Adsorption Characteristics of Activated Carbon for the Recovery of Ni (II) and Pd (II) from Synthetic Electroless Plating Solutions

Thesis submitted in partial fulfillment of the requirements for the degree of

DOCTOR OF PHILOSOPHY

by

Yennam Rajesh

Department of Chemical Engineering

Indian Institute of Technology Guwahati

Guwahati–781039, India

Adsorption Characteristics of Activated Carbon for the Recovery of Ni (II) and Pd (II) from Synthetic Electroless Plating Solutions

Thesis submitted in partial

fulfillment of the requirements for the degree of

DOCTOR OF PHILOSOPHY

by

Yennam Rajesh
Roll No.: 09610723

Department of Chemical Engineering

Indian Institute of Technology Guwahati

Guwahati – 781039, India

July 2014

Dedicated

to

my grandmother, parents and my family members

Department of Chemical Engineering
Indian Institute of Technology Guwahati
Guwahati – 781039, Assam, India

CERTIFICATE

It is certified that the work contained in this thesis entitled **"Adsorption Characteristics of Activated Carbon for the Recovery of Ni (II) and Pd (II) from Synthetic Electroless Plating Solutions"** submitted by **Mr. Yennam Rajesh** for the award of the degree of Doctor of Philosophy has been carried out in Department of Chemical Engineering, Indian Institute of Technology Guwahati under my supervision and this work has not been submitted elsewhere for the award of any other degree or diploma.

(Dr. Ramgopal V.S. Uppaluri)
Professor
Department of Chemical Engineering
IIT Guwahati, India-781039

Adsorption Characteristics of Activated Carbon for the Recovery of Ni (II) and Pd (II) from Synthetic Electroless Plating Solutions

Yennam Rajesh

Acknowledgement

I would like to express my gratitude to all those who helped me in different ways in completing this research work within the time span of four years and seven months, directly or indirectly. First and foremost, I would like to express my deep felt gratitude to my supervisor, **Prof. Ramgopal V. S. Uppaluri** for providing me with continuous inspiration and guidance throughout the entire course of my work. I am indebted to him for his useful suggestions and constant encouragement throughout the entire period.

He also provided me with continuous support, involved me in interesting discussions and also gave the freedom to handle different issues. I am grateful to his expertise in analyzing experimental data and modelling them suitably. His uncompromising approach to complete the experimental part, data analysis, writing manuscripts as well as thesis within the stipulated time period plays a major role in completing my research work. The numerous brain storming sessions during the project meetings with him were very useful in enriching my analytical power.

I would like to express my sincere gratitude to **Dr. Anugrah Singh** of the Department of Chemical Engineering for his valuable suggestions and guidance that helped me in choosing a research area of my interest and understanding. I am also thankful to **Dr. Anil Verma** for providing me with precious equipment like the peristaltic pump and **Dr. Pakshi Rajan** for providing me with the necessary set up for column studies experiments.

My most heartfelt thank you to all my doctoral committee members-**Dr. Mihir K. Purkait, Dr. Subrata K. Majumdar** of the Department of Chemical Engineering and **Dr. R. Swaminathan** of the Department of Biotechnology, for their valuable suggestions and contributions which further improved and enhanced the quality of my research work.

I also thank all the faculty members of the Department of Chemical Engineering for their kind cooperation during my stay in the department. I am also thankful to all the staff members and scientific officers for their genuine help. Special thanks to **Mr**. **Kastumony Deka** and **Mr. Lukumoni Borauh** for their wonderful support during the characterization analysis. I also acknowledge the financial support provided by the Department fund**.**

I am also deeply thankful to the scientific officers at the Central Instruments Facility of IIT Guwahati for allowing me to carry out **SEM and EDX** analysis on my own. These played a crucial role in my research work. In this regard, I must also acknowledge the help of **Mr. K. K. Senapati** and **Mr. Singh,** Scientific Officer, Central Instruments Facility, IIT Guwahati. They taught me how to use the SEM and EDX instruments in order to take images at various critical conditions of the sample. I am also thankful to **Mr. N.K. Das,** Technical Superintendent of Central Workshop, IIT Guwahati for helping me in the fabrication of my experimental setup which was very much essential in my research work.

I was fortunate enough to get excellent lab mates like Mr. E. Sri Harsha, Ms. Amrita Agarwal, Mr. P. Murali, Mr. K. China Malakondaiah, Mr. B. Chandrasekhar and my friends Mr. D. Anand Babu, Mr. A. Leela Manohar, Mr. T. Anil, Mr. K. Suresh, Mr. Santhi Raju Pilli Mr. P. Ravi Kumar and Mr. P. Bharath Kumar for their friendly support and timely assistance whenever I needed it. I am also thankful to Mr. N. Srinu, Ms. M. Mery Kumari, Ms. Y. Sruthi, Ms. Y. Prathyusha, Ms. Supriya, Ms. Shreya Paul and Mrs. Sowjanya for their friendly behaviour and assistance. Special thanks to **Ms**. **Namrata Gummalla** for her assistance and co–operation in editing the thesis files of my research work. My sincere thanks to my seniors Dr. Ashok kumar, Dr. J.P. Anand kumar, Dr. Praveen kumar and Dr. Mahesh Gagarai for their valuable suggestions in my PhD thesis work.

I am also thankful to my Christian Fellowship Families and friends like Bro. Ravi Bolleddu and family, Bro. Agile Mathew and family, Bro. Simon Peter and family, Bro. Kamal Kumar and family, Dr. Roy Sir and family, Haokip Sir and family, Bro. Venu Babu, Bro. Rohit, Sis. Swaroopa, Sis. Raji, and Pradeep for their love and encouragement in my spiritual life. My Special thanks to Sis. Mani, Sis. Anitha and Mangayamma for their care and love towards my health and well-being.

Last but definitely not the least, I would like to express my deepest gratitude to my beloved grandmother, grandfather, parents and family members. My lovable niece children Akshaya, Anshul and Missie for getting peaceful mind while talking and playing with them. Their love, care, sacrifice and encouragement have made it possible for me to come so far. I will be forever indebted to the courage, understanding and dedicated support shown by all of them through all the testing times that lay in our path.

Yennam Rajesh

Abstract

Among various adsorbents, activated carbon has been prominent for industrial applications like heavy metal removal and wastewater treatment. This work addresses the preparation and characterization of biosorbents and activated carbon for the evaluation of Ni (II) and Pd (II) adsorption characteristics from aqueous and synthetic electroless plating (ELP) solutions. While early research efforts focused towards developing an efficient adsorbent from plant waste biomass for Ni (II) adsorption, the later studies aimed at developing a high quality laboratory fabricated activated carbon adsorbent for Pd (II) adsorption from aqueous and synthetic ELP solutions. The carried out research in the thesis has been presented in five sections, namely:

a) Preparation, characterization and batch adsorption characteristics of plant waste biomass based adsorbents for Ni (II) adsorption from aqueous solutions. The adsorbents were prepared using phosphoric acid activation method. For comparative purpose, Ni (II) adsorption studies were conducted with synthetic ELP solutions and commercial AC adsorbent.

b) Preparation, characterization and batch adsorption characteristics of laboratory fabricated and commercial activated carbon adsorbents for the Pd (II) recovery from synthetic ELP solutions. The laboratory fabricated AC adsorbent was achieved using optimal combinations of sintering temperature (600-900 ^{o}C) and acid to bamboo ratio (4:1 by weight).

c) Continuous Pd (II) adsorption and desorption characteristics using commercial AC adsorbent beads and aqueous/synthetic ELP solutions.

d) Preparation, characterization and batch adsorption studies of chitosan-commercial AC composite adsorbents for the Pd (II) recovery from synthetic ELP solutions. The prepared

adsorbents correspond to impregnated (CH-AC-I and CH-AC-IS) and cross-linked (CH-AC-C) chitosan activated carbon composite adsorbents.

FTIR, LPSA, BET and SEM based characterizations were conducted for the adsorbent samples. Further, point of zero charge analysis was also conducted for several cases.

Among pineapple and bamboo stem plant waste biomass sources, the activated carbon prepared with bamboo stem (BSAC) provided optimal performance for Ni (II) adsorption from aqueous solutions. For the BSAC adsorbent, whose BET surface area is 116 m^2/g, optimal batch adsorption parameters were evaluated as 150 min of contact time, pH of 5 and 2 g/L adsorbent dosage respectively. For a variation in Ni (II) solution concentration from 50–300 mg/L, the BSAC adsorbent metal uptake and removal percentage varied from 23.23–98.07 and 92.74-65.38%, respectively. The BSAC adsorbent was observed to provide 45% higher metal uptake than that reported in the literature. Freundlich and pseudo-second order models were the most suitable to represent the measured data. Further, commercial AC adsorbent was analyzed to provide lower metal uptake (5.56–17.75 mg/g) and removal efficiencies (44.54–14.2%) for Ni (II) synthetic ELP solutions prepared with nickel sulphate, trisodium citrate and sodium hydroxide.

For a variation in Pd (II) solution concentration from 50–500 mg/L, the commercial AC with a BET surface area of 1057.7 m^2/g provided a metal uptake and percentage removal of 5.76–43.33 mg/g and 69.12–52 % respectively using agitated assisted adsorption and 6.34–45.5 mg/g and 76.12-54.61 %, respectively, using sonication assisted adsorption. For the same adsorbent, Pd (II) adsorption characteristics were relative better for synthetic ELP solutions containing CTAB surfactant. This is possibly due to the pertinent variations in the interface properties of AC in the

presence of CTAB. For all cases, Freundlich and pseudo-second order models were evaluated to represent the measured equilibrium and kinetic data.

The BSAC14 adsorbent prepared with 4:1 acid to bamboo ratio at a sintering temperature of 700 ^{o}C possessed a BET surface area of 1014.4 m^2/g. This is comparable to the surface area of commercial AC (1057.7 m^2/g). For a variation in Pd solution concentration from 50–500 mg/L, the BSAC14 adsorbent provided a metal uptake and removal efficiency of 6.01-43.23 mg/g and 72.12–53.2%, respectively, for agitation assisted adsorption and 6.35-45.08 mg/g and 76.24–54.1%, respectively, for sonication assisted adsorption. These adsorption characteristics are similar to those obtained using commercial AC adsorbent. Compared to the results reported in the literature for Pd (II) recovery using AC, insignificantly lower metal uptake (29.10 mg/g at 300 mg/L Pd (II) solution concentration) has been obtained for the BSAC14 adsorbent. This is possibly due to the complex chemistry involved in synthetic ELP in comparison with the aqueous solutions.

15% (w/w) poly vinyl alcohol (PVA) was used to prepare the commercial AC beads for continuous Pd (II) adsorption studies. At a bed height of 5 cm, flow rate of 15 mL/min and for an initial metal ion concentration of 50–150 mg/L, the metal uptake and removal efficiency was evaluated to vary from 18.09-152.39 mg/g and 52.93-9.60%, respectively, for aqueous solutions and 10.78-68.66 mg/g and 34.27-5.21%, respectively, for synthetic ELP solutions. This indicates that poor Pd (II) adsorption characteristics exist for synthetic ELP in comparison with those obtained with aqueous solutions. Amongst various models, BDST provided the best fitness for data obtained with aqueous solutions and a satisfactory fitness for the data obtained for ELP solutions. Based on desorption studies, it was evaluated that the AC beads provide lower elution efficiencies of 40–68 and 50–70% for aqueous and synthetic ELP solutions respectively.

Among all adsorbents, the cross-linked chitosan–AC adsorbent possessed the maximum BET surface area of 1317.2 m^2/g. The Pd (II) adsorption characteristics were evaluated for various cases that correspond to synthetic ELP solution (a) without surfactant on CH-AC-I adsorbent (b) without surfactant on CH-AC-IS adsorbent (c) without surfactant on CH-AC-C adsorbent (d) with surfactant on CH-AC-C adsorbent. For a variation in Pd solution concentration from 50-500 mg/L, the highest removal efficiency was obtained for case (d) (98.04–88.87%), followed by case (c) (97.04–84.17%), followed by case (b) (78.78–51.41%) and case (a) (68.78–34.81%). Among various cases, only CH-AC-C adsorbent provided better removal than that reported in the literature. Also, the highest metal uptake (capacity) was obtained for case (d) (8.17–74.06 mg/g), followed by case (c) (8.08–70.14 mg/g), case (b) (6.56–42.54 mg/g) and case (a) (5.73–29.01 mg/g). In comparison with the literature reported chitosan-AC composite adsorbent (BPMC), the obtained data indicate higher metal uptake but lower removal efficiencies for CH-AC-C adsorbent with Pd (II) synthetic ELP solutions. This is attributed to complex solution chemistry of the electroless plating solutions in comparison with aqueous solutions. Batch desorption studies for AC and CH-AC-C adsorbents indicate that the adsorbents can be subjected to desorption effectively with NaOH. With NaOH solution, the desorption efficiency of commercial AC and CH-AC-C adsorbents prepared with an ELP solution initial concentration of 300 mg/L were 4.5 and 23.6 respectively. This indicates the possibilities of significant irreversible chemisorption during the Pd (II) adsorption process.

In summary, the thesis provides substantial amount of data for Ni (II) and Pd (II) adsorption from synthetic ELP solutions. The specific novelty of the thesis refers to the following aspects:

a) Optimality of bamboo stem waste plant biomass for the preparation of low and high quality AC adsorbents.

b) Compared to the existing literature, 45 % higher metal uptake was achieved for Ni (II) batch adsorption using BSAC adsorbent.

c) Optimality of sintering temperature (600 ^{o}C) and high acid to bamboo ratio (4:1) to achieve high quality laboratory fabricated AC adsorbent whose BET surface area is comparable with that of the commercial AC.

d) Insignificant variation in Pd (II) adsorption characteristics for sonication assisted adsorption and agitation assisted adsorption.

e) Significant role of solution complexity in influencing both batch and continuous Pd (II) adsorption characteristics. For batch adsorption, lower removal efficiency but similar metal uptake was obtained for synthetic ELP solutions not containing CTAB surfactant. For continuous Pd (II) adsorption, it has been evaluated that Pd (II) metal uptake and removal efficiency are significantly lower for ELP solutions than those obtained with aqueous solutions.

f) Relative better metal uptake and removal efficiency for Pd (II) batch adsorption from CTAB containing synthetic ELP solutions in comparison with solutions not containing CTAB surfactant.

g) Fitness of Freundlich, pseudo-second order and BDST models to represent batch and continuous Pd (II) adsorption data.

h) Crosslinking process has been identified as optimal choice to achieve high quality chitosan-AC composite adsorbents. The composite CH-AC-C adsorbent has been evaluated to provide about 20 mg/g excess metal uptake than commercial AC for Pd (II) adsorption at 500 mg/L solution concentration.

Considering these aspects, it is envisaged that the data presented in the thesis would serve as a useful reference for furthering research in the field of the recovery and reuse of Pd (II) from electroless and electroplating solutions. This is especially relevant for the industrial electroplating waste solutions case where multiple metals and further complexity of other additives is anticipated to further reduce the metal uptake and removal efficiency. On the other hand, the prepared Pd-AC and Pd-CH-AC-C adsorbents are important functional products that can be utilized for high temperature and low temperature catalysis applications. Despite being highly cost effective, the overall analysis indicates that Pd (II) adsorption from synthetic ELP solutions is characterized with lower combinations of adsorption and desorption efficiency and metal uptake. These useful insights would be relevant to further engineer research in the vast field of adsorption based noble metal recovery and reuse from complex synthetic and industrial solutions and waste streams.

Contents

List of Tables

List of Figures

Nomenclature

Abbreviation

AC	Activated Carbon
PS	Pineapple Stem
BSAC	Bamboo Stem Activated Carbon
BP	Banana pith
CH-AC-I	Chitosan Activated Carbon Impregnated
CH-AC-IS	Chitosan Activated Carbon Impregnated with Surfactant
CH-AC-C	Chitosan Activated Carbon Crosslinked
BPMC	Biopolymer Modified Carbon
MBAC	Melocanna Baccifera Activated Carbon
MBRC	Melocanna Bacifera Raw Charcoal
OSHA	Occupational Safety and Health Act
WHO	World Health Organization
PGM	Palladium Group Metals
BET	Brunauer-Emmett-Teller
DKR	Dubinin-Kanger-Radushkevich
LPSA	Laser Particle Size Analysis
AAS	Atomic Absorption Spectrometer
UV	Ultra Violet Visible Spectroscopy
EDX	Energy Dispersive X-ray spectrometer
FTIR	Fourier Transform Infrared Rays

SEM	Scanning Electronic Microscope
PZC	Point of zero charge
CMC	Critical miscilinaceous concentrations
ELP	Electroless plating solutions
BDST	Bed Depth Service Time
CTAB	Cetyl Trimethyl Ammonium Bromide
EDTA	Ethylenediaminetetraacetic acid
Pd-E-CH-AC-C	Palladium Electrolessplating treated Chitosan Activated Carbon Crosslinked
Pd-ES-CH-AC-C	Palladium Electrolessplating treated Chitosan Activated Carbon Crosslinked

Notations

C_o	Initial concentration of metal in aqueous solution, mg/L
C_e	Equilibrium adsorption concentration of metal, mg/L
W	Adsorbent dosage, g
V	Volume of aqueous solution, mL
q_e	Mass of solute adsorbed per mass of adsorbent at equilibrium, mg/g
q_{max}	Langmuir monolayer capacity, mg/g
b	Langmuir equilibrium constant
K_R	Separation factor
k_f	Freundlich isotherm coefficient
m	Amount of adsorbent taken per l L of aqueous solution, mg/L
A, B	Redlich-Peterson isotherm constants, L/mg.
A_T, b_T	Temkin isotherm constants L/mg.
T	Absolute temperature, ^oC
q_t	Mass of solute adsorbed per mass of adsorbent at ‘t’ min, mg/g

t	Agitation time, min
k_1	Psuedo First order rate constant, min-1
k_2	Pseudo second order rate constant, g.mg-1.min-1
K_{id}	Intra Particle rate constant ($time^{-1}$)
q_t	Mass of solute adsorbed per mass of adsorbent at 't' min, mg/g
R	Universal gas constant (8.314 J/K. mol)
ΔG^o	Change in Gibbs free energy (kJ)
ΔS^o	Change in Entropy (kJ/ K. mol)
ΔH^o	Change in Enthalpy (kJ/mol)
k_d	Equilibrium constant at constant temperature
E_r	Error function
i	Index for adsorption experiment corresponding to specific initial solution concentration of metal
n	Total number of adsorption experiments carried out with variant concentration
Er_{max}	Error maximum
Er_{min}	Error minimum
$Er_{average}$	Average Error
Er_{rms}	Root mean square Error
V_n	Throughput volume at n^{th} reading
C_n	The effluent adsorbate concentration at n^{th} reading (mg/L)
I	Influent adsorbate load (I)
(V_{eff})	Throughput volume (mL)
Mus	Mass of adsorbate not removed (mg)
Mr	Mass of the adsorbate removed (mg)
Mad	Adsorbate uptake by adsorbent (mg)
Δt or Z_m	Mass transfer zone (cm)

t_b	Breakthrough time (min)
t_e	Exhaustion time (min)
Z	Bed heights (cm)
t	Service time (*min*)
N_o	Dynamic bed capacity (mg/L)
ν	Linear flow rate (cm/h)
F	Volumetric flow rate (cm^3/h) or mL/min
A_c	Cross-sectional area of the bed (cm^2)
K_{ad}	Rate constant of adsorption ($l\ mg^{-1}\ h^{-1}$)
C_b	Breakthrough metal ion concentration (mg/L)
m_x	Slope
C_x	Intercept
K_{TH}	kinetic coefficient or Thomas model rate constant (mL/mg. min)
M	Total mass of the adsorbent loaded in the column (*g*)
K_{YN}	Rate constant (per min)

Chapter 1:

Introduction and Literature Review

Chapter 2:

Experimental and Modeling Approaches

Chapter 3:

Equilibrium and Kinetic studies of Ni (II) adsorption using Pineapple and Bamboo Stem based adsorbents

Chapter 4:

Pd (II) adsorption characteristics of commercial AC adsorbents with synthetic electroless plating solutions

Chapter 5:

Development of activated charcoal adsorbent from bamboo (Bambuseae) waste for the recovery of Pd (II) from synthetic electroless plating solutions

Chapter 6:

Packed-bed Pd (II) adsorption studies for commercial AC adsorbent

Chapter 7:

Preparation, Characterization and Pd (II) adsorption characteristics of chitosan-AC composite adsorbents

Chapter 8:

Conclusions and Recommendations for Future Work

Appendix

Publications

References

Introduction and Literature Review

Sections 1.1-1.3 of this chapter present a brief over view on heavy metal and precious metal ion containing wastewaters. Section 1.4 addresses various competent technologies for heavy and precious water treatment and the recovery and reuse of noble metals. Section 1.5 presents a brief overview of adsorption technologies. Subsequently, in sections1.6 and 1.7the chapter focuses on the state of the art in adsorption and ion exchange resins for the competent adsorption of Ni (II) and Pd (II) from their aqueous and synthetic solutions respectively. Section 1.8 details on the scope for further research with emphasis towards the development of biomass based adsorbents and activated carbon based adsorbents for Ni (II) and Pd (II) adsorption studies. Lastly, section 1.9 briefly presents the objectives of the thesis followed with organization related details presented in section 1.10.

1.1 Introduction

Today, environmental pollution has become a key issue of concern in both developed and developing countries. While developed countries might have good systems in practice to reduce environmental pollution, developing countries such as India and China need to implement stringent environmental legislations and establish associated process systems. Environmental pollution can be broadly classified as water pollution, air pollution and noise pollution. Prominent pollution issues include lower quality of air, contamination of drinking water and degradation in the water used to cultivate crops and excessive increase in noise levels. All indicate towards a degrading quality of life. Among various pollution problems, the pollution of water resources is of greater concern in poor and developing countries. This is due to the reason

that among all natural resources, water is of paramount importance. While water covers more than three-fourth of the total area available on planet earth, only 0.6–0.7 % of total water is available in the form of rivers, lakes and ponds for appropriate human utilization (Wollamann *et al*., 1962).

The ever increasing contamination of aquatic sources with several pollutants is endangering bio-diversity and leads to a shortage of potable water resources. Major contributors of aquatic pollution are domestic activities, mining activities, municipal wastes, modern agricultural practices, marine dumping, radioactive wastes, oil spillage, underground storage leakages and industries. Amongst these, industrial units are the major sources for indiscriminate discharge of toxic chemicals in effluents. Textile, steel, oil, tanneries, canneries, refineries, mines, fertilizers production units, detergent production units, electroplating, electroless plating industries and sugar mills are major contributors to water pollution and have been identified to cause hazardous effects on flora and fauna (Rai *et al*., 1998, Singh and Singh, 2000; Gavrilescu, 2004; Iqbal and Edyvean, 2004; Akar and Kiran, 2005). Industrial and other pollution streams refer to homogeneous/heterogeneous systems of several inorganic and organic compounds with varying compositions and activity. Based on extensive research in the field of pollution abatement related to wastewater treatment, the following challenges have been highlighted for urgent attention:

- Efficient water conservation and management with effective implementation of policies and practices at the local level.
- Treatment of generated wastewater streams with cost effective methods including low cost biological treatments.
- Managerial policies targeting the reuse of treated wastewaters.

- Development of eco-friendly technologies that can potentially replace existing technologies which are not environmentally sustainable.

1.2 Heavy metal pollutants in wastewaters

1.2.1 Classification

Heavy metals being non-biodegradable and extremely persistent make up some of the most harmful pollutants in the environment. They enter into the water resources through both natural and anthropogenic sources. The term heavy metal refers to any metallic chemical element that has a relatively high density. Their density is usually more than 5.0 g/cm^3. Even at aqueous concentrations in the order of ppm or mg/L, these heavy metals are toxic to organisms.

1.2.2 Sources

Heavy metals such as arsenic, cadmium etc. occur naturally as constituents of the earth's crust. Heavy metals include transition metals, some metalloids, lanthanides and actinides. Of late, there has been an increase in their concentration levels in the environment due to rapid and widespread industrialization and urbanization. Industrial wastewater streams are the primary means by which heavy metals are released into the environment (LeVan, 1998; Das *et al*., 2008).

Heavy metals may enter water supply systems through industrial or consumer wastes which release heavy metals into streams, lakes, rivers and groundwater. Heavy metals are non-biodegradable and hence pose a tough challenge for environmentalists. The Minamata disease which was caused by Mercury pollution in Japan is one of the well-known examples of environmental disasters caused by heavy metals.

Irrigation water that comes in contact with effluents released from paper mills and fertilizer factories also pollutes water resources with heavy metals (Singh, 1994; Fazeli *et al*., 1998).Some of the common industrial sources for the generation of toxic heavy metal containing wastewater

are summarized in Table 1.1.

Table 1.1: A summary of various sources for heavy metal wastewater generation (Singh, 1994; Fazeli *et al*., 1998)**.**

Metal	Common sources
Chromium	Chrome plating industries, petroleum refineries, electroplating industry, leather tanning industries, textile manufacturers and pulp processing units.
Nickel	Galvanized products, paint powder, batteries processing units, metal refineries and super phosphate fertilizers.
Lead	Petrol based materials, pesticides, leaded gasoline, and mobile batteries.
Copper	Electroplating industry, plastic industry, metal refining and industrial emissions.
Zinc	Rubber industries, paints, dyes, wood preservatives and ointments.
Cadmium	Batteries, electroplating industries, phosphate fertilizers, detergents, refined petroleum products, paint pigments, pesticides, galvanized pipes, plastics, polyvinyl and copper refineries.
Iron	From metal refineries, engine parts.
Aluminum	Industries preparing insulated wiring, ceramics, automotive parts, aluminum phosphate and pesticides.
Arsenic	Automobile exhaust/industrial dust, wood preservatives and dyes.
Mercury	Electric/light bulb, wood, preservatives, leather, tanning, ointments, Thermometers, adhesives and paints.

Table 1.2: Common health problems caused by heavy metals to human beings (Singh, 1994; Fazeli *et al*., 1998)**.**

Metal	Health risks
Chromium	Irritation, nausea and vomiting, cancer, and ulcers. Long-term exposure can cause kidney and liver damage, and damage to circulatory and nervous tissue.
Nickel	Dermatitis, chronic rhinitis, hypersensitivity reactions in the immune system, which in turn cause hyper allergenic reactions to various substances, Long-term, toxicity may lead to liver necrosis and carcinoma, myocardial infarction, respiratory illnesses such as asthma, heart and liver damage, skin irritation.
Lead	Weight loss, cognitive dysfunction and decreased coordination, memory loss, nerve conductions. The central nervous system is most sensitive to the effects of lead.
Copper	Biliary obstruction (inability to excrete excess copper), liver disease, renal dysfunction, fibromyalgia symptoms, muscle and joint pains, depression, chronic fatigue symptoms, irritability, tumor, anemia, learning disabilities and behavioral disorders, stuttering, insomnia, niacin deficiency, leukemia, high blood pressure.
Zinc	Nausea and vomiting.
Cadmium	Hypertension or high blood pressure, dulled sense of smell, anemia, joint, soreness, hair loss, dry scaly skin, loss of appetite, decreased production of T- cells and, therefore, a weakened immune system, kidney diseases and liver damage, emphysema, cancer and shortened lifespan,
Aluminum	Gastrointestinal disturbance, fatigue, headache, poor calcium metabolism, decreased liver and kidney function, forgetfulness, speech disturbances and memory loss, weak and aching muscles, seizures, vertigo and loss of balance Headache, confusion, drowsiness, convulsions, changes in fingernail
Arsenic	Pigmentation, vomiting, diarrhea, bloody urine, muscle cramps, convulsions, gastrointestinal upsets and coma.
Mercury	Anxiety, depression, confusion, irritability, insecurity and fatigue.

1.2.3 Health risks

As trace elements, some of these heavy metals (e.g. copper, selenium, zinc) play a crucial role in maintaining the metabolism of the human body. However, at higher concentrations they are toxic and may even lead to poisoning. Poisoning due to heavy metals could be due to drinking-water contamination, high concentrations in ambient air near emission sources or intake via the food chain. Heavy metals are dangerous because they bio-accumulate. Bioaccumulation refers to an increase in the concentration of a chemical in an organism over time, compared to its concentration in the environment.

In humans, heavy metals accumulate in living tissues. The health risks of heavy metals ingestion thus are of wide range. Some metals cause physical discomfort while others may cause life-threatening illnesses, damage to vital body systems or other damages. Thus, it is very necessary to control emission of heavy metals into the environment.

Table 1.2 summarizes few common harmful effects and health risks for human beings due to heavy metals.

1.3 Precious metals in wastewaters

1.3.1 Classification

Platinum group metals (PGMs) refer to precious metals (PMs) such as Ruthenium (Ru), Rhodium (Rh), Palladium (Pd), Osmium (Os), Iridium (Ir), Platinum (Pt), Gold (Au) and Silver (Ag).The term ‘precious’ has been coined for them because of their economic value and rare occurrence in nature. Gold occurs as a metal in nature. Silver, gold and platinum metals are also recovered in the electrolytic refining of copper. The precious metals do not have the tendency to form oxides under standard conditions with the exception of Osmium which forms OsO_4 even at room conditions. Silver and gold are not susceptible to oxidation by hydrogen ions under

standard conditions, and hence, together with platinum, they are used in jewelry and ornaments. Due to their favourable properties such as resistance to corrosion and oxidation, high melting points, electrical conductivity, catalytic activity and biological inertness, precious metals have several applications in chemical, electrical, electronic, glass, medicine and automotive industries (Kasaini *et al.*, 2009).

1.3.2 Sources

The average concentration of PGMs metals in the earth's crust has been estimated in the range of 0.001-0.005 mg/kg for Pt, 0.015 mg/kg for Pd, 0.0001 mg/kg for Rh, 0.0001 mg/kg for Ru, 0.005 mg/kg for Os and 0.001 mg/kg for Ir (Ravindra *et al*., 2004).Generally, all PGMs are associated with one another in earth's crust and therefore Pd exits with other PGMs in the nature.

The rapid growth in industrialization has polluted the environment. Since recent years sewage waters have been used for irrigation. There are greater concerns about precious metals contamination in the receiving earth and water. For centuries, these precious metals have been sought after in the form of jewelry and ornaments. As scientists uncovered the physical and chemical properties of these metals, their application expanded to many other fields. Among the PGMs, Palladium has unique catalytic activity. Palladium is mostly used in the hydrogen separation application for the fuel cell technology and in the production of Pd- activated charcoal catalysts. It is also the most ideal of the PGMs, and therefore it is the most difficult to dissolve in aqueous solutions (Kayanuma *et al*., 2004).Two of the most important sources of palladium are the nickel-sulphide ores found in South Africa and Canada, which contain approximately 0.1% palladium (Greenwood and Earnshaw, 1989).

In industrial wastewaters with chloride concentrations and typically low pH, such as PGMs refinery wastewaters, PGMs are present in the form of anionic chloro complexes with complex

solution chemistry. For such cases, the PGM species composition needs to be specified along with other factors such as chloride concentration, pH, ionic strength, temperature, and age of the solution (for Palladium especially). Some of the common industrial units releasing toxic PGMs metals into environment are listed in Table 1.3.

Table 1.3: Common industrial units releasing precious metal containing wastewaters to water bodies (Benguerel *et al*., 1996)**.**

Metal	Common sources
Platinum	Electroplating and refining industries, Jewelry and Coins, catalytic convertors on cars, trucks, buses manufacturing.
Palladium	Electroplating and Electroless plating industries, Jewelry, hydrogenation and dehydrogenation reactions, Dental alloys, Gold decolorization, Metal refining and acid mining industries.
Silver	Development of photographs, Dental alloys, Soldier and brazing alloys, Electrical contacts and batteries, Sterling silver for jewelry, Ornaments and silverware.
Gold	Gold coins, gold ingots, and gold bars, gold is available in many forms including pure gold and alloys as gold flakes, foil gauzes (meshes), grain, powders, sheet, sponges, tubes, wires and even single gold crystals.
Rhodium	Copper-nickel sulphide ores, Alloys used in electrodes, furnace windings, crucibles and thermocouple elements.
Iridium	Batteries manufacturing units, nickel refineries, Pen tips and compass bearings alloys.

1.3.3 Health risks

The emission of Pd, Pt, and Rh members of the platinum group metals (PGMs) from automobile catalysts into the urban environment is very harmful for human health. Palladium does not impact the environment greatly. It is present in very less quantities in some soils, and the leaves of trees have been found to contain 0.4 mg/L of Pd (Vijay *et al*., 2011). Although most plants tolerate it, some plants such as the water hyacinth get killed with exposure to low level of palladium salts.

Bringing awareness among people on the health dangers caused by Pd is major concern as even very low doses of Pd are sufficient to cause allergies in human beings. Also, a person with some form of nickel allergy may be especially susceptible to get affected by Pd as well. Miners, dental technicians and chemical workers are especially exposed to Pd which can cause skin and eye irritations. The general population may come into contact with palladium mainly through mucosal contact with dental restorations and jewelry containing palladium and possibly via emissions from Pd catalysts. Their protection from the adverse effects caused by Pd may be achieved by the use of alloys with high corrosion stability and minimal release of palladium. In general, in dental patients who are sensitive to Pd, restorations are not recommended with Pd-containing materials even though Pd has been evaluated without allergic effects for some individuals. Further, those patients who have an allergy to Pd should be informed that use of Pd-containing dental materials may cause Pd allergy, although the chances are less for the allergies to get manifested. On the other hand, $PdCl_2$ was formerly prescribed as a treatment for tuberculosis at the rate of 0.065 g per day (approximately 1 mg/kg) without many negative side effects. Silver up to a concentration of 20-200 μg/mL is permissible in order to control antimicrobial activity without any risk to human health (OSHA-2002; Kielhorn *et al*. 2002).

1.3.4 Cost issues

Palladium commonly occurs along with other PGMs. It exists in three oxidation states: Pd^0 (metallic), Pd^{2+}, and Pd^{4+}. It is found abundantly in the earth's crust (≤1±10 mg/kg) and in sea water (2.2×10^{-8} mg/kg) and is one of the scarcely available metallic elements. Because PGMs are very expensive to mine and purify, a high proportion of them (20 %) are being increasingly recycled by the users or by the producers (WHO, 2002; Johnson Matthey, 2001).

Palladium is a metal whose output has been doubled in the past ten years (Fig.1.1). This increase in Pd demand is mainly due to its application as an automotive emission control catalyst. There has been significant enhancement in the research and development in this field. This is due to the implementation of stricter standards and legislation on allowable emissions from road vehicles. For example, in 1996, 60 percent of new European gasoline cars and also many Japanese and American cars were equipped with palladium-containing catalysts. In Europe, most car manufacturers are adding increasing amounts of palladium to catalysts in order to meet the tighter EU Stage III and Stage IV emissions regulations. In 2000, this resulted in 25 % increase in the demand of Pd (60 metric tons) (Johnson Matthey, 2001).

Palladium also has applications in electrical equipment. Palladium metal or palladium-silver pastes are used as active components in diodes, transistors, integrated circuits, hybrid circuits, and semi-conductor memories. They are also an integral part of many passive electronic components such as very small multilayer ceramic capacitors, thick-film resistors or conductors. Pd is also used as an industrial catalyst in the production of vinyl acetate monomer and for production of terephthalic acid (PTA), a feedstock in the manufacturing of packaging materials and artificial fibres (WHO, 2002). Fig. 1.1 illustrates the forecasted world palladium demand for various applications from 1990-2001 (Johnson Matthey, 2013).

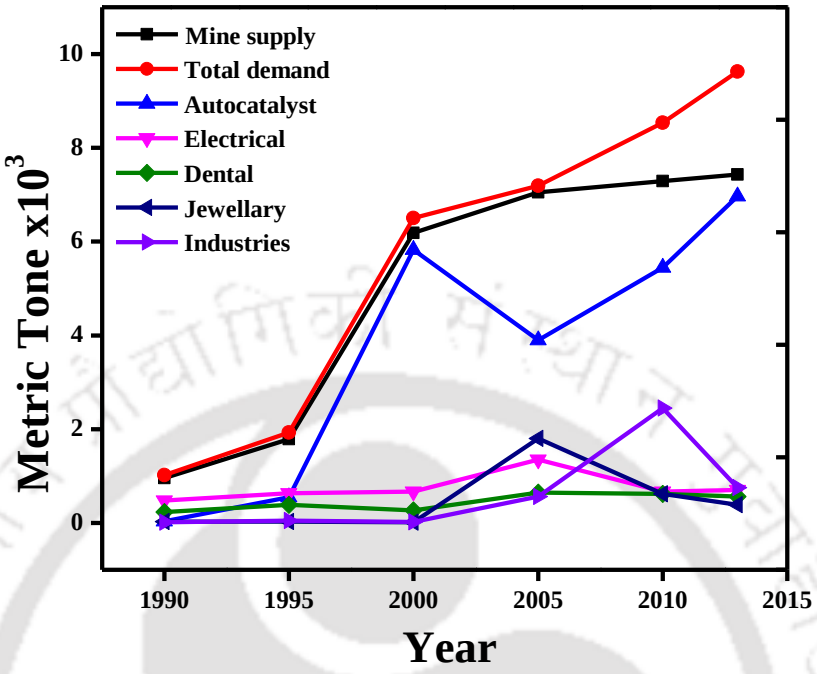

Fig. 1.1: World Palladium demand for various industries (Johnson Matthey, 2013).

1.4 Technologies for the treatment of heavy and precious metal containing industrial effluents

Removal of the above mentioned noble metals from industrial wastewater is a challenging task. For example, from Pd electroless plating industry, the industrial wastewater could consist other various components such as Na_2EDTA, EDTA, CTAB and liquor ammonia. These components complicate the interactions between the noble metal (adsorbate) and adsorbent. It is well known that in the presence of Na_2EDTA and NH_3, Pd forms a complex whose adsorption on the adsorbent might be different from the adsorption of Pd (II) on the adsorbent in aqueous solutions. In addition, the presence of CTAB surfactant is prone to significantly vary pertinent interfacial phenomena which might strongly alter noble metal adsorption characteristics.

For the recovery and reuse of precious metals and treatment of heavy metal containing wastewaters, the most prominent methods can be classified into (a) chemical (b) physical and (c) biological treatment methods. A brief account of these methods is presented in the following sub-sections.

1.4.1 Chemical methods

Few conventional chemical methods used to reduce heavy/precious metals concentrations from wastewater streams include electrochemical treatment, chemical reduction and chemisorption (ion exchange).

1.4.1.1 Chemical coagulation

Chemical coagulation is the most common method for the aggregation of components present in wastewaters. It is a widely used process to remove pollution caused by suspended particles. Due to their small size, suspended particles cannot be settled under gravity and hence they cannot be removed by physical processes. Some suspended particles interact with colloid surfaces and these results in repulsion. Hence, these particles do not agglomerate to form flocs. The process of coagulation involves neutralizing the charges present on the particle surfaces with the help of coagulants and the flocculants. These additives enable the formation of flocs by slow agitation. Typically, coagulation and flocculation are followed by settling process during which resultant flocs are removed from wastewater.

In general, coagulants such as alum, lime, $Al_2(SO_4)_3$, $FeSO_4$ or Fe_2SO_4 and $MgCl_2$ are used to remove heavy metals like Zn, Mn, Ni, Cr, and As etc. from industrial waters. The percentage recoveries obtained for the elements were Cd 66%, Cr 78%, As 69%, Ni 84%, Cu 62% and Zn 73%. These results validate the experimental procedures used in chemical analysis. By comparing the effectiveness of $Al_2(SO_4)_3$, $FeSO_4$, the optimum coagulant dose and pH values for

obtaining maximum removal of metals are determined. Among all coagulants available, $Al_2(SO_4)_3$and $FeSO_4$are chosen as an optimum coagulant for metal removal because they require lowest coagulant dose and minimal settled sludge volume. This results in maximum metal removal from industrial water. Further, these coagulants are economically viable.

1.4.1.2 Ion-exchange process

Among many physicochemical methods developed for the removal of heavy and precious metals from wastewater, ion-exchange is fast becoming a popular method and has received a lot of attention in recent years. Ion-exchange is a unit process in which ions of a given species are displaced from an insoluble exchange material by ions of a different species in solution. During chromium separation ion-exchange process, chromium containing solution enters one end of the column under pressure and passes through the resin bed. This results in chromium being removed from the solution. Once the resin capacity is exhausted, the column is backwashed to remove trapped solids and is then regenerated. The matrices that are commonly used for ion-exchange are synthetic organic ion exchange resins. For Ni removal, 97.04% and 98.06%has been reported for ion-exchange resins (Senthil Kumar *et al*., 2010).

Several ion exchange resins have been identified to perform well for Pd (II) removal. Ion exchange process greatly depends on the pH of the solution. The major disadvantage of ion-exchange method for heavy metal removal is that the resins used in these methods are very selective. A resin must be so chosen that it selectively removes the metal contaminant of concern. Also, ion exchange equipment can be expensive and there can be incomplete removal of the heavy metals from the aqueous solution. Besides, the resins cannot handle concentrated metal solution as the matrix gets easily fouled by organics and other solids in the wastewater.

1.4.1.3 Electrochemical Precipitation

Electrochemical precipitation utilizes an electrical potential to facilitate the precipitation of heavy metal from contaminated wastewater. It is the most common method for removing toxic heavy metals up to parts per million (ppm) levels from water. Using this process, Ni (II) and Pd (II) concentration could be reduced from 500 mg/L to less than 0.3 mg/L (Macaskie *et al*., 2007).The main disadvantage of the process is that it generates large amount of sludge. The sludge contains toxic compounds and therefore needs the resolution of hazard issues. Typically, the efficiency of this cost effective process is affected by the presence of other ions as well as a low pH. Further, the sludge formation requires several additional chemicals for further treatment.

1.4.2 Physical methods

Prominent physical methods include membrane filtration processes and adsorption techniques. Various membrane filtration processes refer to nano-filtration, reverse osmosis and electro dialysis. Membrane processes have a limited lifecycle due to membrane fouling. Further, the cost analysis of the process shall include the cost of periodic replacement of the membrane. The following sub-sections present a brief over view of various membrane processes.

1.4.2.1 Membrane processes

1.4.2.1.1 Reverse Osmosis

During reverse osmosis, heavy metals are separated using a semi-permeable membrane. The process occurs at a pressure greater than the osmotic pressure provided by the solutes dissolved in the waste stream. The major disadvantages of the method are utilization of higher pressures (and hence higher operating cost) and periodic replacement of membrane modules (Ozaki *et al*., 2002).

Membrane filtration technique has gained importance for the treatment of wastewater. It utilizes the principle of the application of external pressure to achieve about the desired separation through the semi-permeable membrane. Various types of membranes like inorganic, polymeric and liquid can be employed for Ni (II) and Pd (II) removal (Sabermahani *et al*., 2013).

1.4.2.1.2 Nano-filtration

The removal of Ni (II) and Pd (II) using nano-filtration composite polyamide membranes was reported by Sabermahani *et al*., (2013). The authors varied concentration and pH of the membrane feed solution. Two membranes were used for the study; which have been characterized as higher and lower rejection membranes. It was found that the percent rejection of palladium increased with the pH of the feed solution, while it decreased with increasing feed concentration. On the other hand, rejection trends were transitionary below and above pH 7.0. The major disadvantages of the process are expensive process, incomplete metal removal, high reagent and energy requirements and generation of toxic sludge or other waste products that require further disposal solutions.

1.4.2.2 Adsorption process

Liquid-phase adsorption is a very popular method for the removal of pollutants from wastewater. A proper design of the adsorption process will facilitate the generation of high-quality treated. Adsorption process is especially viable for the case of inexpensive adsorbents. Further, adsorption usually does not require prior pre-treatment steps.

Adsorption is used in most natural, physical, biological and chemical systems. The most commonly used adsorbents are activated sludge, activated charcoal, activated carbon, zeolites, silicates etc. In the past few years, adsorptive separation processes have gained importance for many important separations in the chemical industries. A detailed study on the adsorption

process that outlines its importance, advantages/disadvantages, applications and limitations are presented in the section 1.5 of the thesis.

1.4.2.3 Electro dialysis

Electrodialysis is a membrane separation process in which instead of pressure, an electric field is applied across a series of membranes. The membranes used are inorganic in nature and are broadly divided into two categories namely cation exchange membrane and anion exchange membrane. Cathode and anode are placed at the two ends of the cell. Raw wastewater is fed continuously from the allotted compartments. The common problems that affect the performance of the electrolysis unit are similar to those faced by reverse osmosis units. In addition, availability of power and its cost play a crucial role in altering the economics of the technology.

1.4.3 Biological treatments

Biological treatment methods are often the most economical alternative in comparison with other physical and chemical processes. Biodegradation methods such as fungal decolorization, microbial degradation, adsorption using microbial biomass (living or dead) and bioremediation systems are commonly applied to the treatment of industrial effluents. These methods utilize the ability of various microorganisms like yeasts, algae and fungi to accumulate and degrade different pollutants. Their application, however, is often restricted because of technical constraints. Biological treatment requires a large land area and is constrained because of the toxic nature of some chemicals, and less flexibility in design and operation. Biological treatment is yet to provide satisfactory metal removal with the currently available biodegradation technologies.

1.4.4 Summary

Except a few, the above mentioned treatment technologies are effective for removal of metals from water with high concentration of metals. For lower concentrations (ppm level) of heavy and precious metals, many of these techniques are not very useful. These methods also have other disadvantages, such as incomplete metal removal, less tolerance to pH change, high cost of equipment and monitoring system requirements, high reagent or energy requirements and generation of toxic sludge or other waste products that require disposal (Yan and Viraraghavan, 2001; Aksu *et al*., 2002; Gavrilescu, 2004; Alimohamadi *et al*., 2005; Wang and Chen, 2006). Few literatures have indicated that many of these techniques may be ineffective or extremely expensive when metal concentration in wastewater is in the range 1-500 mg/L (Mehta and Gaur, 2005).

The continued concern about the contamination of water bodies with by heavy metals has initiated significant number of researches to find possible technological solutions for heavy metal pollution abatement. To overcome the high cost of the physico-chemical treatments, there is a need for developing inexpensive and efficient technology for the treatment of metal containing wastes so that metal concentration can be reduced to environmentally acceptable levels (Wilde and Benemann, 1993; Sandau *et al*., 1996a; Aksu*et al*., 1998; Gavrilescu, 2004). The use of biomass plant wastes and chitosan for metal removal/recovery is considered to be an available alternative to the above discussed conventional methods.

In summary, researchers have widely studied the removal/recovery of heavy/precious metals from aqueous/ industrial wastewater using different types of several separation technologies. In many separation technologies, various draw backs exist. Among these, adsorption process can be viewed as the most effective for metal adsorption with low cost adsorbents and it also provides a

wide variety of industrial applications. Further details with respect to adsorption are presented in the next section.

1.5 Adsorption processes

1.5.1 Working principle

Adsorption occurs due to the affinity of the solute/components to a fluid the surface of a solid. The affinity is due to the existence of unbalanced forces of the species that are getting adsorbed on the solid surface. After adsorption, both repulsive and attractive forces get balanced. Typically, adsorption is an exothermic process and therefore is favored at lower temperatures.

Depending upon the type of forces between adsorbent and adsorbate, adsorption process can be classified as physical adsorption (due to Vander Waal forces) and chemical adsorption (activated adsorption). During physical adsorption, there is a preservation of the individuality of the adsorbate and adsorbent. On the other hand, during chemisorption, there is either transfer or sharing of electrons between adsorbate and adsorbent or transformation of adsorbate into radicals that are bounded to the adsorbent surface. Thus, during physical adsorption, the intermolecular forces of attraction that exist between the molecules of the adsorbate and adsorbent are greater than those which exist between the molecules of the adsorbate.

During the early stages of physical adsorption, monomolecular or monolayer adsorption occurs fastly. During this process, a single layer of adsorbent molecules gets adsorbed onto the adsorbent surface. In due course of time, if the pores of the adsorbent have similar sizes with that of the adsorbing molecules, greater adsorption is facilitated due to the additive filling of the pores with the adsorbate. Such adsorption process is termed as multi molecular or multi-layer

adsorption. There by, the maximum adsorbent capacity will be a function of the pore volume but not the surface area, which is not the case for monolayer absorption.

On the other hand, during chemisorption, chemical bonds are formed only between adsorbent and adsorbate along with the release of heat higher than the heat of condensation. Ion-exchange and chelating resins involve ions transfer or electron transfer mechanisms and are therefore classified as chemisorbing adsorbent. The solution chemistry (liquid phase adsorption) or chemistry of gaseous mixture that is subjected to adsorption can alter the mechanisms of adsorption. In several cases, while physisorption could be dominant, chemisorption cannot be ruled out as the complex solutions/gas mixture chemistry can facilitate the chemical bonding between the adsorbent and adsorbate. Thus, physisorption need not always be the governing mechanism. Chemisorption is a slow and irreversible process in comparison with physisorption. During catalysis, chemisorption occurs and most commercial adsorption processes adapt physical adsorptions.

1.5.2 Advantages and Disadvantages

Adsorption process is highly effective for wastewater treatment applications involving heavy or precious metals. This is due to the various promising features of adsorption such as low cost, ability to process multi component streams with very low concentrations, higher adsorption capacity, cheaper and easier methods of adsorbent preparation etc.

While commercial adsorbents may not have high adsorption capacity, biomass based adsorbents (living or non-living) may provide superior performance. Some of the disadvantages of adsorption technologies are:

(a) Limited shelf life of the adsorbent.

(b) Adsorbent regeneration.

(c) Feed pretreatment to eliminate particles that can plug the adsorbent.

(d) Cooling of feed stream.

(e) Possibility of spent adsorbent to be a hazardous waste.

Generally, adsorption should be coupled with desorption to completely address pollution abatements and hazard issues.

In the field of noble metal recovery from waste streams and solutions, the coupling of adsorption and desorption process will generate noble metals aqueous or acidic solutions. The re-utilization of these solutions in various industries such as plating industries will enable better control of the plating process. This is due to the elimination of metal nuclei in the solution which facilitate unwanted precipitation in the solution. Thus, the recovery and reuse of noble metal from spent solutions/streams generated in the metal finishing industries is a very important area of research, where adsorption-desorption technology can be very useful to sustain and enhance electroplating process efficiency an important role. While it may be argued that commercial ion-exchange resins (lewatit TP-214) may provide very high adsorption capacities, they are highly expensive and therefore it is important to visualize the tradeoff associated with cost and adsorbent performance.

1.5.3 Industrial Applications

Adsorption technologies have been established in process industries for both physical and chemical systems. Activated charcoal and synthetic resins have proven to be ideal materials for the implementation of various adsorption and pollution control methods on an industrial scale. The application of activated charcoal has also been proven to be promising for heavy metal removal from wastewater streams and solutions. Thus, adsorption with activated charcoal can be inferred to possess good potential for precious metal recovery and reuse (Cavalcante, 2000).

1.6 State of the art for Ni (II) removal from aqueous, synthetic and industrial wastewaters

The thesis targets the evaluation of adsorption characteristics of Ni (II) and Pd (II) from aqueous and synthetic electroless plating solutions. Therefore, the state of the art has been first summarized for Ni (II) removal from aqueous, synthetic and industrial wastewaters. Eventually state-of-the-art for Pd (II) adsorption studies has been presented. Nickel is a non-biodegradable toxic heavy metal ion present in wastewater. The main source of nickel pollution in the water is from industrial production processes such as galvanization, smelting, mining, battery manufacture and metal finishing. Nickel can cause serious health and ecological problems beyond a threshold limit in water bodies (WHO-1982; Senthil Kumar *et al*., 2009).

The Ph.D. thesis targets the evaluation of adsorption characteristics of activated carbon adsorbents for the recovery of Ni (II) and Pd (II) from synthetic electroless plating solutions. In the following sub-sections, the state-of-the-art has been confined to the studies carried out for Ni (II) adsorption with adsorbents such as biosorbents (section 1.6.1), activated carbon (section 1.6.2) and chelating resins (section 1.6.3).

1.6.1 Biosorbents

Low *et al*., (1995) had evaluated the performance of banana pith (*Musacea Zingiberales*) for the biosorption of copper and nickel. The copper, nickel-loading phase was carried out with a continuous aqueous stream of electroplating waste containing Cu (2.61 g/mL) and Ni (6.66 g/mL). The pH of the solution was adjusted to 4.4. The equilibrium data followed the Langmuir isotherm model with maximum capacities of 8.55 and 13.46 mg/g for Cu in electroplating waste and synthetic solution respectively. The removal efficiency for Ni (II) varied from 90.81-2.59% for initial concentrations ranging from 50-5000×10^{-6}M (0.28 – 28 mg/L).

Ferda *et al*., (2012) studied adsorption of Ni (II) ions from aqueous solution onto orange peel adsorbent. The optimal pH value for Ni (II) adsorption onto the orange peel was found to be 5.0. Adsorption data was modeled using Langmuir and Freundlich adsorption isotherms. The adsorption kinetics was found to follow pseudo-second-order rate kinetic model, with a good correlation (R^2>0.99) and intra-particle diffusion as one of the rate determining steps.

Ajmal *et al*., (2012) employed orange peel for Ni (II) removal from simulated electroplating wastewater. The adsorption followed first-order kinetics. The process was endothermic and indicated monolayer adsorption of Ni (II).It was evaluated that a maximum adsorption of 96% was provided by the orange peel adsorbent at 50 ^{o}C for an initial Ni (II) concentration of 50 mg/L and pH of 6. At these conditions, the capacity was found to be 6.01 mg/g. Desorption study was carried out with 0.05 M HCl and was found to provide a removal efficiency of 95.83% in column and 76% in batch process, respectively. The removal and recovery study was also carried out in wastewater and was found to be 89% and 93.33%, respectively.

McKay *et al*., (2008) studied upon the fitness of pseudo-second order rate equation for the kinetics data obtained during sorption of divalent metal ions onto sphagnum moss peat at different initial metal ion concentrations. It was evaluated by the authors that the removal of Ni^{+2} from the synthetic solution was maximum at a pH of 4-5. Maximum metal uptake was found to be 53.65 mg/g. Further, an adsorption capacity of 8.85 mg Ni/g was achieved at an initial Ni (II) concentration of 50 mg/L for activated carbon prepared from peat.

1.6.2 Activated Carbon

Kadirvelu *et al*., (2001) has studied the adsorption of nickel in an aqueous solution using activated carbon prepared from coir pith. Ni (II) adsorption fit well with the Langmuir and Freundlich models. The adsorption capacity evaluated from Langmuir isotherm was 62.5 mg Ni

(II)/g at initial pH of 5.0 at 30°C for the adsorbent particles within size of 250-500 μm and at an initial Ni (II) concentration of 300 mg/L. The adsorption of Ni (II) increased with pH from 2 to 7 and remained constant up to a pH of 10.

Hasar *et al*., (2003) prepared activated carbon adsorbent from almond husk. Activation was carried out with and without H_2SO_4 at different sintering temperatures. Optimal conditions for Ni (II) adsorption were pH 5.0, carbonization temperature of 700 °C, 50 min of contact time and adsorbent concentration of 5 g/L. The maximum metal uptake of 37.17 mg/g was obtained at a pH of 5.0. The removal of Ni (II) was found to be 97.8% at an initial concentration of 25 mg/L and adsorbent dosage of 5 g/L.

Lalhruaitluanga *et al*., (2011) studied on activated carbon prepared from *Melocanna baccifera* (Bamboo).Bamboo is the most abundant plant in the state of Mizoram in India. The batch mode experiments were conducted with variant adsorption parameters such as pH (2.0-7.0), adsorbent dose (0.1-0.5 g), contact time (15-360 min) and metal ion concentrations (50-300 mg/L). The maximum adsorption of Ni (II) was obtained as 9.452 and 52.91 mg/g for MBRC (*Melocanna baccifera raw charcoal)* and MBAC (*Melocanna baccifera activated charcoal)*, respectively. Zn (II) q_{max} value was 4.723 and 40.485 mg/g for MBRC and MBAC, respectively. The kinetics of adsorption followed pseudo-second-order reaction.

Namasivayam *et al*., (1995) prepared activated carbon from peanut hulls (PHC), an agricultural waste by-product. The adsorbent was used for the adsorption of Ni (II) from aqueous solution. The adsorption data fit well for both Freundlich and Langmuir adsorption isotherms. The applicability of Lagergren kinetic model has also been investigated. A metal uptake of 85 mg/g was obtained from 20 mg/L Ni (II) feed concentration and pH range of 4.0-10.

1.6.3 Chelating Resins

Senthil kumar *et al*., (2010) carried out Ni (II) adsorption studies using aqueous adsorbate solutions concentration of 500 mg/L and ceralite IR 120 cationic exchange resin (CXR) adsorbent. Batch adsorption studies indicated that maximum Ni (II) removal was at pH of 5.0. The adsorption process followed Langmuir and Freundlich adsorption isotherms. The monolayer adsorption capacity was evaluated to be 28.57 mg/g. Kinetics data confirmed the fitness of the adsorption kinetics of pseudo-second order model for the resin.

Tharanitharan *et al*., (2009) prepared modified adsorbents through the complete mixing of cross-linked phenol-formaldehyde polymeric resin (Duolite XAD-761), sodium dioctylsulfosuccinate (SDOSS) and EDTA-disodium salt (chelating agent) in an aqueous solution. Batch adsorption experiments were conducted with optimal conditions for agitation time (24 h), pH (5), adsorbent dosage (2g/L) and Ni (II) solution concentration (10-100 mg/L). Adsorption data was found to fit well with Langmuir isotherm. The Langmuir monolayer metal uptake was estimated to be 34.50 and 6.89 mg/g for samples prepared with distilled water and tap water, respectively. The adsorption kinetics of Ni (II) on modified XAD-761 resin can be best described with pseudo second order model.

Dave *et al*., (2011) studied the removal of nickel from plating wastewater using weakly basic chelating anion exchange resins such as Dowex 50x4, 50x2 and Dowex M-4195. The adsorption process with the resins indicated maximum Ni (II) removal in the pH range 4-6 for an initial nickel concentration of 5-30 mg/L and resin dosage of 25-700 mg/L. The experimental data have been analyzed using Freundlich and Langmuir isotherms. The monolayer adsorption capacities of 1.75 and 1.63 mg/g were observed for Dowex 50x4 and Dowex M-4195, respectively.

1.6.4 Process alterations

Aniruthan *et al*., (2005) prepared banana stem (*Musa paradisiacal*) biosorbent (BS) by drying the plant biomass at 100^{o}C for four days. The optimum pH range for the maximum removal of lead (II) from synthetic solutions was 5-9. At a pH of 6.0, the maximum removal efficiency of 98.5 and 89.9% was obtained for an initial Pb concentration of 10 and 25 mg/L, respectively. The surface area obtained for the adsorbent from N_2 adsorption isotherm was found to be 108.54 and 214.13 m^2/g for BS and FPBS (Formaldehyde polymerized banana stem) respectively.

Namasivayam *et al*., (2008) studied Cr (VI) adsorption using an adsorbent prepared from coconut coir pith, which is an agricultural solid waste. The adsorbent was subsequently modified with hexa- decyltrimethyl ammonium bromide cationic surfactant. The optimum pH for Cr (VI) adsorption was found to be 2.0. Further, the reduction of Cr (VI) to Cr (III) occurred insignificantly during Cr (VI) removal. Langmuir, Freundlich and Dubinin- Radushkevich (D–R) isotherms were used to model the measured adsorption equilibrium data. It was analyzed that the measured data fit well with all three isotherms. The adsorption capacity of the biosorbent was evaluated to be 76.3 mg/g at an initial concentration of Cr (VI) of 100 mg/L. The adsorbent was also tested for the removal of Cr (VI) from electroplating effluent.

Chi *et al*., (2009) reported activated carbon adsorbents which were impregnated with sodium dodecyl sulphate (SDS), sodium dodecyl benzene sulfonate (SDBS) and dioctyl sulfosuccinate sodium (DSS) anionic surfactants. The maximum Cd (II) uptake of the SDS impregnated activated carbon was 0.198 mmol/g. The maximum adsorption occurred at pH 6and was more than the maximum adsorption value evaluated for Cd (II) removal with activated carbon that was not subject to modification with surfactant. The optimum metal uptake was 0.016 mmol/g, at a

pH of 6. A separation factor value of about 1.7×10^{-3}-$4.7 \times 10^{-3}$for the Langmuir isotherm indicated that the Cd (II) adsorption by the surfactant modified biosorbent was feasible.

Lin *et al*., (2002) reported surfactant modification of clay for the adsorption of Cu^{2+} and Zn^{2+}in the concentration range of 4.5-45 mmoL. The mixture (100 mL) was shaken for 3 h and then centrifuged at 2500 rpm for 10-60 min. The Dubinin-Kanger-Radushkevichin (DKR) and Langmuir equations were used to describe the sorption isotherms of single solute systems. The sorption energy E determined in the DKR equation (-12.6 kJ/moL for Zn^{2+}, -13.8 kJ/moL for Cu^{2+}) revealed the nature of ion exchange mechanism in both systems. The sorption of metal ions on modified clay was rapid during the first 10 min and the equilibrium was attained within 2 h. The pseudo-first-order rate constants for Zn^{2+} and Cu^{2+} sorption were found to be 6.64×10^{-4} and 3.14×10^{-3} min^{-1}, respectively at 25 ^{o}C.

Oualid *et al*., (2009) reported that the leaves of olive tree (*Olea europaea*) can be used as a novel low-cost non-conventional sorbent for the removal of cadmium from aqueous solutions. The authors carried out adsorption studies with and without ultrasound. The sorption significantly increased in the presence of ultrasound. The fitness of Langmuir isotherm inferred that the monolayer sorption capacities of olive leaves were 42.19, 55.87 and 64.94 mg/g for the conventional method, the ultrasound-assisted method and the combined method, respectively. The kinetic data fit very well with the pseudo-second-order kinetic model.

1.6.5 Time dependent studies

Soumik *et al*., (2009) used live biomass of *Trichoderma harzianum* and prepared biosorbent pellets by inoculating 2g of the biomass in a flask and incubating the flasks for different time periods (4, 5, 6, 7 and 8 days). It was observed that a nickel concentration up to 60 mg/L was tolerated by the micro-organisms and the inhibition for mycelia growth was 33.3 %. A further

enhancement in nickel concentration reduced the growth and total inhibition occurred at 200 mg/L. It was observed that a pH of 4-5 and a bio-sorbent prepared with an incubation time period of 7 days provided maximum metal removal (90.2 %) and further incubation did not increase the metal uptake on the biomass.

Moonis *et al*., (2012) studied the biosorption potential of mustard oil cake (MOC) for adsorbing Ni (II) from aqueous medium. Optimum biosorption was observed at a pH of 8. Kinetics studies indicated the fitness of pseudo-second-order model. Breakthrough and exhaustive capacities for 5 mg/L initial Ni (II) concentration were 0.25 and 4.5 mg/g. These values for 10 mg/L initial Ni (II) concentrations were 4.5 and 9.5 mg/g, respectively. Batch desorption studies confirmed maximum Ni (II) recovery in acidic medium. Regeneration studies by batch and column process confirmed reutilization of biomass without appreciable loss in the biosorption process.

Helen *et al*., (2010) studied the adsorption behavior of Ni and Zn from aqueous systems onto activated carbon prepared from *Hevea brasiliensis*. Sawdust was used in batch and column mode studies under various operating conditions. The maximum adsorption capacity of Ni and Zn were found to be 17.21 and 22.03 mg/g at a concentration of 50-200 mg/L, respectively, at 30 ^{o}C. Eventually, an attempt was also made to model the data generated from column studies using Adam-Boharts model and Thomas models. The column regeneration studies were carried out for three adsorption-desorption cycles. The eluent used for the regeneration of the adsorbent was0.1 M H_2SO_4.

Vijayaraghavan *et al*., (2004) investigated the ability of crab shell to remove Ni (II) ions from aqueous solution in a packed bed up-flow column with an internal diameter of 2cm. The experiments were performed for different combinations of bed heights (15-25cm) and flow rates (5-20mL/min) to obtain experimental breakthrough curves. The eluent used for the regeneration

of sorbent was 0.01M EDTA (disodium) solution at a pH of 9.8, which was achieved using NH_4OH. The breakthrough time decreased uniformly from 28.1 to 9.5for an increase in cycle number from one to seven, whereas nickel uptake remained approximately constant throughout the seven cycles. The life-factors for crab shell in terms of critical bed length and breakthrough time for the crab shell were found to be 1.1cm/cycle and 0.17 per cycle, respectively. The elution efficiency was greater than 99.1% for all seven cycles.

Chenxi *et al*., (2009) conducted experiments to examine the effectiveness of 4.0-4.75mm crushed shells and *Sphagnum* peat moss as low-cost natural adsorbent filter materials for the removal of cadmium and nickel ions from binary aqueous solutions. The effect of column depth and flow rate on effluent metal breakthrough, metal removal and pH were investigated as a function of throughout volume (TPV). During the column testing, a flow rate of 1.5 mL/min (surface loading of 27.5cm^3/cm^2day) and bed depth of 15cm were found to be the optimum operational conditions, where 47.9% and 42.7% cadmium and nickel cumulative removals were obtained, respectively.

Nur *et al*., (2012) studied the removal of Ni (II) from synthetic wastewater using a strong acidic cation exchange resin in a fixed bed column. The experiments were conducted at different pH (3-7) and initial heavy metal concentrations (1.8, 2.8 and 3.8g Ni/L). Thomas model was found to fit well with the measured data.

Ruey *et al*., (2006) investigated the removal of Ni (II) from synthetic electroplating wastewater using a strong-acid resin in a fixed bed. Besides $NiSO_4$, water contained NH_4Cl, anionic NaH_2PO_4ligands and citrate. Batch studies confirmed that the adsorption isotherms fit well with Langmuir isotherm model. Column experiments were performed with different pH values (0.5-5.0), metal concentrations (5.1-11.9moL/m^3), volumetric flow rates (5-12cm^3/min) and bed

Table 1.4: Summary of literature data for Ni (II) (a) batch and (b) continuous adsorption characteristics for various adsorbents.

(a)

Type of adsorbent	Adsorbent name	BET surface area (m^2/g)	Type of solution	pH	Solution concentration(mg/L)	Capacity(Q_{max}) (mg/g)	Recovery or Efficiency (%)	Author
Biosorbent	Banana pith	37 – 1285	Electroplating	4.5	50-500	8.55	90.81	(Low *et al.*, 1995)
	Orange peel	-	Aqueous	5	10-200	62.89	-	(Ferda *et* al., 2012)
	Orange peel	-	Electroplating	5	50-300	6.01	96	(Ajmal *et* al., 2012)
	Peat moss	-	Aqueous	5	10-50	8.85	-	(Mckay *et* al., 2008)
Activated charcoal	Coir pith-AC	-	Aqueous	5	50-300	62.5	-	(Namasivayam *et al.*,2001)
	Coir pith-AC	-	Electroplating	5	50-300	-	92	(Namasivayam *et al.*,2001)
	Almond husk-AC	-	Aqueous	5	50-300	30.69	97.8	(Hasar *et al.*, 2003)
	Bamboo stem-AC	6.2-222.8	Aqueous	6	50-300	52.91	80	(Lalhruaitluanga *et al.*, 2011)
	Peanut hulls	-	Aqueous	6.5	30-90	53.65	-	(Namasivayam *et al.*, 1995)

Type of adsorbent	Adsorbent name	BET surface area (m^2/g)	Type of solution	pH	Solution concentration(mg/L)	Capacity(Q_{max}) (mg/g)	Recovery or Efficiency (%)	Author
Chelating Resin	Ceralike SR120	-	Aqueous	5	100-500	28.57	96.4	(Senthil kumar *et al.*,2010)
	XAD-761 and SDOSS	-	Aqueous	5	10-100	34.5 and 6.89	-	(Tharanidharan *et al.*,2009)
	Dowex 50x4 and Dowex M-4195	-	Aqueous	4-6	5-30	1.75,1.63	-	(Dave *et al.*, 2011)
Alternate methods	BS and FPBS	108.54 and 214.13	Aqueous lead	6	10-25	-	98.5 and 89.9	(Anirudhan *et al.*,2005)
	Coconut coir pith, Agricultural – cationic surfactant	-	Chromium electroplating	2	20-100	76.3	-	(Namasivayam *et al.*, 2008)
	Ac-anionic surfactant	-	Aqueous cadmium	6	-	-	-	(Chi *et al.*,2009)
	Clay–SDS surfactant	-	Aqueous cu and zn	3.3	1-5	2.54 and 2.02	-	(Lin *et al.*, 2002)
	Olive tree-sonication	-	Aqueous cadmium with sonication	-	-	55.87	-	(Oualid *et al.*, 2009)

(b)

Adsorbent	**Solution type**	**pH**	**Feed concentration (mg/L)**	**Z**	**q**	**M**	**% Adsorption**	**% Desorption**	**Capacity mg/g**	**Author**
(Trichoderma harzianum)	aqueous	3-5	50-200	-	-	-	-	90.2	-	(Soumik *et al.*, 2009)
Mustard oil cake	Aqueous	8	5-10	-	-	-	66	87.3	9.5	(Moonis *et al.*, 2012)
Ac-Hevea brasiliensis saw dust	aqueous	6	50-200	50-200 cm	5-20	-	68	57.16	43.44	(Helen *et al.*, 2010)
Crab shell	aqueous	9.8	100	15-25cm	5-20	31-51 g	62.95	99.1	23.99	(Vijayraghavan *et al.*, 2004)
Peat moss	aqueous	9.4	19.4-36.3	15-25 cm	1.5-4.5	53.3-160.3	83.8	-	-	(Chenxi *et al.*,2009)
Cation exchange resin	aqueous	3-7	1.8-3.8 g/L	-	-	-	-	-	-	(Nur *et al.*,2012)
strong-acid resin	electroplating	3	5.1-11.9 moL/m3	5-12 cm3/min	-	-	-	-	-	(Ruey *et al.*, 2006)

volumes (3.7-9.8cm^3). The evaluated breakthrough curves agreed with the measured ones (standard deviation 6%), except for the curves obtained before breakthrough time at pH values greater than 3.0. The non-zero Ni (II) concentration in the effluent at the early stage of the whole process was possibly due to the presence of anionic ligands in the adsorbent.

1.6.6 Summary

Table 1.4 presents a summary of various relevant literatures for the adsorption based Ni (II) removal from aqueous synthetic and industrial wastewater solutions and streams.

1.7 State of the art for Pd (II) removal from aqueous, synthetic and industrial wastewaters

In this section, a brief review of studies carried out for the adsorption based recovery of Pd (II) from aqueous, synthetic and industrial wastewaters is being presented. This section has been categorized for various types of adsorbents.

1.7.1 Biosorbents

Remoudaki *et al.*, (2007) studied the biosorptive palladium uptake capacities for six selected strains of microbial biomass. The authors did not address the genetic characterization, culturing conditions, biochemical (i.e. metal binding proteins, secondary metabolites) and cellular parameters (i.e. cell charge, functional groups, exo-polymers production). For biosorption experiments, the effect of pH was studied. Bio-sorption of palladium was favourable for both ionic species ($Pd(NH_3)_4^{2+}$ and Pd (II)) and for all the strains tested. It was evaluated that higher bio-sorption capacities exist for tetra ammonium palladium complexes. The maximum biosorption capacity of microbial biomass for Pd (II) was determined to be 72 mg/g at an initial palladium solution concentration of 1000 mg/L.

Sari *et al.*, (2009) has investigated the biosorption potential of *Racomitrium lanuginose* as an aquatic moss biosorbent for the removal of Pd (II) from aqueous solution. Samples were washed with deionized water and inactivated by heating in an oven at 70 ^{o}C for 48 h. The inactivated dried moss biomass was ground and sieved through different sizes and 180-300 µm sized fraction was used in all experiments. The maximum biosorption capacity of *R. Lanuginosum* for Pd (II) was determined to be 37.2 mg/g at an initial palladium solution concentration of 200 mg/L.

Zhongyu *et al.*, (2002) studied the mechanism of the interaction of microorganisms with Pd^{2+} for by *Bacillus licheniformis* RO8 biomass. When dry powder RO8 biomass (800 mg/L) was mixed with Pd^{2+} (for 45 min at 30 ^{o}C and pH 3.5), the biosorptive maximum metal uptake was 6.01 mg/g. The biosorptive interactions of Pd^{2+} with R08 biomass were also characterized with AAS, TEM, XRD and FTIR.

Park *et al.*, (2010) reported upon a new type of biosorbent that provided very good Pd metal uptake. The authors started with a waste biomass E.coli and cross linked it with polyallylamine hydrochloride (PAH). The PAH-modified biomass was investigated for the removal and recovery of Pd (II), in the chloro-complex Pd (II) from aqueous solution. It has been evaluated that the adsorption performance of *E. coli biomass* was significantly enhanced after surface modification with PAH. At a pH of 3, the maximum Pd (II) uptake of PAH-modified biomass was 265.3 mg/g. For the raw *E. coli biomass*, the Pd (II) uptake was significantly low (141.1 mg/g).

1.7.2 Activated Carbon

Sharififard *et al*., (2012) studied the adsorptive performance of commercial activated carbon for palladium and platinum removal from aqueous solutions. The authors reported that the optimum

operating conditions for palladium and platinum removal with activated carbon were pH of 2, 0.21 mm of particle size of adsorbent and adsorbent dosage of 10 g/L. Under these optimum operating conditions, more than 98% of palladium and platinum were removed by activated carbon in 3 h. The equilibrium adsorption data were well described by Langmuir and Freundlich models. For an initial Pd (II) concentration of 300 mg/L, commercial activated carbon provided palladium and platinum adsorption capacity of 35.7 and 45.5 mg/g, respectively. The adsorption kinetics of palladium and platinum on these adsorbents was analyzed to fit well with pseudo-second-order model.

Kasani *et al*., (2000) carried out batch adsorption tests to separate Pd (II), Rh (III) and Ru (III) from chloride aqueous media using commercial activated carbon pellets (0.8 SUPRA, Norit). The activated carbon pellets exhibited a strong affinity for Pd (II) with wide HCl concentration range (0.005-2.0 M). Also, it was easy to remove Pd (II) from a ternary solution (1.5-2.0 M HCl) containing equal metal concentrations (120 mg/ L) using 0.2-0.3 g of dry carbon. It was found that the adsorption of Rh (III) and Ru (III) occurred simultaneously within a narrow solution pH range (2.3-2.6). However, the overall adsorption rate of Rh (III) was threefold higher than that of Ru (III). At an initial solution concentration of 20 mg/L, the adsorption capacities of Pd (II), Rh (III), and Ru (III) in single-component solutions were evaluated to be 27, 15, and 4 mg/g, respectively. Also, it was inferred that noble metal adsorption enhanced with solution pH up to 8.8 and was reversible at high HCl concentration. Except for Ru (III), the adsorption data for all other metals fit well with the Langmuir isotherms.

1.7.3 Chelating Resins

Fujiwara *et al*., (2007) prepared L-lysine cross-linked chitosan biosorbent resin. To do so, the authors started with 6 g of chitosan resin and added 50 mL of glycoxylic acid solution, E-Pure

(EP) water and stirred the contents at 160 rpm for 24 h at 25 ^{o}C. Eventually, the solid product was filtered and washed with methanol and EP water (1:1). The characterization of the adsorbent was carried out using FTIR spectra of CCR and LMCCR. It was observed that the adsorbent had good selectivity towards metal adsorption for Pt (IV), Pd (II) and Au (III) and this was confirmed by the spectral shift at a 3420 cm^{-1}.

Wang *et al*., (2010) describes the preparation of a chelating resin from chemically modified chitosan. The resin was synthesized by using O-carboxymethylated chitosan to cross-link a polymeric Schiff's base of thiourea/glutaraldehyde and was characterized by IR. The maximum uptake of Ag (I) was 3.77-mmol/g at a pH of 4.0 and silver solution concentration of 20 mg/L.

Table 1.5: Pd (II) adsorption characteristics of commercial ion exchange resins.

Name of adsorbent	Type of solution	Cost of the resin/100 g (₹)	Solution concentration	pH	Adsorption capacity (mg/g)	Reference
Lewatit TP 214	Acidic Solution	3653	100mg/L	8	10.57	Zbigniew *et al*., (2009)
Amberlyst A 21	Acidic Solution	1550	100 µg/cm^3	8	9.81	Hubucki *et al*., (2009)
Dowex MSA 1	Acidic Solution	2552	50 mg/dm^3	8	8.8-9.7	Wolowicz *et al*., (2009)
Amberlite IRA 458	Acidic Solution	5800	100 mg/dm^3	8	7.8	Wolowicz *et al*., (2009)
Lewatit monoplus TP-220	Acidic solution	4800	50 mg/dm^3	4.5	9.95	Wolowicz *et al*., (2009)
MFT chelating resin	Aqueous solution	9587	50-100 mg/L	4	15.29	Birinci *et al*., (2009)

*Cost has been taken from Sigma Aldrich Corporation

The results also indicated that the adsorption process was exothermic and fit well with the pseudo-second-order kinetic model. The Ag (I) desorption was evaluated to be about 99.23% using 0.5M thiourea-2.0M HCl solution.

Chassary *et al*., (2005) studied thiourea modified chitosan for adsorption of Pd and Pt from aqueous solutions. Metal desorption was studied using 5 M HCL and NH_4OH. It was observed that the desorption efficiency of palladium was greater than that platinum. While HCl removed 55% Pd for the resin, NH_4OH provided 80% removal. Platinum recovery was more than 70%.

The overall summary of various commercial ion-exchange and developed resins are shown in Table 1.5.

1.7.4 Time dependent studies

Snyders *et al*., (2013) investigated the recovery of platinum group metals (PGMs) from a dilute cyanide leach solution containing base metals. The leach solution is used for gold extraction in a typical CIP process. The authors focused on both adsorption and elution stages. Adsorption tests were performed on an alkaline leach solution (0.15 ppm Pt, 0.38 ppm Pd and 0.1 ppm Au) obtained from cyanide extraction process. For activated carbon adsorbent, the initial adsorption rates of platinum, palladium, and gold were very fast and recoveries of these three metals were 100%, 97.4%, and 99.9% respectively after 72 h. Platinum and palladium elution from activated carbon almost reached completion in 4 to 5 bed volumes at 80 ^{o}C. However, the elution of gold at the temperature was slow, with a significant amount of gold still left to be eluted after 16 bed volumes.

Wolowicz *et al*., (2009) studied the applicability of weakly basic anion (WBA) exchange resins for Pd (II) removal from acidic solutions. Pd (II) adsorption data was obtained for Amberlite IRA-92, Amberlite IRA-95, Amberlite IRA-96, Dowex 66, Varion ADAM and Lewatit MP-62

and was compared with that obtained for Amberlyst A-23, Amberlyst A-24, Dowex WGR-2 and Amberlyst A-21. The sorption capacity was as high as 121.48 mg/g for varion ADAM resin. Pd (II) adsorption studies with fixed-bed columns also confirmed the greater affinity of varion ADAM for Pd (II) than other weakly basic anion exchangers. The kinetics of Pd (II) with ADAM were well described with pseudo-second order model.

Wolowicz *et al*., (2009) studied the use of strongly basic anion exchange resins. Type 1 resins such as Lewatit MP-500 and Lewatit MP-500A were evaluation for the adsorption of palladium (II) complexes working anion exchange capacities for Lewatit MP-500 (0.029g/cm^3; 0.028g/cm^3) and for Lewatit MP-500A (0.028g/cm^3; 0.027g/cm^3) using 1.0M NaCl and 0.1M HCl–1.0M NaCl solutions, respectively. Lewatit MP-500 possessed slightly higher values of capacities, and therefore is insignificantly more efficient in the adsorption process of palladium (II) ions than Lewatit MP-500A. The equilibrium adsorption capacities varied in the range of 8.84-9.99 and 8.40-9.38mg/g respectively for Lewatit MP-500 and between 8.12-9.57 and 7.268.85mg/g respectively for Lewatit MP-500Afor 0.1M HCl-1.0 M NaCl and 0.1 M HCl-2.0 M NaCl solutions, respectively.

Zbigniew *et al*., (2009) studied two types of ion exchange resins such as chelating (Lewatit TP 214, Purolite S 920) and cationic (Chelite S, Duolite GT 73) ion exchangers were used for the recovery of Pd (II) complexes from chloride media (0.1-2.0M HCl-1.0M NaCl-0.0011 M Pd (II); 0.1-2.0M HCl-2.0M NaCl-0.0011M Pd (II)). The authors studied upon influence of concentration of HCl, NaCl as well as the phase contact time on the degree of recovery of Pd (II) complexes.

Hubucki *et al*., (2009) studied two anion exchange resins-strongly basic Amberlyst A 29 and weakly basic Amberlyst A 21for Pd (II) adsorption. These resins were used for the adsorption of

palladium (II) complexes from HCl-NaCl solutions over a range of acid concentrations (0.1-2.0M) in 1.0 and 2.0M NaCl using static and dynamic methods. The breakthrough curves of Pd (II) were used to calculate the ion exchange capacity, weight and bed distribution coefficients. It was inferred that Amberlyst A21 is more promising for the adsorption of Pd (II) chloro-complexes from acidic chloride solutions than Amberlyst A29.

Yu *et al.,* (2002) has carried out biosorption studies using TCF for Pt, Pd and Hg. The adsorption conditions, adsorption flow rates, saturation adsorption quantities, desorption conditions and interfering factors along with methods for their elimination were focused. The saturation adsorption quantities of various heavy metal ions were evaluated in the concentration range of 10-70 mg/g. Except for As and Se, the solution flow rate with 0.1 g of TCF in a column is 10-30 mL/min. It was evaluated that the noble metal recovery is about 85 % for all natural water based samples and all 19 trace elements have been successfully separated in these samples.

The possibility of adsorbent regeneration (desorption) and metal recovery was primarily studied based on the general assumption that regeneration of adsorbent is directly linked to the economics of the process. Sudha and Abraham (2012) have inferred that solutions of alkali highly alkaline salts (NaOH, $NaHCO_3$ and Na_2CO_3) were better eluting agents than acids or mineral salts for heavy metal desorption from immobilized fungal biomass. Chassary *et al.*, (2005) concluded that Pd (II) can be loaded sorbents using HCl and NH_4OH. About, 50-70% of Pd (II) recovered from this process.

1.7.5 Composite Adsorbents

Chantaraporn *et al*., (2012) developed a novel bio-based adsorbent for CO_2 adsorption. Palm shell based activated carbon was immersed in agitated aqueous chitosan solutions in the concentration range of 0.1-2 g/L. A series of chitosan impregnated activated carbon adsorbents were there by achieved in which chitosan varied from 0.12-0.98%. The chitosan impregnated activated carbon prepared with 0.1 g/L chitosan solution yielded 0.12% chitosan-AC adsorbent and was the optimal for CO_2/H_2 separation. For CO_2/CH_4 separation, the chitosan-AC adsorbent prepared with 2 g/L chitosan solution (0.76% chitosan) was the optimal adsorbent.

Sharififard *et al*., (2012) studied bio-polymer modified commercial activated carbon adsorbent (BPMC) for the adsorption of palladium and platinum from aqueous solutions. The Taguchi approach was adopted for the design of experiments. In the modification process, it was observed that BET surface area reduced from (AC) 922.33 to (BPMC) 362.3 m^2/g. The authors inferred that the optimum operating conditions for palladium and platinum removal were pH of 2, particle size of 0.21 mm and adsorbent dosage 10 of g/L. Under these optimum operating conditions, more than 98% of palladium and platinum were removed by activated carbon in 3 h. The equilibrium adsorption data were well described by the Langmuir and Freundlich models. The commercial activated carbon had the palladium and platinum adsorption capacity of 43.48 and 52.63 mg/g of palladium and platinum, respectively. Adsorption kinetics of palladium and platinum on these adsorbents could be well analyzed with pseudo-second-order model.

Morisada *et al.*, (2011) prepared chemically treated tannin gel (TG) as biosorbent. For this purpose, the authors dissolved 28 g of wattle tannin powder in 45mL of 0.25M NaOH solution at

Table 1.6: Summary of literature data for Pd (II) (a) batch and (b) continuous adsorption characteristics for various adsorbents.

(a)

Type of adsorbent	Adsorbent name	BET surface area (m^2/g)	Type of solution	pH	Solution concentration(mg/L)	Capacity(Q_{max}) (mg/g)	Recovery or Efficiency (%)	Author
Biosorbent	Microbial biomass	-	Acid and base	3 and 8	100-1000	72	-	(Remoudaki *et al.*, 2007)
	Racomitrium lanuginose	-	Aqueous	5	25-200	37.2	98	(Sari *et al.*, 2009)
	Bacillus licheniformis RO8 biomass	-	Electroplating	3.5	116.5-800	6.01	-	(Zhongyu *et al.*,2002)
	E.coli	-	Aqueous	3	10-50	265.3 and 145	-	(Park *et al.*, 2010)
Activated charcoal	AC	922	Aqueous	2	50-300	35.7	98	(Sharififard *et al.*, 2012)
	Carbon pellts	951	Chloride solution	2.3-2.6	20-120	27.6	-	(kasani *et al.*, 2000)
Chelating Resin	L-lysine cross-linked chitosan resin	82.4	Aqueous	2	100-400	70.34	75.6	(Fujiwara *et al.*,2007)
	Thiourea	-	Aqueous	2	-	3.73mmol/g	95% Ag	(Wang *et al.*, 2010)
	Thiourea	192	Aqueous	2	48.8	-	-	(Ma *et al.*, 2006)
	Thiourea modified chitosan	-	Aqueous	2	50-200		55 and 80.2	(Chassary *et al.*, 2005)

Alternate methods	BPAC	362	Aqueous	2	50-300	43.6 and 53.5	98	(Sharififard *et al.*, 2012)
	$CHAC\text{-}CO_2$	-	Gas mixture	10.1	20-100	0.1-2	-	(Chantaraporn *et al.*, 2012)
	tannin gel (TG)	-	Aqueous	8.8	50-200	11.4	-	(Morisada*et al.*, 2011)

(b)

Adsorbent	**Solution type**	**pH**	**Feed concentration (mg/L)**	**Z (Bed length) (cm)**	**Q (Flow rate) (mL/min)**	**M (Weight of adsorbent) (g)**	**% Adsorption**	**% Desorption**	**Capacity mg/g**	**Author**
AC	Leaching solution	10	38	-	-	-	-	97.4 and 99.9	-	(Synders *et al.*, 2013)
WBA	Chloride solution	2	100-2000	-	-	-	-	-	121.7	(Wolowicz *et al.*, 2009)
Lewatit MP-500 and Lewatit MP-500A	aqueous	2	0.1-1	-	-	-	-	-	8.12-9.17	(Wolowicz *et al.*, 2009)
Chelating resins	Chloride solutions	2	0.1-2	-	-	-	-	-	-	(Zbigniew *et al.*, 2009)
Anion exchange resin	Chloride solutions	-	0.1-6	-	-	-	-	-	-	(Hubucki *et al.*, 2009)
TCF	aqueous	-	10-70	-	10-30	-	-	85	-	(Yu *et al.*, 2002)

room temperature. Eventually, 6 mL of 37 wt % formaldehyde solution was successively added as a cross-linker. After gelation at 353 K for 12 h, the gel obtained was ground into small particles and sieved by screens with mesh sizes of 125 and 250 μm. To confirm the amine modification of the TG by the ammonia treatment, solid-state CP-MAS 13C NMR spectra of the tannin molecule (TM), the TG, and the ATG (Ammonia treated Tanning gel) were obtained. The macro porous ATG with the three-dimensional gel network has 60-70 wt % of water content on a wet basis and resulted in a high adsorption capacity and low intra particle mass transfer resistance.

1.7.6 Summary

Table 1.6 (a) and (b) respectively summarize the Pd (II) batch and continuous adsorption characteristics of various adsorbents and adsorbate studied till date.

1.8 Possible scope for further research

A detailed literature review presented in the previous section indicates upon the possible scope for further research in the following sub-sections.

1.8.1 Preparation and characterization of biosorbents using dead biomass from the North-eastern region of India for Ni (II) adsorption

Strict environmental legislations coupled with wider and large scale integrated chemical processing necessitate the development of low cost technologies for wastewater treatment. Typical permissible limit for Ni in water and wastewaters is about 0.01-0.1 mg/L and 1-3 mg/L (Senthil kumar *et al.,* 2009; WHO- 1982). Several technologies suggested for the removal of Ni (II) from wastewater streams include adsorption, chemical precipitation, electrochemical reduction, sulphide precipitation, cementation, ion-exchange, reverse osmosis, electro dialysis, solvent extraction and evaporation (Anand kumar and Mandal, 2009; Lalhruaitluanga *et al*.,

2011). Amongst these alternatives, adsorption using conventional and novel adsorbents is an attractive option for large scale Ni (II) removal from wastewater streams because of its cost, design simplicity and ability to offer wide range of choice for selecting an adsorbent with superior combinations of metal uptake and removal efficiency.

Early research in the development of adsorption technology involved studies related to activated carbon/charcoal adsorbent due to its superior adsorbent characteristics for heavy metal removal from aqueous solutions and wastewater streams. Recently, the development, engineering and deployment of functional adsorbents from non-living biomass towards Ni (II) removal from aqueous solutions have received significant attention. These refer to adsorbents developed using bale tree leaf (Senthil kumar *et al*., 2009), Melocanna baccifera (Lalhruaitluanga *et al*., 2011), bamboo charcoal (Li *et al*., 2008), pineapple stem (Hameed *et al*., 2009), pineapple crown leaves (Tran *et al*., 2006), bagasse fly ash (Gupta *et al*., 2003), citrus reticulate fruit peel (Ajmal *et al*., 2000), chlorella sorokiniana (Akthar*et al*., 2004), wheat straw (Doan *et al*., 2008), fabric histosal (Covelo *et al*., 2008), turkish fly ashes (Bayat, 2002), pine bark and blast furnace (Nehrenheim and Gustafsson, 2008), black gram husk (Saeed *et al*., 2005), modified jute fibres (Shukla and Pai, 2005), palm fruit bunch (Nassar, 1997), rice husk (Low and Lee, 1997), hazel nut shell (Kobya, 2004), coconut shell (Sekar*et al*., 2004), peats (Brown *et al*., 2000), coir pith (Kadirvelu *et al*., 2001), granular activated carbon (Kinhikar, 2012; Paola *et al*., 2011), walnut shell (Wang *et al*., 2010), odinawodier bark carbon (Vijayakumaran and Srivoli, 2011) and tannic acid immobilized activated carbon (Uer *et al*., 2006). Till date, adsorption studies for Ni (II) removal from aqueous solutions reported variant feed concentrations (50-300 mg/L), adsorbent dosages (1-30 g/L) and pH (2-10), to achieve good combinations of adsorbent metal uptake and removal efficiencies ranging from 0.683 to 124.85 mg/g and 52.74-96.8%

respectively. Amongst these adsorbents, the susceptibility of various adsorbents to withstand stringent environmental conditions and possess extended shelf life is of primary concern and activated carbon is one of the several promising options of adsorbents that can be used for industrial applications, as it has been proven to have a good shelf life and durability for wastewater treatment applications.

Thus, the preparation, characterization and application of activated charcoal adsorbents from dead biomass resources is an important area of research. Amongst several dead bio-mass resources, bamboo and pineapple stem are few amongst the world's best known natural resources for the development of activated charcoal adsorbents. These resources are available abundantly in South Asian countries. In India, bamboo forests account for 45% of world's bamboo reserves and contribute towards maintaining the ecological balance and socio-economic sustainability. Similarly, pineapple is cultivated throughout north-eastern India and possesses higher degree of cellulosic content (70-80%). Till date, only two literatures addressed adsorbent preparation and characterization from bamboo sources towards Ni (II) removal from aqueous solutions. Lalhruaitluanga *et al*., (2011) reported the development of *melcoanna baccifera* (bamboo) based charcoal for the removal of Ni (II) and Zn (II) from aqueous solutions. KOH treatment has been carried out by the authors to enhance the surface area of the charcoal from 6.26 to 222.81 m^2/g. The maximum adsorption of Ni (II) from aqueous solutions was about 9.452 and 52.91 mg/g for raw and activated charcoal with the kinetics of adsorption following pseudo-second order reaction. Li *et al*., (2008) reported the adsorption of Ni (II) on bamboo based charcoal and indicated that the optimal adsorbent dosage, pH and equilibrium time have been 30 g/L, 7 and 180 minutes respectively. Further details with respect to the adsorbent characterization parameters are not available.

Thus, the specific research involving the development of good quality activated charcoal adsorbents from bamboo stem and pineapple stem resources and their subsequent application for heavy metal ion removal from aqueous solutions/wastewater solutions received little attention till date and should be the concerned attention of this thesis. Even for comparative purposes, it can be observed that the maximum adsorption capacity of bamboo based activated charcoal reported by Lalhruaitluanga *et al*. (2011) is 52.91 mg/g, which is very low. Thus, this work needs to address efficient fabrication techniques to achieve good quality bamboo stem based activated charcoal adsorbents which can provide adsorption capacities higher than those reported in the literature. Also, the adsorption characteristics of native biosorbents prepared from pineapple stem have also not been investigated and are targeted in this work. A further objective of this work is to compare and contrast Ni (II) adsorption from aqueous and electroless plating solutions. The long term goal of the research carried out is to envisage the potential of bamboo/pineapple stem based adsorbents for application towards the removal and recovery of Pd (II) from aqueous and synthetic wastewater electroless plating solutions.

1.8.2 Adsorption of Pd (II) from synthetic electroless plating solutions using commercial and laboratory fabricated activated carbon

There is good scope for further research in the area of Pd (II) adsorption from synthetic ELP solutions with commercial and laboratory fabricated activated carbon. Details for the scope of further research have been elaborated in two sub-sections that are presented as follows:

1.8.2.1 Preparation and characterization of laboratory fabricated activated carbon for Pd (II) adsorption from synthetic electroless plating solutions

Metallurgical and metal finishing industries produce wastewaters with heavy metal and noble metals. Today, there is increasing demand for the recovery and reuse of noble metals from

wastewater streams due to stringent environmental legislations and the high cost of the noble metals. As per OSHA-1982, for Pd, the permissible exposure limit is about 5 mg/L due to several health hazards such as skin and eye irritation (Kielhorn *et al*., 2002; Wu *et al*., 1999). Therefore, competent technologies need to be identified that can economically recover and reuse noble metals from industrial waste streams (Hsieh *et al*., 2000).

Conventional methods for the separation, pre-concentration and recovery of palladium and other PGM metals are solvent-extraction (Mizuta *et al*., 2004, Cashton and Sercombe, 1961), co-precipitation (Ramesh *et al.*, 2008), electro-deposition, chlorination (Zhou *et al*., 2009), leaching, cyanidation (Snyder's *et al*., 2013), cloud point extraction (Saria *et al*., 2009), ion-exchange (Wang *et al*., 2010), and adsorption process (Woinska and Godlewska, 2011). Amongst these, sorption processes (both adsorption and ion-exchange) have been widely investigated for their ability to recover PGMs from dilute acidic solutions. When compared to other conventional methods, adsorption has less harmful environmental effects and is more economical because of its low cost, availability, profitability, ease of operation and high removal efficiency (Shafaghat *et al*., 2011; Awoyale *et al*., 2013). The recovery of noble metals using adsorbents is also an attractive option due to their utility as viable products in industrial processing schemes (Hsieh *et al*., 2000, Mizuta *et al*., 2004). For instance, Pd impregnated activated carbon is a well-known catalyst for hydrogenation reactions in petrochemical and pharmaceutical industries (Cashton and Sercombe, 1961).

Amongst various adsorbents, activated charcoal adsorbent offers several advantages. Firstly, it can be easily fabricated from abundant natural resources. Secondly, wider variations in its physical structure, purity, content of trace elements, complexity in pore structure, specific surface area can be targeted. Thirdly, activated carbon possesses good chemical stability due to

oxygen containing functional groups on the surface, which ensure maximum shelf life. With such variegated features, activated carbon has been widely used for water and wastewater treatment and gas filtration/separation.

In the literature, mature procedures and methodologies that target the preparation of high quality activated carbon adsorbent from agricultural waste and dead bio-mass (Shafaghat *et al.*, 2011) have been described. Traditional methods include chemical activation, physical activation, steam activation, oxidation and a combination of physical and chemical activation processes (Awoyale *et al*., 2013; Dhiraj *et al*., 2008). Various chemicals used for the activation of waste and dead bio-mass include H_2SO_4 (Sun *et al*., 2011), NaOH (Fan *et al*., 2010), and H_3PO_4 (McKay *et al*., 2008). Amongst these, H_3PO_4 based activation is highly promising due to its ability to swell and open the surface structure, stabilize the adsorbent during activation, filling the cavities of the cellulosic structure and easier evaporation from cavities at the carbonization temperature. Also, it has been mentioned that phosphoric acid treatment facilitates the formation of phosphate linkages. There by, the formation of phosphate and polyphosphate esters favours the cross linking of biopolymer structures, which can be subjected to further treatment steps (Jagtoyen *et al*., 1998).

Amongst various dead biomass resources, bamboo waste is an important source for the preparation of high quality activated carbon adsorbents. Few literatures elaborated upon the achievement of high quality activated carbon from dead biomass resources using phosphoric acid based activation. Using a bamboo to acid ratio of 1:5 and a sintering temperature of 600 ^oC, Hosokawa and Minamide (1991) achieved AC adsorbent with a BET surface area of 900 m^2/g. McKay *et al*. (2008) achieved very high quality activated charcoal using a bamboo: acid ratio of 1:5 in flowing N_2 gas at sintering temperatures of 600-900 ^oC. The AC adsorbent prepared by the

authors possessed a BET surface area of 2123 m^2/g which is the maximum value reported till date in the literature. Taking these aspects into consideration, it is important to understand how good quality activated carbon adsorbent can be prepared with the most competent waste biomass source in the north eastern region of India.

Prior to carrying out experimental investigations in this work, commercial activated carbon had been procured whose BET surface area is about 1057.7 m^2/g. Considering the commercial activated carbon (Merk India Limited) adsorbent as a reference case, there is enough scope for research to be addressed in this thesis. Firstly, it is envisaged to target the preparation of good quality activated charcoal from bamboo waste with BET surface area comparable to that of the commercial activated carbon. Secondly, the prepared activated charcoal adsorbent from most competent waste biomass from north eastern region needs to be investigated for the Pd (II) adsorption characteristics using synthetic electroless plating solutions. These solutions are characterized to offer more complex chemistry with additional constituents such as stabilizer (Na_2EDTA), liquor ammonia and cationic surfactant CTAB (optional). Specific novelty issues that are of relevance are presented as follows:

a) The literature utilized H_3PO_4 in the ratio of 1:5 and is intended to further reduce the total amount of acid utilized to prepare high quality AC. The effect of the variation in biomass acid ratio has not been investigated and could provide further insights towards the preparation of inexpensive AC.

b) Literature confines to Pd (II) adsorption characteristics using Pd aqueous solutions for commercial activated charcoal (Sharififard *et al*., 2012), and there is a need to further the understanding towards Pd (II) adsorption characteristics from spent or synthetic electroless and electroplating solutions. The synthetic electroless plating solutions

considered in this work constitute Na_2EDTA stabilizer, liquor ammonia and an optional CTAB surfactant which complicate the Pd (II) adsorption characteristics in comparison to that reported for Pd (II) aqueous solutions.

c) A comparative assessment of sonication assisted adsorption and agitation assisted adsorption has not been reported till date for Pd (II) adsorption characteristics. Such a study could be important from the perspective of minimizing contact time required to achieve mass transfer equilibrium. Thus, experimental investigations need to as well addresses sonication assisted adsorption in addition to agitation assisted adsorption.

In summary, the Pd (II) adsorption characteristics on activated carbon derived from plant waste biomass has not been investigated till date from synthetic electroless plating solutions.

1.8.2.2 Pd (II) adsorption from synthetic electroless plating solutions using commercial activated carbon adsorbent

Till date, simple and inexpensive adsorbents such as activated carbons and modified activated charcoal with polymer (Sharififard *et al*., 2012), carbon pellets (Kasaini *et al*., 2000), cross-linked chitosan resin (Fujiwara *et al*., 2007), tannin gel (Morisada *et al*., 2011) racomitrium lanuginosum (Saria *et al*., 2009), bayberry tannin immobilized collagen fibre (BTICF) (Ma *et al*., 2006), carbonaceous adsorbents (Foersterling *et al*., 1990), aminated lignin derivatives (Parajuli *et al*., 2006), anion exchange resins and activated carbon (Kononova *et al*., 2007), thiourea-modified chitosan microspheres (Zhou *et al*., 2009) have been studied for the Pd (II) adsorption using aqueous solutions. For several cases corresponding to waste stream complexity, complex resin adsorbent such as amberlite (Park *et al*., 2000) has been evaluated. Amongst these adsorbents, activated charcoal appears to be highly efficient towards the palladium recovery

from waste streams with relatively lesser complexity in terms of the chemical constituents in the stream.

In a unique study, few authors inferred that commercial activated charcoal provided adsorption capacity of 35.7 and 45.5 mg/g for Pd and Pt respectively with aqueous Pd (II) solutions (300 mg/L) (Sharififard *et al.*, 2012). Corresponding removal efficiency for both the metals was reported to be 98 % respectively. The equilibrium adsorption data were well described by the Langmuir and Freundlich models and the adsorption kinetics of Pd and Pt followed by pseudo second order model.

Thus, the literature indicates towards the lack of studies with synthetic/industrial metal finishing industry effluent streams and therefore there is a need to address Pd (II) adsorption on commercial activated carbon for such solutions where solution chemistry and pH are anticipated to significantly influence adsorption characteristics in terms of capacity and % removal. The literature also does not also outline upon the role of ultrasound as a mass transfer enhancement technique to supplement the adsorption of precious metals.

Hence, the combinatorial role of stabilizer, liquor ammonia and surfactants to influence the adsorption characteristics of palladium over commercial activated charcoal has not received any attention and shall be the objective of the present work. Another objective of this work shall be to evaluate the potential of ultrasound assisted adsorption for Pd recovery from electroless plating solutions. Thereby, it is intended to compare the performance characteristics of commercial and laboratory fabricated activated carbon for Pd (II) adsorption from synthetic electroless plating solutions.

1.8.3 Adsorption of Pd (II) from aqueous and synthetic solutions using activated carbon packed beds

Activated carbon adsorbent has several advantages to effectively recover and reuse Pd (II) from metal finishing industry wastewaters. A critical insight into the literature indicates that time dependent adsorption studies using adsorbent packed beds are important to outline upon the possibility of industrial scale processing. While several studies have been addressed for Ni (II) adsorption using activated carbon columns, there are no literatures with respect to the Pd (II) adsorption using activated carbon, even from aqueous solutions. Therefore, it is important to consider the time dependent Pd (II) adsorption studies using activated charcoal packed columns for both aqueous and synthetic electroless plating solutions. Such studies will be helpful to provide reference data for furthering the research in the field of relevant biosorbents and chelating resins that may have better adsorption capacity and removal efficiency in comparison with the activated charcoal adsorbent. Also, time desorption studies are equally important to consider, given the fact that the recovery and reuse of adsorbed Pd (II) is a strong function of the time dependent desorption characteristics. In addition, relevant modeling efforts also need to be considered to identify the fitness of the most competent model to represent the time dependent Pd (II) adsorption from aqueous and synthetic electroless plating solutions. Further, the study will also provide insight with respect to the role of solution chemistry in influencing Pd (II) adsorption and desorption characteristics.

1.8.4 Preparation, Characterization and Pd (II) adsorption from synthetic electroless plating solutions using chitosan-AC composite adsorbents

In the past two decades, many researchers have studied various adsorbents such as activated carbon, clays, metal oxides, silica and zeolite for the removal and recovery of heavy and precious

metals. Amongst these, activated charcoal has been extensively studied due to its high adsorption capacity, high adsorption rate, porous structure, large internal surface area and good resistance to abrasion. AC has been proven to be capable to adsorb wide varieties of undesired species from gaseous or liquid phase systems. On the other hand, research in the field of Pd (II) adsorption and recovery from aqueous and synthetic wastewater solutions has led to the development of various synthetic chelating ion-exchange resins (Sharififard *et al*., 2012). In general, anion-exchange resins have been studied for the removal of Pd, Pt and Rh from their chloride containing aqueous solutions. However, research investigations have not been directed towards evaluating Pd (II) adsorption characteristics from synthetic and real industrial wastewater streams such as electroplating wastewaters, metal finishing wastewaters etc.,

As an alternative to expensive synthetic chelating resins, bio-adsorption using biopolymers have been suggested due to the abundance and low cost of these resources. Very recently, biopolymer impregnated and cross-linked adsorbents on AC have been studied. This is due to the greater enhancement in adsorbent performance for a fractional increase in the adsorbent cost. Among several polymers, chitosan is the preferred bio-polymer due to its wider availability in nature and lower cost in comparison with synthetic chelating polymers (Kasaini *et al*., 2000; Xiong *et al*., 2009; Garcia *et al*., 2008; Chand and Goyal, 2005).

Typically, chitosan bio-polymer is extracted from crustacean shells or from fungal biomass. Thus, chitosan is freely available in the environment and is only next to cellulose in terms of abundance in nature. Besides this, chitosan has high porosity and exhibits excellent binding properties for heavy and precious metals. Due to this reason, chitosan has been deployed in water purification plants to remove oil, grease, heavy metals (such as Cd, Cu, Pb, Hg and Cr) and turbidity caused by fine particulate matter in wastewater streams (Hsieh *et al*., 2000). Chitosan is

a renewable bio-polymer and hence a promising ingredient for green engineering and technology. Other features of chitosan include low cost, polymeric structure, non-toxicity to environment and human beings. Chitosan has a striking feature of providing no side effects or allergy even after implantation on the human body.

The hydroxyl and amine functional groups of chitosan enable stronger binding with the metal ions through various mechanisms. These include chelation (chemical interactions) and electrostatic interactions by the formation of ion pair or ion exchange. These interactions are also dependent upon the metal type, chemical constituents of the interacting medium and pH of the solution. Chitosan and its derivatives have been studied for both heavy and precious metal removal in the form of raw chitosan, cross-linked chitosan with synthetic polymeric structures, chitosan beads, impregnated chitosan activated carbon composites, cross-linked chitosan–AC adsorbents etc., Also, existing literature have focussed towards aqueous solutions whose chemical constitution is simpler in comparison with the real industrial wastewater streams where solution chemistry is bound to be complex.

Two important studies in the literature have elaborated upon the preparation of chitosan–AC adsorbents. These refer to impregnation method (Chantaraporn *et al*., 2012) and cross-linking methods (Sharififard *et al*., 2012). For impregnated chitosan AC adsorbents, BET surface area has been reported to have lower than that of the activated carbon Chantaraporn *et al*., (2012). This was not the case for chitosan cross linked AC adsorbents. However, despite having lower BET surface area than AC, the impregnated chitosan-AC adsorbents were able to provide better separation of binary $CO_2/CH_4$and CO_2/CH_2 gas mixtures than those obtained with AC (Chantaraporn *et al*., 2012). However, the same has not been studied for Pd (II) adsorption from aqueous electroplating adsorbates.

While the impregnated chitosan-AC adsorbent performed well for CO_2 adsorption, the efficacy of cross-linked chitosan-AC adsorbent has been reported for aqueous Pd solutions within the feed concentration range of 40-300 mg/L. Thus, research needs to emphasize upon the relevance of chitosan–AC adsorbents for the Pd (II) recovery and reuse from synthetic electroless plating solutions whose composition is similar to real electroless plating solutions. No data has been provided for synthetic ELP solutions for both classes of composite biosorbents. No data is available even for Pd (II) adsorption from aqueous solutions using chitosan impregnated adsorbents. All these are relevant areas of research that can be addressed in this thesis.

1.9 Objectives of the Thesis

Based on the identified scope for further research, the broad objectives of the thesis have been outlined as follows:

- Preparation and characterization of adsorbents from plant stem wastes.
- Adsorption characteristics of plant waste based adsorbents for Ni (II) adsorption from aqueous solutions.
- Ni (II) adsorption studies with synthetic ELP solutions.
- Batch adsorption of Pd (II) from synthetic electroless plating solutions using laboratory fabricated and commercial activated carbon adsorbents.
- Column studies for Pd (II) adsorption from aqueous and synthetic electroless plating solutions using commercial AC adsorbent.
- Preparation, characterization and Pd (II) adsorption characteristics of AC-chitosan composite adsorbents using synthetic ELP solutions.

1.10 Organization of the Thesis

From the detailed discussion presented in section 1.8, it is apparent that there is significant scope for further research in the field of adsorption based Pd (II) recovery. While the objectives of the thesis presented in the earlier section have briefly summarized various important tasks that need to be addressed, this section presents a brief summary of the thesis. The thesis has been organized in seven additional chapters.

Chapter 2 details upon the experimental and modeling approaches involved throughout the thesis. These include a) preparation and characterization of plant biomass waste based biosorbents b) batch adsorption of Ni (II) on plant based biosorbents followed with modeling approaches to represent evaluated adsorption characteristics c) preparation and characterization of activated carbon adsorbent using the most competent plant waste biomass d) batch adsorption of Pd (II) from synthetic electroless plating solutions with commercial and laboratory fabricated activated carbon adsorbent e) Time dependent Pd (II) adsorption on commercial activated carbon packed bed with synthetic electroless plating solutions and f) Preparation and characterization of chitosan-AC composite adsorbents for Pd (II) adsorption from synthetic electroless plating solutions.

The adsorbent and adsorbate characterizations have been conducted using FTIR, LPSA, EDX, SEM and AAS. NaOH and H_3PO_4 activation methods have been followed out to achieve the desired classes of adsorbents including biomass based adsorbents and activated carbon adsorbents. Impregnated and cross-linked chitosan-AC composites have been prepared using procedures presented in relevant literature. Batch adsorption equilibriums were modeled using Langmuir and Freundlich isotherms. Batch adsorption kinetics was modeled using Psuedo first order, pseudo second order and intra-particle diffusion models. Pd (II) adsorption using activated

carbon packed beds has been modeled using BDST model, Thomas model and Yoon-Nelson model respectively. Further, for Pd (II) batch adsorption experiments with commercial and laboratory fabricated activated carbon, agitation assisted adsorption and ultrasound assisted adsorption have been studied, whose details have also been mentioned in the relevant sections of this chapter.

Chapter 3 summarizes the results obtained for Ni (II) adsorption on biosorbents derived from plant biomass waste. The optimality of adsorption parameters such as equilibrium time (min), pH, dosage (mg) have been identified. Following this, the adsorption efficacy of various biosorbents was evaluated in terms of capacity and removal efficiency at various concentrations. Finally, results obtained from equilibrium and kinetic modelings were presented. Also, this chapter addresses a comparative assessment of Ni (II) adsorption using commercial AC from synthetic ELP solutions.

Chapter 4 addresses Pd (II) adsorption characteristics of commercial activated carbon with synthetic electroless plating solutions. The role of CTAB surfactant has been investigated for both agitated and sonication assisted adsorption approaches. Relevant modeling efforts also have been carried out to identify the best fit models.

Chapter 5 details with respect to the results obtained for the preparation and characterization of laboratory fabricated activated carbon. Subsequently, Pd (II) adsorption characteristics and fitness of best models among equilibrium and kinetic models have been presented for both laboratory fabricated AC adsorbent. Both agitation and sonication assisted adsorption were considered. The primary aspect of the experimental investigations is to compare and contrast the adsorptive performance of laboratory fabricated AC adsorbent was evaluated with respect to that of the commercial AC adsorbent.

Chapter 6elaborates upon the results obtained for the continuous adsorption characteristics with palladium metal from both aqueous and electroless plating solutions using commercial activated charcoal beads. The effects of various adsorption parameters such as flow rate, bed height and feed concentration on the adsorption characteristics have been elaborated. Further, desorption characteristics have also been considered. Eventually, the studies were carried out to evaluate the fitness of few standard models to represent continuous Pd (II) adsorption data for both aqueous and synthetic electroless plating solutions. In this regard, the chapter intends to address the comparative variation of time dependent Pd (II) adsorption characteristics for synthetic electroless plating solutions and aqueous solutions.

Chapter 7presents the results obtained for Pd (II) adsorption on impregnated and cross-linked chitosan-AC adsorbents. Thereby, the discussion coverage's towards the identification of the best adsorbent. The obtained results have been compared with the results presented in the literature for aqueous Pd solutions. Relevant equilibrium and kinetic models have been evaluated for their fitness with the measured data.

Chapter 8 summarizes the conclusions that can be drawn based on the research findings in this work. Eventually, the chapter also presents a brief overview of the future research work that can be initiated in the chosen area of research.

Experimental and Modeling Approaches

The contents in this chapter are presented in five sections. The first section addresses the materials required for the preparation of nickel and palladium aqueous as well as electroless plating stock solutions. The second section details upon various methods adopted to prepare and utilize activated carbon adsorbents for adsorption studies. The third section presents methodologies adopted for surface characterization. Section 2.4 briefly describes procedures followed for batch and continuous adsorption studies. Eventually, section 2.5 presents modeling related procedures followed towards the fitness of measured data. Finally, section 2.6 summarizes few details with respect to cost analysis of laboratory fabricated AC adsorbent.

2.1 Materials

2.1.1 Preparation of Nickel stock solution

Nickel stock solution (1000 ppm) was prepared by dissolving analytical grade nickel sulfate (Merck, India) in millipore water. For all adsorption experiments, the nickel concentration of aqueous solutions varied from 50 to 300 mg/L. Further, few adsorption studies were carried out with synthetic nickel electroless plating bath composition using chemicals such as nickel sulfate, trisodium citrate and sodium hydroxide. All chemicals used were of analytical grade purity. Few experimental investigations were conducted for the Ni (II) adsorption characteristics using synthetic ELP solutions. For these cases, the composition of the synthetic Ni (II) ELP solution has taken as: 0.239-2.39 g/L of $NiSO_4.7H_2O$ (equivalent to 50-500 mg/L of Ni (II) solution concentration), 0.626-626 g/L of TSC, 4 g/L (0.1M) of NaOH in aqueous media.

Table 2.1: Composition of synthetic Pd (II) electroless plating solutions for adsorption studies.

Name of the component	Palladium solution concentration (mg/L)					
	50	**100**	**200**	**300**	**400**	**500**
$PdCl_2$ (mg/L)	83.31	166.63	333.27	499.90	666.54	833.17
Na_2edta (g/L)	1.39					
NH_3 solution (25%), mL/L	10.33					
CTAB, mg/L (if any)	335-1340					

2.1.2 Palladium stock solution precursors

Palladium chloride (99.9% pure obtained from SRL Chemicals Pvt. Ltd., India), Na_2EDTA (Merck India), liquor ammonia (25%) (Merck India), N-Cetyl-N, N, N-Trimethyl Ammonium Bromide (CTAB) (Merck India Ltd.) and millipore water (Make: milliQ) were used for the preparation of metal solutions. The pH of the solution was adjusted by using analytical grade HCl, NaOH solutions and pH meter (Make: VSI- 301).

2.1.3 Preparation of Palladium stock solution

The synthetic ELP solution composition was chosen based on the extensive research work conducted by Murali *et al*., (2014) for the fabrication of dense Pd composite membranes using Pd electroless plating solutions. The stock solution of $PdCl_2$ (1000 mg/L) was prepared using synthetic electroless plating bath composition presented in Table 2.1. The synthetic solution was prepared by mixing the specific constituents in 1000 mL deionized water using an incubator. Mixing was carried out for 15 min at 120 rpm to obtain complete dissolution. Subsequent solutions of varying palladium (II) concentrations were prepared by diluting the stock solution. All chemicals/reagents used were of analytical grade purity. The composition essentially refers to a stabilizer (Na_2EDTA), an optional cationic surfactant (CTAB) in a highly alkaline solution

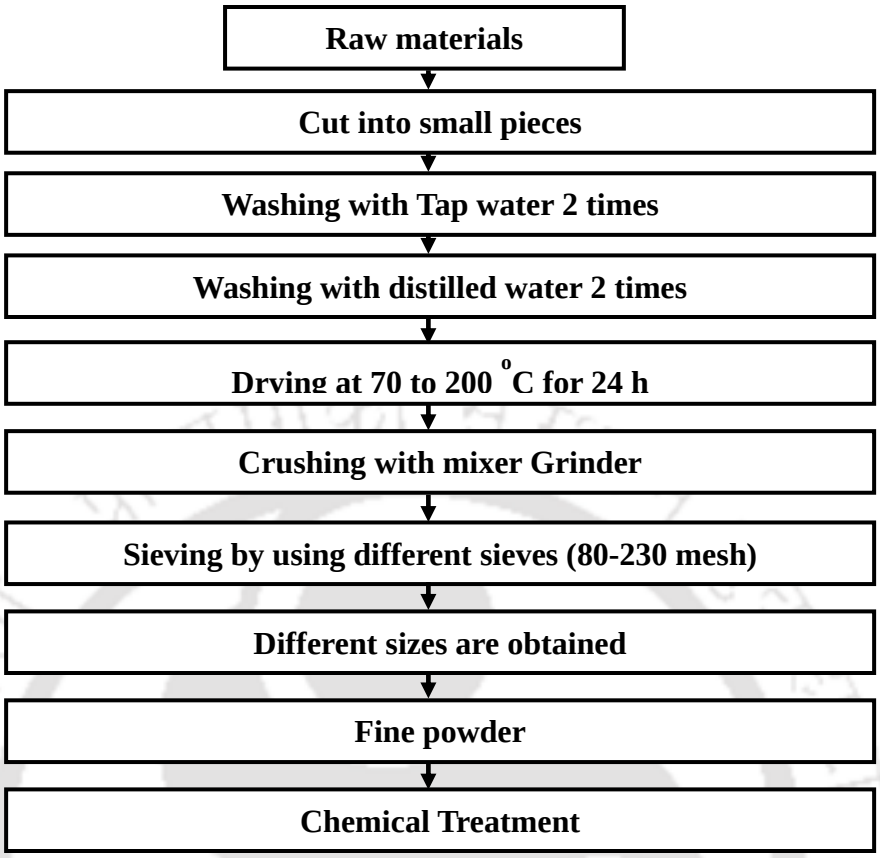

Fig. 2.1: Steps followed for the preparation of bio-sorbents.

prepared with liquor ammonia. The Pd concentration of the prepared stock solution varied between 50 -500 mg/L.

2.2 Development of biosorbents and AC adsorbent

Fig.2.1 depicts the overall procedure adopted to obtain biosorbent powder from plant wastes that are available in north eastern part of India, Assam. The procedures are similar to those presented in the literature (Loderro *et al*., 2004).

2.2.1 Preparation of biosorbent from banana pith

Banana pith obtained from IIT Guwahati region was dried, ground and sieved to less than 1 mm. The sieved materials were treated separately with 0.5M NaOH, 0.5 M HNO_3 and distilled water

and labeled as alkali treated, acid-treated and distilled-water-treated banana piths respectively. A typical pre-treatment process with HNO_3 is as follows. Banana pith (10 g) was soaked in 300 ml of 0.5M HNO_3 for 2 h. It was filtered and rinsed with distilled water until the filtrate was nearly neutral. The acid-treated material was dried to constant weight before experimentation. For the alkali-treated banana pith, the pith was boiled with 0.5M NaOH solution for 2h. Subsequently, it was treated in the similar way as the acid-treated banana pith. Distilled water-treated pith followed the same treatment process except, only distilled water was used to remove water-soluble products (Low *et al*., 1995). It was filtered and rinsed with distilled water until the filtrate was almost neutral and dried for subsequent analysis and characterization.

2.2.2 Preparation of biosorbent from pineapple stem wastes

Pineapple stem adsorbent (PS) was prepared by adopting the procedure outlined in the literature (Hameed *et al*., 2009). Pineapple stems were collected from a nearby market and were washed with distilled water several times to remove all the dirt particles. Subsequently, the stems were cut into small pieces (1-3 cm) and were dried in a hot air oven at 70 ^{o}C for 48 h. Eventually, the stem pieces were ground in a laboratory grinder and screened to obtain untreated adsorbent within the particle size range of 300 µm. Finally, the pineapple stem powder was repeatedly washed with hot distilled water until the filtered water was obtained as a clear solution. Thereafter, the pineapple stem adsorbent was dried at 70 °C for 24 h in an oven to obtain the adsorbent for further characterization and studies.

2.2.3 Preparation of activated charcoal (AC) adsorbent from bamboo stem wastes

Samples of bamboo waste were collected from a site located near IIT Guwahati, Assam. The preparation procedure for bamboo stem adsorbent is similar to that presented in the literature (McKay *et al*., 2008). The ash content of the tree waste was determined by heating the raw

material to 150 ^{o}C for 4 h, which is about 1.95 wt %. The bamboo stem was first cut into small pieces and then grinded in a laboratory grade grinder and sieved to a particle size fraction of 78 µm. Eventually, 10-20 g of bamboo stem powder was mixed with 14 ml of phosphoric acid and the mixture was subjected to low temperature treatment at 150 ^{o}C in a muffle furnace operated with flowing nitrogen gas at atmospheric pressure for 2 h. The final heat treatment step involved sintering the treated bamboo mixture till 600 ^{o}C with very fast heating rate, followed with a heating rate of 10 ^{o}C/min to elevate the temperature to 700 ^{o}C, at which the sample was sintered for 4 h. After the heat treatment, the carbonaceous adsorbent was cooled to room temperature in flowing N_2. The mixture was filtered and the adsorbent thus obtained was washed thoroughly with hot deionized water until the pH of the washed solution reached a pH of 7. Finally, the adsorbent was dried at 105 ^{o}C for further analysis and characterization of two types of adsorbents, namely, bamboo stem adsorbent after grinding and sieving (BS) and bamboo stem activated charcoal adsorbent after acid and heat treatment (BSAC). Also, few bamboo adsorbent samples were prepared by following procedures involving utilization of higher concentrations of phosphoric acid (acid to adsorbent ratio enhanced from 1.4 mL/g to 4 mL/g) and higher degree of carbonization (heating the sample in a muffle furnace in an inert environment upto 900 ^{o}C. The obtained adsorbent samples termed as high quality BSAC (HBSAC) were subjected to BET surface area analysis. To evaluate upon the role of bamboo to acid ratio on the surface area enhancement, various classes of BSAC adsorbents were prepared (Fig. 2.2) by varying the bamboo to acid ratio from 1-4. Thus, four different sets of adsorbents BSAC 11, BSAC 12, BSAC 13 and BSAC 14 respectively have been prepared using various sets of bamboo to acid ratio namely 1:1, 1:2, 1:3 and 1:4.

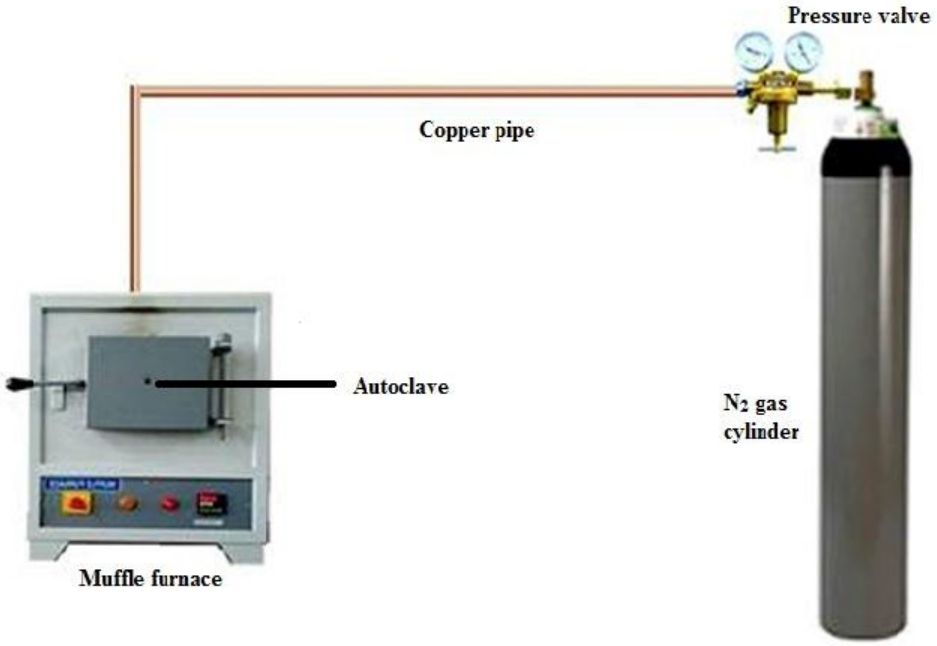

Fig. 2.2: Setup for the preparation of BSAC and BSAC 14 adsorbents.

2.2.4 Preparation of activated charcoal beads for column studies

The activated charcoal beads were prepared using (w/w) poly-vinyl alcohol (PVA). To prepare the beads, a specified amount of commercial AC adsorbent was mixed with PVA and the mixture was constantly stirred under warm conditions (50 ^{o}C) until the PVA gets dissolved. Spherical AC adsorbent with a size of about 65 µm was prepared by rolling with hands. Subsequently, the beads were soaked in water at ambient conditions for 48 h to evaluate upon the bead adhesion capabilities. The trial and error procedure involved in AC beads preparation referred to varying PVA composition from 5-20%. From such investigations, it was evaluated that the beads prepared with less than 10% PVA swelled and lost their texture upon conducting the soaking test and the beads prepared with 15% PVA retained their texture even after being exposed to a water environment for more than 40 h. Thereby the prepared beads with 15% PVA were dried in a hot air oven for 6h at 70 °C to remove the moisture. Finally, the beads were preserved in airtight polyethylene bags to further use them for continuous adsorption studies (Pilli *et al*., 2012).

2.2.5 Preparation of activated charcoal-chitosan composites

Chitosan impregnated activated charcoal adsorbents:

The procedure to prepare chitosan impregnated activated carbon adsorbent was outlined by Chataraporn *et al*., (2012) and the same was followed to achieve impregnated adsorbents prepared with CTAB surfactant. To prepare the chitosan impregnated AC adsorbents, the activated charcoal powder was washed with deionized water to remove fines and dirt and was then dried in an oven at 100 ^{o}C for 24 h before the impregnation process was conducted. Later, the AC was sieved to sizes ranging from 60-65 µm to prepare two types of adsorbents, namely, chitosan impregnated activated charcoal (CH-AC-I) and chitosan-surfactant impregnated activated charcoal (CH-AC-IS). The first adsorbent (CH-AC-I) was prepared by wet impregnation method with a solution concentration of 2 g/L of AC and variant chitosan initial concentrations (0.1-2 g/L). Using similar solution concentrations, the CH-AC-IS adsorbent was prepared using additional CTAB surfactant of solution concentration of 1-2 CMC. Subsequently, the impregnated adsorbents were prepared by keeping the prepared mixture of the adsorbent, chitosan and surfactant (if any) in an orbital shaker (agitation speed of 200 rpm at 25 ^{o}C) for 3 days. The modified AC powder was separated from chitosan solution by filtration. Using a calibration chart that was prepared apriori (Appendix B), the final chitosan concentration in the solution was done by evaluating the absorbance of the effluent solution using UV-visible spectrometer (Make: Perkin Elmer, Model: Lamda). The peak wavelength for chitosan detection using UV-Visible Spectrophotometer is about 205 nm in the literature (Chantaraporn *et al*., (2012)). However, based on experimental investigations carried out in this work, the peak wavelength corresponds to 197 nm. The capacity and removal of the chitosan during the impregnation process was evaluated using Eq. (2.1) and (2.2) that are presented in section 2.4 of

the chapter. Finally, the chitosan impregnated AC adsorbents (CH-AC-I and CH-AC-IS) were dried in a hot air oven at a temperature of 100 ^{o}C for 24 h. The amount of chitosan impregnated on the activated charcoal was cross-checked with the evaluation of weight gain after the impregnation process.

Cross linked Chitosan - Activated charcoal adsorbent:

The cross linked chitosan (CH) activated charcoal (CH-AC-C) adsorbent was prepared by the following method that was outlined by Sharififard *et al*., (2012). Firstly, to prepare oxalic acid treated adsorbent, 20 g of AC was mixed in 0.2 M oxalic acid and stirred for 4 h. Subsequently, the AC was filtered and washed with deionized water and then dried in an oven at 70 °C for 12 h. The formation of chitosan-oxalic acid gel was carried out by mixing 10 g of chitosan in 1 L of 0.2 M oxalic acid under continuous stirring conditions at 45-50 °C for 1 h. After the gel preparation process was complete, about 20 g of acid treated AC was added slowly to the chitosan gel and stirred for 16 h at 45-50 °C. Subsequently, the gel-AC mixture was added drop wise into 0.7 M NaOH precipitation bath (1 L) at 50 ^{o}C. Finally, the cross-linked adsorbent was filtered from NaOH bath, and was washed several times with deionized water to achieve neutral pH in the washed water. Prior to sieving, the CH-AC-C adsorbent was dried in a hot air oven at 50 ^{o}C for 6 h for further usage towards characterization and batch adsorption studies.

2.2.6 Commercial AC adsorbent

Commercial activated charcoal (AC) (CAS No.7440-44-0) was purchased from Merck India Limited, Mumbai and was used as the adsorbent without any further pre-treatment for Ni (II) and Pd (II) adsorption from synthetic ELP solutions.

2.3 Surface characterization

The AC characterization studies involved measurements using Laser particle size analyser (LPSA), Braummer Emmet Teller (BET), Fourier Transform Infrared Ray (FTIR), Energy Dispersive X-Ray spectroscopy (EDX) analysis, Scanning Electron Microscopy (SEM) and zero point charge.

Laser particle size analyser (Make: M/s Malvern Instruments Ltd.) was used to estimate the average particle size (μm) distribution of the adsorbents. BET instrument (Make: Backman Coulter) has been used to determine the specific surface area of the adsorbents based on N_2 adsorption-desorption at 150 °C. The surface area analyser was used to determine the 3-point BET and pore size distribution using BJH method (Brunauer *et al*., 1938; Sing *et al*., 1985). Based on spectral analysis obtained due to vibrations in the molecules within the light wave frequency of 500-4500 cm^{-1}, FTIR (M/s Toshvin Analytical Pvt Ltd.) spectral analysis enables to identify various functional groups on the adsorbent surface. The morphology of the adsorbent and elemental composition present on the adsorbent surface was analysed using scanning electronic microscopy (SEM) (Make: Leo 1430vp, Model: Oxoford) and Energy dispersive X-ray spectrometer (EDX) respectively.

Point of zero charge (PZC) corresponds to the solution pH at which the observed charge on the adsorbent surface is zero (Yang *et al*., 2004). The point of zero charge (PZC value) of AC was determined by the pH drift method. The method involved preparing a solution of 0.005 M $CaCl_2$ which was boiled to remove dissolved CO_2 and was subsequently cooled to room temperature. The pH adjustment in the range of 2-12 was facilitated with 0.5 M HCl and NaOH solutions. Eventually, the adsorbent was added to 20 mL of the prepared solution in a capped vial and was equilibrated for 24 h, to eventually measure the final pH. Based on the measured data for various

sets of initial and final pH, a curve was plotted between various sets of final and initial pH. The PZC value was evaluated to be corresponding final pH value of a co-ordinate obtained with the intersection of 45° line and the curve on the same graph. The physical significance of PZC is summarized as follows. When the adsorbent is in contact with a solution whose pH is less than that of PZC, due to the protonation of functional groups on the adsorbent's surface, the adsorbent becomes positively charged and will not be favourable for the adsorption of positively charged metal ions. However, when the adsorbent pH is more than that of the PZC, due to less protonation, the adsorbent shall enable maximum adsorption at higher pH (Ho *et al*., 2002).

2.4 Batch adsorption studies

2.4.1 Adsorption of Ni (II) from aqueous and synthetic ELP solutions

Batch mode experiments were carried out using 0.01-0.1 g of selected adsorbents (PS and BSAC) powder and with 50 mL of aqueous solution. The initial solution concentration was varied from 50 to 300 mg/L at a natural pH of 5. The experiments were performed in wrist action shaker (Make: Lab Tech., India) for a period of 1 hour at 200 rpm, using 250 ml flasks containing 50 ml solutions of specified Ni (II) concentrations at room temperature (25 ^{o}C). Continuous mixing was provided during the experimental period with a constant agitation speed of 200 rpm so as to ensure the achievement of mass transfer equilibrium. Subsequently, the mixture was filtered using Whatman filter paper (No. 40). Ni (II) concentration was determined using fast sequential atomic absorption spectrometer (Make: Spectra AA220FS), at a wavelength of 232.8 nm. The calibration curve for the evaluation of Ni (II) solution concentration is presented in Appendix A. Using the measured concentrations, various adsorption parameters namely, mg/g (Amount of adsorption at equilibrium) and metal removal % were estimated using the following equations:

$$q_e = \frac{(C_o - C_e)V}{W} \quad (2.1)$$

$$\text{Removal } \% = \frac{(C_o - C_e)}{C_o} \times 100 \quad (2.2)$$

Similar procedures were followed for batch Ni (II) adsorption from synthetic ELP solutions using commercial AC adsorbent.

2.4.2 Pd (II) adsorption on activated carbon adsorbents

Batch mode experiments were carried out using 0.05-0.3 g of AC powder and 50 mL of synthetic electroless plating solution. The initial solution concentration varied from 50 to 500 mg/L at a natural pH of 9-10. The experiments were performed in a wrist action shaker (make: Lab Tech., India) for a period of 1-5 hours at 200 rpm, using 250 mL flasks containing 50 mL solutions of specified Pd (II) concentrations at room temperature (25 ^{o}C). Continuous mixing was provided during the experimental period with a constant agitation speed of 200 rpm, so as to ensure the achievement of mass transfer equilibrium. Subsequently, the mixture was filtered using Whatman filter paper (No. 40) to obtain the spent electroless plating solution whose Pd (II) concentration was determined using Atomic Absorption Spectrophotometer (AAS) (Make: Varian spectra, FS240) equipped with air-acetylene flame detector at a wavelength of 247.6 nm respectively (Merdivan *et al*., 1997). The calibration curve for the evaluation of Ni (II) solution concentration is presented in Appendix B. Using the measured concentrations, various adsorption parameters namely q_e (Amount of adsorption at equilibrium) and metal removal % were estimated using equations (2.1) and (2.2).

For all experiments conducted with solutions consisting of CTAB surfactant, the solution concentration of CTAB surfactant was varied in the range of 1-4 CMC (335-1340 mg/L).

Further, few batch adsorption experiments were conducted by deploying sonication assisted adsorption instead of physi-sorption. These experiments involved placing the adsorbent and adsorbate solution in an ultrasonic cleaning bath (Make: Elma S30 H) at a temperature of 30 ^{o}C under degas mode for a contact time of 120 min to facilitate equilibrium.

2.4.3 Pd (II) adsorption on chitosan modified activated carbon adsorbents

For CH-AC-I adsorbent, batch adsorption studies were conducted for synthetic electroless plating solutions. Thus, the adsorbents obtained after such Pd (II) adsorption studies have been referred to as Pd-E-CH-AC-I, Pd-E-CH-AC-IS for adsorbents obtained from CH-AC-I and CH-AC-IS respectively. The adsorbents obtained after batch adsorption studies using CH-AC-C adsorbents have been referred to as Pd-E-CH-AC-C and Pd-ES-CH-AC-C for solutions deployed without and with CTAB surfactant respectively. For all cases, Pd solution concentration was varied from 50-500 mg/L and for cases where CTAB surfactant is included in the solution formulation, its composition corresponds to 2 CMC. Batch adsorption studies were not conducted for impregnated adsorbents with surfactant containing Pd (II) ELP solutions due to the objective of evaluating the surfactant competence in the impregnation procedure itself.

For both CH-AC-I and CH-AC-IS adsorbents, the optimal set of batch adsorption process have been assumed to be similar to the values obtained from the batch adsorption studies conducted for Pd adsorption on AC. This is due to the fact that impregnation does not enable significant chemical bonding with the activated carbon and therefore the optimal batch adsorption parameters for AC could be relevant for the CH-AC-I and CH-AC-IS adsorbents. However, for CH-AC-C, batch adsorption studies were conducted in the parametric range of 2-14 for pH, 50-400 min for equilibrium time and 1-7 g/L for adsorbent dosage.

Sample calculations for Pd (II) batch adsorption are presented in Appendix C. A summary of error analysis is presented in Appendix D. Appendix E summarizes images of various prepared adsorbents and packed bed adsorption setup.

2.5 Continuous adsorption studies

2.5.1 Pd (II) continuous adsorption studies on activated carbon adsorbent

Fig. 2.3 illustrates the schematic of experimental setup used for Pd continuous adsorption studies. The setup consists of a packed column (2.5 cm diameter and 50 cm height) in which activated carbon beads were loaded from the top. During the experiment, aqueous/synthetic ELP solutions were circulated in the upward direction using a peristaltic pump at the specified flow rate.

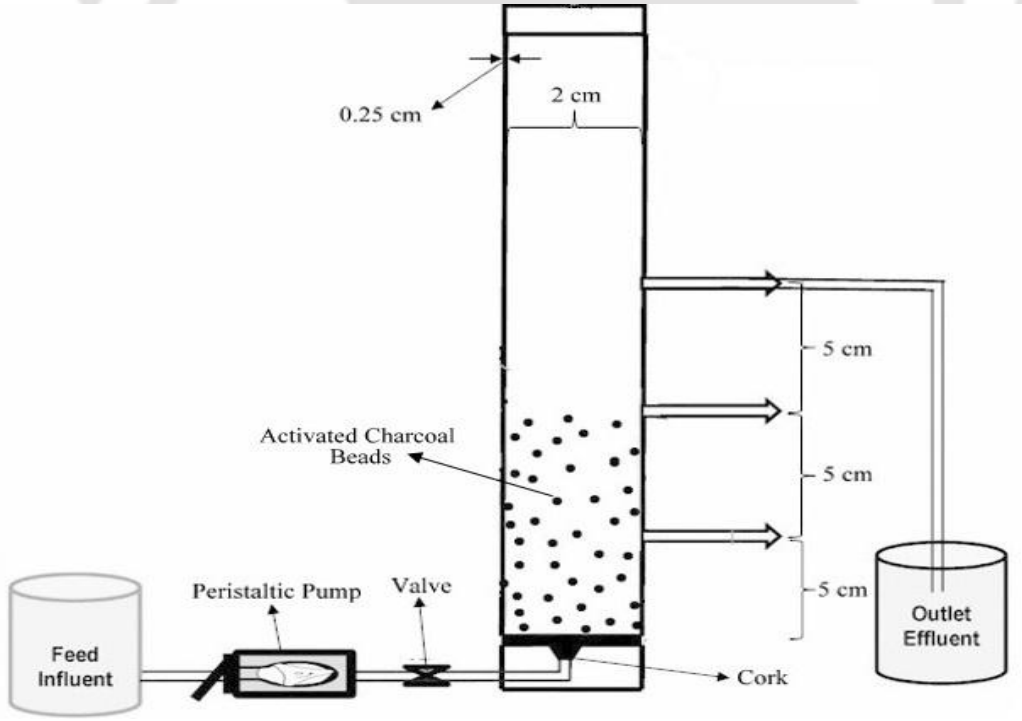

Fig. 2.3: Experimental setup for continuous Pd (II) adsorption studies using AC packed bed.

The effluent was taken from the top section of the packed column at various time intervals to evaluate the time dependent concentrations of unabsorbed palladium metal ions using Atomic absorption spectrometer (AAS) (Make: Varian spectra, FS240). The experimental run was terminated upon saturation of the adsorbent bed after 3 h. The packed bed adsorption

2.5.2 Continuous Pd (II) adsorption data analysis

Breakthrough curves are standard plots that are deployed for the analysis of continuous metal adsorption in packed bed columns. The breakthrough curve is expressed as a time dependent variation of C_e/C_o where C_e and C_o refers to the effluent and influent concentrations. Thus, in due course of time, the ratio of C_e/C_o shall gradually increase, which refers to the saturation of the packed column in terms of the capacity. Several variables associated to the performance of packed columns for continuous adsorption studies refer to effluent volume (V_{eff}), sorption zone (Δt), mass transfer zone (L_m), % Removal and equilibrium metal uptake (q_e). Along with suitable expressions for other parameters, the above parameters can be evaluated from the breakthrough curves as follows (Pilli *et al*. 2012):

a) Breakthrough time (t_b) was evaluated as the time taken from the start of the experiment to achieve an outlet Pd (II) concentration of 1 mg/L.

b) Bed exhaustion time (t_e) was evaluated as the time taken from inception to achieve the outlet Pd (II) concentration equivalent to 95% of the inlet Pd (II) concentration

c) The overall sorption zone (Δt) can be evaluated as the difference between breakthrough and exhaustion time:

$$\Delta t = t_e - t_b \qquad (2.3)$$

d) The length of the mass transfer zone (L_m) can be evaluated as a function of the bed height, evaluated breakthrough and exhaustion time is expressed as:

$$L_m = L\left(1 - \frac{t_b}{t_e}\right) \tag{2.4}$$

e) The effluent volume (V_{eff}) is evaluated as a function of flow rate and exhaust time and is given as:

$$V_{eff} = Ft_e \tag{2.5}$$

f) The area under the curve (A) for the breakthrough curve can be evaluated using Trapezoidal rule. For a specified inlet concentration, the total adsorbed metal quantity (m_{ad}, g) can be estimated as a function of flow rate and evaluated area and is expressed as:

$$m_{ad} = \frac{FA}{1000} \tag{2.6}$$

g) The total amount of metal sent to the column (m_{total}) is evaluated as:

$$m_{total} = \frac{C_o F t_e}{1000} \tag{2.7}$$

h) Using evaluated values of m_{ad} and m_{total}, the % removal of the Pd metal during continuous adsorption is evaluated as:

$$\text{Removal}(\%) = \frac{m_{ad}}{m_{total}} \times 100 \tag{2.8}$$

i) The elution efficiency (E) can be eventually calculated as:

$$E(\%) = \frac{m_d}{m_{ad}} \times 100 \tag{2.9}$$

where m_d corresponds to the total metal desorbed during desorption experiments and was evaluated using expressions similar to Eq. 2.6. The area under the curve for the desorption case corresponds to the area obtained for the desorption breakthrough curve.

j) The equilibrium metal update q_{eq} can be evaluated using the expression:

$$q_{eq} = \frac{m_{total}}{W} \times 100 \qquad (2.10)$$

The efficacy of the continuous adsorption process can be quantified based on the above variables. For an adsorbent that facilitates efficient adsorption, L_m (length of mass transfer zone) shall be low. Similarly, higher combinations of elution efficiency and equilibrium metal uptake shall be applicable along with lower value of removal efficiency.

Also, the breakthrough time (t_b) and the corresponding metal ion concentration (breakthrough metal ion concentration C_b) that can be only obtained from the breakthrough curves. These variables are of relevance for the evaluation of fitness of BDST model which will be summarized later in section 5.4.1 of the thesis.

2.6 Desorption studies

2.6.1 Batch Pd (II) desorption on commercial AC adsorbent

For commercial activated carbon adsorbent, batch desorption was carried out by using 0.1 M NaOH and HCl. The commercial AC adsorbent obtained with an initial Pd (II) concentration of 300 mg/L was used for desorption studies. For the desorption experiments, 60 mg of Pd (II) adsorbed AC was used with 50 mL of elutant solution for a contact time of 300 min. Thereby, the Pd (II) recovery from desorption was evaluated as a function of initial and final Pd (II) adsorbent concentrations. The final Pd (II) adsorbent concentration was determined using mass balance approach in which elutant Pd (II) concentration after desorption was obtained from AAS analysis.

2.6.2 Batch Pd (II) desorption on CH-AC-C adsorbent

For CH-AC-C adsorbent, batch Pd desorption studies were conducted using the adsorbent obtained after reaching adsorption equilibrium with an initial solution concentration of 300 mg/L. Based on the carried out study, the Pd adsorbed CH-AC-C adsorbent was evaluated to have a capacity of 44.34 mg/g for the chosen initial concentration. The batch adsorption studies were conducted with 0.1 M HCl and 0.1 M NaOH that were prepared using Millipore water. For the batch desorption experiments, 0.12 g of adsorbent was used to achieve saturated desorption Pd solution concentration in 50 mL reagent solution. The desorption experiments were conducted for a time period of 300 min. Subsequently, using the final solution concentrations evaluated from AAS analysis, mass balance was conducted to estimate the Pd (II) surface concentration on the adsorbent after desorption experiment. Eventually, the Pd recovery after desorption has been evaluated as a function of the initial and final Pd adsorbent concentrations.

2.6.3 Continuous Pd (II) desorption on AC adsorbent

The continuous Pd desorption experiments were conducted similar to the continuous adsorption experiments conducted for the AC adsorbent. Desorption experiments were conducted with Pd-AC adsorbents obtained from continuous adsorption experiments. Thus, the Pd-AC adsorbents correspond to the adsorbents obtained with an initial Pd solution concentration of 50-150 mg/L. For desorption experiments, 0.1 M NaOH was used. For the continuous Pd desorption experiments, other parameters were taken similar to those taken for continuous Pd adsorption i.e., bed height 5-15 cm (4.2-13.04 g adsorbent loading) and flow rate of 15-25 mL/min. Subsequent analysis of the effluent solutions was conducted with AAS to evaluate upon the time dependent Pd desorption characteristics of the Pd-AC adsorbent.

2.7 Modeling and Error analysis for Batch adsorption

2.7.1 Isotherm modeling

Analysis of equilibrium sorption data is important to optimize the design of sorption systems. The adsorption process depends on the interaction between the surface of the adsorbent and the adsorbed species. The interaction may be due to chemical bonding, hydrogen bonding, hydrophobic and Vander Waals forces. The adsorption isotherms represent the relationship between the amount adsorbed by a unit weight of solid adsorbent and the amount of solute remaining in the solution at equilibrium.

Langmuir and Freundlich isotherm models are frequently used to describe the adsorption of metal ions on various adsorbents. Either Langmuir or Freundlich isotherms fit well with the equilibrium data of adsorbents. This suggests that either monolayer or multilayer adsorption could occur on the adsorbent surface. The Langmuir model assumes that sorption takes place on the homogeneous surface of the adsorbent and a saturation monolayer is formed, while the Freundlich expression is an empirical equation based on the adsorption on a heterogeneous surface. However, heavy metal adsorption on heterogeneous adsorbents has been interpreted using Langmuir isotherm as well. In addition there are other standard models (Redlich-Peterson and Temkin models) that can be as well as considered to model measured Ni (II) and Pd (II) adsorption data (Ho *et al*., 2002).

Assuming complete monolayer coverage on homogenous adsorbent surface without any interaction between adsorbed ions, Langmuir equilibrium isotherm model is commonly represented as (Langmuir, 1916).

$$\frac{C_e}{q_e} = \frac{1}{bq_{max}} + \frac{1}{q_{max}} C_e \qquad (2.11)$$

Typically, the favorability of the adsorption based on Langmuir isotherm model is expressed in terms of separation factor (K_R) defined as:

$$K_R = \frac{1}{(1 + bC_o)} \tag{2.12}$$

From the shape of the isotherm, the separation factor (K_R) indicates whether the adsorption is favourable or not. Typically, favourable adsorption indicates a K_R value that is within the range of 0-1.

Assuming exponential distribution of active centers and with characteristics of heterogeneous surface and infinite surface coverage, Freundlich isotherm model is commonly represented as (Freundlich, 1906):

$$\log(q) = \log(k_f) + \frac{1}{n}\log(C_e) \tag{2.13}$$

Incorporating both the features of Langmuir and Freundlich models, Redlich and Peterson (Redlich *et al*., 1959) presented an isotherm model expressed as:

$$\ln\left(A\frac{C_e}{q_e} - 1\right) = g\ln(C_e) + \ln(B) \tag{2.14}$$

Although a linear analysis is not possible for a three parameter isotherm, three isotherm constants, A, B and g, can be evaluated from the pseudo-linear plot represented by Eq. (2.14) using a trial and error optimization method.

The Temkin isotherm assumes that the reduction in the heat of sorption is linear but not logarithmic with increasing metal concentration and is typically expressed as (Aharoni et al., 1977)

$$q_e = \frac{RT}{b_T} \ln(A_T C_e) \qquad (2.15)$$

The fitness procedure of various equilibrium models towards experimental data involves graphical (for Langmuir, Freundlich and Temkin isotherms) or non-linear optimization procedures (Redlich and Peterson Model).

2.7.2 Kinetic modeling

Typically, standard kinetic models are subjected to fitness studies for the sorption of metal ions onto adsorbent surface. Generally, adsorption kinetics is represented using either pseudo-first order or pseudo second order models. The pseudo-first order model used to represent adsorption kinetics is expressed in terms of Lagergren equation (Aharoni *et al*., 1977):

$$\log(q_e - q_t) = \log(q_e) - \frac{k_1}{2.303} t \qquad (2.16)$$

On the other hand, the process can be described by a pseudo-second order model based on the assumption that the rate limiting step may be chemical sorption or chemisorption involving valency forces through sharing or exchange of electrons between sorbent and sorbate. The parameter influencing on the kinetics of the sorption reaction was the sorption equilibrium capacity, q_e, which is a function of initial metal ion concentration and nature of the solute ion. Pseudo second order kinetic model is expressed as (Ho *et al*., 1999):

$$\frac{t}{q} = \frac{1}{k_2 q_e^{\ 2}} + \frac{1}{q_e} t \qquad (2.17)$$

Other than these two models, intra particle diffusion model is also typically deployed to study the significance of intra particle diffusion. Typically the model is expressed as:

$$q_t = K_{id} t^{0.5} + C \qquad (2.18)$$

Therefore, if the plot of q_t versus $t^{0.5}$ is linear and passes through the origin, the intra particle diffusion is the sole rate-limiting step (Srivastava *et al*., 2006). However, in case the plot is non-linear in nature, the plot can be analyzed to infer about various processes that contribute towards the adsorption. The first sharper region in the non-linear plot corresponds to the instantaneous external surface adsorption. The second region refers to a gradual adsorption stage where Intraparticle diffusion is the rate limiting step. In some cases, a third region exists that corresponds to the final equilibrium with the reduction in intra particle diffusion at larger contact times and reduction of solute concentration in the solution.

2.7.3 Estimation of thermodynamic parameters

Thermodynamically, Van't Hoff equation describes the variation of equilibrium constant with temperature and is suitably expressed as (Jossens *et al*., 1978).

$$\frac{d\ln K_a}{dT} = \frac{\Delta H^o}{RT^2} \qquad (2.19)$$

From the above equation, k_a can be determined.

Knowing ΔH^o and k_a, other thermodynamic parameters (ΔG^o), and (ΔS^o) were obtained using the expressions:

$$\Delta G^o = -RT\ln K_a \qquad (2.20)$$

$$\Delta G^o = \Delta H^o - T\Delta S \qquad (2.21)$$

2.7.4 Error Analysis

The fitness of the above three models towards experimental data can be easily carried out by a graphical procedure and the model with best combinations of coefficient of correlation (R^2)

along with lowest values of minimal, maximum, average and RMS error will be regarded as the best fit model.

For all models summarized in sections 2.7.1 and 2.7.2 various errors have been calculated using the following equations (2.24-2.28).

$$Er_i = \frac{\left|C_i^{exp} - C_i^{model}\right|}{C_i^{exp}} \times 100 \quad (2.24)$$

$$Ermax = Max(Er_i) \quad (2.25)$$

$$Ermin = Min(Er_i) \quad (2.26)$$

$$Eravg = \frac{\sum_{i=1}^{n} Er_i}{n} \quad (2.27)$$

$$RMSE = \frac{\sqrt{\sum_{i=1}^{n} Er_i^{\,2}}}{n} \quad (2.28)$$

2.8 Modeling and Error analysis for Column studies

Modeling of continuous Pd adsorption process is required for the design and analysis of the adsorption process. The analysis of the process will be of particular interest with respect to the cost and economics of the process. For modelling continuous Pd adsorption process, standard continuous adsorption models are often investigated for their fitness. This section elaborates upon the same.

Using the breakthrough curves $\frac{C_e}{C_o}$ obtained for different bed heights (Z), flow rates (F) and initial solution concentration (C_o), various relevant variables required for modelling column

studies can be estimated. In general, three standard mathematical models are typically studied for their fitness to represent experimentally determined column adsorption data. These refer to Bed depth service time (BDST), Thomas and Yoon-Nelson models. In the following sub-sections, details with respect to various models are being presented.

2.8.1 Bed Depth Service Time (BDST) model

Bed service time is an important design principle for packed bed absorbers. Evaluated service time values for operating absorbers are often used to compare the uptake capacity of the columns. Emphasizing upon the service time concept, the BDST model was derived by assuming that the intra-particle diffusion and external mass transfer resistance are negligible and that the adsorption kinetics is controlled by surface chemical reaction between solute and the unused adsorbent. Service time is typically defined as the time period required for the adsorbent to remove the specified amount of adsorbate from the influent solution before there is a need for regeneration. The BDST model is a modification of the Bohart-Adams model (Tan *et al*., (2007); Muralidharan *et al*. (1994); Bohart and Adams *et al*., 1920,) which was originally expressed as:

$$\ln\left(\frac{C_o}{C_b}-1\right)=\ln\left(\exp\left(\frac{KN_oZ}{\nu}\right)-1\right)-KC_ot \qquad (2.29)$$

The above equation has been subsequently modified by Hutchins (1973) as a linear relation between the bed depth and service time parameters and is expressed as:

$$t_b=\frac{ZN_o}{C_o\nu}-\frac{1}{K_{ad}C_b}\left(\frac{C_o}{C_b}-1\right) \qquad (2.30)$$

In the above expression, t_b is service time at breakthrough point; N_o is dynamic bed capacity (mg/L); Z is the bed height of the column (cm); C_o is the initial concentration of solute in the

liquid phase (mg/L); ν is linear flow rate (cm/h); defined as the ratio of the volumetric flow rate F (cm^3/hr) to the cross-sectional area of the bed A_c (cm^2); K_{ad} is rate constant of adsorption (l mg^{-1} h^{-1}) and C_b is the breakthrough metal ion concentration (mg/L). Using the expression derived by Hutchins, one needs to only carry out a minimum of three fixed-bed tests to obtain the relevant data based on a straight line fit of evaluated data parameter sets.

Eq. 2.30 can be represented as a straight line using the expressions:

$$t_b = m_x Z - C_x \tag{2.31}$$

where

$$C_x = \frac{1}{K_{ad} C_b} \ln\left(\frac{C_o}{C_b} - 1\right) \tag{2.32}$$

$$m_x = \frac{N_o}{C_o \nu} \tag{2.33}$$

The procedure for the fitness of BDST model and subsequent calculations is outlined as follows:

a) Using the breakthrough curves ($\frac{C_e}{C_o}$ vs t), t_b values can be estimated for a given set of F, Z and C_o. In the breakthrough curve, t_b corresponds to time at which the breakthrough curve slope increases significantly. Thus, the t_b has been estimated using experimental continuous Pd adsorption data.

b) Eventually, a plot of t_b (service time) vs. Z (bed height) with minimal three data sets could indicate a straight line fit for the validity of the BDST model. From the plot, the slope and intercept of the plot can be determined.

c) The slope of the graph corresponds to $\frac{N_o}{C_o \nu}$ using which for known values of C_o and ν, N_o can be determined.

d) Using the intercept value of the plot, K_{ad} can be determined using Eq. (2.32). To determine K_{ad}, the breakthrough metal ion concentration (C_b) will be required, which corresponds to the effluent concentration at breakthrough time (t_b) in the breakthrough curve.

2.8.2 Thomas Model

Following Langmuir kinetics of adsorption-desorption with no axial dispersion and assuming constant separation factor and rate driving force adopting second-order reversible reaction kinetics, Thomas model had been derived by Thomas *et al*., (1944). The model is expressed as:

$$\frac{C_e}{C_o} = \frac{1}{1+\exp\left(\frac{k_{TH}}{F}\left(q_o M - C_o V_{eff}\right)\right)} \tag{2.33}$$

The linearized equation for the Thomas model is expressed as:

$$\ln\left(\frac{C_o}{C_e} - 1\right) = \frac{k_{TH} q_o M}{F} - k_{TH} C_o t \tag{2.34}$$

where the kinetic coefficient (or Thomas model rate constant K_{TH}) and the maximum adsorption capacity (q_o) can be determined for known values of all other parameters in the above equation. Also, in the above equation, C_o and C_e are palladium ion concentrations (mg/L) in the influent and effluent, respectively, F *is* the flow rate (L/h), q_o is the maximum solid-phase concentration of the solute (mg/g), M *is* the total mass of the adsorbent loaded in the column (*g*) and V_{eff} is the volume of palladium solution (*L*) that passed through the column.

The procedure for evaluating the fitness of Thomas model and subsequent calculations can be summarized as follows:

a) Using the experimentally obtained breakthrough curve data, a plot of $\ln\left(\frac{C_o}{C_e}-1\right)$ vs t will provide a straight line fit for the validity of the Thomas model.

b) Upon good fitness of the Thomas model, the slope of the plot corresponds to the $-k_{TH}C_o$. For known value of C_o, k_{TH} can be determined.

c) The intercept of the plot corresponds to $\frac{k_{TH}q_oM}{F}$ using which q_o can be estimated. Subsequently, the experimentally determined q_o is matched with that obtained from the Thomas model.

2.8.3 Yoon-Nelson Model

In this model it is assumed that the rate of decrease in the probability of adsorption for each adsorbate molecule is proportional to the probability of adsorbate adsorption and adsorbate breakthrough on the adsorbent (Yoon and Nelson *et al*., 1984). Without requiring details such as physical properties of the adsorption bed, characteristics of adsorbate and adsorbent, Yoon and Nelson equation can be used to model Pd continuous adsorption using the expression:

$$\frac{C_e}{C_o}=\frac{\exp\left(k_{YN}t-\tau k_{YN}\right)}{1+\exp\left(k_{YN}-\tau k_{YN}\right)} \qquad (2.35)$$

The linear expression for the above equation is given as:

$$\ln\left(\frac{C_e}{C_e-C_o}\right)=k_{YN}t-\tau k_{YN} \qquad (2.36)$$

where k_{YN} is the rate constant (per min); τ is the time required for 50 % adsorbate breakthrough (min) and t is the breakthrough (sampling) time (min).

The procedure for evaluating the fitness of Yoon and Nelson model and subsequent calculations is summarized as follows:

a) First, a graph is drawn between $\ln\left(\frac{C_e}{C_e - C_o}\right)$ and t. If a straight fit is obtained for the same, it indicates the fitness of Yoon and Nelson model.

b) The slope of the graph refers to k_{YN} and using the intercept τ can be estimated. The τ determined from the model is subsequently compared with the τ obtained from the breakthrough curve (i.e., time corresponding to 50 % adsorbate breakthrough).

2.9 Cost analysis of the BSAC and commercial activated carbon adsorbent

Conceptual cost estimation has been carried out for both BSAC and activated carbon adsorbents. The following assumptions are applicable for the cost analysis:

a) The energy requirement for BSAC is 20 kWh (2 kW for 10 h) to process 250 g of adsorbent.

b) Inert gas requirements have been estimated as 0.2 m^3 to process 250 g of adsorbent

c) Costs of various commodities such as electricity, nitrogen gas and phosphoric acid have been assumed as ₹ 7/kWh, ₹ 300/m^3 and ₹ 150/L respectively.

d) Cost estimation has been carried out for 10 kg of BSAC. To do so, power law model has been adopted with an exponent value of 0.6.

Chapter 3

Equilibrium and Kinetic Studies of Ni (II) Adsorption using Pineapple and Bamboo Stem based Adsorbents

In this chapter, results obtained for the Ni (II) adsorption of synthetic aqueous solutions have been presented for pineapple and bamboo stem waste based biosorbents. Section 3.2 presents surface characterization results for the adsorbents. Sections 3.3 and 3.4 details upon batch adsorption characteristics followed by model fitness to measured adsorption equilibrium data for both adsorbents. Sections 3.5 and 3.6 addresses kinetic data and thermodynamic model parameters respectively. Section 3.7 presents cost analysis data for the prepared adsorbent followed with summary in section 3.8.

3.1 Introduction

This chapter addresses the development of low cost adsorbents developed using pineapple and bamboo stem waste which were used for the removal of Ni (II) from aqueous solutions. The primal role of phosphoric acid activation for the surface area enhancement of the adsorbent has been considered. Adsorbents characterization studies involved Fourier transform infrared (FTIR) spectral analysis, Brummer Emmett Teller (BET) adsorption and Laser Particle Size Analysis (LPSA). Further, for both the adsorbents, Ni (II) adsorption experiments were carried out with various combinations of solution concentrations (50-300 mg/L), adsorbent dosage (2 g/L), contact time (30-300 minutes) and pH (2-10). Equilibrium and kinetic modelling of adsorption process have been addressed using various isotherms. The next section elaborates with respect to adsorbent characterization.

3.2 Adsorbent Characterization

Fig. 3.2(a) and 3.2(b) present the obtained FTIR spectra for PS and BSAC respectively. As shown in the figure, several functional groups exist on both adsorbents. For the BSAC adsorbent before nickel adsorption, peaks were observed at specific wavelengths of 2939.3, 2897.2, 1716.4, 1651.8, 1519.3, 1508.1, 1338.4, 1165, 1056.5 and 898.6 cm^{-1}. However, after adsorption on BSAC, FTIR spectral peaks were observed at 2924.6, 2850.8, 1720.4, 1654.8, 1045.3 and 902.9 cm^{-1}. Similarly, for PS adsorbent, spectral peaks were observed at 2931.2, 2908.6, 2357, 1728.2, 1600.91, 1369.3 and 1246.01 cm^{-1} for the raw adsorbent and these shifted to 2920.2, 2368.5, 1735.9, 1627.8, 1365.3 and 1242.1 cm^{-1}, respectively, after Ni (II) adsorption. The spectral shifts indicate that there were binding processes taking place on the surface of both BSAC and PS adsorbents. Specific functional group interactions can be analyzed to indicate C≡N (2939 cm^{-1}), stretching vibration of C=O (1651.8 cm^{-1}), $–CH_3$

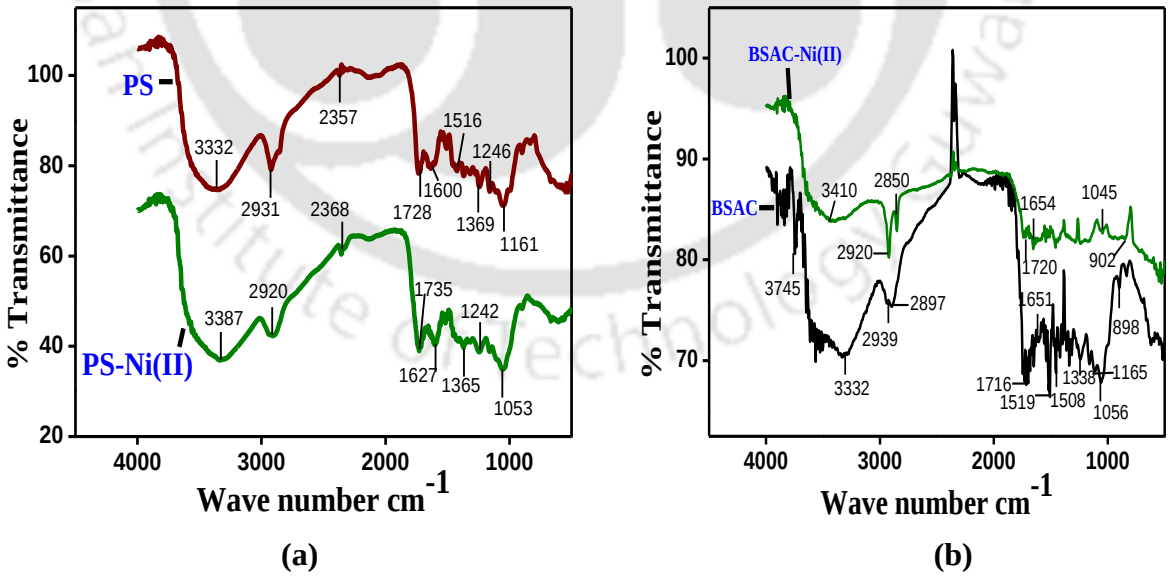

Fig. 3.1: FTIR spectra of fresh and Ni (II) adsorbed (a) PS and (b) BSAC adsorbents.

wagging (at 1365 cm^{-1}) and C–O stretching vibration (at 1056 cm^{-1}) (Lalhruaitluanga *et al*., 2011; Hameed *et al*., 2009; McKay *et al*., 2008).

Affinity towards Ni (II) ions and hence their adsorption to the adsorbent surface can be analyzed through the evaluated functional group related band shifts. For the C≡N, lone pair of electrons exists on N and partial negative charge is also prevalent on both C and N (depending on the direction in which the bond shift occurs). Thereby, the prevalent negative charge induces affinity towards the positively charged Ni (II) ion or its complex. Similarly, for the C=O, the lone pair of electrons present on the O and the partial negative charge present on either of the atoms will induce affinity towards the positively charged metal ion species. For the C-O, the lone pair of electrons on O might induce the affinity of Ni (II) ion to the adsorbent surface. The extent of reversible chemisorption or physisorption could not be confirmed by the FTIR spectra due to the inability to provide quantitative information with respect to the actively prevalent bonds and their distributions. Nonetheless, the FTIR spectral analysis has been useful to confirm upon the possibilities of strong irreversible chemisorption which can be further confirmed through desorption studies.

The BET surface area values were evaluated as 11.47 m^2/g and 116 m^2/g for PS and BSAC, respectively. This indicated that the chemical treatment of phosphoric acid contributed towards larger adsorption capacity of BSAC (Lalhruaitluanga *et al.*, 2011) and chemical treatment contributed towards enhancement of surface area which could reduce the optimal dosage and enhance adsorptive efficacy of the developed adsorbent.

The particle size analysis of the prepared adsorbents indicated an average particle size of 300 and 78 µm for PS and BSAC respectively for the adsorbents screened using various mesh sizes ranging from 80-230. The lower size of the prepared adsorbents promising due to the

reason that particle size strongly influences metal uptake and removal efficiency. Using the pH drift method, the PZC values of BSAC and PS have been obtained as 4.5 and 4.08 respectively. This indicates that for the adsorbents and for the solution pH lower than these PZC values, adsorption shall not be significant and this is evident from the results presented later in section 3.3.2 (Fig. 3.3). Also, the inability to have higher adsorption at higher pH (above pH of 5) is indicative towards the fact that complex chemistry is involved with the binding of Ni metal ions to the adsorbent surface and based on PZC and pH study, the optimal pH value corresponds to the value slightly above the PZC value for both the adsorbents (Singh *et al*., 2013; Alhawas *et al*., 2013). Thus, PZC being the lower limit of adsorption has also been confirmed by both PS and BSAC adsorbents for Ni (II) adsorption from aqueous solutions.

3.3 Adsorption characteristics

For both BSAC and PS, based on hierarchial selection of various operating parameters, the adsorbent performance studies were conducted. Firstly, the optimality of the contact time had been targeted by considering a fixed choice of adsorbent dosage (0.02 g/L), pH (5-6) and initial Ni (II) solution concentration of 50 mg/L. Eventually, the corresponding contact times for the adsorbents were fixed and the adsorption studies were conducted for variant pH (2-10) and fixed choice of adsorbent dosage (0.02 g/L), Ni (II) solution concentrations (50 mg/L) and optimized contact times (obtained from the first set of adsorption experiments). These studies identified optimal pH as 5. Finally, for the fixed choice of pH (obtained from second set of adsorption experiments), contact time, Ni (II) solution concentration (50 mg/L) and the adsorbent dosages were varied (0.02-0.1 g/L) to evaluate the adsorption performance of PS and BSAC. For all cases, adsorbent performance was evaluated in terms of metal uptake

(mg/g) and removal % which were determined using Eq. (2.1-2.2). Finally, the performance of PS and BSAC were studied for various solution concentrations (50-300 mg/L), by choosing all other parameters from results obtained with above mentioned preliminary adsorption studies. Further details with respect to the results obtained from the three sets of adsorption experiments are presented below.

3.3.1 Effect of contact time

Fig. 3.2 presents the variation in % adsorption and metal uptake (mg/g) with contact time for BSAC and PS. Corresponding choice of other parameters include adsorbent dosage, pH and Ni (II) concentration as 0.02 g/L, 5-6 and 50 mg/L respectively. It can be observed that the minimum time required to achieve equilibrium (i.e., maximum adsorption) is 300 and 90

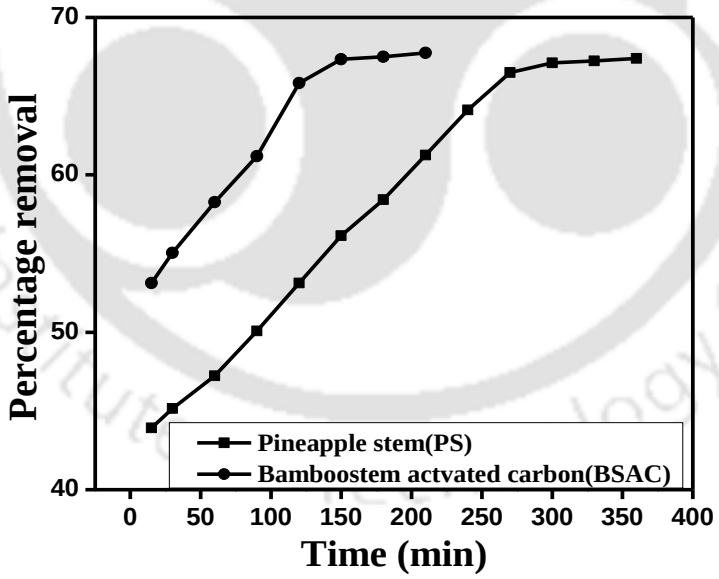

Fig. 3.2: Effect of contact time on Ni (II) removal efficiency for BSAC and PS adsorbents. Other experimental conditions were C_o = 50 mg/L, T = 25 ^oC, RPM = 200 and V = 50 mL.

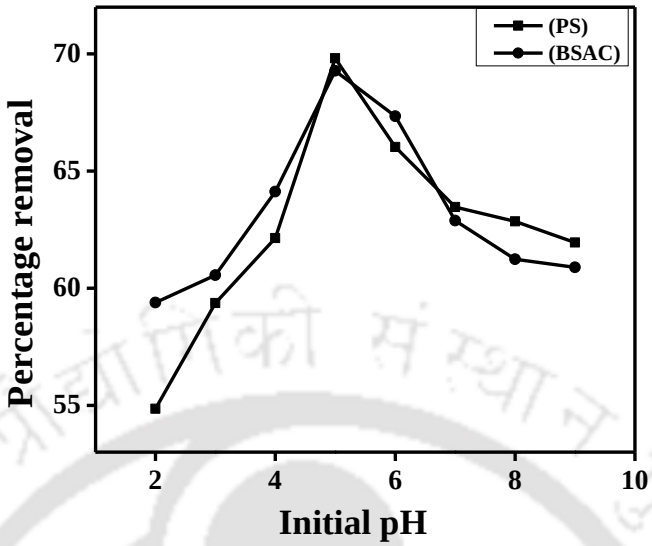

Fig. 3.3: Effect of pH on Nickel (II) removal using BSAC and PS adsorbents. Other experimental conditions were C_o = 50 mg/L, T = 25 ^oC, RPM = 200 and V = 50 mL.

minutes for PS and BSAC respectively. For these cases, the maximal removal % was estimated at 67.12 and 67.34% respectively. Corresponding metal uptake (mg/g) for the adsorbents were 83.9 and 84.17 mg/g respectively. The observations are in good agreement with those available in the literature (Lalhruaitluanga *et al.*, 2011; Hameed *et al.*, 2009).

3.3.2 Effect of pH

Fig. 3.3 presents the effect of pH on the adsorbent performance of BSAC and PS. Corresponding choice of other parameters include adsorbent dosage, Ni (II) solution concentration and contact time are 0.02 g/L, 50 mg/L and 90 (BSAC), 300 (PS) min respectively. It can be observed in these figures that adsorption and metal uptake curves reach a maximum at a certain pH and eventually reduce at higher pH values. For the PS, the % removal and adsorption capacity increased to 69.82% and 87.27 mg/g with an increase in pH

from 2-5. Similarly, for the BSAC the % removal and metal uptake increased to 86.67 mg/g and 69.28% respectively. It can be observed in these figures that adsorption and metal uptake curves reach a maximum at a certain initial pH and eventually reduce at higher initial pH values. These observations are in agreement with that presented in the literature for PS and BSAC adsorbents (Lalhruaitluanga *et al*., 2011; Hameed *et al*., 2009; McKay *et al*., 2008). The enhancement in Ni (II) adsorption with increasing initial pH is due to the competence of both H^+ and metal ion to get adsorbed at lower initial pH which reduced metal ion binding to the adsorbent surface at lower pH. At a higher initial pH, the sorbent surface develops more negative charges and hence can strongly attract more number of metal ions. A further increase in initial pH enables the formation of anionic hydroxide complexes which reduce the availability of the metal ion in the solution and restrict the adsorptive capacity (McLean and Bledsoe (1992)).

3.3.3 Effect of Dosage

The effect of dosage variation on Ni (II) removal using developed adsorbents is presented in Fig.3.4. Corresponding choice of other parameters include pH, Ni (II) solution concentration. The contact time are 5, 50 mg/L and 90 (BSAC), 300 (PS) min respectively. It can be observed that with an increase in dosage from 0.02 to 0.15 g/L, the maximum metal uptake and % removals are 21.3175, 23.185 mg/g and 85.27, 92.74 for PS and BSAC respectively. The enhancement in adsorption for higher dosages is due to the availability of more active sites for binding the metal to the adsorbent surfaces. Similar results are reported in the literature (Lalhruaitluanga *et al.*, 2011; Hameed *et al.*, 2009).

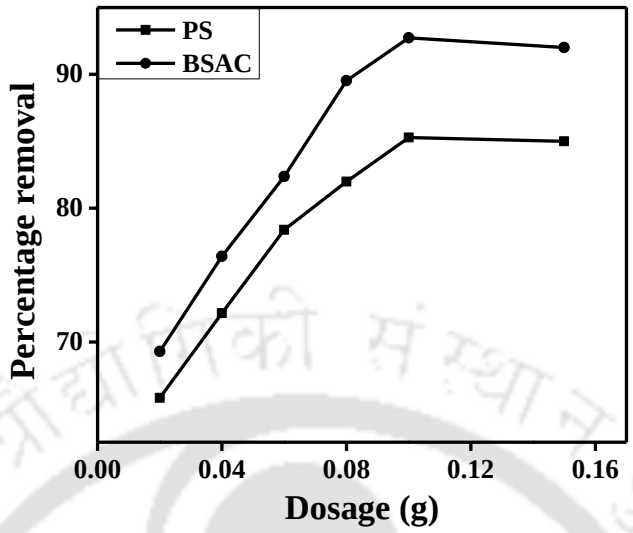

Fig. 3.4: Effect of adsorbent dosage on Ni (II) removal efficiency using BSAC and PS adsorbents. Other experimental conditions were C_o = 50 mg/L, T = 25 ^oC, RPM = 200 and V = 50 mL.

3.3.4 Ni (II) adsorption characteristics of AC using synthetic ELP solutions

The evaluation of Ni (II) adsorption characteristics using synthetic ELP solutions was carried out using commercial activated carbon adsorbent. Based on the preliminary batch adsorption experiments conducted for the adsorption of Ni (II) from aqueous solutions using BSAC adsorbent, the optimal adsorption parameters correspond to a pH of 5, equilibrium time of 90 min and dosage of 2 g/L. Using activated carbon, the optimal set of adsorption parameters for Ni (II) adsorption from synthetic electroless plating solutions correspond to a pH of 10-11, equilibrium time of 120 min and dosage of 4 g/L. While Ni (II) adsorption characteristics were studied for BSAC adsorbent and aqueous solutions in the concentration range of 50-300 mg/L, the Ni (II) adsorption studies with synthetic ELP solutions were carried out in the concentration range of 50-500 mg/L.

Fig. 3.5 (a) and (b) present the variation in metal capacity and removal efficiency respectively with a variation in solution concentration for both ELP and aqueous solutions. It can be observed in Fig 3.5 (a) that the metal uptake varied from 16.84-91.59 mg/g for aqueous solutions in the Ni (II) concentration range of 50-300 mg/L. However, significantly lower metal uptake variations exist (5.56-17.75 mg/g) for the synthetic Ni (II) ELP solutions in the concentration range of 50-500 mg/L. The most relevant literature data for comparison purpose refers to the Ni (II) adsorption data for banana pith based AC adsorbent and electroplating solutions. The reported metal uptake in the literature refers to 11.42 mg/g for a solution concentration of 5000 × 10^{-6}M (28 mg/L). Thus, it is apparent that significantly lower Ni (II) metal uptake values have been obtained for the synthetic ELP solutions in compared to those measured for AC adsorbents for both aqueous (this work) and electroplating (Low *et al.*, 1995) solutions. This indicates that the solution chemistry plays an important role in altering the capacity characteristics of the AC adsorbents.

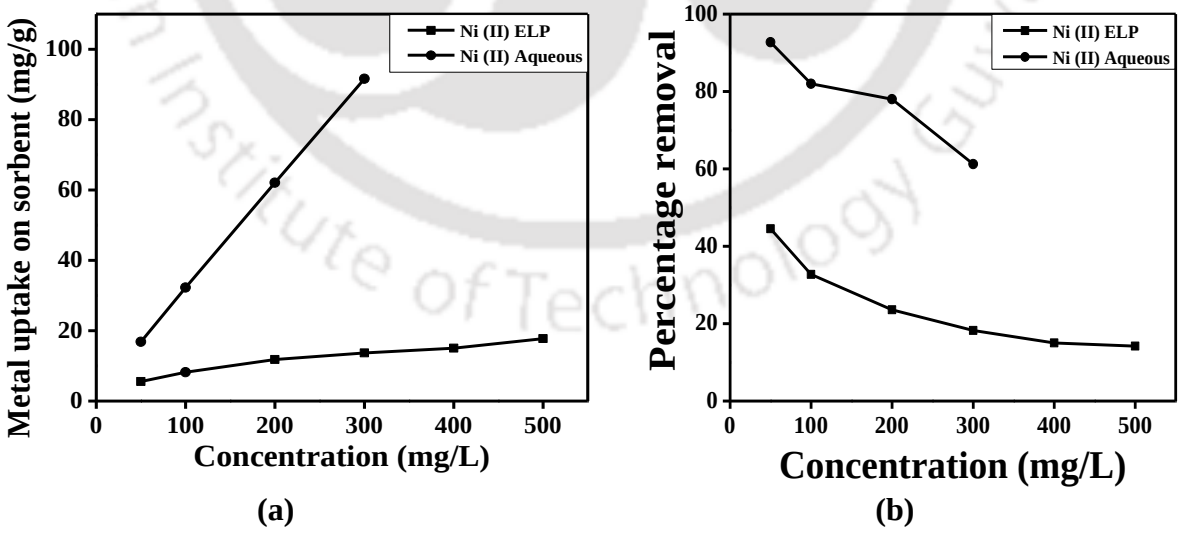

Fig. 3.5: Ni (II) adsorption characteristics for BSAC (aqueous) and AC (synthetic electroless plating solutions) adsorbents: (a) Metal uptake (b) Removal efficiency.

Fig. 3.5 (b) summarizes the removal efficiency characteristics of BSAC and AC adsorbents for aqueous and synthetic ELP solutions respectively. It has been evaluated that the Ni (II) removal efficiencies varied from 92.74-61.23% for aqueous solutions in the concentration range of 50-300 mg/L and 44.54-14.2% for synthetic ELP solutions in the concentration range of 50-500 mg/L. The literature data corresponds to 90.81-2.59 % removal efficiency for electroplating waste solutions for a Ni (II) initial solution concentration of 50-5000 × 10^{-6} M (0.280–28 mg/L). Thus, it is apparent that poor adsorption characteristics exist for synthetic ELP solutions. This is possibly due to variations in solution pH (which was 5 for aqueous phase and 10-11 for synthetic ELP solutions), inclusion of other stabilizing agents such as trisodium citrate for synthetic ELP solutions. Thus, it is inferred that the complex ELP solution chemistry was not favourable for the preferential sorption of Ni (II) on the AC adsorbent.

Table 3.1: Comparative performance indices of PS, BSAC and literature reported adsorbents for Ni (II) removal from aqueous solutions.

Adsorbent	**Present Study**			**Literature**		
	Concentration range(mg/L)	**%Removal**	q_{max} **(mg/g)**	**Concentration range(mg/L)**	**%Removal**	q_{max} **(mg/g)**
Pineapple stem	50-300	85.24	2.4	25-300	96 (Hameed *et al.*, 2009)	119.09 (Hameed *et al.*, 2009)
Bamboo stem	50-300	92.7	121.72	50-300	84.5 (Lalhruaitluanga *et al*, 2011)	52.9 Lalhruaitluanga *et al*, 2011)

Table 3.1 summarizes a comparison of the performance of the low cost adsorbents with respect to the values reported in the literature. The prepared activated carbon adsorbent from bamboo stem provided an adsorption capacity of 121.45 mg/g, which is higher than several native and carbonized adsorbents such as acid treated banana pith (17.06 mg/g), oil palm fibre (1.91 mg/g), coconut husk (8.66 mg/g), moss (27.06 mg/g), solanumelaeagnifolium (6.5 mg/g), alkali treated banana pith (11.42 mg/g), pineapple stem (2.4 mg/g, present work) and bamboo activated charcoal (52.91 mg/g). As shown, the prepared BSAC adsorbent performed significantly better than those presented in the literature, with BSAC metal uptake being 45 % more than the values reported in the literature (Lalhruaitluanga *et al.*, 2011). Thus, the fabricated low cost adsorbents appear to be promising and further research is required towards enhancement of their surface area and other factors which will make them suitable for utilization with real time waste water.

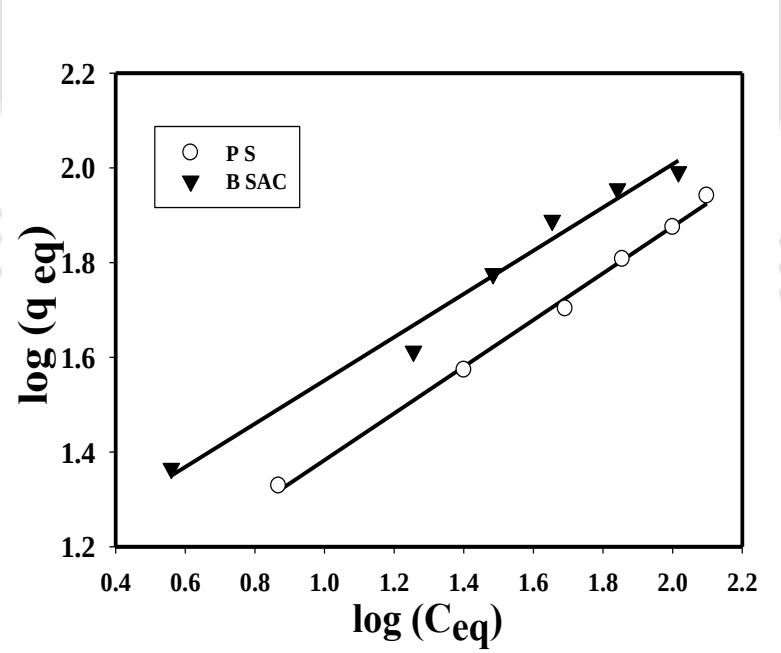

Fig. 3.6: Freundlich isotherm fitness plot for measured Ni (II) adsorption data with BSAC and PS adsorbents.

3.4 Adsorption Equilibrium studies

Amongst various isotherm models such as Langmuir, Freundlich, Redlich–Peterson and Temkin, it was evaluated observed that only Langmuir and Freundlich isotherms fit well to represent the experimental adsorption data. The fitness of Langmuir and Freundlich isotherm models to represent Ni (II) adsorption on the low cost adsorbents BSAC and PS are summarized in Table 3.2. As shown in Fig. 3.6, for both BSAC and PS, the coefficient of correlation (R^2) has been evaluated as 0.9797 and 0.9964 for Freundlich isotherm and 0.9659 and 0.9434 for Langmuir isotherm. The variation of various errors namely RMS, average, correlation (R^2) has been evaluated as 0.9797 and 0.9964 for Freundlich isotherm and 0.9659 and 0.9434 for Langmuir isotherm. The variation of various errors namely RMS, average, maximum, minimum for these isotherms is also presented in the Table 3.2**.** From both error values and coefficient of correlation (R^2), it can be observed that only Freundlich isotherm provided the best fitness towards experimental data for both adsorbents. Corresponding maximum, minimum, average and RMS error values for Freundlich isotherm are 3.414, 0.240, 1.50, and 1.813 for BSAC adsorbent respectively.

Table 3.2: Langmuir and Freundlich isotherms parameters for Ni (II) adsorption on BSAC and PS adsorbents.

Adsorbent	Model	R^2	% Error				Q_{max} (mg/g)		n	Model parameters
			RMS	Average	Max	Min	Exp	Cal		
BSAC	Langmuir	0.9659	116.87	107.16	160.20	18.69	98.07	121.726		b=0.0380 K_R =0.344
BSAC	Freundlich	0.9797	1.813	1.50	3.414	0.240	-	-		K_f=0.9136 n=2.189
PS	Langmuir	0.9434	1.33	11.79	39.28	2.09	85.24	2.40		b = 0.0213 K_R = 0.483
PS	Freundlich	0.9964	0.727	0.5968	1.24	0.076	-	-		K_f= 0.776 n=2.087

The values for the PS adsorbent are 1.24, 0.076, 0.5968 and 0.727 respectively. Further, the evaluated value of K_R indicated that the adsorbents are favourable for adsorption. Hence, it is concluded that adsorption equilibrium studies indicate towards a satisfactory performance of BSAC and PS adsorbents for Ni (II) adsorption (Lalhruaitluanga *et al*, 2011; Hameed *et al.*, 2009).

3.5 Adsorption kinetics

Among various kinetic models such as pseudo first order, pseudo second order and intra particle diffusion, it has been evaluated that only pseudo second order kinetic model fit well to represent the experimental adsorption data (Fig. 3.7 and Fig. 3.8). The fitness of pseudo

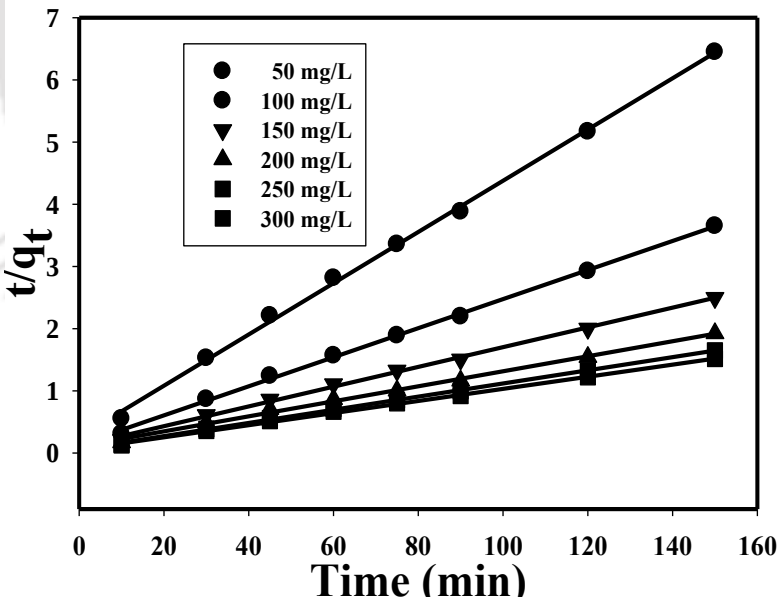

Fig. 3.7: Pseudo second order kinetic model fitness plot for Ni (II) adsorption on BSAC adsorbent.

second order kinetic model to represent Ni (II) adsorption kinetics has been expressed in terms of the coefficient of correlation (R^2), and errors namely RMS, average, maximum and minimum. These are summarized in Table 3.3 and Table 3.4 for BSAC and PS respectively. Within the concentration range of 50-300 mg/L, it can be observed that R^2 values varied from 0.9985-0.9983 and 0.9967-0.9890 for BSAC and PS respectively. For the BSAC, the RMS, average, maximum and minimum errors varied from 7.8-9.1, 4.2-4.8, 21.3-25.1, 0.13-0.11 etc. respectively. For the PS, these errors varied from 16.82-25.23, 7.8-11.9, 57.4-85.1, 0.3-0.27 etc. respectively. The pseudo second order rate constant k_2 is found to decrease with an increase the initial metal solution concentration. This indicates that at lower metal solution concentration equilibrium is attained faster and vice-versa. This is possibly due to the reduction in metal ion diffusion into the boundary layer at higher solution concentration.

Table 3.3: Pseudo-second order kinetic model parameters for Ni (II) removal using BSAC adsorbent.

C_0 (mg/L)	q_e (mg/g)		R^2	$k_2 x 10^{-3}$ (L/min.)	%Error			
	Exp	Cal			RMS	Average	Max	Min
50	23.18	24.27	0.9985	6.5	0.78	4.26	21.33	0.13
100	41.09	42.73	0.9987	3.9	0.75	4.08	20.41	0.09
150	59.76	62.89	0.9976	2.2	1.04	5.59	28.77	0.077
200	77.45	82.64	0.9958	1.3	12.79	6.90	34.77	0.085
250	90.28	94.33	0.9988	1.8	7.89	4.14	21.62	0.17
300	98.07	103.09	0.9983	1.6	6.16	5.9	60.09	4.73

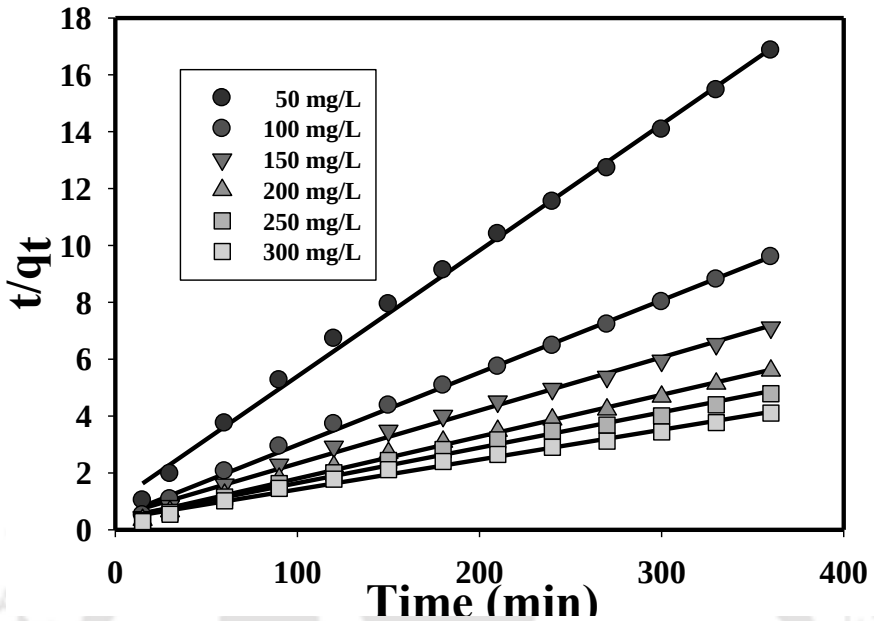

Fig. 3.8: Fitness of pseudo second order kinetic model for Ni (II) adsorption on PS adsorbent.

Table 3.4: Pseudo-second order kinetic model parameters for Ni (II) removal using PS adsorbent.

C_0 (mg/L)	q_e (mg/g)		R^2	$k_2 \times 10^{-3}$ (L/min.)	%Error			
	Exp	Cal			RMS	Average	Max	Min
50	21.31	22.57	0.9967	2.0	16.82	7.80	57.43	0.318
100	37.425	39.37	0.9976	1.4	16.90	7.39	58.74	0.152
150	50.422	53.76	0.9939	0.7	20.46	9.75	68.71	0.419
200	64.15	68.02	0.9956	0.6	18.50	8.66	62.47	0.298
250	74.95	80.64	0.9899	0.3	23.51	11.44	79.31	0.706
300	87.3	95.23	0.9890	0.2	25.23	11.97	85.18	0.273

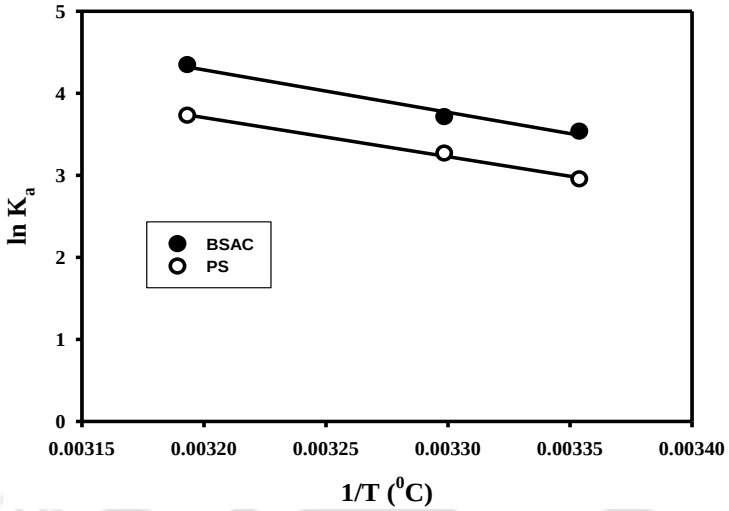

Fig. 3.9: Van't Hoff plot for Ni (II) adsorption on PS and BSAC adsorbents.

3.6 Thermodynamic Parameters

Fig. 3.9 presents the Van't Hoff plot with which thermodynamic parameters for Ni (II) adsorption characteristics on PS and BSAC adsorbents were obtained. Both enthalpy and entropy calculations were conducted in the temperature range of 25 – 35 °C. The thermodynamic parameters, namely, ΔH^o and ΔS^o were evaluated to be 43.07 kJ/mol and 0.173 kJ/K. mol for BSAC adsorbent. Similarly, for the PS, these were evaluated as 39.62 and 0.157 kJ/K. mol respectively. The positive values of ΔH^o and ΔS^o indicate that Ni (II) adsorption with BSAC/PS is endothermic and irreversible, which is in agreement with the findings in the literature (Lalhruaitluanga *et al.*, 2011; Hameed *et al.*, 2009).

3.7 Cost Analysis of the Bamboo stem Activated Charcoal.

Table 3.5 presents a summary of the cost analysis carried out for BSAC and commercial activated carbon. It can be observed that the cost of BSAC is 0.0072 $/g which is comparable

Table 3.5: Cost parameters and analysis of BSAC and commercial AC adsorbents.

S.No.	Head	Unit cost	Adsorbent Cost $\frac{\text{Rs.}}{250\,\text{g}}$
1.	Electricity	$7\ \frac{\text{Rs.}}{\text{kWh}}$	$10\,\text{hrs}\times 2\,\text{kW}\times 7\,\frac{\text{Rs.}}{\text{kWh}} = 140$
2.	Nitrogen Gas	$300\ \frac{\text{Rs.}}{\text{m}^3}$	$1\,\text{m}^3\times 300\,\frac{\text{Rs.}}{\text{kWh}} = \text{Rs.}300$
3.	Phosphoric acid	$1044\ \frac{\text{Rs.}}{\text{L}}$	$\frac{331}{1000}mL\times \text{Rs.}1044 = \text{Rs.}345$
4.	Bamboo stem	$60\ \frac{\text{Rs.}}{5\,\text{kg raw wood}}$	$60\,\text{Rs.}\times\frac{1250\,\text{g powder}}{5\,\text{kg raw wood}}\times\frac{1}{5} = \text{Rs.}12$
Total (items 1 to 4)			797
Miscellaneous Operating Costs (2%)			16
Grand total cost (Retail)			813
Retail cost of adsorbent $\frac{\$}{\text{g}}$			$813\,\frac{\text{Rs.}}{259\,\text{g}}\times\frac{1\ \$}{55\,\text{Rs.}} = 0.057$
Retail Waste stream processing cost index for low cost sorbent $\frac{\$}{\text{L feed}}$			$0.057\,\frac{\$}{\text{g}}\times\frac{0.1\,\text{g}}{50\,\text{mL}}\times\frac{1000\,\text{mL}}{50\,\text{mL}} = 0.114$
Cost of Commercial Activated Carbon			$322\,\frac{\text{Rs.}}{500\,\text{g}}\times\frac{1\ \$}{55\,\text{Rs.}} = 0.011$
Waste stream processing cost index for commercial activated carbon $\frac{\$}{\text{L feed}}$			$0.011\frac{\$.}{\text{g}}\times\frac{1\,\text{g}}{\text{L.}} = 0.011$
Scaling Factor, Ratio of commercial cost index to low cost sorbent cost index			$\frac{0.114}{0.011}\approx 10$

with the cost of commercial activated carbon of 0.0114 $/g. From a waste stream processing perspective, the cost of BSAC is about 0.0144 $/L feed, which is comparable with that of the commercial activated carbon (0.011 $/L feed) (Lalhruaitluanga *et al.*, 2011). Thus, it can be inferred that the prepared BSAC adsorbent is comparable with commercial activated carbon with respect to cost analysis (Radenovic *et al*., 2011). It should be further noted that the cost

calculations provided in Table 3.5 are conceptual and could be further modified to provide a better estimate.

3.8 Summary

This chapter summarized the preparation and characterization of low cost adsorbents from plant (Bamboo and Pineapple) biomass resources in the north eastern region. The adsorbents prepared in this work indicate that BSAC is a promising adsorbent that offers a BET surface area of 116 m^2/g. Further, the BSAC adsorbent provided the highest monolayer adsorption capacity (121.72 mg/g) amongst adsorbents prepared from various other native biomass for the adsorption of Ni (II) from aqueous solutions, and has 45% higher metal uptake than the corresponding bamboo based activated charcoal reported in the literature for aqueous solutions. The performance of PS adsorbent has not been mentioned so far in the literature and this work can serve as a yardstick for further research towards the preparation of pineapple adsorbent with better adsorption and heat resistance characteristics. Further heat treatment research will be promising for BSAC adsorbent, which had been taken up in this work.

Further, based on equilibrium and kinetic studies, the Ni (II) adsorption on both BSAC and PS has been inferred to fit with Freundlich isotherm and pseudo second order model respectively. Further, thermodynamic studies indicated that the biosorption of Ni (II) is endothermic and irreversible in nature. A preliminary cost analysis of the BSAC adsorbent indicates that the cost of the prepared adsorbents is comparable with the commercial activated carbon.

The commercial AC provided very low metal uptake and removal efficiency (%) for synthetic ELP solutions in comparison to obtained data for Ni (II) containing aqueous solutions. This indicates that solution chemistry strongly affects Ni (II) sorption on AC adsorbents.

Chapter 4

Pd (II) Adsorption Characteristics of Commercial AC Adsorbents with Synthetic Electroless Plating Solutions

The results in this chapter are presented in three sections. Section 4.2 details with respect to the surface characterization results of the adsorbent. Section 4.3 presents Pd (II) batch adsorption characteristics of commercial AC. Section 4.4 details with respect to equilibrium, kinetic and thermodynamic model fitness. Finally, summary is presented in section 4.5.

4.1 Introduction:

Literature is scarcely available for the adsorption characteristics of palladium from synthetic electroless/electroplating solutions using activated carbon. Palladium electroless solutions necessarily consist of a stabilizer (Na_2EDTA) in a highly alkaline medium consisting of liquor ammonia. Several studies reported in the literature for palladium recovery present adsorption characteristics for aqueous solutions. Further, cationic surfactants such as CTAB are also added to the electroless plating solutions to maximize plating rates and obtain a good surface finish. Hence, the combinatorial role of stabilizer, liquor ammonia and surfactants to influence the adsorption characteristics of palladium over activated carbon has not received any attention and is the objective of this work. Further, sonication assisted adsorption has also been relatively less studied and the dominance of adsorption/desorption characteristics with the supplement of ultrasound during adsorption is an interesting area of research and needs further investigation and insights. With these limitations in literature, this work addresses the adsorption characteristics of palladium on commercial activated carbon using synthetic electroless plating

solutions. A deeper objective of this work is to also examine the role of ultrasound in influencing the adsorption characteristics of palladium from electroless plating solutions.

Adsorption characterization has been carried out using Fourier transform infrared (FTIR) spectral analysis, Brummer- Emmett-Teller (BET) adsorption, Laser Particle Size Analysis (LPSA) Scanning Electronic Microscopy (SEM) and Energy dispersive X-ray spectroscopy (EDS) analysis. The role of sonication as a supplement to favour mass transfer enhancement has also been investigated for various cases. For optimized adsorbent dosage, contact time and pH, adsorption experiments were conducted for wide range of Pd (II) solution concentrations (50 – 500 mg/L). The specific influence of various additives such as CTAB (surfactant), Na_2EDTA (stabilizer) and liquor ammonia (NH_3) on the adsorption characteristics of Pd (II) using commercial activated carbon was addressed. Equilibrium adsorption data was tested using various isotherm models such as Langmuir and Freundlich models. Both pseudo first order and second order kinetic models were evaluated for their fitness to represent the kinetics of adsorption. The next section addresses results obtained from surface characterization.

4.2 Characterization of the Adsorbent

4.2.1 Surface area Analysis

Adsorbents with higher BET surface area enable the reduction in adsorbent dosage and contribute to adsorption efficiency (Brunauer *et al*., 1938). An estimate of the AC surface area and pore size was obtained using the N_2 adsorption/desorption isotherm at 77 K with the BET surface area analyser. Prior to the measurement, the samples were degassed at 200 ^oC in vacuum for 60 min. Fig. 4.1 (a) presents the N_2 adsorption-desorption isotherms of AC adsorbent. It can be observed that the isotherms were of type IV and H_4 hysteresis loop, which according to IUPAC (International Union of Pure and Applied Chemistry) classification indicated the

existence of narrow slit-like pores (Altunoglu., 1994). Also, it can be seen that the isotherm grew sharply during the early stages of adsorption which is due to the micropore filling effect.

Fig. 4.1 (b) represents Barrett-Joyner-Halenda (BJH) pore size distribution (Sing, 1985; Gelb, 1999) of AC that was obtained for both adsorption and desorption. The pore size distribution indicated that the adsorbent possessed cylindrical pores and the BJH analysis provided sharper peaks than the isotherm data presented in Fig. 4.1 (a). Fig. 4.1 (c) illustrates the variation obtained in pore area distribution with pore diameter. It can be seen that the pore area of the adsorbent was more sensitive with respect to the adsorption process than with the desorption which is in agreement with the trends presented in the literature (Sing, 1985; Gelb, 1999). In summary, the surface area analysis indicated that the AC possessed good surface texture properties (Table 4.1) and pore size distribution.

Table 4.1: Physical properties of commercial AC adsorbent.

Surface Properties of Activated Charcoal	Value
BET Surface Area (m^2/g)	1057.17
BET Monolayer Volume (cc/g)	242.89
Langmuir surface Area (m^2/g)	1197.5
Langmuir Monolayer Volume (cc/g)	275.123
Total Pore Volume (mL/g) (Ps/Po=0.9814, Adsorption)	0.9814

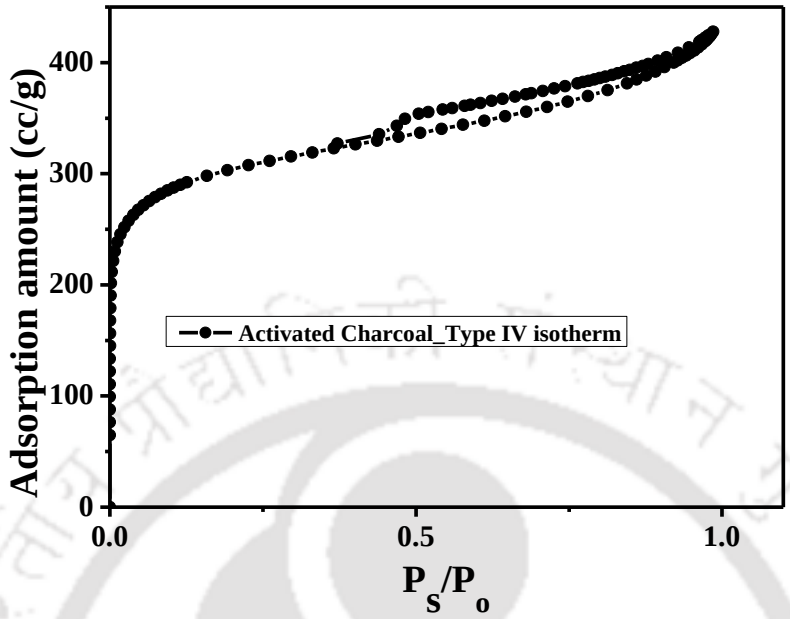
Adsorption amount (cc/g)
400
300
200
100
0
0.0
0.5
1.0
P_S/P_o
Activated Charcoal_Type IV isotherm

(a)

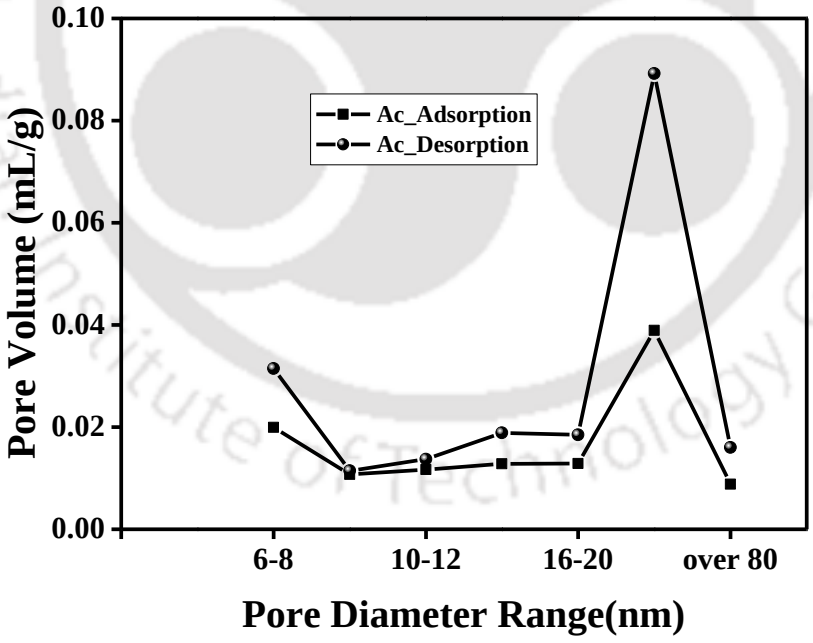
Pore Volume (mL/g)
0.10
0.08
0.06
0.04
0.02
0.00
Ac_Adsorption
Ac_Desorption
6-8
10-12
16-20
over 80
Pore Diameter Range(nm)

(b)

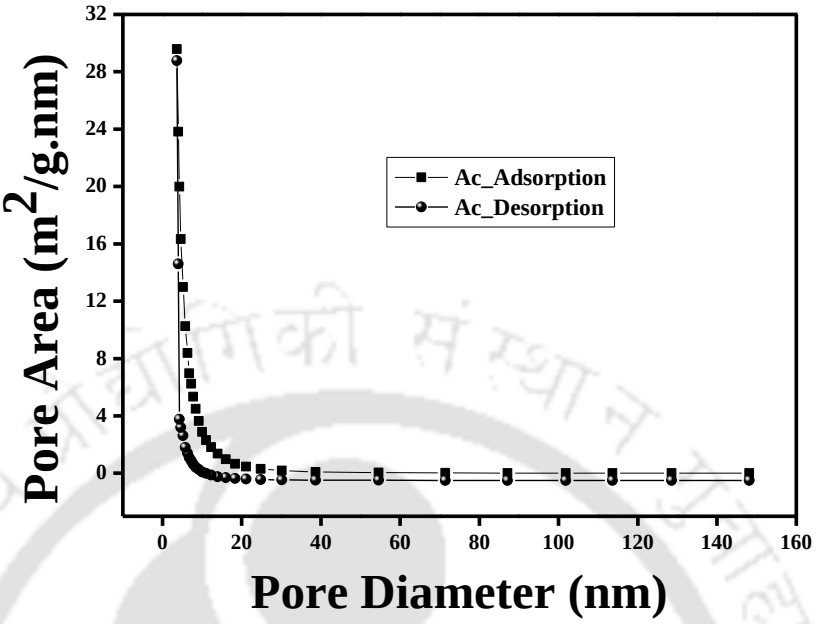

(c)

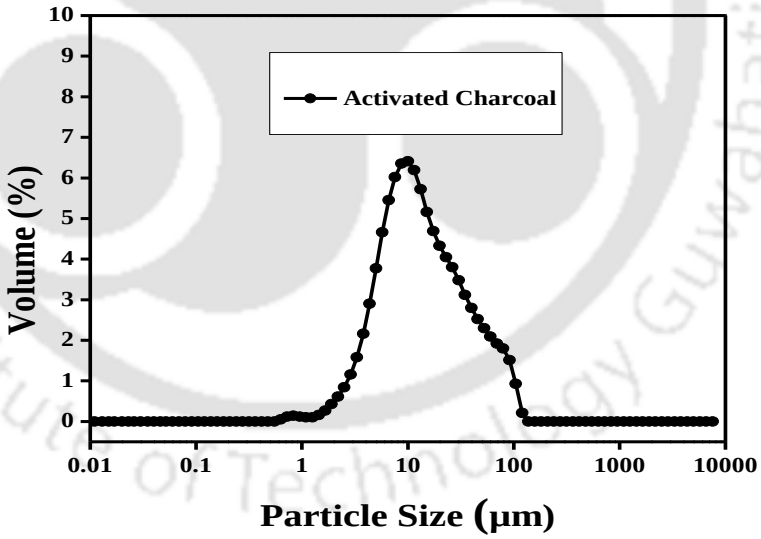

(d)

Fig. 4.1: Surface properties of commercial AC adsorbent (a) Hysteresis isotherm (BET) (b) Variation of pore volume with pore diameter (BET) (c) Variation of pore area with pore diameter (BET) (d) Particle size distributions (LPSA).

4.2.2 Particle size distribution

Fig. 4.1 (d) represents the particle size distribution of activated charcoal, using which the average particle size of the AC was evaluated as 25.47 µm. The narrow particle size distribution and average particle size of the adsorbent is promising given the fact that particle size strongly influences the metal uptake and efficiency (Sharififard *et al*.,, 2012; Gelb, 1999)

4.2.3 FTIR Analysis

FTIR analysis was conducted for both raw AC sample and samples obtained after Pd (II) batch adsorption experiments. The FTIR analysis (Fig. 4.2) indicated the existence of several functional groups on the adsorbent surface. For the raw sample (AC), several peaks were found at the wave number values of 3722, 3616, 3296, 2333, 1700, 1521, 1340 and 956 cm^{-1}. For the case where adsorbent was contacted with Pd aqueous solutions, peaks were observed at wave numbers of 3736, 3624, 3288, 2970, 2416, 2301, 1706, 1510, 1338 and 962 cm^{-1}. For the AC adsorbent that was contacted with Pd, Na_2EDTA and liquor NH_3 but not CTAB, the peaks were observed at wavenumbers of 2924.1, 2858.9, 2364.7 and 2330.3 cm^{-1}(Pd (E)-AC-AAA). On the other hand, for the case of AC that was contacted with CTAB using both agitation and sonication assisted adsorption, the peaks were observed at 3738, 3612, 3288, 2970, 2414 , 2291, 1705, 1527, 1346 and 964 cm^{-1} (Pd (E)-AC-SAA) with a distinct peak observed at 966 cm^{-1} for the case of only agitation assisted adsorption. Therefore, comparing the FTIR peaks obtained for all cases, Pd (II) adsorption corresponds to common peaks that were obtained at wave numbers of 3736, 3624, 3288, 2970, 2416, 2301, 1706, 1510, 1338, and 962 cm^{-1} and Pd (II) adsorption in the presence of CTAB indicated the existence of two peaks at 1706 and 962 cm^{-1}. Also, several spectral peaks can be observed to have shifted from low to high intensity.

Thus, spectral functional group interactions indicate C-H aliphatic stretching (2920.2 cm^{-1}), -O-CH_3 of aldehyde group (2858.5 cm^{-1}), stretching of C-O or O-H deformation in carboxylic acids (1647.3 cm^{-1}). Thus, it is apparent that Pd (II) interaction with carbonyl and carboxyl groups enabled shift in the peaks and their intensities and thereby infer that palladium ions have chemical interaction with surface chemical groups of activated charcoal during the adsorption process. The chemical interactions and bond formations of Pd (II) with carbonyl and carboxylic groups are because of the lone pair of electrons present on O atom and due to the partial negative charge present on both C and O atoms, which is dependent on the direction in which the direction in which the bond shift occurs (Sharififard *et al*., 2012; Dastgheib *et al*., 2002; Ma *et al*., 2013).

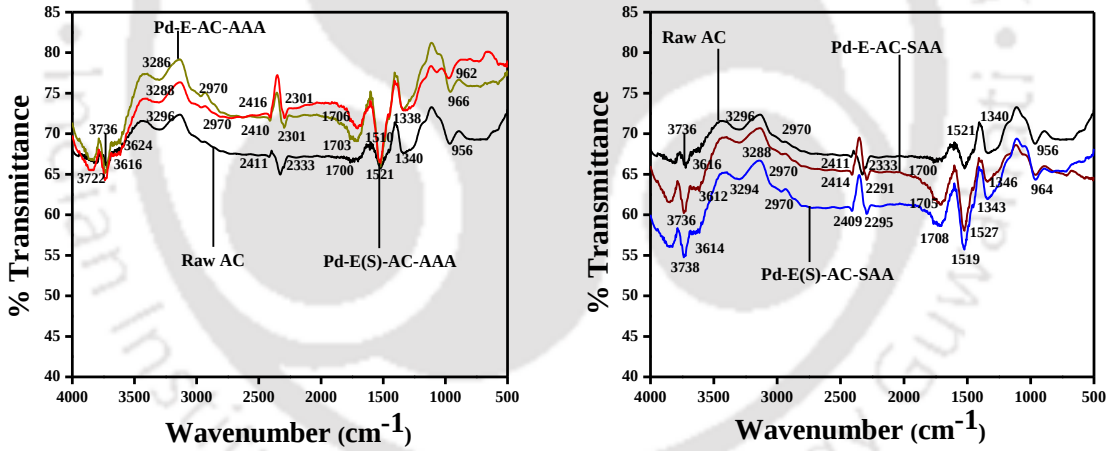

(**a**) Agitation assisted adsorption (**b**) Sonication assisted adsorption

Fig. 4.2: FTIR spectra of AC adsorbent before and after Pd adsorption for (a) agitation and (b) sonication assisted Pd (II) adsorption.

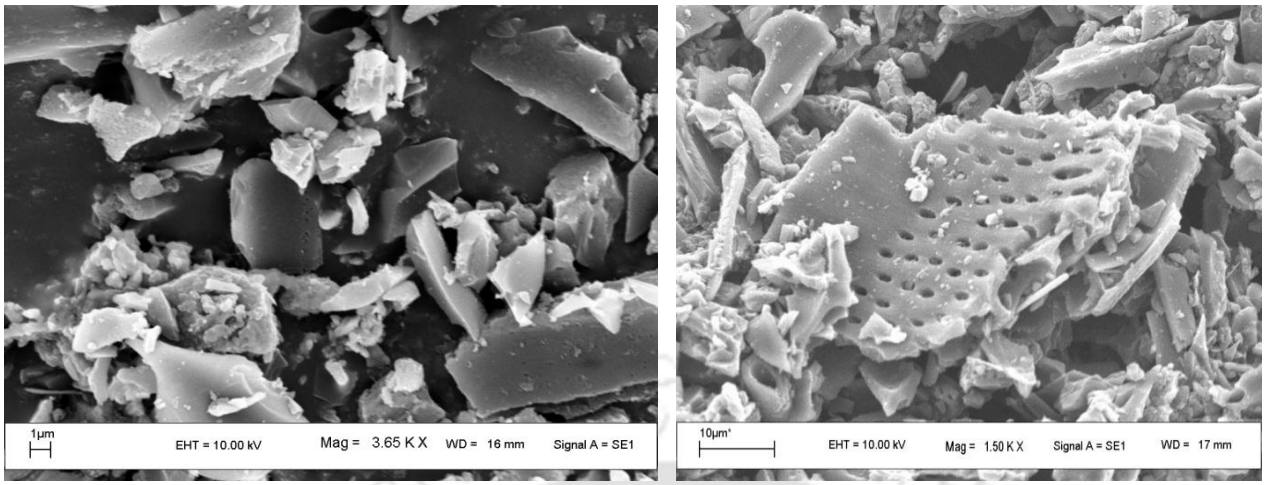

(a) Before adsorption of AC **(b)** After Pd adsorption of AC

Fig. 4.3: Scanning electronic micrographs (SEM) of the AC adsorbent before and after agitation assisted Pd (II) adsorption.

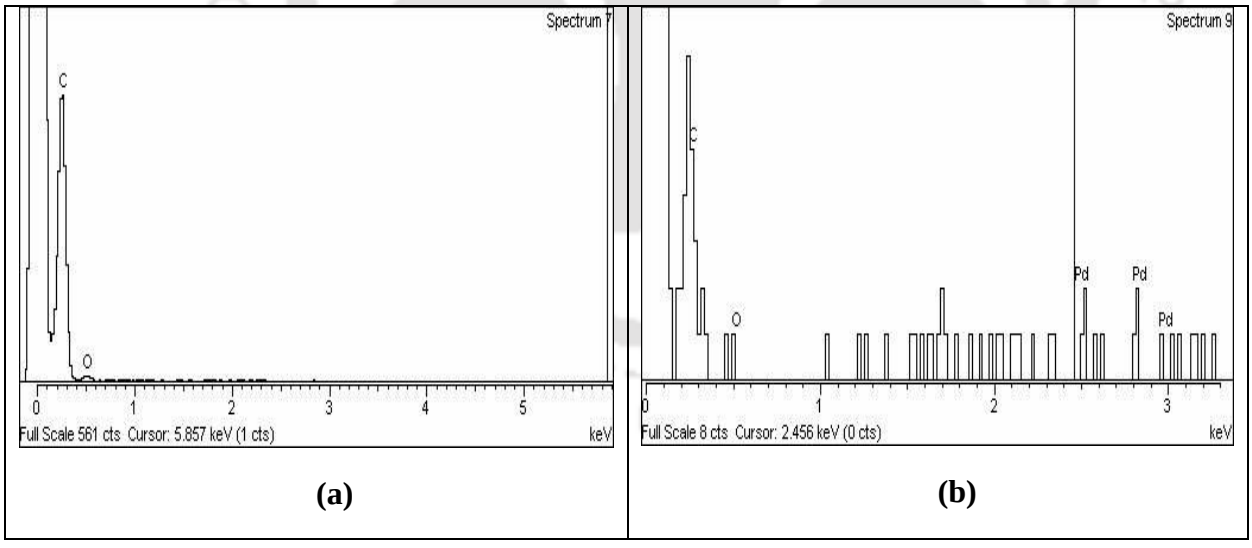

(a) **(b)**

Fig. 4.4: Energy dispersive X-ray spectra (ED) of AC (a) before and (b) after Pd (II) adsorption.

Table 4.2: ED spectral analysis of AC adsorbent before and after Pd (II) adsorption with 500 mg/L initial Pd solution concentration.

Element	Before Adsorption Weight%	After Adsorption Weight%
Carbon	88.77	52.39
Oxygen	11.23	13.68
Palladium	0.0	33.93

4.2.4 SEM analysis

Fig. 4.3 (a) and (b) respectively illustrate the SEM based surface morphology of the raw adsorbent (AC) and adsorbent obtained after adsorption with synthetic Pd (II) electroless plating solution. It can be observed from the SEM images that palladium adsorption occurred as indicated by a new bulky coated layer on the porous surface and Pd occupied the surface porous texture of the AC. The obtained images are similar to those reported by Sharififard *et al*., (2012).

4.2.5 Energy dispersive X-ray spectroscopy (EDS) analysis

Fig. 4.4 (a) and (b) present the EDX spectra of the raw adsorbent and Pd adsorbed AC respectively. Corresponding quantitative information is presented in Table 4.2. It was observed in the spectra that for the raw adsorbent case, carbon and oxygen elements existed on the adsorbent surface. This is in accordance with the literature data (Sharififard *et al*., 2012), where it was conveyed that raw AC adsorbents constitute several carbon and oxygen groups that could be acidic (carboxylic and lactonic), non-acidic (ether, quinine and carbonyl), phenol groups and anhydride groups. Further, for the Pd adsorbed AC, it can be observed that in addition to the carbon and oxygen peaks, Pd specific peaks have been identified in the EDS analysis. The typical composition of Pd adsorbed on the AC surface is summarized in Table 4.2, which

indicates that the Pd content on the spent adsorbent is 33.93 %. Corresponding Pd metal uptake on the AC adsorbent which is obtained from batch adsorption experiments is 44.03 mg/g for a Pd solution concentration of 500 mg/L. Thus, the evaluated metal uptake and the measured Pd concentration on the adsorbent are in good agreement.

4.2.6 PZC Analysis

Using pH drift method, the PZC value of the AC was estimated to be 9.5. In the literature, it was reported that for AC and BPMC, PZC is 6.5 (Sharififard *et al*., 2012). However, Senthil Kumar *et al*., (2006) reported that the PZC for AC is about 8 – 8.5. Considering these values, the obtained PZC value for the commercial AC is close to that obtained by Senthil Kumar et al. (2006) and is marginally higher than the value reported by the authors. In conjunction with the observed Pd adsorption trends that confirm higher adsorption at initial pH values above 10, the obtained PZC value of 9.5 is appropriate. This is relevant for the given hypothesis that adsorption is always favoured for the case where pH is greater than the PZC. The same statement has also been presented by Sharififard *et al*., (2012) based upon their experimental investigations for Pd (II) adsorption from aqueous solutions.

4.3 Batch adsorption studies

4.3.1 Optimality of adsorption process parameters

Agitation assisted adsorption batch experiments were conducted using synthetic Pd electroless plating solutions. The composition of the solution corresponds to the data presented in Table 2.1 without CTAB. Based on the adsorption characteristics (metal uptake and removal efficiency), preliminary batch experiments were conducted to identify optimal operating conditions such as equilibrium time (min), pH and dosage (g).

Firstly, the optimality of the contact time was targeted by considering a fixed choice of adsorbent dosage (1 g/L), pH (9-10) and initial Pd (II) solution concentration of 50 mg/L. For the corresponding optimized contact time, second set of batch adsorption experiments were conducted for variant pH (2-14), fixed dosage (1 g/L) and initial Pd solution concentration of 50 mg/L and optimized equilibrium times (obtained from the first set of Adsorption experiments). After identifying the optimal pH as 10, the third set of batch adsorption experiments were conducted for the fixed choice of contact time, pH (obtained from the second set of adsorption experiments) and Pd (II) plating solution concentration 50 mg/L, and the adsorbent dosage variation (1–6 g/L) was examined for the optimality of adsorbent characteristics. Finally, the adsorption performance of AC was studied for various solution concentrations (50-500 mg/L), by selecting all the other parameters obtained from preliminary adsorption studies mentioned above. Results obtained from the three sets of adsorption experiments are presented as follows.

4.3.1.1 Effect of contact time

Fig. 4.5 (a) shows the variation of metal uptake and removal efficiency with variation in contact time. From the figure, it can be observed that the minimum time required to reach equilibrium (i.e., maximum adsorption) is 300 min. For this case, the maximum % removal and metal uptake (mg/g) have been evaluated as 68.4 and 34.2 respectively. Similar results were reported by Sharififard *et al*., (2012) for Pd removal from aqueous solutions using AC adsorbent.

4.3.1.2 Effect of pH

Fig. 4.5 (b) presents the effect of pH on the Pd (II) adsorption characteristics using AC. It can be identified that the optimum pH was 10 where maximum % removal (62.94) and metal uptake (31.14 mg/g) have been obtained. pH of the solution affects metal ion solubility, concentrations

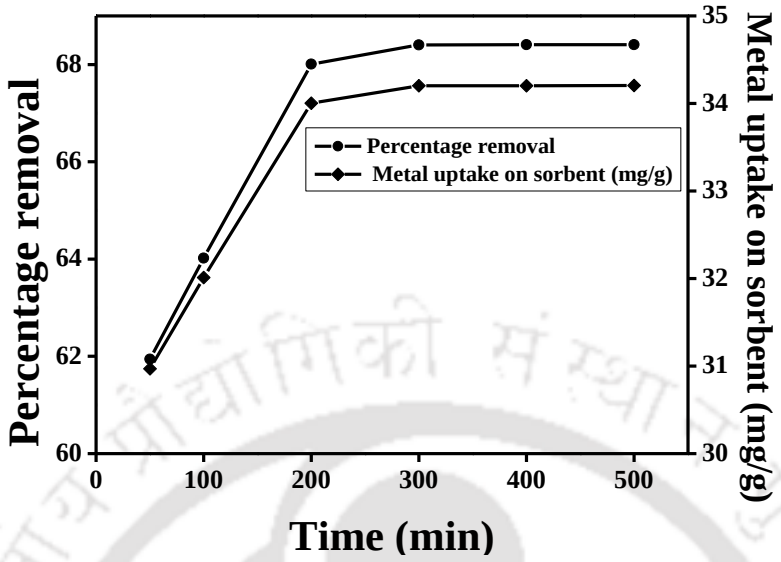

Fig. 4.5 (a): Effect of contact time (min) on the Pd (II) removal efficiency for commercial AC adsorbent.

of counter ions on the adsorbent functional groups and degree of ionization of the adsorbate. It can be observed that the metal removal increased with an increase in pH from 2 to 10 after which it steadily declined. At low pH, H^+ enables protonation effect and this does not favour the adsorption of Pd (II) on AC due to the competitive adsorption of NH_4^+ and Pd (II) on the active sites (Saria, 2009; Ma, 2006). However, as pH increases, protonation effect reduces and the availability of OH^- on the adsorbent surface favours the electrostatic attraction of the positively charged Pd (II) ions. Beyond a pH of 10, there might be complexification of NH_3 with Pd (II), which does not favour further adsorption of Pd (II). For aqueous solutions, an optimal pH of 2 has been suggested Sharififard *et al*., (2012), which indicates the significance of NH_3 in affecting the optimality of pH in this work. The evaluated maximum adsorption of Pd (II) at a pH of 10 is in good agreement with the adsorption of Pd (II) from leached cyanide solutions (Snyder's et al., 2013).

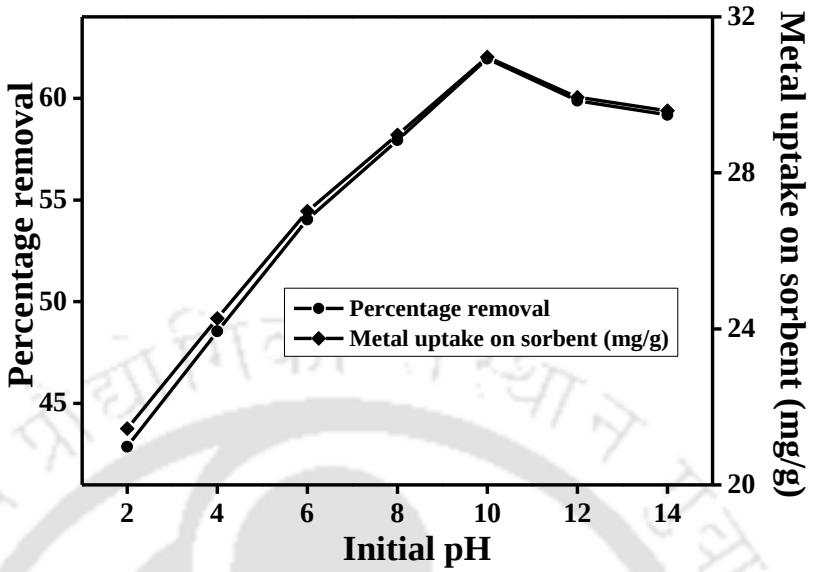

Fig. 4.5 (b): Effect of pH on the Pd (II) removal efficiency for commercial AC adsorbent.

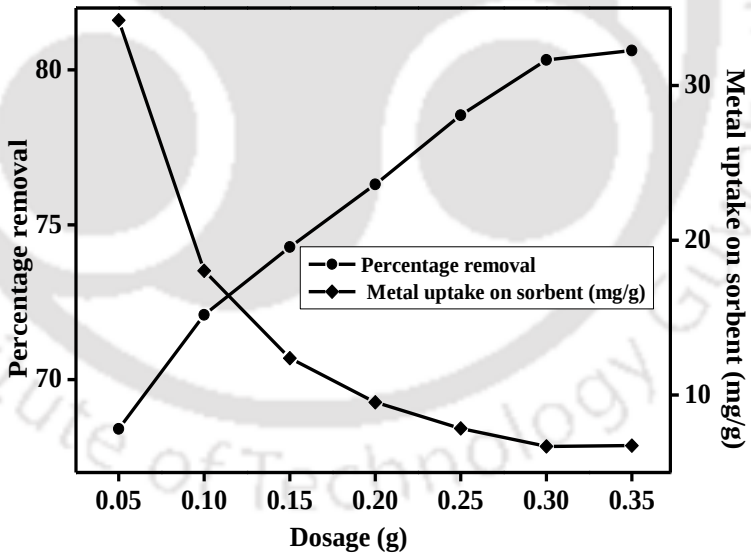

Fig. 4.5 (c): Effect of adsorbent dosage on the Pd (II) removal efficiency for commercial adsorbent.

4.3.1.2 Effect of Dosage

The influence of adsorbent dosage on palladium removal using AC is shown in Fig. 4.5 (c). From the figure, it can be observed that increasing adsorbent dosage from 1 to 7 g/L enhanced metal removal (80.32 %), which is also in agreement with the lower average particle size (25.7 µm) of the adsorbent. The enhancement of adsorption with an increase in adsorbent at higher adsorbent dosage is due to the enhancement in adsorbent surface area and availability of more metal active sites. Similar values for optimal adsorbent dosage have been presented in the literature for Pd (II) adsorption from aqueous solutions. The capacity reduces with an increase in adsorbent dosage due to significant increase in the denominator (weight of adsorbent after adsorption) in comparison to the enhancement in the numerator (metal adsorbed due to more active sites).

4.3.2 Adsorption Characteristics for Synthetic Electroless Plating Solutions

In this work, the synthetic electroless plating solution compositions have been considered to obtain insights into the adsorption characteristics of Pd (II) adsorption from complex solutions. Both variations in palladium solution and surfactant concentrations were considered to obtain sufficient data with which adsorption characteristics can be analysed and better understood. For the cases, the adsorption experiments have been conducted using optimized operating parameters (contact time 300 min, pH 10 and dosage 6 g/L). Composition variations have been targeted for three different sets of experiments. In the first set of experiments, only agitation assisted adsorption of a single synthetic electroless plating solution composition without surfactant has been studied at various levels of dilution. The second set of experiments involved both agitation assisted adsorption and sonication assisted the adsorption for same Pd (II) compositions in the

presence of 2 CMC surfactant concentrations in the original composition. Finally, the third set of experiments were conducted at variant surfactant solution concentrations (1–4 CMC) for similar palladium solution compositions studied in the first and second experimental sets. Various compositions investigated in this work have been summarized in Table 2.1.

4.3.2.1 Agitation assisted adsorption and Sonication assisted adsorption of Pd (II) from synthetic electroless plating solutions.

Fig. 4.6 (a) presents the adsorption characteristics of Pd (II) on activated charcoal for the case involving synthetic electroless plating solutions without CTAB surfactant. As shown, for both cases, i.e. agitation assisted adsorption (Fig. 4.6 (a)–(i)) and sonication assisted adsorption (Fig. 4.6 (a)–(ii)), with on increasing Pd (II) solution concentrations, while capacity (or metal uptake) increased, the metal removal efficiency reduced. For the case of agitation assisted adsorption, the metal uptake and removal percentage varied from 5.76–43.33 mg/g and 69.12–52 % respectively with a variation in Pd solution concentration from 50–500 mg/L. On the other hand, for the sonication case, the metal uptake and removal percentage varied from 6.34–45.5 mg/g and 76.12-54.61 % respectively with variant Pd solution concentration. Thus, it is apparent that both agitation and sonication assisted adsorption provided similar adsorption characteristics with only insignificant improvement in the capacity values achieved with sonication assisted adsorption. However, it is important to note that while agitation assisted adsorption involved a time period of 300 minutes, sonication assisted adsorption was carried out for 120 min. Therefore, sonication could be considered to reduce the time required to achieve mass transfer equilibrium for Pd (II) adsorption on activated charcoal.

The enhancement in metal uptake with increasing concentration of noble metal in the solution is due to the increased driving force for mass transfer at higher concentration gradients. At lower

solution concentrations, Pd (II) could bind with the active sites and hence could provide higher removal efficiency. On the other hand, the reduction of metal removal with increasing metal concentration is due to the reduction in available active surface area at higher noble metal loading.

Table 4.3 summarizes a comparison of evaluated Pd (II) metal uptake from synthetic electroless plating with the data available in the literature for aqueous solutions. It can be observed that the evaluated metal uptake values are comparable with those evaluated for aqueous solutions with activated charcoal. Only for chitosan modified adsorbents higher metal uptake have been obtained and this is due to the enhanced adsorption characteristics of chitosan modified resins. These resins cannot be compared with the activated charcoal adsorbents, given that the cost of activated charcoal is significantly lower than the cost of these resins. Amongst the available data, the data presented by Sharififard *et al*., (2012) provides the best data in terms of maximum metal uptake. For aqueous solutions, indicated that the adsorption capacities varied from 5.3-35.57 mg/g for a variation in palladium solution concentrations from 50–300 mg/L. In comparison with the data available in the literature for the adsorption of Pd (II) from aqueous solutions using AC, it can be observed that the capacities obtained in this work indicate lower metal uptake (32.41 mg/g) at higher Pd solution concentration (300 mg/L). Thus, it is apparent that the adsorption characteristics of synthetic electroless plating solutions are significantly different from those obtained with the aqueous solutions and this is due to the complex chemistry involved with other additives such as Na_2EDTA and liquor ammonia.

Table 4.3: A summary of Pd (II) metal uptake data for various adsorbents.

Adsorbent	Solution	Pd solution concentration (mg/L)	Adsorbent Capacity (mg/g)	Reference
Activated carbon	Aqueous	50-300	5.3-35.7	(Sharififard *et al*., 2012).
BPMC	Aqueous	50-300	6-43.4	(Sharififard *et al*., 2012).
Activated carbon	Aqueous chloride solution	20-225	1.5-27	(Kasaini *et al*., 2000)
Cross linked chitosan resin	Aqueous	50-400	9.5-109.7	(Fujiwara *et al*., 2007)
Racomitrium lanuginosum	Aqueous	25-300	5-30.2	(Saria *et al*. 2009)
BTICF	Aqueous	43.8-48.8	22.4-27.5	(Ma *et al*., 2006)
Thiourea-modified chitosan	Aqueous	10-400	8.28-112.4	(Foersterling *et al*., 1990)
Activated carbon	Synthetic ELP solution	50-500	5.76–43.33 (Agitation assisted adsorption)	This work
Activated carbon	Synthetic ELP solution	50-500	6.34–45.5 (Sonication)	This work
Activated carbon	Synthetic ELP solution + CTAB	50-500	6.69–50.13 (Agitation assisted adsorption)	This work
Activated carbon	Synthetic ELP solution + CTAB	50-500	7.52–60.03 (Sonication)	This work

4.3.2.2 Pd (II) adsorption from ELP solutions containing CTAB surfactant

For both agitation (Fig. 4.6 (b)–(i)) and sonication assisted adsorption (Fig. 4.6 (b)–(ii)). Fig. 4.6 (b) summarizes the variation of adsorption capacities and removal for Pd (II) adsorption on AC in the presence of CTAB at its solution concentration of 2 CMC. As shown, the Pd (II) adsorption characteristics on AC are significantly affected due to the presence of the surfactant. A typical adsorption characteristic of heavy and noble metals from aqueous solutions involves a simultaneous enhancement in capacity and reduction in removal efficiency with increasing metal solution concentration. While this trend is seen even in the presence of CTAB surfactant, there is a significant increase in the adsorption parameters when compared to the ELP solutions without

surfactant. The significant increase in metal uptake is attributed to the presence of the surfactant which alters the pertinent interfacial and surface characteristics of the adsorbent.

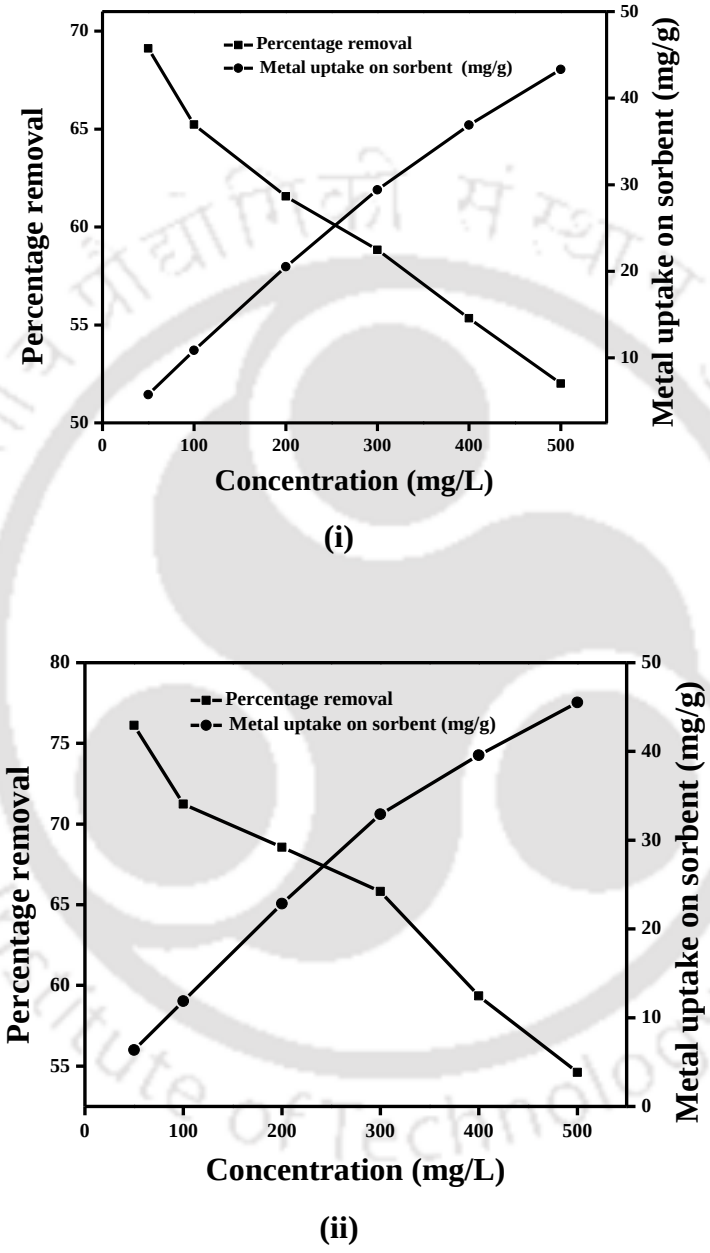

Fig. 4.6(a): Pd(II) adsorption characteristics for synthetic electroless plating solutions not containing CTAB surfactant (i) agitation assisted adsorption and (ii) sonication assisted adsorption.

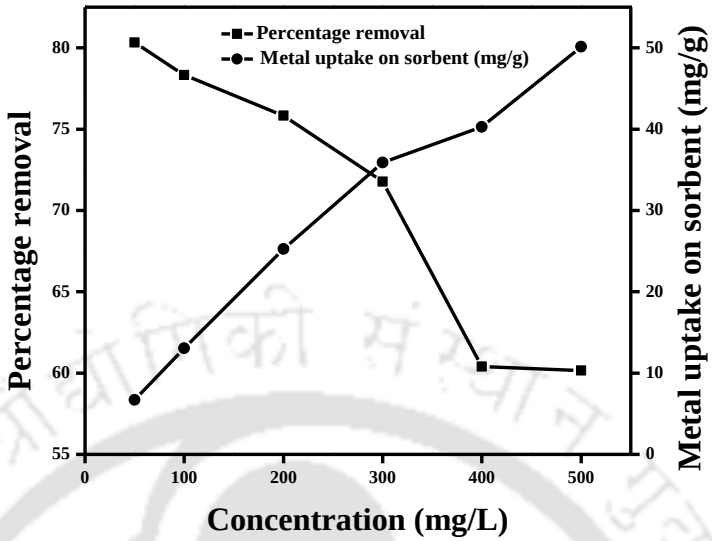

(i)

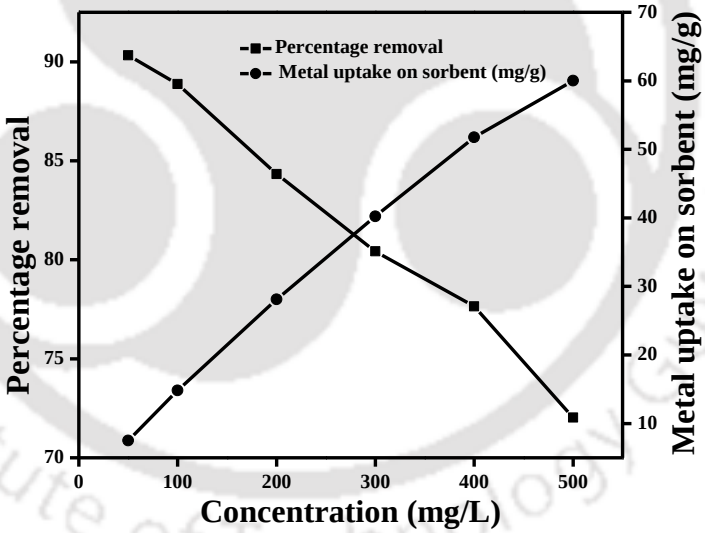

(ii)

Fig. 4.6(b): Pd(II) adsorption characteristics for synthetic electroless plating solutions containing CTAB (2 CMC) surfactant (i) agitation assisted adsorption and (ii) sonication assisted adsorption.

As shown in Fig. 4.6 (b)–(i), for the agitation assisted adsorption case, the capacities and % adsorption varied from 6.69–50.13 mg/g and 80.32–60.16% with variation in Pd solution concentration from 50–500 mg/L. On the other hand, for the case of sonication assisted adsorption, Fig. 4.6 (b)-(ii) the capacities and % adsorption varied from 7.52–60.03 mg/g and 90.32–72.03 % with variation in Pd solution concentration from 50–500 mg/L. Therefore, once again, it can be inferred that sonication did not significantly enhance the capacity and removal percentage when compared to the agitation assisted adsorption. The increase in metal uptake and adsorption efficiency values can again be attributed to the enhancement of adsorbent characteristics due to presence of the surfactant. In the literature, only one article (Ahn *et al*., 2009) addressed the removal of Cd (II) from aqueous solution using activated carbon impregnated with anionic surfactants. No literature data is thus available for the adsorption of surfactant containing Pd (II) solutions.

Table 4.3 summarizes the comparative variation of Pd (II) adsorption metal uptake from synthetic ELP solutions containing surfactant. In this work, the metal uptake for Pd solution concentration of 300 mg/L is about 34 mg/g. This is in good agreement with the value reported in the literature (35.57 mg/g for a similar solution concentration by Sharififard *et al*. (2012). Also, the removal efficiency in this work is significantly lower (80.32%) than that reported by the authors (98%). Thus, the generalization of relating experimental adsorption data obtained for Pd (II) aqueous solution towards the design and operation of an adsorption process for electroless plating solution is not applicable, as significant differences have been evaluated for removal efficiency.

4.3.2.3 Effect of surfactant solution concentration

Fig. 4.6 (c)-(i) and (ii) respectively present the variation of metal uptake and removal efficiency for the agitation assisted adsorption of Pd (II) on activated charcoal for various cases of surfactant solution concentration (1–4 CMC). As shown, the metal uptake capacity increased with increasing surfactant solution concentration, which indicates that the insitu adsorption of surfactant on AC significantly favoured Pd adsorption as it leads to the improvement in the surface properties of the adsorbent. For a variation in Pd solution concentration from 50–500 mg/L, the metal uptake and removal efficiency varied from 6.31–6.8 mg/g and 75.78–56.16% respectively (1 CMC), which increased to 6.69-50.13 mg/g and 80.32-60.16% respectively at 2 CMC surfactant concentration and 7.19-51.83 mg/g and 86.32-62.19% respectively at 4 CMC surfactant concentration. Similar adsorption characteristics have been observed (Fig. 4.6 (c))., (iii and iv) for the sonicated assisted adsorption, where the metal uptake and efficiency respectively varied from 7.36–59.75 mg/g and 88.3–71.70% for 1 CMC surfactant concentration, 7.52–60.03 mg/g and 90.32–72.03% for 2 CMC surfactant concentration and 7.81–62.46 mg/g and 93.82–74.96% for 4 CMC surfactant concentrations. Once again it can be analysed that sonication performed slightly better than agitation assisted adsorption of Pd (II). Thus, it is clearly evident that increasing surfactant solution concentration increased Pd adsorption in comparison with the case where surfactant was not involved. This is attributed to the role of surfactant adsorption on activated charcoal adsorbent.

The experimental adsorption data has also been analysed with respect to the variation of surfactant concentration for a fixed of palladium solution concentration. Using agitation assisted adsorption, Fig. 4.6 (d) summarizes the variation of metal uptake (i) and removal efficiency (ii)

with surfactant solution concentration (1–4 CMC) for various cases of feed Pd solution concentration (50–500 mg/L). As shown, an increase in both surfactant and palladium solution

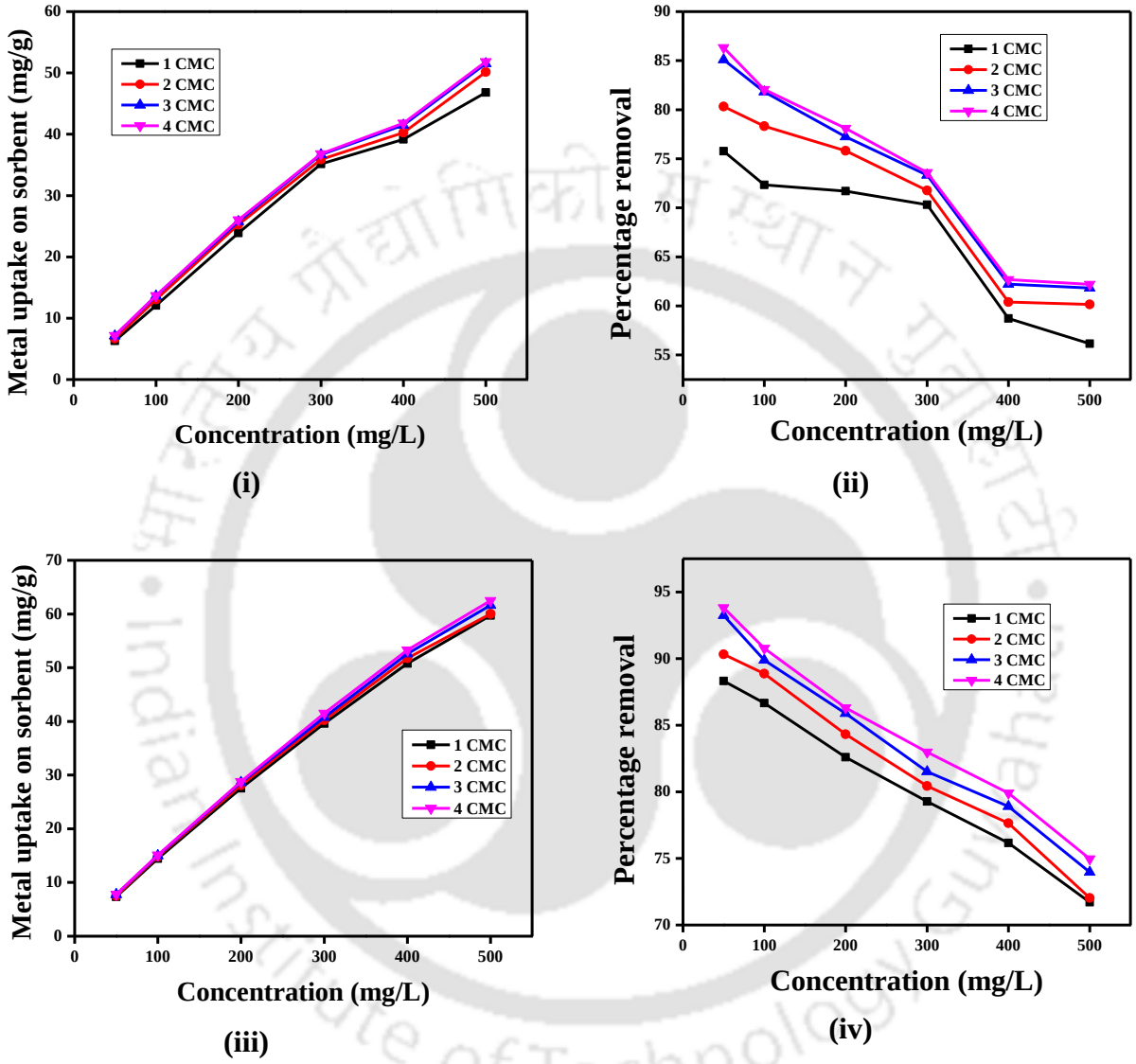

Fig. 4.6(c): Effect of initial Pd solution concentration on the adsorption characteristics for synthetic electroless plating solutions containing CTAB surfactant (1–4 CMC)

(i) metal uptake and (ii) removal efficiency for agitation assisted adsorption

(iii)metal uptake and (iv) removal efficiency for sonication assisted adsorption.

concentrations significantly removal efficiency values, but not metal uptake values. For a feed Pd solution concentration of 50 mg/L, the metal uptake and removal efficiency varied from 6.31–7.19 mg/g and 75.78–86.32% respectively for a variation in surfactant solution concentration from 1–4 CMC. These adsorption characteristic parameters enhanced to 23.9–26.03 mg/g and 71.71–78.09% respectively for 200 mg/L Pd solution concentration and 46.8–51.83 mg/g and 56.8–62.19% respectively for 500 mg/L Pd solution concentration. Similar trends were observed in Fig. 4.6 (d), (iii and iv) for the sonicated assisted adsorption, where the metal uptake and removal efficiencies were evaluated as 7.36–7.81 mg/g and 88.32–93.82% respectively for 50 mg/L Pd solution concentration. These values increased to 59.75–62.46 mg/g for 200 mg/L Pd solution concentration and 71.7–74.96% for 500 mg/L Pd solution concentration.

In summary, the evaluation of higher adsorption capacity and metal uptake for higher surfactant solution concentrations is advantageous for wastewater treatment, given the fact that wastewater solutions would contain higher amounts of Pd and surfactants. Further, the evaluated removal efficiency of 71.7–74.96% at 500 mg/L is also attractive in the perspective of noble metal recovery from spent electroless plating solutions.

With respect to the data presented in the literature, for the 4 CMC case for a solution concentration of 300 mg/L, the metal uptake and removal efficiency have been evaluated as 41.49 mg/g and 82.98% respectively. On the other hand, for aqueous solutions, corresponding literature values correspond to 35.57 mg/g and 98 % respectively. Thus, it is apparent that the 4 CMC case provides higher metal uptake but lower removal efficiency in comparison with the literature data.

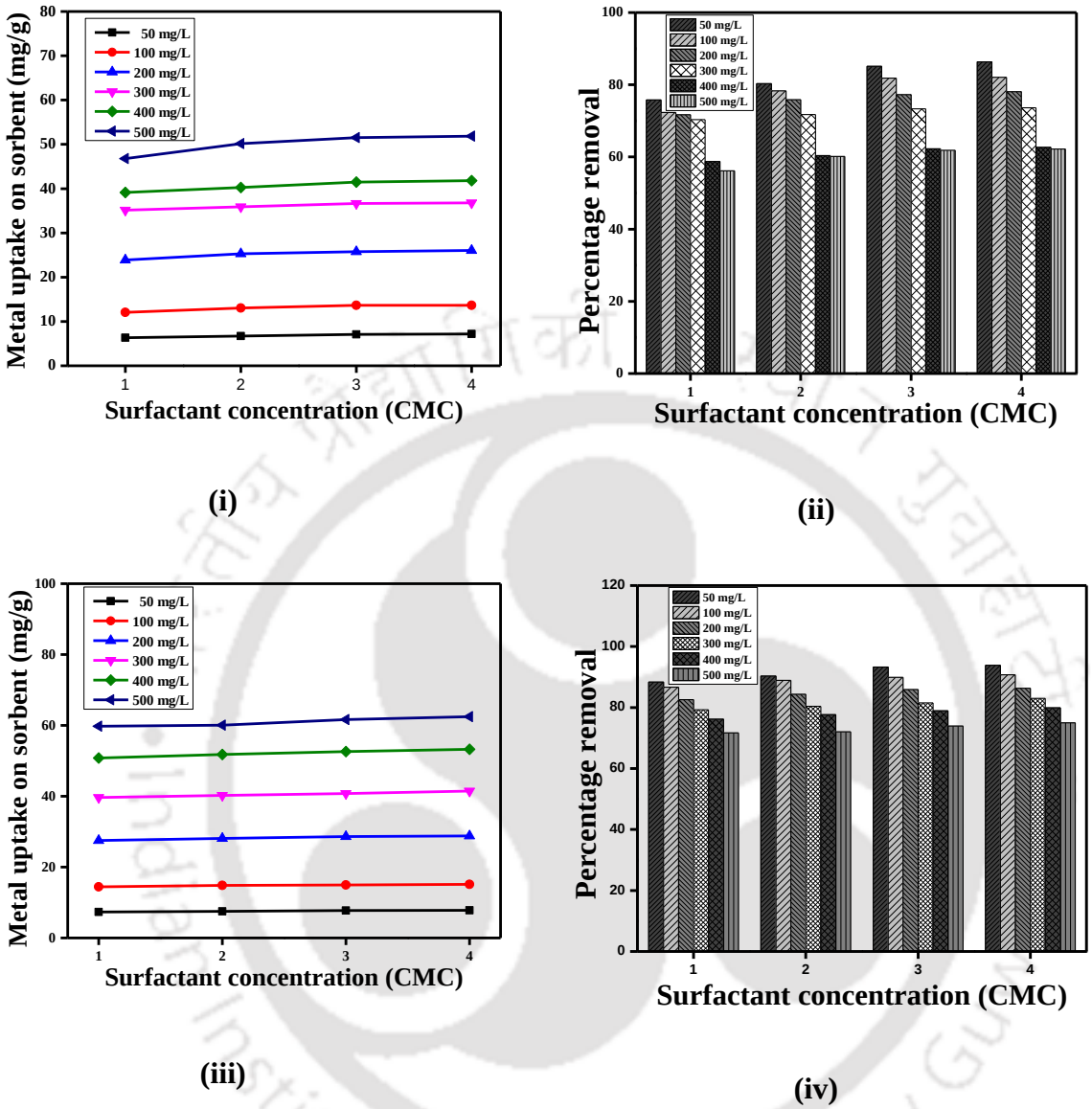

Fig. 4.6(d): Effect of surfactant solution concentration on the adsorption characteristics for various cases of initial Pd solution concentration (50 – 500 mg/L). (i) metal uptake and (ii) removal efficiency for agitation assisted adsorption and (iii) metal uptake and (iv) removal efficiency for sonication assisted adsorption.

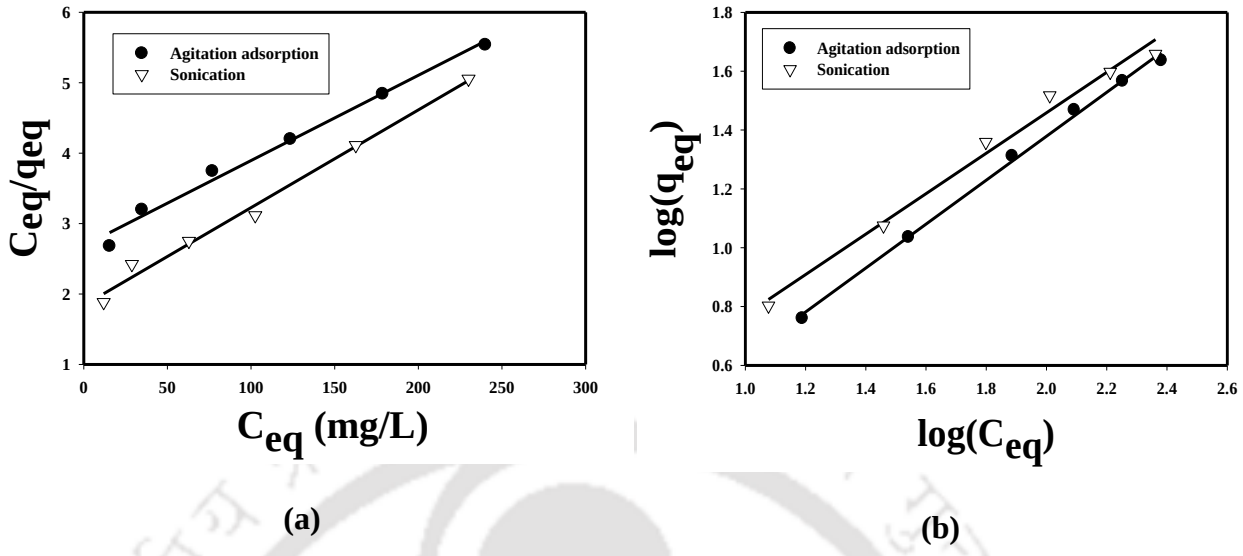

(a) **(b)**

Fig. 4.7: (a) Langmuir and (b) Freundlich isotherm fitness plots for Pd (II) adsorption from synthetic electroless plating solutions not containing CTAB surfactant.

4.4 Modelling and Methodology

4.4.1 Adsorption Equilibrium

Table 4.4 and Fig. 4.7 (a-b) illustrate the fitness of Langmuir and Freundlich isotherm for both agitation assisted adsorption and sonication assisted Pd (II) adsorption on activated charcoal using synthetic electroless plating solutions not containing the cationic surfactant.

For this case, it can be observed that both Langmuir and Freundlich isotherm models provide good fitness to represent the equilibrium adsorption data and among these two, Freundlich isotherm provided maximum fitness (R^2 = 0.997 and 0.987 for agitation assisted adsorption and sonication assisted adsorption respectively), thus indicating that heterogeneous adsorption is the underlying physical mechanism. Corresponding summary of the RMS error values has been presented in Table 4.4, which indicates that Freundlich isotherm provided lowest error values. For the experimental data, the Freundlich isotherm modeling constants refer to k_f = 0.768 and n

= 1.34 for agitation assisted adsorption and k_f = 1.21 and n = 1.45 for sonication assisted adsorption.

Table 4.5 and Fig. 4.8 (a) and 4.8 (b) summarize the results obtained for the fitness of Freundlich isotherm for the Pd (II) adsorption using synthetic electroless plating solutions containing CTAB surfactant. For this case also, it has been evaluated that the Langmuir isotherm did not fit well with the measured experimental adsorption parameters (R^2 = 0.835 and 0.865 for agitation assisted adsorption and sonication assisted adsorption respectively). On the other hand, the coefficient of correlation for the Freundlich equilibrium isotherm indicated better fitness (R^2 = 0.993 and 0.985 for agitation assisted adsorption and sonication assisted adsorption respectively). At 500 mg/L, significant deviation has been observed for the fitness. The observed data trends are in agreement with the hypothesis presented by Fredrik *et al*., (1994); Paria *et al*., (2004) for the surfactant adsorption on silica-water interface. The authors indicated that the surfactant adsorption can be presented in terms of a graph between the logarithmic plot of amount adsorbed and equilibrium concentration, which follows three distinct regimes (Fredrik *et al*., 1994; Paria *et al*., 2004):

a) Regime I: This occurs at lower solution concentration and follows Henry's law to indicate a straight line profile with a slope of 1 for the adsorption characteristics.
b) Regime II: This occurs at higher solution concentration which provides higher adsorption capacity due to the interaction between the surfactants to result in their surface aggregation. The slope of the graph will be greater than 1 in this case.
c) Regime III: This indicates a slower rate of surfactant adsorption due to saturation and therefore the graph will have a slope lower than obtained for the Regime II.

For the experimental data trends observed in this work, the Freundlich isotherm refers to a logarithmic plot between equilibrium metal concentration and capacity. Regime I is not existent as the Pd solution concentrations are significantly higher. However, regimes II and III were existent, with Regime III existent within the Pd solution concentration of 400–500 mg/L. The onset of Regime III indicates the significant influence of Vander wal's forces in altering the heterogeneity of AC at higher Pd solution concentrations in the presence of the surfactant. Thus, it is apparent that the Pd adsorption on AC in the presence of surfactant followed the mechanism elaborated in Regime II for Pd solution concentrations within the range of 50–400 mg/L and regime III within the concentration range of 400–500 mg/L.

The fit Freundlich equilibrium isotherm constants are presented in Table 4.5 for both agitation assisted adsorption and sonication assisted adsorption. As presented, k_f varied from 2.48–4.212 and 1.223–2.52 for increasing surfactant concentration from 1–4 CMC for

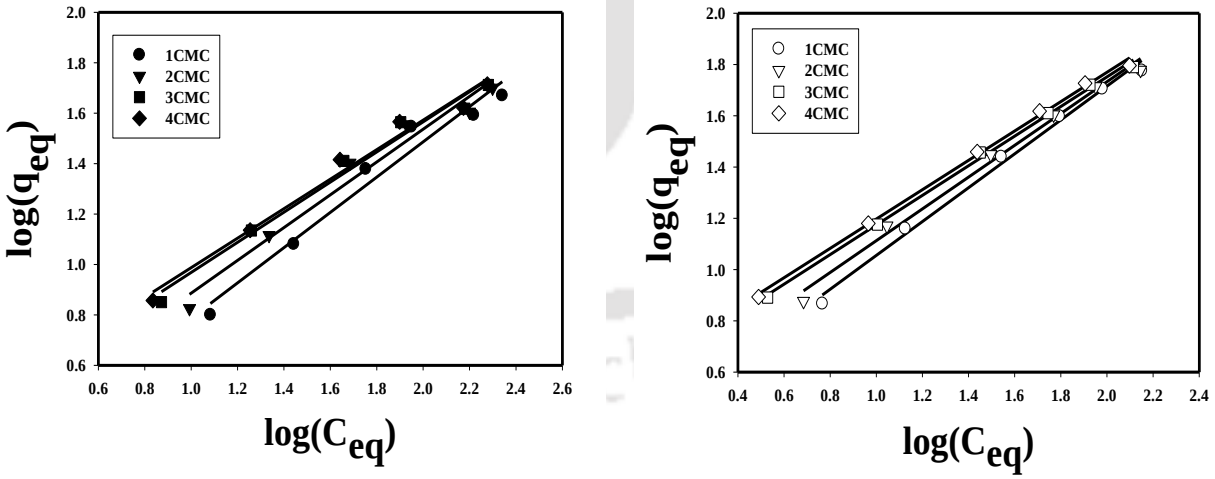

Fig. 4.8: Freundlich isotherm fitness plots for Pd (II) adsorption from synthetic electroless plating solutions containing CTAB surfactant (1 – 4 CMC).

Table 4.4: Langmuir and Freundlich isotherm model parameters for Pd (II) adsorption from synthetic electroless plating solutions without CTAB surfactant.

Mass transfer Technique	Model	R^2	% Error				Monolayer adsorption capacity q_{max} (mg/g)	Model parameters
			RMS	Avg	Max	Min		
Agitation assisted without CTAB	Langmuir	0.988	3.46	2.49	7.08	0.08	42.9	b=0.004 K_R =0.703
	Freundlich	0.997	1.56	1.02	1.66	0.004	-	k_f =0.768, n=1.34
Sonication without CTAB	Langmuir	0.989	4.56	3.52	7.65	0.40	52.4	b=0.007 K_R =0.633
	Freundlich	0.987	2.49	2.24	3.37	0.42	-	k_f=1.21, n=1.45

Table 4.5: Freundlich isotherm model fitness and model parameters for Pd (II) adsorption from CTAB surfactant containing synthetic electroless plating solutions.

Method	Surfactant concentration (CMC)	%Error					Model values	
		R^2	RMS	Avg	Max	Min	k_f	n
Sonication with CTAB	1	0.9931	0.8891	0.468	3.893	0.2212	2.48	2.53
	2	0.9907	1.0412	0.5508	4.602	0.6758	3.107	2.03
	3	0.9973	0.4442	0.233	1.5623	0.1174	3.94	1.67
	4	0.9975	0.4264	0.2353	1.6422	0.2381	4.212	1.61
Agitation assisted adsorption with CTAB	1	0.9643	1.7649	0.9989	6.145	1.38	1.223	11.4
	2	0.969	1.7345	0.9459	6.76	0.999	1.72	4.24
	3	0.9799	1.3184	0.7314	4.8314	0.994	2.34	2.69
	4	0.9816	1.2104	0.644	3.924	0.0108	2.52	2.48

sonication assisted adsorption and agitation assisted adsorption respectively. On the other hand, n varied from 2.53–1.61 and 11.4–2.48 for an increase in the surfactant solution concentration from 1-4 CMC. It can be also observed that while K_f and n followed a systematic trend. The observed trends are in agreement with the hypotheses that at higher surfactant concentrations favor Pd (II) adsorption onto commercial AC adsorbent.

4.4.2 Adsorption Kinetics

Amongst the two kinetic models tested for their fitness towards representing experimentally measured kinetic data of Pd (II) adsorption on activated charcoal in the presence of CTAB surfactant, it has been evaluated that the first order model did not fit well as the plots did not pass through the origin. However, good fitness was observed for the second order kinetic model. Fig. 4.8 (a) presents the fitness of the second order kinetic model for the measured kinetic data for the case of 2 CMC surfactant solution concentration and Pd solution concentrations varying from 50–500 mg/L. Corresponding model parameters and errors are summarized in Table 4.6. As presented in Table 4.6, there is a good agreement with the q_e values determined experimentally and from pseudo second order model. Similar modelling trends were observed for other sets of surfactant concentrations but are not shown. The kinetic results were further analysed with intraparticle diffusion model to elaborate upon the pertinent diffusion mechanism of Pd (II) adsorption with ELP solutions consisting of 2 CMC surfactant. The fitness of measured Pd (II) adsorption kinetic data towards the intraparticle diffusion model is presented in Fig. 4.8 (b) which indicates the existence of two distinct adsorption characteristics. These correspond to initial sharper region where instantaneous external surface adsorption occurs on the adsorbent and the later gradual Pd adsorption that involves intraparticle diffusion as a rate limiting step. At longer time periods, it can be observed that saturation is apparent Sharififard *et al*. (2012).

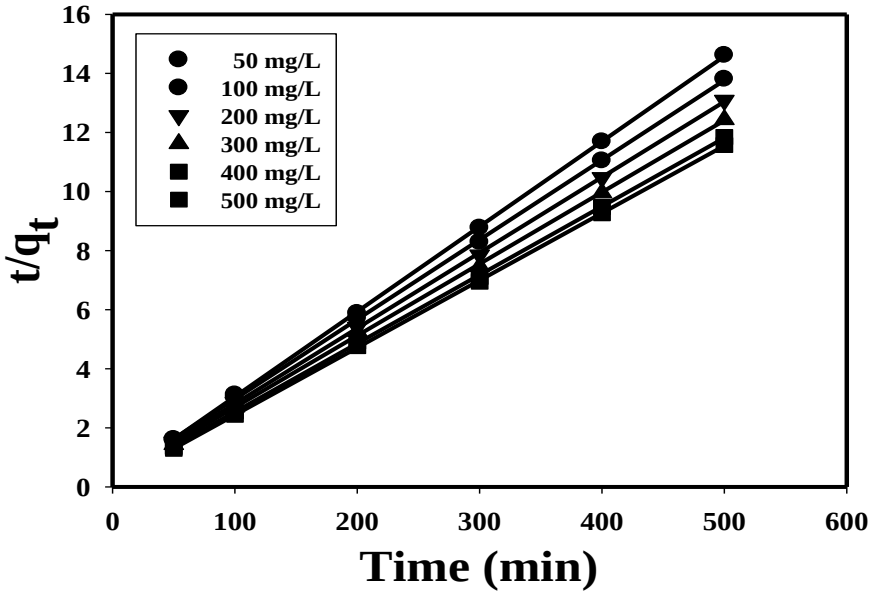

Fig. 4.9(a): Pseudo-second order kinetic model fitness for Pd (II) adsorption from synthetic electroless plating solutions containing 2CMC CTAB surfactant.

4.3.3 Thermodynamic parameters

Since only Pd (II) adsorption data obtained using synthetic electroless plating solutions without CTAB surfactant follow Langmuir equilibrium model, thermodynamic model parameters ΔH^o and ΔS^o have been evaluated for this case only and correspond to 37.8 kJ/mol and 1.94 kJ/K. mol respectively, for agitation assisted adsorption and 49.3 kJ/mol and 1.8 kJ/K. mol for sonication respectively. The positive values of ΔH^o and ΔS^o indicate that the Pd (II) adsorption from synthetic electroless plating solutions is spontaneous and endothermic nature (Sharififard *et al.*, 2012).

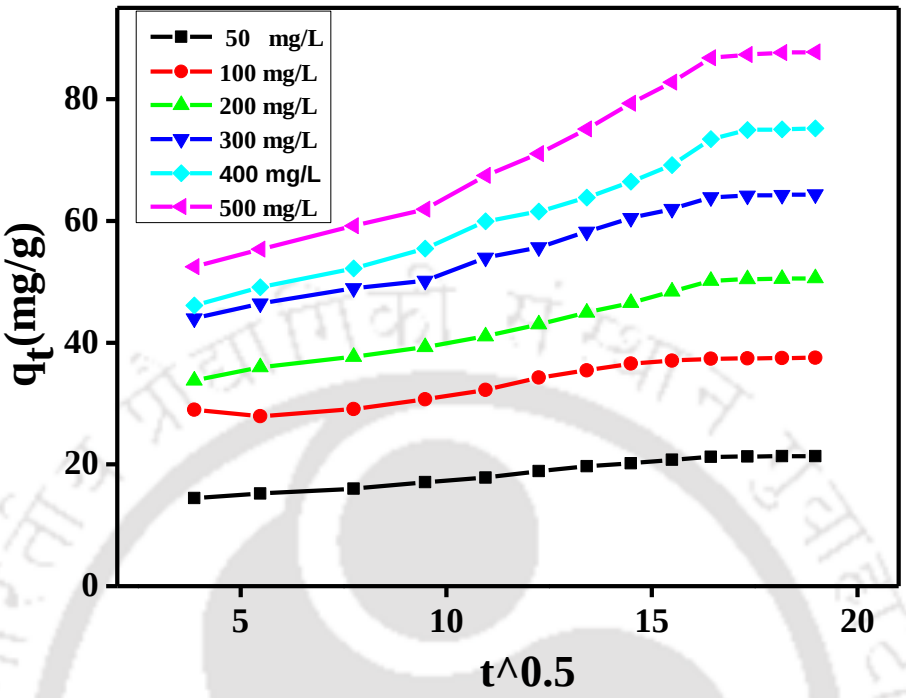

Fig. 4.9(b): Intra particle diffusion model fitness plot for Pd (II) adsorption from synthetic electroless plating solutions containing 2CMC CTAB surfactant.

Table 4.6: Pseudo-second order kinetic model parameters for Pd (II) removal using CTAB (2CMC) containing synthetic electroless plating solutions.

C_e (mg/L)	q_e (mg/g)		R^2	k_2 x 10^{-3} (L/min.)	%Error			
	Exp	Cal			RMS	Average	Max	Min
50	34.25	34.72	0.9999	4.7	0.99	0.66	2.18	0.008
100	36.36	37.03	0.9999	2.6	1.36	1.09	2.43	0.21
200	38.50	39.06	0.9999	2.5	0.93	0.80	1.36	0.23
300	41.21	41.15	0.9999	2.2	1.90	1.36	3.65	0.15
400	42.75	43.10	0.9999	2.2	1.57	1.04	3.49	0.01
500	43.28	43.10	0.9996	2.4	4.13	3.66	7.58	2.07

4.5 Desorption Characteristics

For the Pd-AC adsorbent prepared with 300 mg/L initial solution concentration, the experimentally evaluated metal capacity is 36.525 mg/g. Using 0.1 M HCl, the equilibrium Pd concentration on the adsorbent after adsorption was evaluated to be 80.85 mg/L. Using these two values, the batch desorption efficiency is about 2.25% which is significantly low. Similarly using 0.1 M NaOH, the adsorbent Pd concentration and batch desorption efficiency were evaluated as 39.7 mg/L and 4.45%. Thus, comparing these two cases, it can be concluded that strong irreversible chemisorption occurred during Pd (II) adsorption on AC, as the elution efficiency has been significantly low. Among HCl and NaOH, NaOH provided better elution characteristics due to the PZC of AC being in the basic media range.

4.6 Summary

This work presented Pd (II) adsorption characteristics on activated charcoal from synthetic Pd electroless plating solutions without and with CTAB cationic surfactant. Optimal operating conditions for batch adsorption were identified as contact time = 300 min, pH = 10, dosage 6 g/L within the concentration range of 50–500 mg/L Pd solution concentration. It was observed that the Pd (II) adsorption characteristics from synthetic electroless plating solutions are significantly different from Pd (II) adsorption from aqueous solutions. While the ELP solutions containing the surfactant showed the same trend of increasing metal uptake and decreasing adsorption efficiency with increasing concentration, the values obtained were significantly higher than what were obtained for the corresponding concentrations in the case of ELP solutions without the surfactant. The surfactant containing solutions provided enhancement in metal uptake with increasing concentration. The metal uptake values varied from 5.76–43.33 mg/g and the values for removal efficiency varied from 69.12–52 % with increasing Pd solution concentration. For

ELP solutions with surfactants, the values of metal uptake varied from 6.69–50.13 mg/g and removal efficiency varied from 80.32–60.16%.

Also, the evaluated adsorption characteristics are distinct and indicate higher metal uptake and removal efficiency than those obtained for aqueous solutions. It has been observed that sonication assisted adsorption performed slightly better than the agitation assisted adsorption case for metal uptake and removal efficiency values. Also, it has been observed that both metal uptake and removal efficiency values increased with increasing CTAB surfactant solution concentration, thus indicating that surfactant significantly altered the prevalent surface phenomena associated to Pd adsorption on AC. For all cases, Freundlich equilibrium isotherm and Psuedo second order kinetic model have been evaluated to be the best fit models. In summary, while similar metal uptakes were obtained, lower removal efficiencies were obtained for the case of synthetic ELP solutions in comparison with aqueous solutions. Thus, the experimental and theoretical adsorption characteristics of Pd (II) are anticipated to serve as reference data for the cost effective recovery and reuse of Pd (II) from spent electroless plating solutions using activated charcoal adsorbent.

Chapter 5

Development of Activated Charcoal Adsorbent from Bamboo (*Bambuseae*) Waste for the Recovery of Pd (II) from Synthetic Electroless Plating Solutions

In this chapter, the adsorption characteristics of Pd (II) have been presented for AC adsorbent prepared from bamboo stem activated charcoal. The results are summarized in three sections. Section 5.2 elaborates upon adsorbent surface characterization. Section 5.3 discusses batch adsorption characteristics. Section 5.4 details upon the fitness of relevant equilibrium, kinetic and thermodynamic models.

5.1 Introduction

This chapter primarily addresses two objectives. Firstly, it targets the preparation of good quality activated charcoal from bamboo waste which will have BET surface area comparable to that of the commercial activated carbon. Secondly, the prepared activated charcoal adsorbent from bamboo waste was evaluated for Pd (II) adsorption characteristics using synthetic electroless plating solutions that constitute a stabilizer (Na_2EDTA), liquor ammonia and cationic surfactant CTAB (optional) in addition to the noble metal ions.

The Pd (II) adsorption characteristics on bamboo based activated carbon with synthetic electroless plating solutions has not been reported till date and is targeted in this work. The long term objective of the experimental investigations highlighted in this work is to further enhance the adsorption capacity of activated carbon adsorbent from bamboo stem waste using suitable

surface modification agents such as chitosan. The same will be also addressed in chapter 7 of the thesis.

It has been well documented in the literature that H_3PO_4 activation is highly promising to enhance the BET surface area of the adsorbents (McKay *et al.*, 2009; Anand kumar and Mandal, 2009). The acid to bamboo ratio is an important parameter for evaluation. Various prepared adsorbents were characterized using Fourier transform infrared (FTIR) spectral analysis, Brunauer, Emmett and Teller (BET**)** surface area analysis, Laser particle size analysis (LPSA), Scanning electronic microscopy (SEM) and Energy dispersive spectral (EDS) analysis. Using best quality activated adsorbent prepared from bamboo stem waste, batch adsorption experiments were carried out for variant adsorbent dosages (1-6 g/L), Pd (II) solution concentrations (50-500 mg/L), contact time (50-350 min.) and pH (2-14). The specific influence of various additives such as CTAB (surfactant), Na_2EDTA (stabilizer) and liquor ammonia (NH_3) on the adsorption characteristics of Pd (II) using bamboo based activated carbon has been addressed. Equilibrium adsorption data have been tested for their fitness towards various isotherm models such as Langmuir and Freundlich models. Pseudo first order, second order kinetic and intra-particle diffusion models were evaluated for their fitness to represent the kinetics of adsorption. The next section details upon surface characterization results.

5.2 Characterization of the Adsorbent

5.2.1 Surface Area analysis

Fig. 5.1 (a-c) present the textural appearance of various samples including raw bamboo stem powder Fig. 5.1 (a), chemically activated bamboo stem charcoal Fig. 5.1 (b) and bamboo stem based activated charcoal. It can be observed that the texture of the bamboo stem waste changed from a brown colour to dark black, indicating that carbonization occurred during the sintering

process. Table 5.1 and Fig. 5.1 (d) summarize the physical properties of various adsorbents (BSAC11-14) and hysteresis graph for BSAC 14 adsorbent respectively. As shown, Fig. 5.1 (d) refers to Type IV isotherm with H_4 hysteresis loop which according to IUPAC classification indicated the existence of narrow slit like pores (Sing *et al*., 1985). It can also be observed that the adsorbent surface area got enhanced from 612.8-1014.4 m^2/g with increasing bamboo to acid ratio (1-4). Similar enhancements in monolayer volume (55.237-221.09 cc/g) and total pore volume (0.2331–0.9324 mL/g) can be also observed for various adsorbents. Amongst all adsorbents, BSAC 14 provided the best combinations of BET surface area (1014.4 m^2/g), monolayer volume (221.09 cc/g) and total pore volume (0.9324 mL/g). These are comparable with that of the commercial activated carbon (BET surface area of 1057.7 m^2/g, monolayer and total pore volume of 242.89 and 0.9814, respectively). Similar enhancements in adsorbent properties were reported by Mohanty *et al*., (2005) and Anand kumar *et al*., (2009) for activated carbon prepared from bale shell.

(a)

(b)

(c)

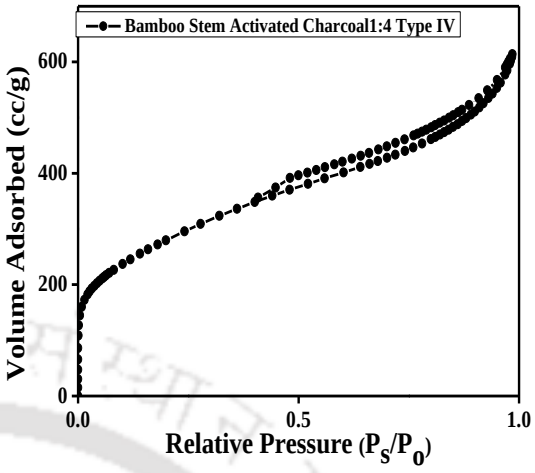

(d)

Fig. 5.1: Images of (a) raw bamboo stem powder, (b) BSAC14 adsorbent, (c) BSAC 14 adsorbent powder and (d) Nitrogen adsorption/desorption isotherm for BSAC 14 adsorbent.

Table 5.1: Physical properties of BSAC 14 adsorbent.

Properties	**H_3PO_4 Treated Bamboo stem Powder Impregnation ratio [BSAC weight (g)/ H_3PO_4 volume (mL)]**			
	BSAC11	**BSAC12**	**BSAC13**	**BSAC 14**
BET Surface Area(m^2/g)	612.8124	725.8752	817.62	1014.4
Monolayer Volume(cc/g)	55.237	127.95	169.56	221.0927
Total Pore Volume(ml/g)	0.2331	0.4896	0.7654	0.9324

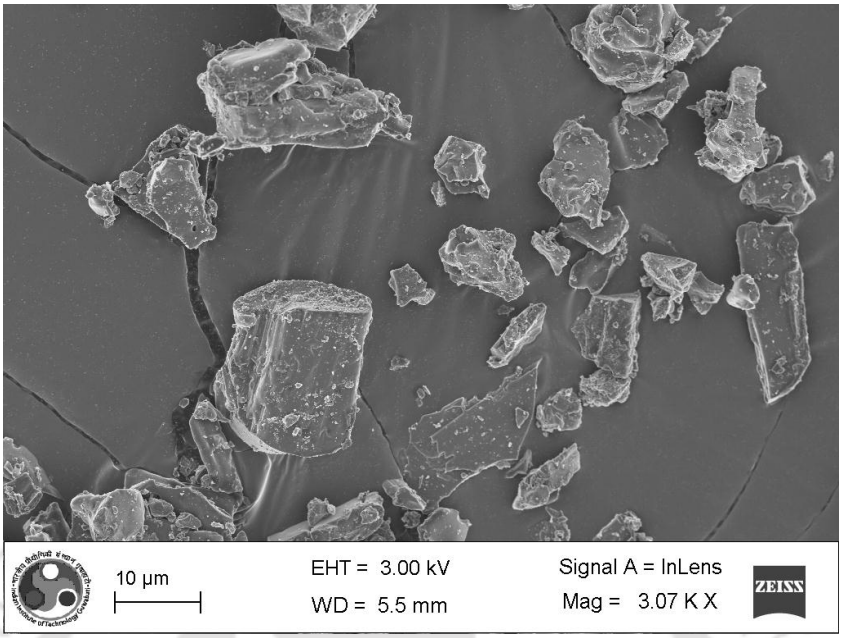
10 µm
EHT = 3.00 kV
WD = 5.5 mm
Signal A = InLens
Mag = 3.07 K X
ZEISS

(a)

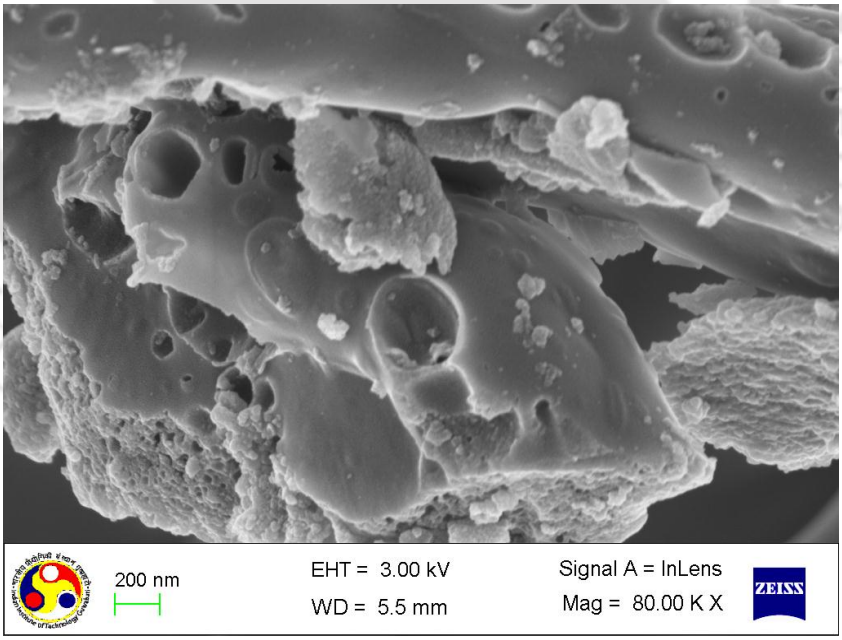
200 nm
EHT = 3.00 kV
WD = 5.5 mm
Signal A = InLens
Mag = 80.00 K X
ZEISS

(b)

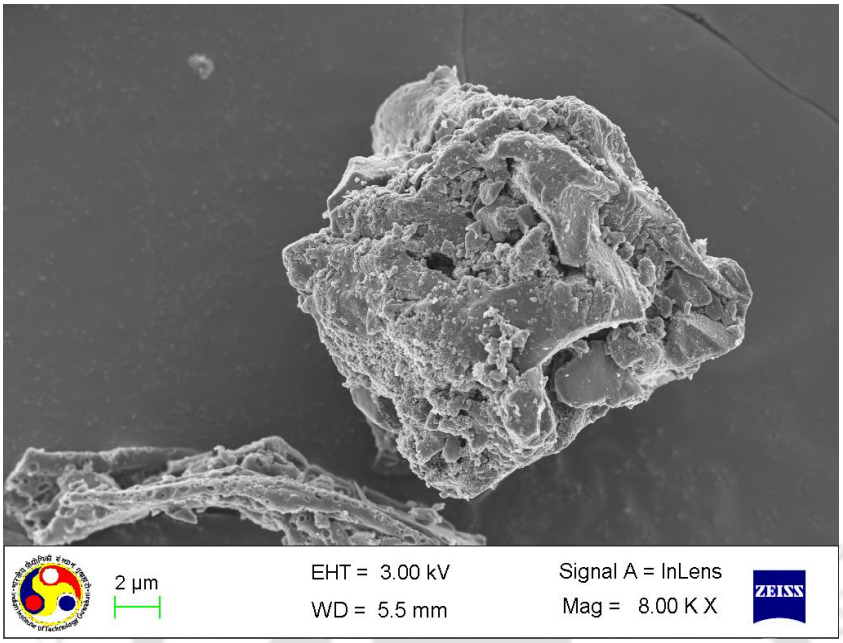

(c)

Fig. 5.2: Scanning electronic micrographs of various samples (a) Bamboo stem powder (b) BSAC 14 adsorbent and (c) Pd (II) adsorbed BSAC 14 adsorbent.

5.2.2 SEM Characterization

Fig. 5.2. (a-c) presents the scanning electron micrographs for raw bamboo stem powder prior to activation, BSAC 14 adsorbent and Pd (II) adsorbed BSAC 14, respectively. It can be observed that compared to the raw bamboo stem, highly porous structure exists for both BSAC 14 and Pd adsorbed BSAC 14 samples. Thus it is apparent that phosphoric acid activation swelled and opened the surface structure. The evaporation during the later stages of the sintering enabled the formation of active pores on the adsorbent surface. The existence of an additional coated layer on the adsorbent surface as observed in Fig.5.2 (c) is indicative towards the surface adsorption of Pd (II) on BSAC 14 (Lalhruaitluanga *et al*., 2011).

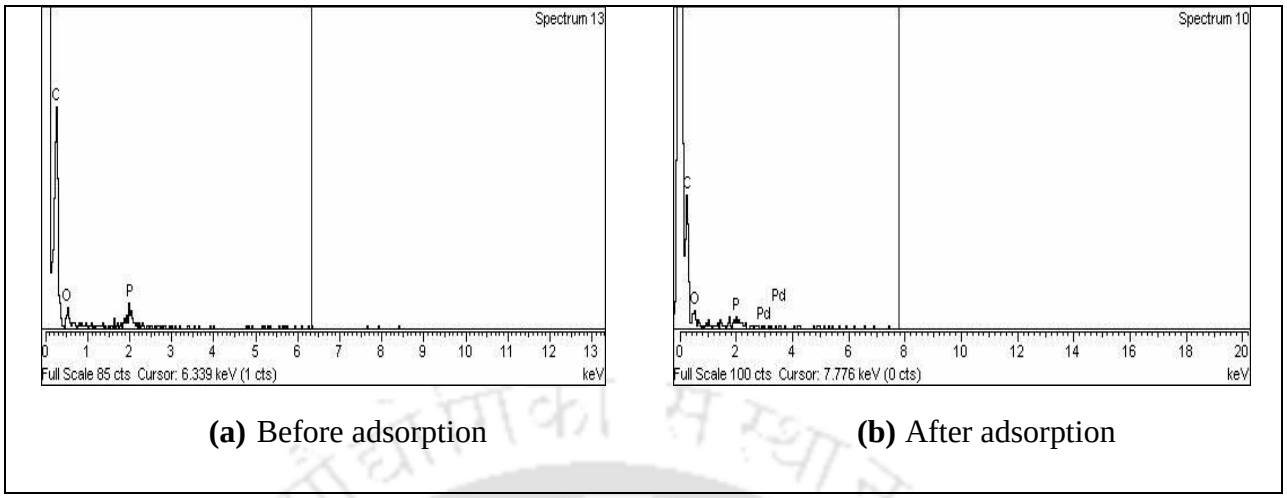

(a) Before adsorption **(b)** After adsorption

Fig. 5.3: ED spectra of (a) BSAC 14 and (b) Pd (II) adsorbed BSAC 14 adsorbents.

Table 5.2: ED spectral analysis of BSAC 14 adsorbent before and after adsorption with 50 mg/L Pd solution concentration.

Element	**Before adsorption**		**After adsorption**	
	Weight%	**Atomic%**	**Weight%**	**Atomic%**
Carbon	36.02	48.19	76.11	83.56
Oxygen	38.37	38.53	18.69	14.99
Phosphorus	25.60	13.28	2.86	1.18
Palladium			2.34	0.27

5.2.3 Energy dispersive X-ray spectroscopy (EDS)

Fig.5.3 (a), (b) and Table 5.2 present the EDS and composition of various elements on BSAC 14 and Pd adsorbed BSAC 14. For both cases, it can be observed that the surface elemental composition refers to carbon and oxygen groups which confirm that the adsorbent possesses several carbon and oxygen groups including acidic (carboxylic and lactonic), non-acidic (ether, quinine and carbonyl), anhydride and phenol groups. Further, for BSAC 14, the Pd elemental

composition corresponds to 2.34 wt %, for a Pd metal uptake of about 6.8 mg/g with an initial Pd (II) solution concentration of 50 mg/L.

5.2.4 Fourier Transform Infrared Spectral Analysis

Fig. 5.4 presents the FTIR spectral analysis for BSAC 14, Pd adsorbed BSAC 14 obtained with agitation assisted adsorption and Pd adsorbed BSAC 14 obtained with sonication assisted adsorption. The FTIR spectral analysis indicated that for the BSAC 14, peak located at 3784 cm^{-1} is due to stretching vibrations of -OH or -NH groups. For these groups, the peak shifted from its earlier frequency to 3744 and 3724 cm^{-1}. Also, the peak that existed for BSAC 14 at 2970 cm^{-1} does not exist for Pd adsorbed BSAC 14. This peak corresponds to the stretching vibrations of C-H groups. The absence of this peak after Pd adsorption is possibly due to the role of Na_2EDTA stabilizer in the synthetic ELP solution. The stretching vibrations of amine groups ($-NH_2^+$ and $-NH^+$) in the BSAC14 correspond to the peaks observed at 2407 and 2299 cm^{-1}. These peaks shifted to 2409, 2287 and 2385, 2301 cm^{-1} frequency values after interaction with ammonia available in the Pd (II) synthetic ELP solution. Similarly, after Pd adsorption, the stretching vibration of carboxylic groups (-CHOO) whose peak was located at a frequency of 1521 cm^{-1} shifted to 1523 and 1519 cm^{-1} after Pd adsorption for both cases (sonication and agitation assisted Pd adsorption). The peaks assigned for COO, C=O groups at a frequency of 1250 cm^{-1} for BSAC14 also shifted to 1156 and 1049 cm^{-1} for both cases.

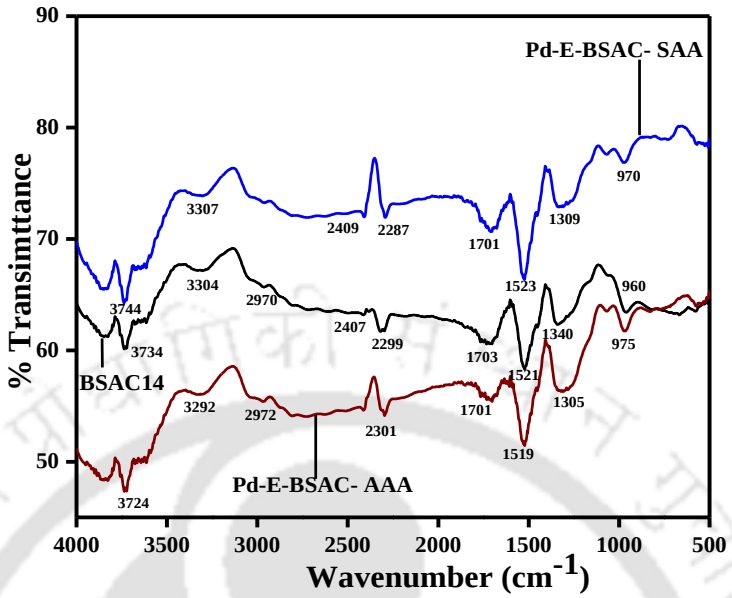

Fig. 5.4: FTIR spectra of Bamboo stem, BSAC 14 and Pd (II) adsorbed BSAC 14 adsorbents.

5.2.5 Particle Size Distribution

Fig. 5.5 shows the average particle size distribution for BSAC 11-14 adsorbents. It can be observed that the particle size distribution varied from 2.6-2046.6, 2.7-2046.7, 2.7-2046.8 and 2.0465-893.3785 μm for BSAC 11-14 adsorbents respectively. Corresponding volume % distribution varied from 0.09-0.18, 0.08-0.07, 0.08-0.05 and 0.05-0.06 for BSAC 11-14 adsorbents respectively. The average particle size reduced with increasing the acid to bamboo ratio during activation step and varied from 249.96-65.75 μm for BSAC 11-14 respectively. Thus, the achievement of lower average particle size for BSAC 14 is promising towards its efficacy to adsorb Pd (II) from synthetic electroless plating solutions.

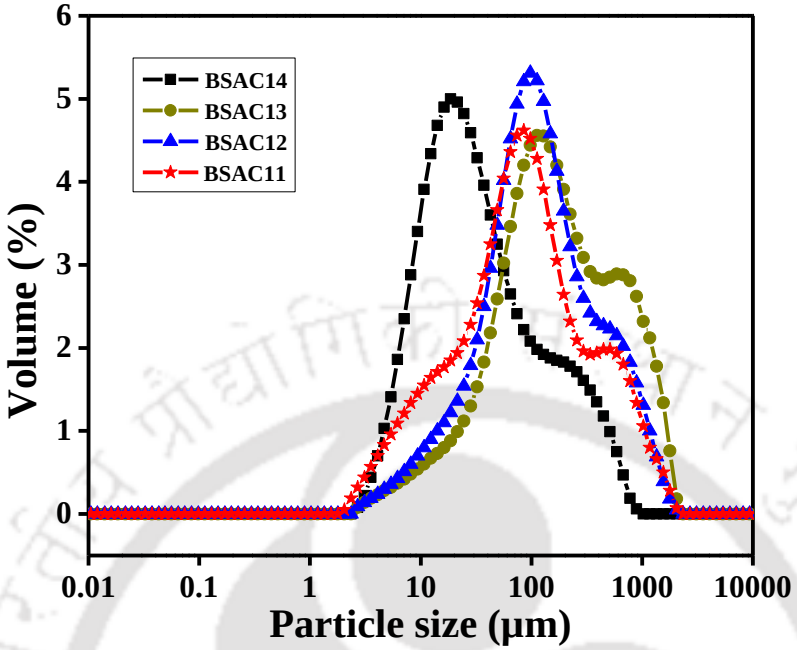

Fig. 5.5: Particle size distribution for BSAC 11-14 adsorbents.

5.3Batch Adsorption

Batch adsorption experiments were targeted by varying either one of the adsorption parameters. These are agitation time, BSAC dosage, pH and initial Pd (II) solution concentration. The first set of experiments targeted the variation of contact time with other adsorption parameters specified as pH = 2-12, dosage = 1 g/L and initial Pd (II) concentration of 50 mg/L. For the second set of experiments, with the optimal contact time identified from the first step, batch experiments were conducted for variation in pH (2-12) and by choosing other adsorption parameters as dosage 1 g/L and initial Pd (II) concentration of 50 mg/L. The third set of batch adsorption experiments were targeted with optimal combinations of contact time and pH for a variation in dosage (1-6 g/L) and chosen initial Pd (II) concentration of 50 mg/L. Finally, the last

set of batch adsorption experiments were carried out for optimal combinations of dosage, contact time and pH and variation in Pd (II) solution concentration from 50–500 mg/L.

5.3.1 Effect of Contact Time

Fig. 5.6 (a) presents the variation of metal uptake and removal efficiency with variation in contact time for Pd (II) adsorption from synthetic electroless plating solutions using BSAC 14 adsorbent. It can be observed that with a variation in contact time from 50-350 min, the metal uptake increased from 13.68-41.01 mg/g and removal efficiency increased from 27.3-82.02 % respectively. Based on the observed profiles for metal uptake and removal efficiency, the optimal equilibrium time has been evaluated as 300 min, where the metal uptake and removal efficiency values are 40.9 mg/g and 81.8%, respectively. For commercial activated carbon, the optimal equilibrium time has been evaluated to be 300 min, which is similar to that obtained for the BSAC 14.

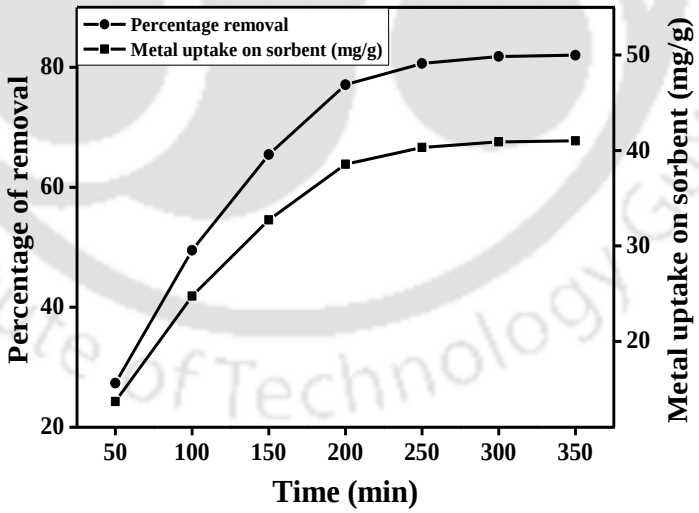

Fig. 5.6(a): Effect of contact time on Pd (II) adsorption characteristics for BSAC 14 adsorbent.

5.3.2 Effect of pH

Fig. 5.6 (b) shows the effect of pH on the metal uptake (mg/g) and removal efficiency for BSAC 14 adsorbent. It can be observed that with an increase in pH, both metal uptake and removal efficiency increased from 9.64-40.55 mg/g and 19.28-81.1% respectively up to a pH of 8 after which they reduced to 34 mg/g and 68.2%, respectively up to a pH of 12. Based on the observed profiles for metal uptake and removal efficiency, the optimal equilibrium pH has been evaluated as 8. Thus, pH is an important parameter to influence the degree of ionization and modification of surface adsorption characteristics. As pH of the solution increases from 2 to 8, greater protonation facilitates better adsorption characteristics of the positively charged Pd ions on the BSAC 14 surface. The reduction in adsorption characteristics at higher pH is due to less protonation at higher pH which facilitates competitiveness for adsorbed ions on the BSAC surface. For commercial activated carbon, the optimal pH has been evaluated to be 10, which is slightly higher to that obtained for BSAC 14.

5.3.3 Effect of Dosage

Fig. 5.6 (c) presents the variation in metal uptake and removal efficiency with increasing dosage of the adsorbent. It can be observed that the metal uptake decreased from 17.58–6.45 mg/g and removal efficiency increased from 35.16-80.42% with increasing adsorbent dosage from 1-6 g/L. Based on the observed profiles for metal uptake and removal efficiency, the optimal dosage has been evaluated as 6 g/L. The decrease in metal uptake with increasing dosage is explained in section 3.2.1. For commercial activated carbon, the optimal dosage has been evaluated to be 6 g/L, which is the same as that obtained for the BSAC 14.

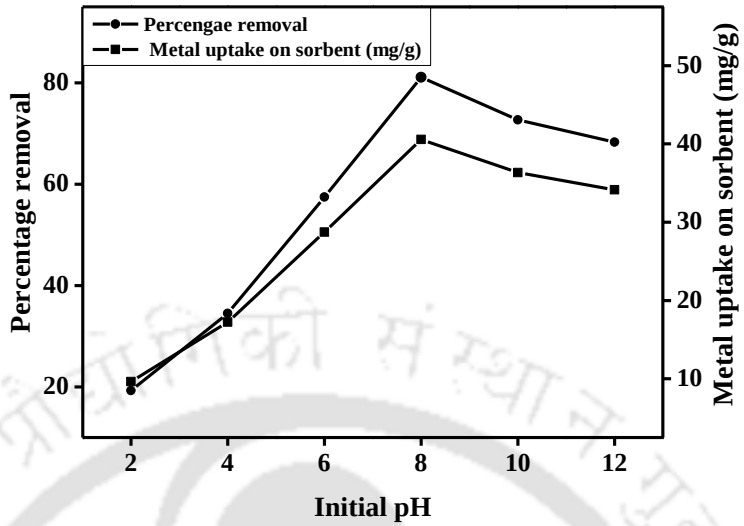

Fig. 5.6 (b): Effect of pH on Pd (II) adsorption characteristics of BSAC 14 adsorbent.

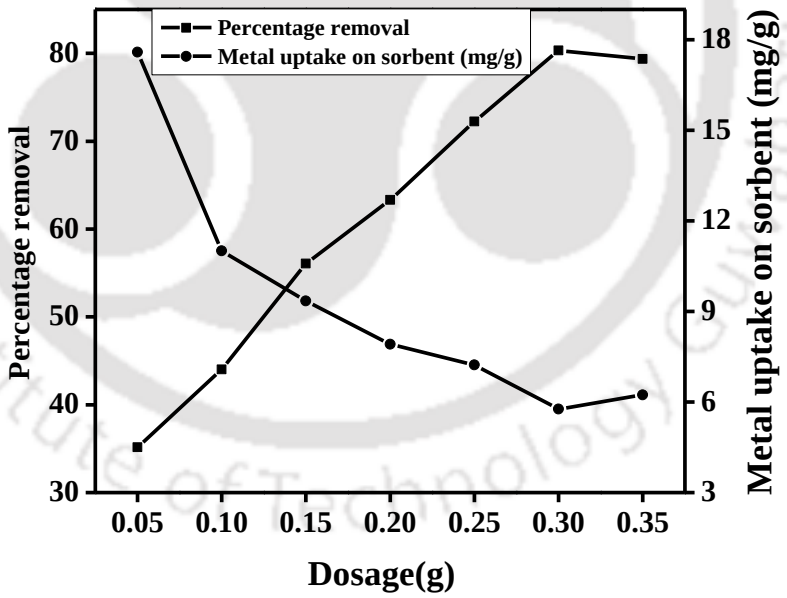

Fig. 5.6(c): Effect of dosage on Pd (II) adsorption characteristics of BSAC 14 adsorbent.

5.3.4 Effect of Pd (II) solution concentration

The effect of variation in Pd (II) solution concentration has been investigated for four different cases, namely, (i) agitation assisted adsorption using synthetic Pd (II) solutions not containing CTAB surfactant (ii) sonication assisted adsorption using synthetic Pd (II) solutions not containing CTAB surfactant (iii) agitation assisted adsorption using synthetic Pd (II) solutions containing CTAB surfactant and (iv) sonicated assisted adsorption using synthetic Pd (II) solutions containing CTAB surfactant. Results obtained are briefly presented in the following sub-sections.

5.3.4.1 Agitation and sonication assisted Pd (II) adsorption from synthetic electroless plating solutions

Fig. 5.7 (i-ii) respectively illustrate the variation of metal capacity (mg/g) and removal efficiency for both agitation and sonicated assisted adsorption of Pd (II) from synthetic electroless plating solutions not containing CTAB surfactant. From Fig. 5.7 (i), it can be observed that the metal capacity varied similarly for both agitation and sonicated assisted adsorption with variation 5.27-42.5 mg/g for agitation assisted adsorption and 6.01-43.23 mg/g for sonication, with increasing Pd solution concentration from 50-500 mg/L. On the other hand, it can be observed in Fig. 5.7 (ii) that the removal efficiency reduced from 65.12-51% for agitation assisted adsorption which is comparatively lower than the corresponding values (72.12-53.2%) evaluated for sonicated assisted adsorption. Thus, while metal uptake remained similar for both adsorption processes, removal efficiency was significantly higher for the sonication assisted adsorption.

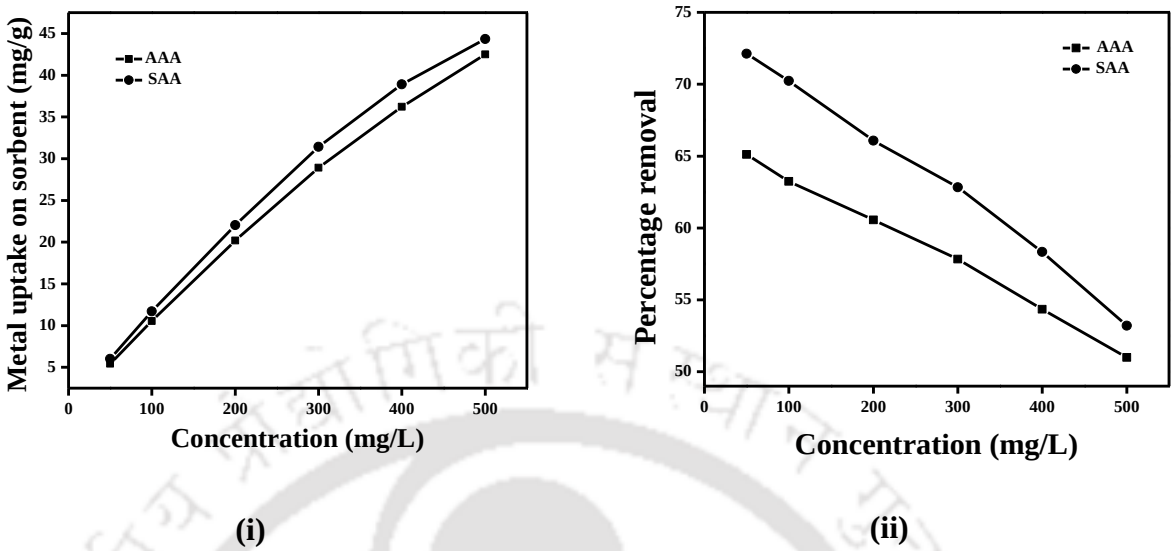

(i) **(ii)**

Fig. 5.7: Pd (II) adsorption characteristics of BSAC 14 adsorbents using synthetic electroless plating solutions: (i) Metal uptake (ii) Removal efficiency.

Comparatively, for commercial activated carbon and similar variation in Pd solution concentration, the metal uptake varied from 5.76-43.33 mg/g for agitation assisted adsorption and 6.34-45.5 mg/g for sonicated assisted adsorption while the removal efficiency varied from 69.12-52% and 76.12-54.61% respectively for agitation and sonicated assisted adsorption. The best literature data with respect to maximum metal uptake for Pd (II) adsorption from aqueous solutions (300 mg/L) had been reported by Sharififard *et al*., (2012) which is about 35.7 mg/g. Thus, a comparative assessment of measured metal uptake and removal efficiency for the developed BSAC 14 adsorbent indicate its competitive performance characteristics with both commercial activated carbon and literature values.

5.3.4.2 Agitation and sonication assisted Pd (II) adsorption from CTAB containing synthetic Pd electroless plating solutions

Fig. 5.8 (i-ii) respectively illustrate the variation of metal capacity (mg/g) and removal efficiency for both agitation and sonicated assisted adsorption of Pd (II) from synthetic electroless plating solutions containing CTAB surfactant. From Fig. 5.8 (i), it can be observed that the metal uptake values increased significantly for both agitation assisted adsorption (6.35-45.08 mg/g) and sonicated assisted adsorption (6.8-53.75 mg/g) with increasing Pd (II) solution concentration (50-500 mg/L), when compared to the solutions without the surfactant. It can be observed from Fig. 5.8 (ii) that the corresponding values of removal efficiency also increased as compared to the solutions without surfactant. The simultaneous enhancement in both metal uptake and removal efficiency values for these two cases is probably due to the role of CTAB surfactant which altered the surface properties of the BSAC 14 adsorbent during the adsorption process and made it a more affective adsorbent by altering its surface area and reactivity. In summary, a comparative assessment of measured metal uptake and removal efficiency for the developed BSAC 14 adsorbent indicate that distinctly better adsorption characteristics exist for Pd (II) adsorption from synthetic electroless plating solutions containing CTAB surfactant.

A summary of the adsorption parameters obtained in this work and those reported in the literature are presented in Table 5.3. It can be observed that the metal uptake reduced insignificantly for synthetic electroless plating solutions in comparison with the aqueous solutions. Also, the BSAC 14 adsorbent performed similarly to that of the commercial activated carbon.

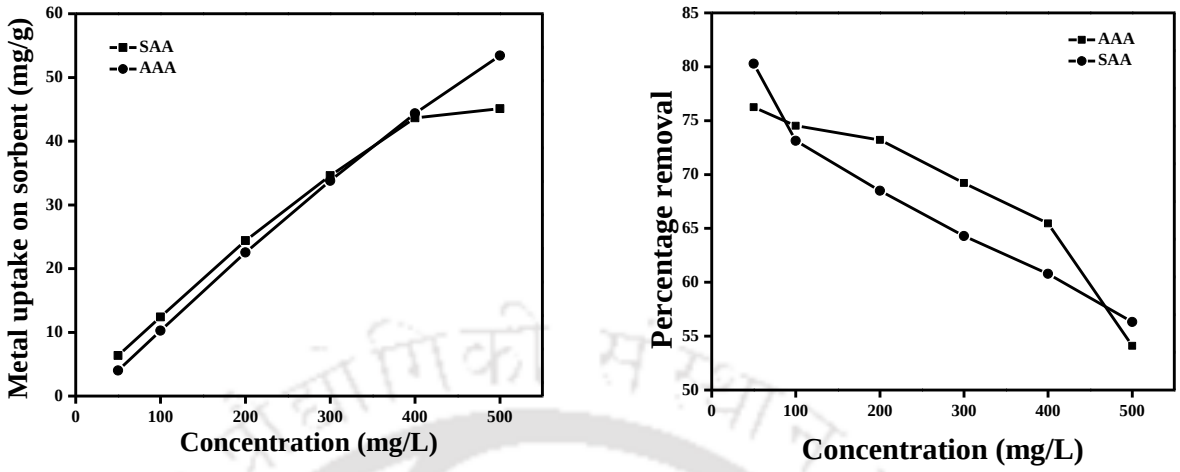

Fig. 5.8: Pd (II) adsorption characteristics of BSAC 14 adsorbent with 2 CMC CTAB containing synthetic electroless plating solutions (i) Metal uptake and (ii) Removal efficiency.

5.4 Modeling

5.4.1 Isotherm modeling

Table 5.4 and Fig. 5.9 (a) (i-ii) illustrate the fitness of Langmuir and Freundlich isotherm for both agitation assisted adsorption and sonication assisted Pd (II) adsorption on activated charcoal using synthetic electroless plating solutions not containing the cationic surfactant. For all cases, it can be observed that both Freundlich and Langmuir isotherm models provided good fitness towards the measured equilibrium adsorption data.

However, Freundlich isotherm provided maximum fitness (R^2 = 0.998 and 0.998 for agitation and sonication assisted adsorption respectively), which indicates that heterogeneous adsorption is the most likely mechanism during the Pd (II) adsorption. It can be also observed in Table 5.4 that the RMS error values were lowest for Langmuir (0.804-1.15) and Freundlich isotherm (0.2-2.7). Table 5.4 presents the Freundlich isotherm constants for these cases which refers to k_f = 1.65 and

n = 1.27 for agitation assisted adsorption and k_f = 1.02 and n = 1.39 for sonication assisted adsorption.

Table 5.4 and **Fig. 5.9**(b) summarize the results obtained for the fitness of Freundlich isotherm for the Pd (II) adsorption using synthetic electroless plating solutions containing

Table 5.3: A summary of measured and literature Pd (II) metal uptake for various adsorbents for an initial solution concentration of 300 mg/L.

Type of adsorbent	Activating agent	Metal	Capacity (mg/g)	Type of Solution	Reference
BSAC	(H_3PO_4)	Ni	121.27	Aqueous solution	(Rajesh *et al*., 2014)
AC	-	Pt	45.45	Aqueous solution	(Sharififard *et al*., 2012)
BPMC	chitosan	Pt	52.63	Aqueous solution	(Sharififard *et al*., 2012)
Racomitrium lanuginosum	Aqueous	Pd	30.2	Aqueous solution	(Sari *et al*., 2009)
AC	-	Pd	27	Aqueous solution	(Kasaini *et al*., 2000)
AC	-	Pd	35.71	Aqueous solution	(Sharififard *et al*., 2012)
BPMC	chitosan	Pd	43.48	Aqueous solution	(Sharififard *et al*., 2012)
Commercial AC	-	Pd	Soni:35.6 Phy:34.2	Pd ELP solution+ CTAB	Chapter 4
Commercial AC	-	Pd	Soni:34.5 Phy:32.4	Pd ELP solution	Chapter 4
BSAC 14	(H_3PO_4)	Pd	Soni:35.1 Phy:34	Pd ELP solution+ CTAB	This work
BSAC 14	(H_3PO_4)	Pd	Soni:31.4 Phy: 29.10	Pd ELP solution	This work

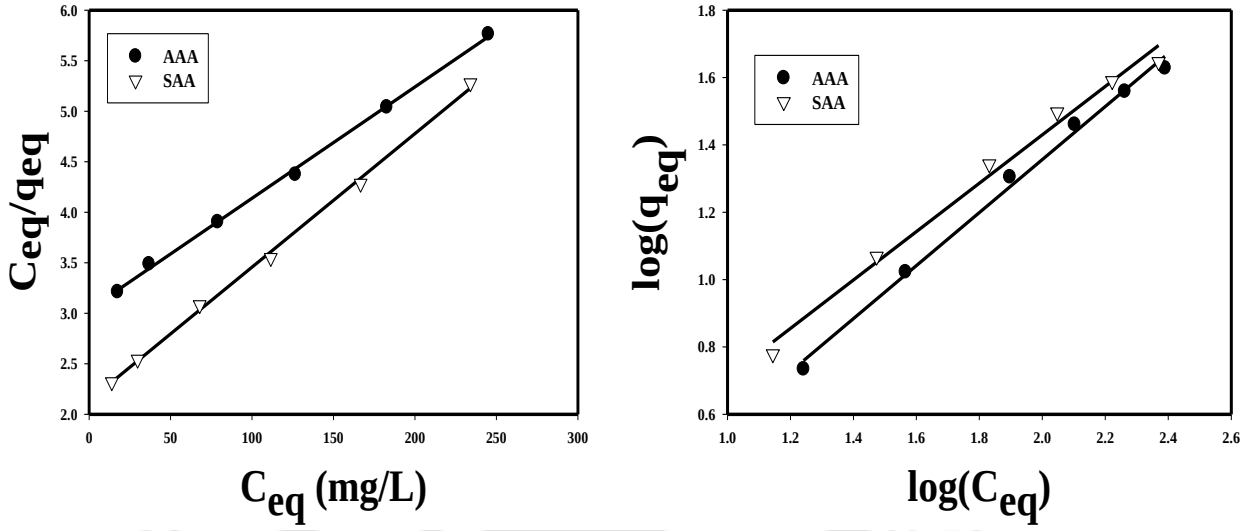

(i) **(ii)**

Fig. 5.9(a): Fitness of (i) Langmuir and (ii) Freundlich isotherm model for Pd (II) adsorption from synthetic ELP solutions on BSAC 14.

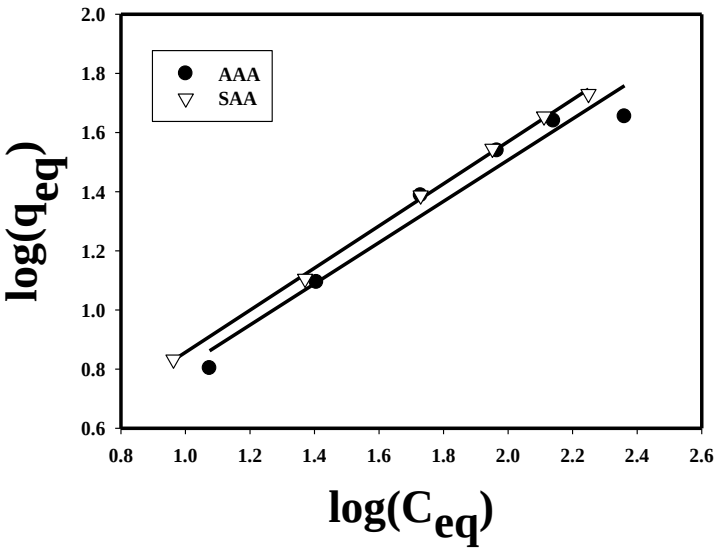

Fig. 5.9(b): Fitness of Freundlich isotherm model for Pd (II) adsorption on BSAC 14 using synthetic ELP solutions containing 2 CMC CTAB surfactant.

Table 5.4: Langmuir and Freundlich isotherm model parameters for Pd (II) adsorption with BSAC14 adsorbent.

Mass transfer Technique	Model	R^2	% Error				q_{max} (mg/g)		Model parameters
			RMS	Avg	Max	Min	Exp	Cal	
AAA without CTAB	Langmuir	0.9987	0.80	0.62	1.39	0.050	42.5	42.8	b=0.0036 K_R =0.053
	Freundlich	0.9984	0.2	1.74	3.35	0.223	-	-	k_f =1.65, n=1.27
SAA without CTAB	Langmuir	0.9982	1.159	1	1.63	0.007	44.3	52.2	b=0.0061 K_R =0.005
	Freundlich	0.9983	2.7	2.32	4.60	0.042	-	-	k_f=1.02, n=1.39
AAA with CTAB	Freundlich	0.9734	0.429	3.67	7.3	0.12	48.8	-	k_f =1.3, n=1.43
SAA with CTAB	Freundlich	0.9987	0.832	0.75	1.36	0.28	54.2	-	k_f =2.8, n=1.4

CTAB surfactant. For this case, it has been observed that the Langmuir isotherm did not fit well with the measured experimental adsorption parameters (R^2 = 0.9597 and 0.9591 for agitation and sonication assisted adsorption respectively). On the other hand, the coefficient of correlation for the Freundlich equilibrium isotherm indicated better fitness (R^2 = 0.9734 and 0.9987 for agitation and sonication assisted adsorption respectively).

The Freundlich isotherm model constants refer to k_f = 1.30 and n =1.43 for agitation assisted adsorption and k_f = 2.84 and n = 1.4 for sonication assisted adsorption. Similar trends were reported by (Paria *et al.*, 2004) for activated carbon impregnated with anionic and cationic surfactants.

5.4.2 Kinetic modeling

For all experimental investigations, it has been evaluated that the pseudo first order model did not fit well to represent the measured kinetic data. Fig. 5.10 (a) presents the fitness of the second order kinetic model for the measured kinetic data with 2 CMC surfactant solution concentration and Pd solution concentration varied from 50-500 mg/L. Corresponding model parameters and errors have been summarized in Table 5.5. As presented in Table 5.5 there is a good agreement with the q_e values determined experimentally and from pseudo-second order model. Similar modeling trends were observed for other sets of surfactant concentrations but are not shown. The kinetic results were further analyzed with intraparticle diffusion model to elaborate upon the pertinent diffusion mechanism of Pd (II) adsorption with ELP solutions consisting 2 CMC surfactant solution concentrations (Aharoni, 1977).

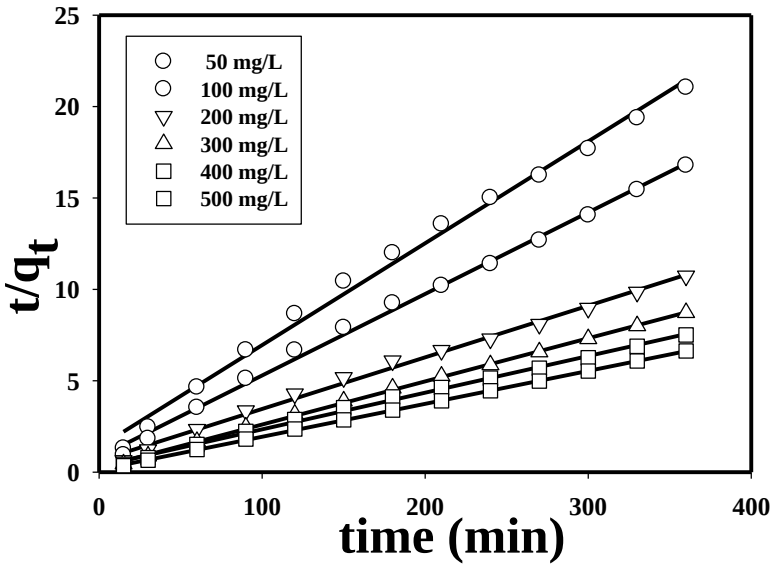

Fig. 5.10(a): Psuedo second order kinetic model fitness plot for Pd (II) adsorption on BSAC 14 adsorbent with 2CMC CTAB containing synthetic ELP solutions.

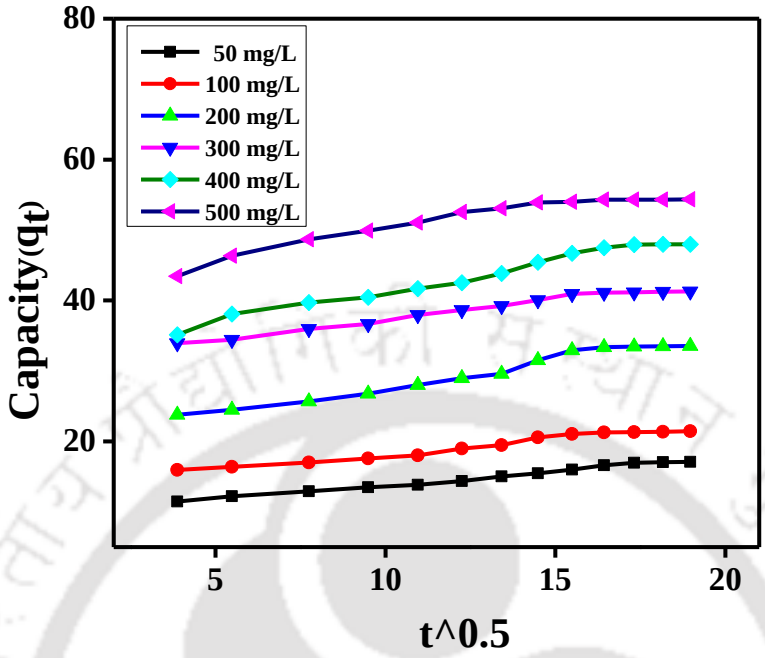

Fig. 5.10(b): Fitness of intraparticle diffusion model kinetic model for BSAC 14 adsorbent and 2 CMC CTAB containing ELP solutions.

Table 5.5: Pseudo-second order kinetic model parameters for Pd (II) adsorption on BSAC 14 from 2 CMC CTAB containing synthetic ELP solutions.

C_e (mg/L)	q_e (mg/g)		R^2	k_2 x 10^{-3} (L/min.)	%Error			
	Exp	Cal			RMS	Average	Max	Min
50	16.96	17.95	0.9923	2.25	20.62	10	69.24	1.06
100	21.33	22.42	0.9964	2.39	17.60	8.21	59.66	0.10
200	33.46	35.46	0.9948	1.26	19.61	9.2	66.56	0.46
300	41.15	42.37	0.9992	2.30	10.09	4.53	34.75	0.23
400	47.95	49.75	0.9972	1.22	14.35	7.04	47.49	0.23
500	54.36	55.55	0.9998	2.40	5.05	2.36	17.25	0.01

The fitness of measured Pd (II) adsorption kinetic data towards the intraparticle diffusion model is presented in Fig. 5.10 (b) which indicates that two distinct kinetic characteristics were prevalent. These correspond to initial sharper region where instantaneous external surface adsorption occurred on the adsorbent and the later gradual Pd adsorption that involves intraparticle diffusion as a rate limiting step which gradually leads to saturation at longer time periods.

5.4.3 Thermodynamic parameters

The thermodynamic model parameters were evaluated for synthetic electroless plating solutions without CTAB surfactant where Langmuir equilibrium model fit reasonably well with the measured equilibrium data. It has been evaluated that ΔH^{o} and ΔS^{o} were 32.3 kJ/mol and 0.137 kJ/K. mol respectively for agitation assisted adsorption and 31.8 kJ/mol and 0.136 kJ/K. mol for sonication assisted agitation assisted adsorption respectively. The positive magnitude of the evaluated thermodynamic parameters indicates that the Pd (II) adsorption followed endothermic spontaneous process.

5.5. Summary

This chapter summarized the results obtained during the preparation of low cost bamboo waste based activated charcoal adsorbents for Pd (II) adsorption from synthetic electroless plating solutions without and with CTAB surfactant. It was analyzed that a bamboo to phosphoric acid ratio of 1:4 provided BSAC adsorbent (1014.4 m^2/g) with adsorbent characteristics similar to those evaluated for commercial activated carbon (1057.7 m^2/g). For the optimized choice of adsorption parameters (pH of 8, dosage of 6 g/L and contact time of 300 min, etc.), the BSAC 14

adsorbent provided a metal uptake and removal efficiency of 29.10 mg/g and 57.83%, respectively for an initial Pd concentration of 300 mg/L using agitation assisted adsorption. Further, sonication provided slightly better adsorption characteristics compared to agitation assisted adsorption. Also, it was observed that CTAB significantly improved Pd (II) adsorbent characteristics. All in all, the Pd (II) adsorption characteristics have been evaluated to be distinct from those measured till date for aqueous solutions using AC adsorbents. Since, BSAC 14 performance is similar to commercial AC, the next chapter addresses Pd (II) continuous adsorption studies with commercial AC, given the fact that BSAC 14 preparation could not be scaled up significantly in the laboratory and abundant availability of commercial AC.

Continuous Pd (II) Adsorption Characteristics of Commercial AC Adsorbent

Results obtained from the batch mode Pd (II) adsorption studies confirmed that activated carbon provides promising Pd (II) adsorption characteristics. As a continuation of batch mode adsorption work this chapter presents the continuous Pd (II) adsorption performance of activated carbon for both aqueous and synthetic electroless plating solutions. Section 6.2 presents the adsorbent characterization results. Section 6.3 discusses the Pd (II) adsorption characteristics of commercial AC. Section 6.4 details upon the fitness of various standard models to represent measured data. The Pd (II) desorption results are briefly presented in section 6.5 followed with summary in section 6.6.

6.1 Introduction

In chapters 4 and 5 of the thesis, data obtained from the batch adsorption studies for Pd (II) ELP solutions with AC adsorbent has been presented and analysed. Based on the batch Pd (II) adsorption characteristics of laboratory fabricated AC and commercial AC, it has been inferred that the laboratory fabricated AC performed similarly to that of the commercial adsorbent and there is insignificant variation in the capacity and removal efficiency of the laboratory fabricated AC adsorbent in comparison with that of the commercial one. However, the BET surface area of laboratory fabricated AC is slightly lower than that of the commercial AC. Due to this reason, the performance of commercial AC is still better for all cases. Considering the fact that laboratory fabricated AC cannot be prepared in the huge quantities that are required for column adsorption studies, the continuous Pd (II) adsorption studies were conducted with the commercial AC adsorbent. Thus, it is concluded that there would not be significant differences in the adsorption behavior of BSAC 14 and commercial

AC for continuous Pd (II) adsorption studies. Hence, continuous Pd (II) adsorption studies have been targeted for the commercial AC adsorbent.

Section 6.2 presents the results obtained from adsorbent characterization achieved after continuous adsorption studies. Section 6.3 summarizes the adsorption profiles obtained for Pd (II) adsorption from aqueous and synthetic ELP solutions in the format of breakthrough curves. The effect of relevant process parameters on adsorption performance have been evaluated from the obtained data have been elaborated in the context of the comparative assessment of both aqueous and synthetic ELP solutions. Section 6.4 summarizes the fitness of various mathematical models such as BDST, Thomas and Yoon-Nelson models. Section 6.5 briefly presents the results obtained from desorption studies followed by summary in section 6.6.

6.2 Adsorbent characterization

The activated charcoal beads-both, treated and untreated-with Pd (II) reshown in Fig. 6.1. The FTIR spectral analysis indicated that for raw activated charcoal, the peaks were observed at frequencies of 3726, 3628, 3298, 2953, 2424, 2315, 1764, 1510, 1355 and 966 cm^{-1}. When treated with poly-vinyl alcohol, these peaks shifted and the new peaks were observed at frequencies of 3724, 3616, 3311, 2964, 2428, 2289, 1720, 1515, 1358 and 962 cm^{-1}. After treatment with Pd (II) aqueous solutions, the activated charcoal beads indicated vibration peaks at frequencies of 3736, 3622, 3304, 2968, 2414, 2330, 1764, 1531, 1336 and 958 cm^{-1}. For beads treated with Pd (II) ELP solutions, the AC beads confirmed vibration peaks at frequencies of 3736, 3616, 3324, 2968, 2418, 2295, 1718, 1517, 1334 and 960. The palladium adsorbed beads were then treated with NaOH, so as to recover Pd (II) from the surface of activated charcoal. For these beads, the peaks shifted to frequencies of 3736, 3624, 3300, 2956, 2420, 2285, 1730, 1519, 1342 and 962 cm^{-1}, which were associated with the

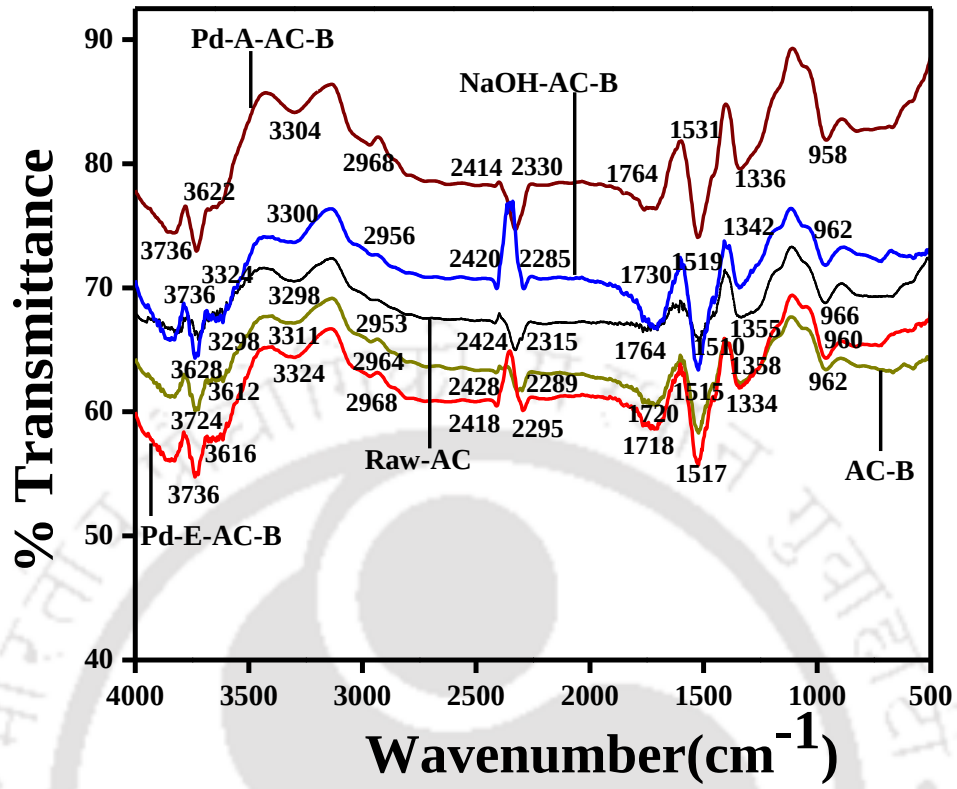

Fig. 6.1: FTIR spectra of fresh and Pd (II) adsorbed AC beads.

presence of various groups like C-H groups, amine groups (-NH^{2+} and –NH^{+}), carboxylic groups (-CHOO), COO, C=O, O-H and carbonyl groups etc. Thereafter, the FTIR spectral analysis indicated that positively charged Pd (II) adsorption from aqueous as well as synthetic electroless plating solutions resulted in significant alteration of the peaks associated to bond shifts. These peaks were associated with the presence of various functional groups like carboxylic acid, amino and hydroxyl groups. These groups have high electron densities because of the two lone pair of electrons on the oxygen atoms, one lone pair of electrons on nitrogen and the partial negative charges on other atoms in the functional groups possess due to the bond-shift. This can cause the attraction and adsorption of the positively charged Pd

Table 6.1: Operating parameters for Pd (II) adsorption with commercial AC packed bed.

Operating Parameter	Value
Contact time	150 min (approximately)
Optional pH	3.5 for aqueous and 10.5 for synthetic ELP
Flow rate used	15, 20 and 25 mL/min
Bed height used	5, 10 and 15 cm
Mass of bed	4.2, 8.52 and 13.04 g
Concentration	50, 100 and 150mg/L

(II) ions. These bond shifts are in accordance with the results obtained from our previous work and the literature available (Rajesh *et al*., 2014; Sharififard *et al*., 2012).

6.3 Continuous Packed bed adsorption for Pd (II) on AC

Continuous adsorption of metals in packed bed column is an effective process for cyclic sorption/desorption as it makes the best use of the concentration difference known to as a driving force for adsorption. The continuous adsorption process thereby allows more efficient utilization of the sorbent capacity and results in a better quality of the effluent. The continuous backed bed adsorption analysis was carried out for both aqueous and electroless plating solutions of Palladium, using AC beads. Various operating conditions for the carried out experiments are presented in Table 6.1. Based on the measurements, the plotted between (C_e/C_o) against time (t) for various chosen conditions listed in the Table 6.1.

6.3.1 Effect of Flow Rate

Based on the data obtained from batch adsorption studies, the pH of the influent solution was maintained at 3.5 and 10.5 respectively for aqueous and electroless plating solutions. The effect of flow rate on the breakthrough curves was investigated by varying the flow rates as

15, 20 and 25 mL/min. For these experimental runs, the initial adsorbate concentration and bed height were maintained at 50 mg/L and 5 cm, respectively. The effect of flow rate on breakthrough performance at the above operating conditions is shown in Fig. 6.2 (a) and 6.2 (b) for aqueous and synthetic ELP solutions respectively. The data corresponds to a time variation from 0 – 180 min for all experimental investigations. It was evaluated that with an increase in flow rate from 15 – 25 mL/min, the time dependent C_e/C_o values decrease from 0 – 0.68966 to 0 – 0.9785 for aqueous solutions and from 0 – 0.68996 to 0 – 0.84497 for synthetic ELP solutions. Thus, higher adsorption efficiencies were obtained at lower flow rate. This can be explained with the reason that at high flow rate, lower metal diffusion reduces Pd metal sorption on the AC. In other words, at higher flow rate, the residence time of the solute in the column is not large enough to achieve adsorption equilibrium and hence the metal solution leaves the column before equilibrium occurs. The breakthrough curves also illustrate upon the efficiency of the process in terms of the adsorption kinetics. It can be observed that the adsorbent saturation occurs fast at higher flow rates. Based on the obtained C_e/C_o trends, the capacity (metal uptake) of the adsorbent has been evaluated to decrease with increasing flow rate. For an increase in flow rate from 15 – 25 mL/min, the saturated adsorbent capacity and % removal have been observed to vary from 18.25-11.23 mg/g and 41.40-29.84 respectively for aqueous solutions and 10.78 – 7.52 and 31.2 –19.4 respectively for synthetic ELP solutions. For aqueous solutions, the adsorption saturation time was evaluated to be 140,130 and 110 min for the flow rate cases of 15, 20 and 25 mL/min respectively. Similarly, for synthetic ELP solutions, the adsorption saturation time was evaluated to be 120,110 and 100 min for 15, 20 and 25 mL/min respectively. To summarise, it can be inferred that the adsorption capacities and removal substantially decreased for synthetic ELP solutions in comparison with aqueous solutions. This is possibly due to the complex chemistry associated with the ELP solutions with the presence of the stabilizer and

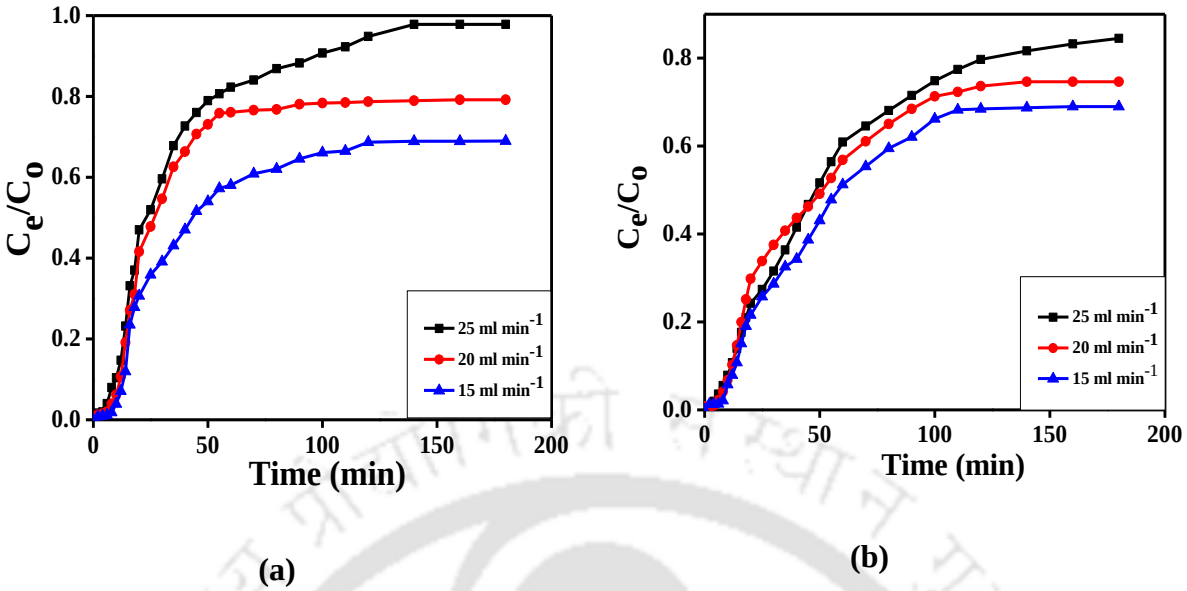

Fig. 6.2: Effect of flow rate on Pd (II) adsorption characteristics (C_o = 50 mg/L Bed Height = 5 cm): (a) aqueous and (b) synthetic electroless plating solutions.

and ammonia (and hence pH) (Emaine, 2006; Mahlatse, 2012; Nasehir, 2011).

6.3.2 Effect of initial adsorbate concentration

To determine the effect of adsorbate concentration on the breakthrough curves, column experiments were conducted by varying the Pd (II) solution concentration from 50 - 150 mg/L. For these experiments, a bed height of 5 cm, a pH of 3.5, 10.5 respectively for aqueous and electroless plating solutions and a flow rate of 15 mL/min were considered. Fig. 6.3 (a) and (b) present the breakthrough curves obtained for aqueous and electroless plating solutions respectively. The data corresponds to a time variation from 2 – 180 min for all experimental investigations. It can be observed that for an increase in solution concentration from 50 – 150 mg/L, the time dependent C_e/C_o values increased from 0 – 0.533 to 0 – 0.9785 for aqueous solutions and from 0 – 0.3265 to 0 – 0.8325 for electroless plating solutions. Thus, it is apparent that with increasing concentrations, adsorption efficiencies reduced for both cases. This is due to the quicker saturation of binding sites on the adsorbent surface at higher

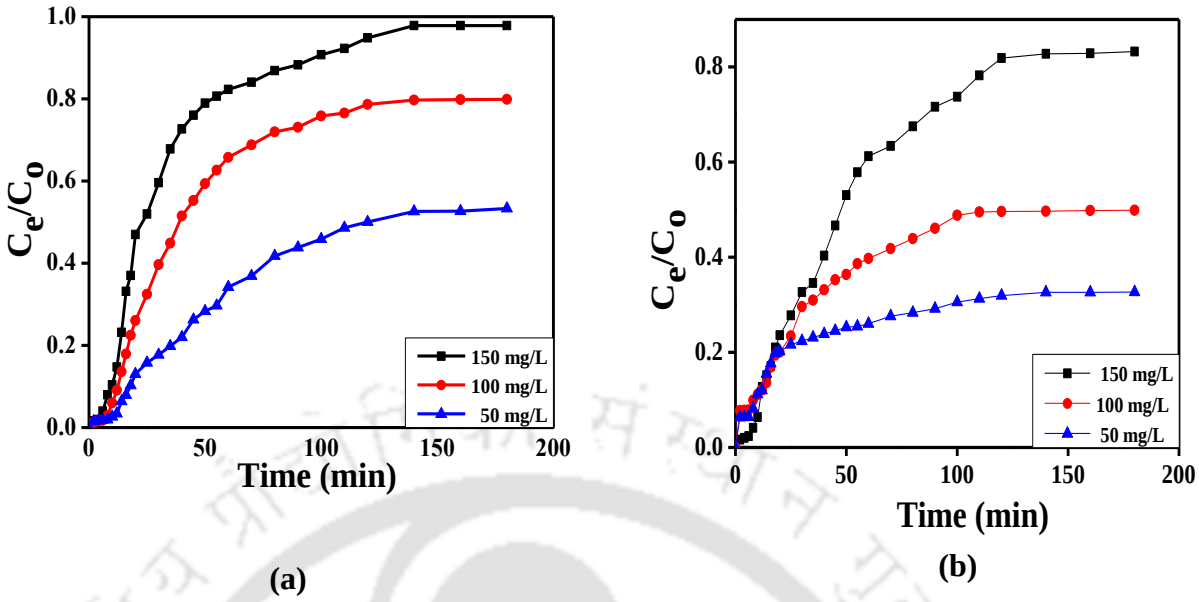

Fig. 6.3: Effect of concentration on Pd (II) adsorption characteristics (C_o = 15 ml/min and Bed Height = 5 cm): (a) aqueous and (b) synthetic electroless plating solutions.

solution concentrations. Based on the obtained C_e/C_o values, for an increase in solution concentration from 50 – 150 mg/L, the saturation removal values decreased from 52.9 – 9.6% and 34.37 – 5.26% for aqueous and synthetic ELP solutions respectively. Corresponding saturation capacity values increased from 18.25-152.64 and 10.78-68.66 for aqueous and synthetic solutions respectively. The enhancement in capacities with increasing solution concentrations is due to an increase in the number of metal ions that can get adsorbed on the adsorbent surface, thus increasing the weight of adsorbate settled on 1gm adsorbent. For the solution concentrations of 50, 100 and 150 mg/L, the saturation adsorption times have been evaluated as 100, 120 and 140 min respectively for aqueous solutions and, 80, 100 and 140 respectively for electroless plating solutions. Thus, it can be observed that for lower Pd solution concentration, lower saturation times exist. Overall, it can be observed that lower Pd solution concentrations facilitated film controlled processes with wide mass transfer zone which was not the case for higher concentrations. In agreement with the trends observed in the previous sub-section, the capacities and removal efficiencies for synthetic ELP solutions

are lower than those obtained for aqueous solutions. This is due to the complex solution chemistry and associated variation in the solution pH. The observed trends for variations in adsorption efficiencies, breakthrough curves and capacities with variation in Pd (II) solution concentration are in agreement with those presented in the literature (Goel *et al.*, 2005).

6.3.3 Effect of bed height

The effect of bed height on the breakthrough adsorbent performance was evaluated for a variation in bed height from 5 – 15 cm. For these experiments, other operational parameters refer to a Pd solution concentration of 50 mg/L, flow rate of 15 mL/min, and a pH of 3.5 and 10.5 respectively for aqueous and synthetic electroless plating solutions. The obtained breakthrough curves have been presented in Fig. 6.4 (a) and (b) for aqueous and synthetic electroless plating solutions respectively. The data corresponds to a time variation from 2 – 180 min for all experimental investigations. For both cases, it can be observed that the slope of the S curve increased with increasing bed height until saturation occurred. This is due to higher contact time with increased bed height.

For a variation in bed height from 5 – 15 cm, the time dependent C_e/C_o values decreased from 0-0.5333 to 0-0.4465 for aqueous solutions and from 0-0.3265- to 0-0.23885 for electroless plating solutions. For the cases of z = 5, 10 and 15 cm, the adsorption saturation time have been evaluated as 100, 120 and 140 min respectively for aqueous solutions and 80, 110 and 140 respectively for electroless plating solutions. Thus, with increasing bed height, saturation time increased. This is due to the reason that with an increase in bed height, the total surface area for adsorption increases to enhance the total number of binding sites available for adsorption. Thereby, adsorption equilibrium is bound to take longer time periods. For aqueous solutions, the saturated metal adsorption capacities have been evaluated to increase from 18.25-74.35 mg/g for an increase in bed height from 5–15 cm.

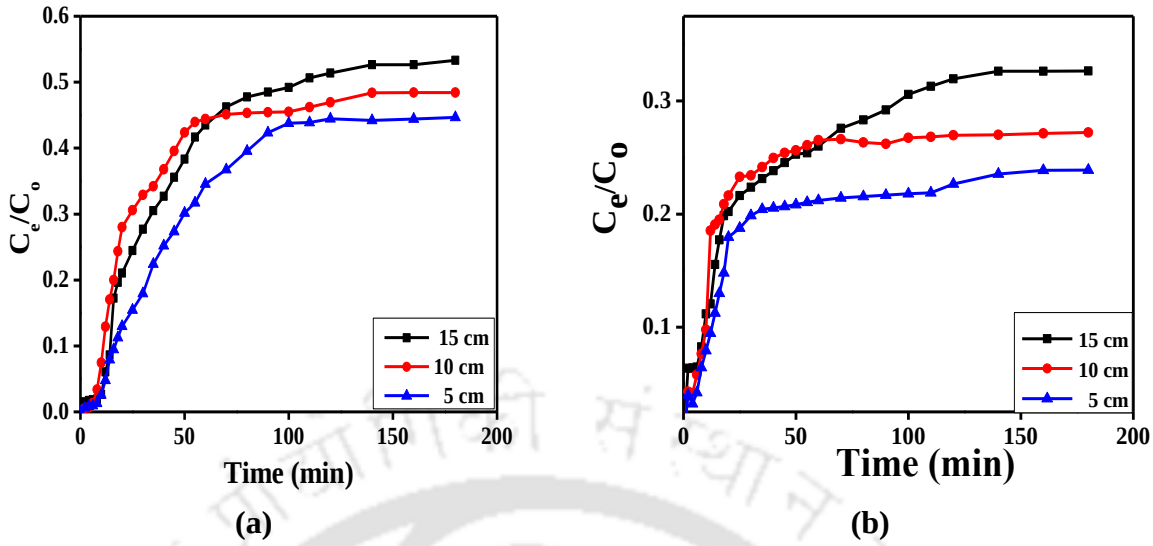

Fig. 6.4: Effect of bed height on Pd (II) adsorption characteristics (C_o = 50 mg/L and Bed Height = 15 mL/min) for (a) aqueous and (b) synthetic electroless plating solutions.

Corresponding capacities for synthetic ELP solutions refer to an enhancement from 10.78-35.7 mg/g. Once again, the solution chemistry and pH was evaluated to strongly influence the variations in metal capacities for both ELP and aqueous solutions. For ELP solutions, lower capacities have been evaluated in comparison with those obtained for aqueous solutions.

6.4 Fitness of standard mathematical models

Based on the continuous adsorption data obtained for various cases, three different standard models, namely, BDST, Thomas and Yoon-Nelson were tested for their fitness. For BDST model, some data obtained from breakthrough curves such as breakthrough time and breakthrough metal concentration were utilized. The detailed procedure for the fitness of various continuous Pd (II) adsorption models has been presented in section 2.4 of this thesis. This section summarizes the relevant results.

6.4.1 BDST model

6.4.1.1 Aqueous solution

For aqueous solutions, a plot of service time (t_b) vs bed height (Z) is presented in Fig. 6.5 (a). Along with correlation coefficients, other variables such as N_o, C_b and K_{ad} for the BDST model (that were derived from slope and intercept) for continuous adsorption data obtained for aqueous solutions is presented in Table 6.2 (a). It can be observed in the table that the correlation coefficients are not very good (0.9231 – 0.9423). This was especially true for the case where flow rate is about 20 mL/min. Further, it should be noted that the data taken refers to 3 data sets only and straight line fit for three data sets could be erroneous. Nonetheless, the obtained trends are indicative to the fact that the fitness of standard models (such as BDST) could be very difficult for Pd recovery from synthetic electroless plating solutions. Obtained modeling trends therefore require additional research investigations in the near future with more values of experimental parameters such as flow rates.

With respect to the obtained data, it can be observed that for various cases, N_o varied from 0.4115 – 0.4692, C_b varied from 0.2437 – 0.5125 and K_{ad} varied from 0.0187 – 0.00615. Lower breakthrough metal concentration values for the Pd (II) adsorption data indicate that active sites of the adsorbent were unoccupied by metal ions and the adsorbent was unsaturated.

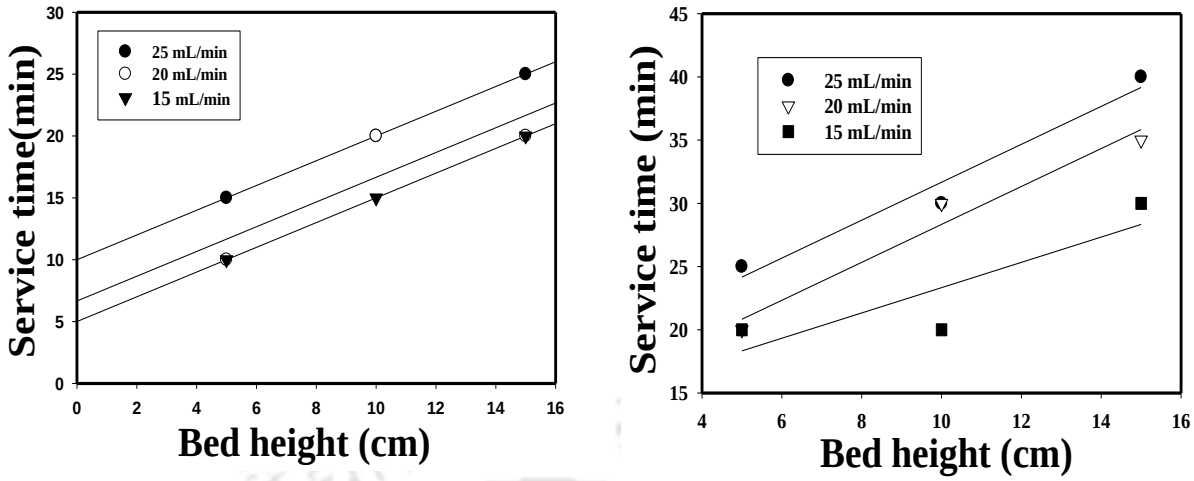

(a) **(b)**

Fig. 6.5: BDST model fitness plot for Pd (II) adsorption with (a) aqueous and (b) synthetic ELP solutions.

6.4.1.2 Synthetic ELP solutions

For synthetic ELP solutions, the plot of service time (t_b) vs bed depth (Z) is presented in Fig. 6.5 (b). Along with correlation coefficients, other variables such as N_o, C_b and K_{ad} for the BDST model (that were derived from slope and intercept) have been summarized in Table 6.2 (b). It can be observed in the table that satisfactory but not excellent correlation coefficients (0.9423–0.75) have been obtained for the fitness of the BDST model. This indicates the complexity involved with the modeling of continuous Pd (II) adsorption from synthetic ELP solutions. It can be also analyzed from the table that for synthetic ELP solutions case, N_o varied from 0.489 – 0.73, C_b from 0.1437 – 0.5125 and K_{ad} from 0.0037 – 0.0032. Compared to the aqueous solutions, higher N_o and lower combinations of C_b and K_{ad} have been obtained for the ELP solutions case. This can be compared with the experimentally determined q0 (using Eq.2.10 presented in section 2.5.2 of the thesis). This indicates that adopting continuous adsorption process, Pd (II) adsorption from ELP solution is significantly challenging in comparison with the Pd (II) adsorption from aqueous solutions (Pilli *et al.*, 2012).

Table 6.2(a): A summary of breakthrough curve and BDST model parameters for Pd (II) adsorption from aqueous solution.

F (mL/min)	Z (cm)	N_o (mg/L)	C_b (mg/L)	K_{ad} (L/mg.h)	R^2
25	5	0.4115	3.125	0.01877	0.9423
	10	0.4115	3.625	0.01767	0.9423
	15	0.4115	5.125	0.01504	0.9423
20	5	0.4230	2.5	0.04374	0.9231
	10	0.4230	3.625	0.03786	0.9231
	15	0.4230	4.25	0.03530	0.9231
15	5	0.4692	2.437	0.00753	0.9423
	10	0.4692	3.825	0.00631	0.9423
	15	0.4692	4.0625	0.00615	0.9423

Table 6.2(b): A summary of breakthrough curve and BDST model parameters for Pd (II) adsorption from synthetic ELP solutions.

F (mL/min)	Z (cm)	N_o (mg/L)	C_b (mg/L)	K_{ad} (L/mg.h)	R^2
25	5	0.489	2.125	0.0037	0.9643
	10	0.489	3.625	0.0030	0.9643
	15	0.489	5.125	0.0026	0.9643
20	5	0.603	1.5	0.0052	0.75
	10	0.603	3.625	0.0038	0.75
	15	0.603	4.25	0.0035	0.75
15	5	0.730	1.437	0.0042	0.75
	10	0.730	3.125	0.0032	0.75
	15	0.730	3.0625	0.0032	0.75

6.4.2 Thomas model

The Pd (II) adsorption data obtained from column studies were subjected to fitness studies the Thomas model to determine the rate constant (K_{Th}) and equilibrium specific palladium uptake (q_0). Tables 6.3 (a) and (b) summarize the results obtained for the fitness of Thomas model

Table 6.3(a): Thomas model fitness and model parameters for aqueous solutions (bed height = 5 cm).

Co (mg/L)	F (mL/min)	K_{Th} (mL/min.mg)	$q_{o,\ theo}$ (mg/g)	$q_{o,exp}$ (mg/g)	R^2
50	15	0.00053	12.53	18.25	0.7446
100	15	0.00031	35.63	40.29	0.7124
150	15	0.00018	66.81	64.169	0.5931
50	20	0.00061	14.68	38.22	0.8123
100	20	0.00022	35.92	80.91	0.4472
150	20	0.00013	62.96	62.99	0.6334
50	25	0.00052	25.65	152.64	0.7758
100	25	0.00026	63.11	212.39	0.5849
150	25	0.00015	107.48	282.39	0.5027

for aqueous and synthetic ELP solutions respectively. For aqueous solutions case, the correlation coefficients varied from 0.7446 – 0.5027 which indicates an unsatisfactory fitness of the Thomas model. Also, for this case, K_{TH} varied from 0.0053 – 0.0015, and theoretical q_o values varied from 18.25 – 282.39 which were significantly lower than those obtained from experimental investigations (12.53 – 107.48 mg/g). Hence, it can be summarized that the analysis of the Thomas model could not predict the performance of the continuous Pd (II) adsorption process using AC adsorbent. It is well known that the Thomas model is applicable where the external and internal diffusions are not the limiting steps and hence the poor fitness indicates that these factors play a significant role in the Pd (II) adsorption.

Table 6.3(b): Thomas model fitness and model parameters for synthetic ELP solutions (bed height = 5 cm).

Co (mg/L)	F (mL/min)	K_{TH} (mL/min.mg)	$q_{o,\ theo}$ (mg/g)	$q_{o,exp}$ (mg/g)	R^2
50	15	0.0421	1.30579	3.9157	0.7842
100	15	0.0165	4.40248	9.5678	0.6503
150	15	0.0042	8.39085	11.587	0.5694
50	20	0.0406	1.88443	4.12587	0.6258
100	20	0.0172	6.4159	9.5538	0.4547
150	20	0.0127	16.0781	11.2971	0.4166
50	25	0.0502	2.71075	2.8674	0.5793
100	25	0.0197	8.27381	11.1578	0.6242
150	25	0.0153	17.9546	15.2743	0.5875

For ELP solutions, similar trends were obtained for the fitness of Thomas model. Correlation coefficients and relevant parameters for the case are summarized in Table 6.3 (b). Based on the correlation coefficients (0.7842 – 0.6242), it can be inferred that there is poor fitness of the Thomas model with the measured data. It can be seen that K_{TH} varied from 0.0421 – 0.0197 and theoretical q_o value varied from 1.305 – 85 mg/g, values which are significantly lower than the experimentally determined q_o values of 0.0042 – 11.587 mg/g.

Based on the results presented in Tables 6.3 (a) and 6.3 (b), Thomas model can be concluded to be unsatisfactory for the prediction of continuous Pd (II) adsorption using AC from both aqueous and synthetic ELP solutions.

Table 6.4(a): Yoon-Nelson fitness and model parameters for aqueous solutions (bed height = 5 cm).

Co (mg/L)	F (mL/min)	τ_{theo} (min)	τ_{exp} (min)	K_{yn} (l/min)	R^2
50	15	112.75	95	0.0264	0.7446
100	15	44.25	50	0.0269	0.7124
150	15	91.64	72	0.0237	0.5931
50	20	56.53	80	0.0332	0.8123
100	20	76.52	90	0.0229	0.4472
150	20	95.88	82	0.0196	0.6334
50	25	71.18	105	0.0398	0.7758
100	25	101.18	100	0.0297	0.5849
150	25	126.49	85	0.0222	0.5027

6.4.3 Yoon and Nelson model

Tables 6.4 (a) and (b) summarize the results obtained for the fitness of Yoon and Nelson Model for the data corresponding to the continuous adsorption of Pd (II) from aqueous and ELP solutions. For aqueous solutions, it can be analyzed that the correlation coefficients varied from 0.7446 – 0.5029. This indicates a poor fitness. Also, a similar fitness range existed for the correlation coefficients obtained for synthetic ELP solutions (0.7842 – 0.5875). It can be further observed that the K_{YN} parameter varied from 0.0264 – 0.0222 and 0.0174–0.0301 for aqueous and synthetic ELP solutions. Further, the deviation between theoretical τ and experimentally determined τ is significant i.e., theoretical τ varied from 112.75–126.49 for aqueous solutions for a corresponding variation in experimentally determined τ from 95–85. Similar deviations existed for the parameters obtained for the ELP

Table 6.4(b): Yoon-Nelson fitness and model parameters for synthetic ELP solutions (bed height = 5 cm).

Co (mg/L)	F (mL/min)	τ_{theo} (min)	τ_{exp} (min)	K_{yn} (l/min)	R^2
50	15	110.88	85	0.0174	0.7842
100	15	98.56	110	0.0055	0.6503
150	15	68.29	120	0.0078	0.5694
50	20	108.18	100	0.0286	0.6258
100	20	129.2	90	0.0084	0.4547
150	20	99.85	70	0.0035	0.4166
50	25	96.78	80	0.0097	0.5793
100	25	122.42	75	0.0146	0.6242
150	25	75.78	60	0.0301	0.5875

solutions. Hence, based on the correlation coefficient values, it can be inferred that Yoon and Nelson model did not fit well with the experimentally measured Pd (II) adsorption data using packed bed AC adsorbent beads.

6.5 Metal Desorption

Pd (II) metal desorption experiments were carried out with a bed height and flow rate of 5 cm and 15 mL/min respectively. Desorption experiments were initiated immediately after the adsorption experiments were terminated and hence the breakthrough curves were reported with respect to the original metal ion concentration (50 – 150 mg/L) for both cases i.e., aqueous and synthetic ELP solutions. Fig. 6.6 (a) and (b) illustrate the desorption breakthrough curves obtained for aqueous and synthetic ELP solutions respectively, It can be analysed that for aqueous solutions, the C_e/C_o values initially increased from 0.2625 - 0.7937,

0.26-0.5893 to 0.142-0.445 for a variation in time from 2–10 min for 150, 100 and 50 mg/L initial metal ion concentrations respectively. However, eventually for a time period of 12–100 min, the desorption profiles reduced from 0.775-0.1225, 0.553-0.0512 to 0.4104-0.0269 for 150, 100 and 50 mg/L, respectively. Based on the breakthrough curves, the saturation time was evaluated as 70 min.

For the ELP solutions case, similar desorption profiles exist. As shown in Fig. 6.6 (b), the corresponding C_e/C_o values increased from 0.2625-0.5937, 0.1725-0.3831 to 0.1825-0.2491 for a variation in time from 2–10 min., and they have eventually decreased from 0.575-0.1625, 0.3562-0.07161 and 0.22-0.0603 for a variation in time from 12–100 min. Thus, it can be analysed that the effluent concentrations for both aqueous and ELP solutions are similar.

Based on the total metal adsorbed during adsorption (m_{ad}) and desorption (m_{de}), the elution efficiency has been evaluated as a ratio of these two and has been expressed in terms of percentage. It has been analysed that the elution efficiencies varied from 40–68% and 50–70% for aqueous and synthetic ELP solutions respectively. In this regard, it can be noted that for chitosan derivates (Chassary *et al.*, 2012), Pd and Pt recovery from bio-component mixtures was analysed to be 49-70% for HCl and NH_4OH, respectively. Thus, the literature desorption values are similar to those presented in the literature for chitosan derivatives.

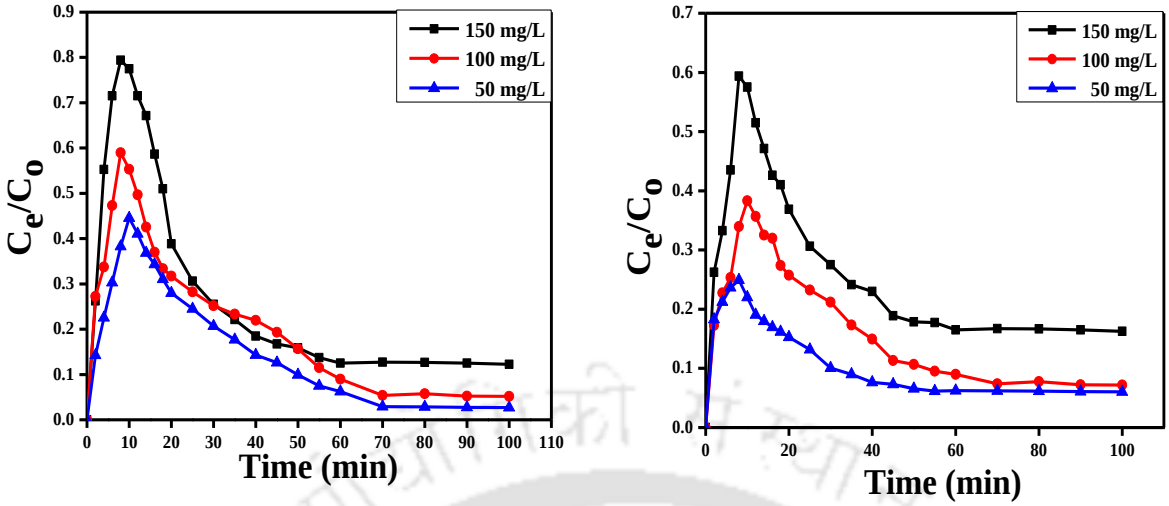

Fig. 6.6. Desorption profiles for Pd (II) removal (5 cm bed height at 15mL/min flow rate) from Pd adsorbed commercial AC (a) aqueous and (b) synthetic ELP solutions.

Table 6.5: A summary of operating parameters and continuous Pd (II) adsorption characteristics for both aqueous and synthetic ELP solutions.

Operating Parameters			Process Variables		
	Aqueous solutions	Synthetic ELP solutions		Aqueous solutions	Synthetic ELP solutions
pH	3.5	10.5	**t_b, min**	6-14	18–40
M, g	4.26 - 13.04		**t_e, min**	55-140	80-140
Z, cm	5 – 15		**V_{eff}, mL**	990-2500	1500-3625
F, mL/min	15 – 25		**L_m, cm**	4.27-13.63	4-11.25
Co, mg/L	50 – 150		**Capacity, mg/g**	18.09-152.39	10.78-68.66
			% Removal	52.93-9.60	34.27-5.21
			% Desorption	68.28-51.81	71.54-40.84

6.6 Summary

Extensive lab scale investigations were conducted to evaluate continuous Pd (II) adsorption using AC adsorbent packed beds with aqueous and synthetic ELP solutions. Overall data summary is presented in Table 6.5. It can be analyzed that the q_o and removal efficiency for aqueous solutions varied from 18.09-152.39 and 9.60-52.93 respectively. Similarly, for ELP solutions, these parameters varied from 10.78-68.66 and 5.21-34.27 respectively.

Thus, it is apparent that the Pd (II) adsorption from synthetic ELP provides lower metal adsorption capacity and removal % in comparison with the aqueous solutions. This is due to the complexity of solution chemistry and pH in influencing the packed bed Pd (II) adsorption characteristics.

The obtained Pd (II) adsorption data for both aqueous and synthetic ELP solutions has been tested for their fitness towards standard mathematical models such as BDST, Thomas and Yoon and Nelson models. Based on the obtained values, only BDST model provided excellent fitness for the data obtained with aqueous solutions and satisfactory fitness for data obtained for synthetic ELP solutions. Relevant modeling parameters were also evaluated, using which, the modeling of Pd (II) continuous adsorption can be carried out. Subsequent desorption studies were promising and provided higher elution efficiency. With respect to the literature reported data, a comparative assessment of obtained data is presented in Table 6.6. Using AC adsorbent, it can be analyzed that lower desorption efficiency was obtained for continuous adsorption of both aqueous and synthetic ELP solutions in comparison with the data presented for leaching solutions (Synders *et al*., 2013). There is no data for solutions with higher pH in the literature and the obtained data is inferred to be useful as a reference for furthering research towards the recovery and reuse of Pd (II) from electroless and electroplating solutions.

Table 6.6: Summary of literature data for continuous Pd (II) adsorption with various adsorbents and resins.

Adsorbent	Solution type	pH	C_o (mg/L)	Z cm	F mL/min	M(g)	% Adsorption	% Desorption	Capacity mg/g	Author
AC	Aqueous solutions	3.5	50-150	5-15	15-25	4.26-13.04	52.93-9.60	68.28-51.81	18.09-152.39	This work
AC	Synthetic ELP solution	10.5	50-150	5-15	15-25	4.26-13.04	34.27-5.21	71.54-40.84	10.78-68.66	This work
AC	Leaching solution	10	38	-	-	-	-	97.4 and 99.9	-	(Synders *et al.*, 2013)
WBA	Chloride solution	2	100-2000	-	-	-	-	-	121.7	(Wolowicz *et al.*, 2009)
Lewatit MP-500 and Lewatit MP-500A	Aqueous	2	0.1-1	-	-	-	-	-	8.12-9.17	(Wolowicz *et al.*, 2009)
Chelating resins	Chloride solutions	2	0.1-2	-	-	-	-	-	-	(Zbigniew *et al.*, 2009
Anion exchange resin	Chloride solutions	-	0.1-6	-	-	-	-	-	-	(Hubucki *et al.*, 2009)
TCF	Aqueous	-	10-70	-	10-30	-	-	85	-	(Yu *et al.*, 2009)

Chapter 7

Preparation, Characterization and Pd (II) Adsorption Characteristics of Chitosan-AC Composite Adsorbents

This chapter presents the results obtained for chitosan modified AC adsorbents. Two types of chitosan-AC composite adsorbents were prepared using cross-linked and impregnated methods. Section 7.3 details upon characterization results of the adsorbents using BET, FTIR and SEM techniques. Section 7.4 presents the adsorption characteristics of the prepared adsorbents followed with model fitness related discussion in section 7.5. Sections 7.6 and 7.7 present a brief overview of desorption performance and summary respectively.

7.1 Introduction

Few literatures have elaborated upon the preparation of chitosan – AC adsorbents by impregnation method (Chantaraporn *et al.*, 2012) and crosslinking method (Sharififard *et al*., 2012). While crosslinked chitosan AC adsorbent has been reported to have higher BET surface area (and hence higher sorption capacity), the impregnated chitosan AC adsorbent has not been reported for its surface area properties in the literature. However, it has been reported that the adsorbent provided better CO_2 capture from biohydrogen, biogas and flue gas mixtures in comparison with the AC adsorbent. For the cross-linked chitosan AC adsorbent, Pd adsorption studies were conducted within the initial Pd solution concentration range of 40 – 300 mg/L and for aqueous solutions. Based on the available state-of-the art, this chapter emphasizes upon relevance of chitosan–AC adsorbents for the Pd (II) recovery and reuse from synthetic electroless plating solutions whose composition is similar to real electroless plating solutions.

Various types of adsorbents were prepared by adopting impregnation method and cross-linking method. Subsequent characterizations of the adsorbents were carried out using BET, FTIR and SEM instruments. Eventually, batch adsorption studies were conducted to evaluate the equilibrium Pd (II) adsorption characteristics with synthetic electroless plating solutions that may or may not contain CTAB surfactant. Few desorption studies have also been carried out to elaborate upon the potential of the adsorbents for the removal of adsorbed Pd (II). The fitness of measured equilibrium data with standard adsorption models was also carried out.

7.2 Chitosan adsorption characteristics for impregnated adsorbents.

The chitosan impregnated activated charcoal (CH-AC-I and CH-AC-IS) was oven dried at 100 ^{o}C for 24 h. The amount of chitosan impregnated on the activated charcoal was cross-checked by evaluating the difference in the weights of chitosan before and after the process of impregnation. In this study, the peak absorbance value of chitosan concentration was observed at a wavelength of 197 nm, approximately, in UV-visible spectrometer (Chantraporn *et al.*, 2012). For chitosan adsorption, based on the calibrated chart prepared for the variation of chitosan concentration in aqueous solution (0.1–1 g/L), the % chitosan removal efficiency and metal uptake for CH-AC-I adsorbent have been evaluated as 59.73-17.05 and 14.93-0.42 mg/g respectively. Further, during the preparation of CH-AC-IS adsorbent, for a chitosan solution concentration of 0.1–1 g/L, maximum chitosan adsorption capacity and removal of 9.32 mg/g and 37.42% respectively have been obtained at a surfactant solution concentration of 1 CMC. For these results, literature data is not available for the comparison and therefore, it is intended that this works serves as a reference for the preparation of chitosan impregnated AC adsorbents.

7.3 Surface characterization

7.3.1 Surface area analyses

In this work the activated charcoal was modified with chitosan using direct impregnation, surfactant assisted impregnation and cross linking approaches so as to develop the chitosan - AC composite adsorbents. Table 7.1 represents the physical properties of chitosan modified AC adsorbents. It can be analysed that only for CH-AC-C, highest BET surface area of 1317.27 m^2/g has been obtained which was not the case for CH-AC-I and CH-AC-IS. For these two adsorbents, lower BET surface area in comparison with the AC has been obtained. Thus, it is apparent that impregnation did not enhance BET surface area and therefore is ineffective to serve as a viable technique to achieve good quality chitosan AC composite adsorbents. Among the adsorbents, it can be also observed from Table 7.1 that the CH-AC-C adsorbent possessed a total pore volume of 1.1117 mL/g, Langmuir surface area of 1256.93 m^2/g and BET surface area of 1317.27 m^2/g. Thereby, it is anticipated that the adsorbent with highest BET surface area will require lower adsorbent dosage and yield highest adsorption efficiency.

Fig. 7.1 (a) presents the N_2 adsorption-desorption isotherms of (CH-AC-C) adsorbent. It can be observed that the isotherms were of type IV and H_4 hysteresis loop which according to IUPAC (International Union of Pure and Applied Chemistry) classification confirms upon the existence of narrow slit-like pores (Sing *et al*., 1985). Also, it can be seen that the isotherm rose sharply during the early stages of adsorption which is due to the micropore filling effect. Hence, the later stages did not indicate significant rise in N_2 adsorption.

Table 7.1: Surface properties of AC, CH-AC-I, CH-AC-IS and CH-AC-C adsorbents.

S.No.	Physical Properties	AC	CH-AC-I	CH-AC-IS	CH-AC-C
1	BET surface area (m^2/g)	1057.17	787.109	914.18	1317.27
2	Total pore volume (mL/g)	0.6567	0.5227	0.7200	1.1117
3	Langmuir surface area(m^2/g)	1197.5	833.83	1125.331	1256.23

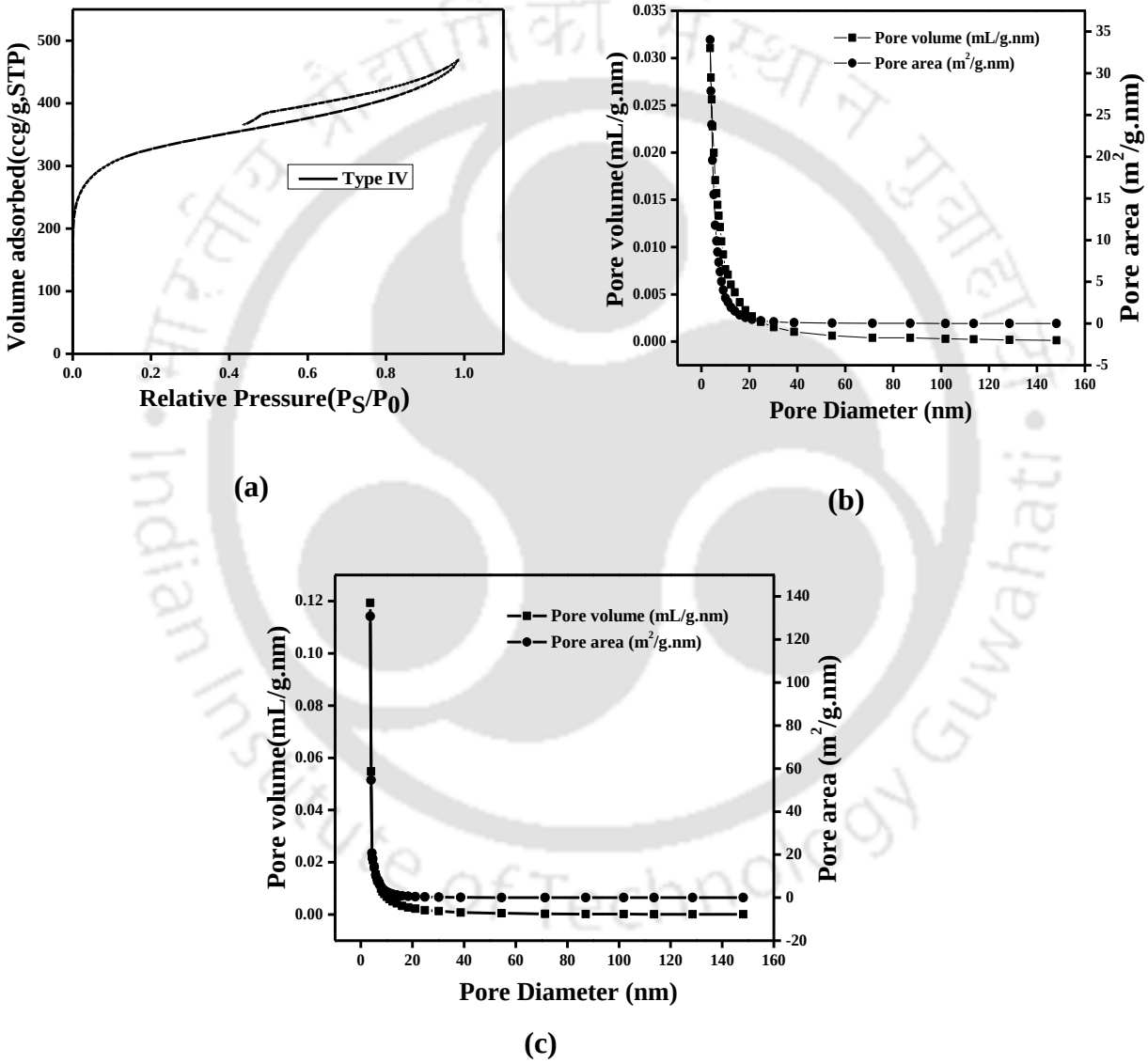

Fig. 7.1: BET surface area plots for CH-AC-C adsorbent: (a) BET isotherm (Type IV); (b) Adsorption BJH Pore volume and pore area distribution and (c) Desorption BJH pore volume and pore area distribution.

Fig. 7.1 (b) represents Barrett-Joyner-Halenda (BJH) pore size distribution (Gelb and Gubbins, 1999) of CH-AC-C that was obtained for both adsorption and desorption. The pore size distribution indicate that the adsorbent possessed cylindrical pores and the BJH analysis provided sharper peaks than the isotherm data presented in Fig.7.1 (a). Fig. 7.1 (c) illustrates the variation in obtained pore area distribution with pore diameter. It can be seen that the pore area of the adsorbent was more sensitive to the adsorption process than the desorption which is in agreement with the trends presented in the literature (Anand kumar and Mandal, 2009; Sharififard *et al*., 2012).

7.3.2 Fourier Transform Infrared Spectroscopy

FTIR analysis was conducted for raw AC, CH-AC-I, CH-AC-C adsorbents and adsorbents obtained after Pd adsorption. Some of these Pd (II) adsorbed adsorbents have been named as Pd-E-CH-AC-C and Pd-ES-CH-AC-C adsorbents. The FTIR spectra for all the adsorbents are depicted in Fig. 7.2. The FTIR analysis indicated towards the existence of several functional groups on the adsorbent surface. For the raw sample (AC), several peaks were found at wave numbers of 3526.3, 3300, 2416, 2328, 1721, 1520, 1330 and 970 cm^{-1}. For the case where adsorbent was impregnated with chitosan solutions (CH-AC-I), peaks were observed at the wave numbers of 3514, 3309, 2412, 2301, 1764, 1521, 1336 and 960 cm^{-1}. For cross linked chitosan-oxalic acid solutions (CH-AC-C), peaks were observed at wave numbers of 3512, 3309, 2420, 2303, 1732, 1525, 1350, and 966 cm^{-1} and after Pd interaction with cross linked adsorbent (Pd-E-CH-AC-C, Pd-ES-CH-AC-C), peaks were observed at the wave numbers as 3520, 3290, 2418, 2295, 1759, 1529, 1328 and 956 cm^{-1}. Also, several spectral peaks, as observed, shifted from low to high intensity. Further, spectral functional group interactions indicate OH stretching (3500 cm^{-1}), C-H aliphatic stretching

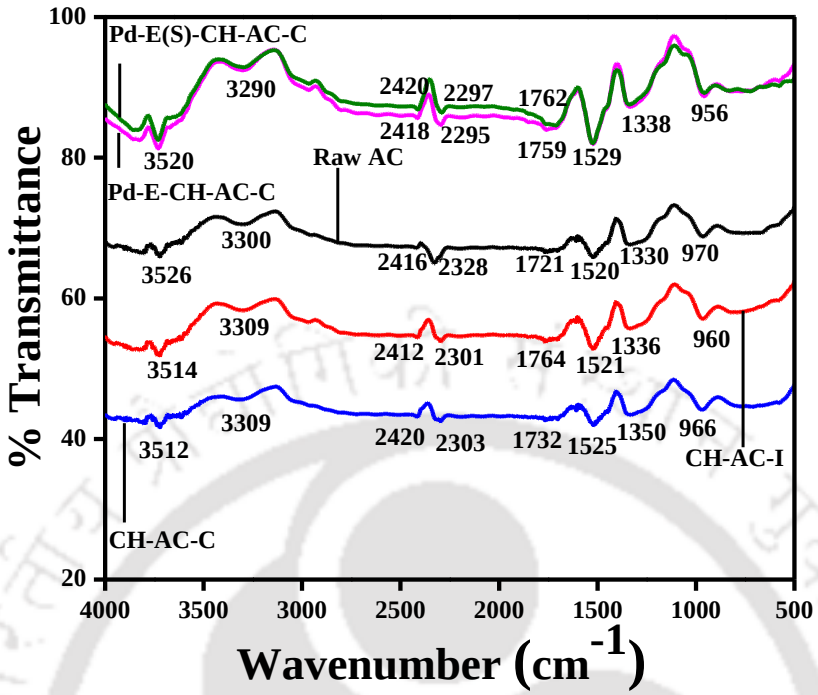

Fig. 7.2: FTIR spectra of raw AC, CH-AC-I, CH-AC-C, Pd-E-CH-AC-C and Pd-ES-CH-AC-C- adsorbents.

(2920.2 cm^{-1}), -O-CH_3 of aldehyde group (2858.5 cm^{-1}), C-H aldehydes (2720 cm^{-1}), C=O aromatic stretching (2350 cm^{-1}), stretching of C-O or O-H deformation in carboxylic acids (1747.3 cm^{-1}), C-O stretching of aromatic ethers, esters and phenols (1280-1240 cm^{-1}), C-C stretching (700 cm^{-1}). Thus, it is apparent that the peaks and intensities shifted for the adsorbents after Pd adsorption occurred on their surfaces. It is well known that the OH bond have two lone pair of electrons on the O which enables the bonding of positively charged metal ions. Similarly, O-CH3, C=O, CHO, COOH, C=O in ethers, esters and phenols have lone pair of electrons on which also Pd (II) could undergo chemisorption (Sharififard *et al.*, 2012). Therefore, there are stronger possibilities for irreversible chemisorption, which will be confirmed further with results from desorption studies.

7.3.3 Scanning electronic microscopy

The SEM images of raw AC, prepared (CH-AC-I, CH-AC-C) and treated (Pd-E-CH-AC-C) adsorbents are shown in Fig. 7.3 (a) to (d). It can observed from Fig. 7.3 (a) that the raw activated charcoal had regular plain surface with no pores on it, However, as shown Fig. 7.3 (b) and 7.3 (c), the SEM images of chitosan impregnated AC and cross linked AC indicate the progressive changes and well developed pores on the surface of the AC. The pore formation of CH-AC-I and CH-AC-C are mainly due to the additional bondage of chitosan to the adsorbent surface due to which structural changes in the adsorbent occurred to give raise to a porous structure. A further structural variation in the adsorbent can be observed in Fig. 7.3 (d) which confirms the adsorption of Pd to the active sites of the CH-AC-C adsorbent.

7.4 Effect of adsorption parameters

To analyse the adsorption performance of CH-AC-C, the optimality of adsorption parameters such as pH, equilibrium time and dosage were evaluated based on the hierarchical selection procedure. For these experimental investigations, synthetic electroless plating solutions without CTAB surfactant were used. The optimality of pH solution was first assessed by considering a fixed choice of adsorbent dosage (2 g/L), contact time 360 min and initial Pd (II) solution concentration of 50 mg/L. At the corresponding optimized pH, whose value was obtained as 12, a second set of batch adsorption experiments were conducted for varying time intervals with fixed values of adsorbent dosage (2 g/L) and initial Pd solution concentration (50 mg/L). After identifying the optimal equilibrium time as 300 min and pH as 12, a third set of batch adsorption experiments were conducted for the fixed choice of contact time, pH (obtained from the first & second set of adsorption experiments), Pd (II) plating solution concentration 50 mg/L with variation in the adsorbent dosage from 1–7 g/L.

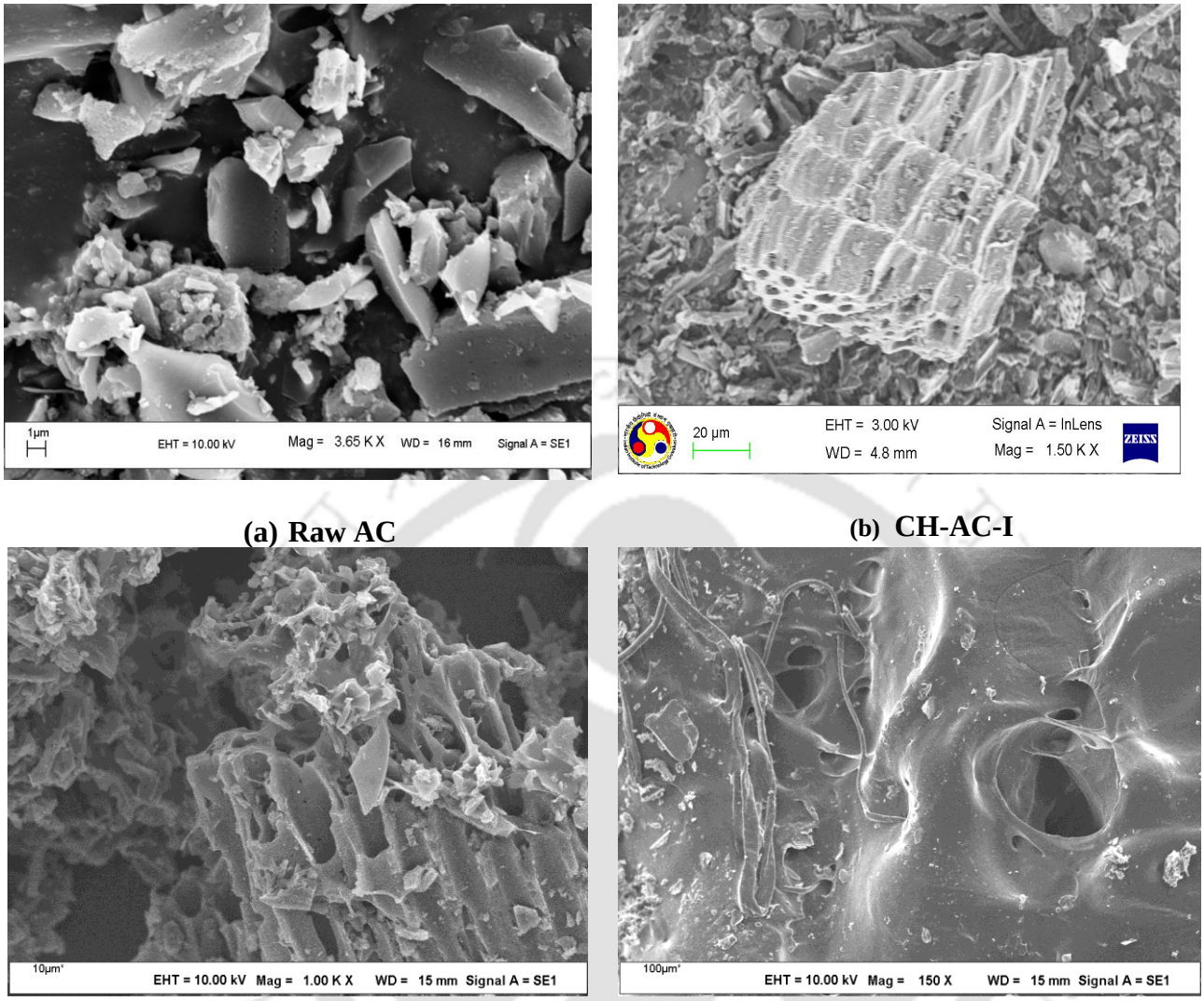

(a) Raw AC **(b) CH-AC-I**

(c) CH-AC-C **(d) Pd-CH-AC-C**

Fig. 7.3: SEM micrographs for various adsorbent samples (a) Raw AC (b) CH-AC-I (c) CH-AC-C and (d) Pd-E-CH-AC-C.

7.4.1 Effect of pH

Fig.7.4 (a) presents the effect of pH on the Pd (II) adsorption characteristics using CH-AC-C adsorbent. For a variation in pH from 2-14 from 50-300 min, the % removal and capacity varied from 35.96-81.16 and 8.99-20.29 mg/g, respectively. The Fig.7.4 (a) also indicates that

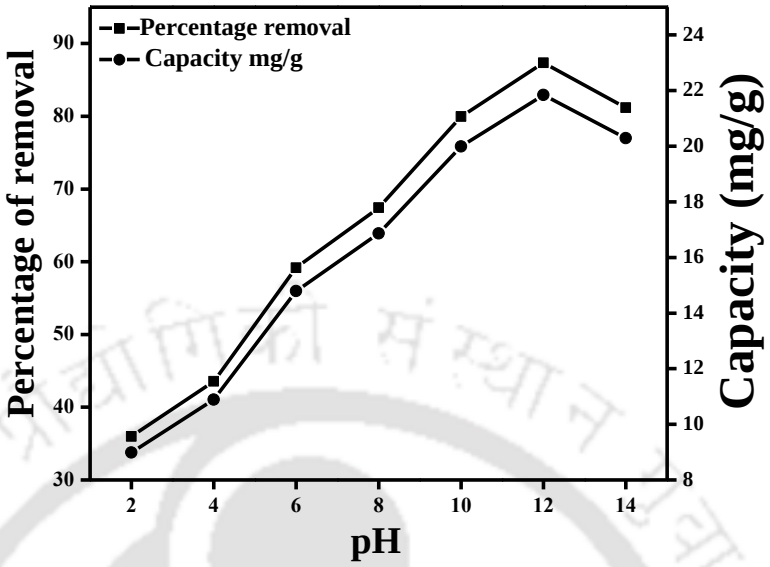

Fig. 7.4 (a) Effect of pH on Pd (II) adsorption characteristics for CH-AC-C adsorbent.

maximum % removal (87.36 %) and metal uptake (21.84 mg/g) have been observed at pH 12, which is the optimum pH identified for further experimental studies. In literature, for the experimental conditions of pH 2, time 300 min, and 10 g/L adsorbent dosage, BPMC adsorbent has been evaluated to provide % removal and capacity of 98 and 16.98 mg/g respectively (Sharififard *et al*., 2012). Thus, it can be seen that the characteristics of Pd (II) adsorption on CH-AC-C for ELP solutions were significantly lower than those obtained for aqueous solutions**.** Solution pH affects metal ion solubility, concentrations of counter ions on the adsorbent functional groups and degree of ionization of the adsorbate. It can be observed that the metal removal enhanced with an increase in pH from 2 to 12 after which it steadily declined. At low pH, H^+ enables protonation effect and this does not favour the adsorption of Pd (II) on AC (Yang *et al*., 2004; Rockstraw *et al*., 2002). However, as pH increases, protonation effect reduces and the availability of OH^- on the adsorbent surface favours the electrostatic attraction

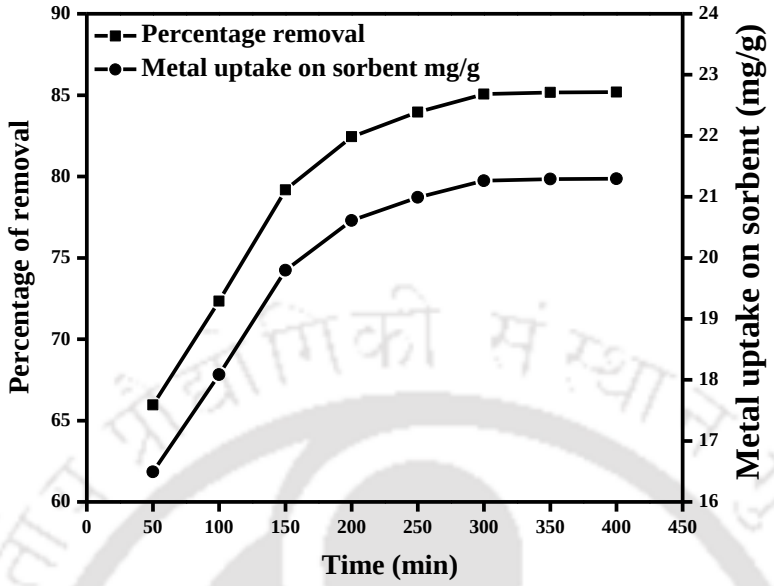

Fig. 7.4 (b) Effect of equilibrium time on Pd (II) adsorption characteristics for CH-AC-C adsorbent.

of the positively charged Pd (II) ions. Beyond a pH of 12, there might be complexification of EDTA, NH_3 with Pd (II) and therefore does not favour further adsorption of Pd (II) onto CH-AC-C. The evaluated maximum adsorption of Pd (II) at a pH of 12 is in good agreement with the reported optimal pH of 10.5 for the Pd adsorption from leached cyanide solutions on AC adsorbent (Snyder's *et al.*, 2013).

7.4.2 Effect of contact time

Fig. 7.4 (b) shows the variation of metal uptake and removal efficiency with variation in contact time. At a pH of 12 and adsorbent dosage of 2 g/L, for a variation in time from 50-400 min, the % removal and capacity varied from 65.9-85.20 and 16.49-21.29 mg/g, respectively. Also, from the figure, it can be observed that the optimal contact time can be evaluated as 300 min, at

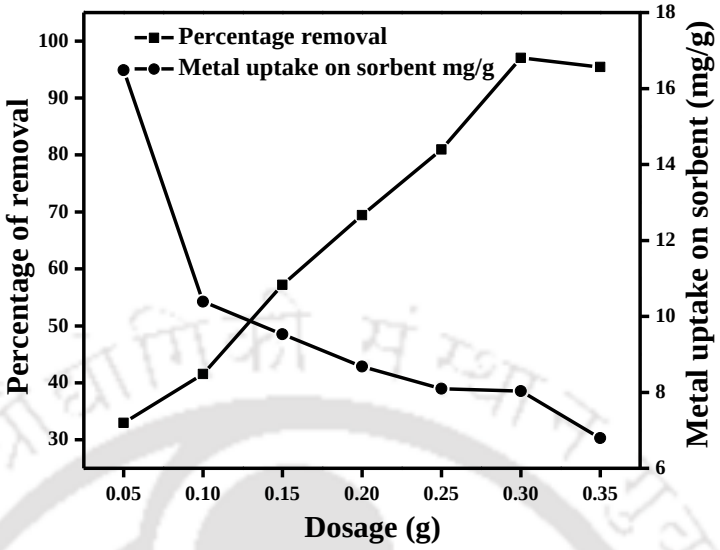

Fig. 7.4 (c) Effect of adsorbent dosage on Pd (II) adsorption characteristics for CH-AC-C adsorbent.

which maximum % removal (85.16) and metal uptake (21.26 mg/g) have evaluated. In the literature, for the experimental conditions of pH 2, time 300 min, and 10 g/L, BPMC adsorbent provided % adsorption and capacity of 98 and 16.8 mg/g respectively. Once again, it can be analysed that the adsorption characteristics of synthetic electroless plating solution are different from aqueous solutions. Thus, as observed for AC adsorbents, capacity and % removal have been obtained for the synthetic ELP solutions with CH-AC-C adsorbent in comparison with the BPMC at the optimal contact time value (Sharififard *et al*., 2012).

7.4.3 Effect of adsorbent dosage

Fig. 7.4 (c) shows the variation of adsorption capacity and removal efficiency with variation in adsorbent dosage. At a pH of 12 and equilibrium time of 300 min, for a variation in dosage from 1-7 g/L, the % removal and capacity varied from 32.96-95.46 and 16.49-6.81 mg/g, respectively. The Fig.7.4 (c) also indicates that maximum % removal (97.04) and metal uptake

(8.08 mg/g) have been evaluated at an optimal adsorbent dosage of 6 g/L. In the literature, for the BPMC adsorbent, the capacity and removal have been evaluated as 98 and 6.8 mg/g for the optimal dosage of 10 g/L. Thus, it can be analysed that significant reduction in the optimal dosage, removal but not metal uptake exist for the CH-AC-C in comparison with the BPMC adsorbent. This indicates upon the need to do experimental investigations such as those reported in this work to confirm upon the effectiveness of the CH-AC-C adsorbent but not to assume that the adsorbent characteristics of aqueous and electroless plating solutions are similar for the adsorbent. Because of the high surface area of the adsorbent (1317.2 m^2/g), a lower dosage of 6 g/L has sufficient binding sites to provides maximum adsorption. The reasons for the enhancement in removal efficiency and metal uptake with increasing adsorbent dosage have already been explained in section 3.2.1 and are also valid for this case

7.4.4 Effect of initial concentration

Based on the preliminary batch adsorption experiments conducted for CH-AC-C adsorbent, the optimal set of adsorption parameters correspond to a pH = 12, equilibrium time = 300 min and dosage = 6 g/L. Based on the Pd adsorption characteristics obtained for activated carbon adsorbent, the optimal pH, equilibrium time and dosage have been taken as 10, 300 min and 6 g/L for CH-AC-I and CH-AC-IS adsorbents. For CH-AC-C adsorbent, both synthetic plating solutions with and without surfactant have been studied for the evaluation of the initial Pd (II) solution concentration effect. For CH-AC-I and CH-AC-IS adsorbents, synthetic plating solutions without CTAB surfactant was used for the evaluating the initial concentration effect. For all cases, the Pd solution concentration was varied from 50 – 500 mg/L. For cases where CTAB was considered, its solution concentration corresponds to 2 CMC.

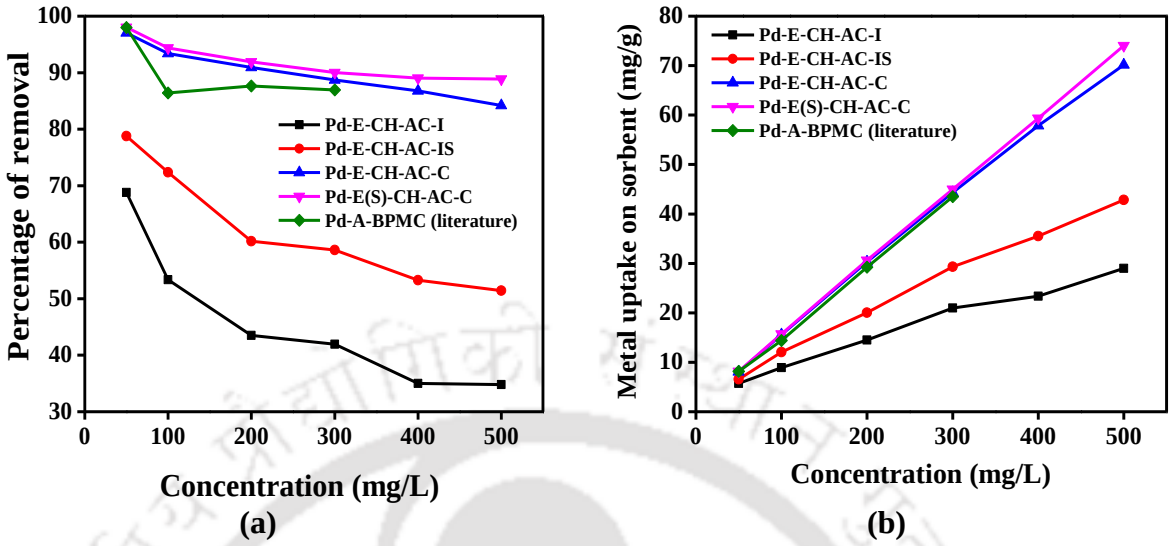

Fig. 7.5: Effect of initial Pd solution concentration on Pd (II) adsorption characteristics for CH-AC-I, CH-AC-IS, CH-AC-C adsorbents: (a) percentage removal and (b) capacity.

Fig. 7.5 (a) and (b) presents the variation of % removal and capacity for all cases. These correspond to Pd adsorption from synthetic ELP solution (a) without surfactant on CH-AC-I adsorbent (b) without surfactant on CH-AC-IS adsorbent (c) without surfactant on CH-AC-C adsorbent (d) with surfactant on CH-AC-C adsorbent. For comparison purposes, literature data presented for the Pd adsorption from aqueous solutions on BPMC adsorbent has also been presented. For a variation in Pd solution concentration from 50 -500 mg/L, it can be analysed from the figure that highest removal has been obtained for (d) 98.048 – 88.874% followed by (c) 97.04 – 84.17%, (b) 78.78 – 51.41% and (a) 68.78– 34.81 %. In comparison with the literature, only CH-AC-C adsorbent provided better removal than that reported for BPMC. Thus, the prepared adsorbent has been evaluated to be effective for Pd adsorption from synthetic ELP solutions with and without CTAB surfactant.

It can be also analysed from Fig. 7.5 (b) that the capacity increased almost linearly with an increase in initial feed concentration. In comparison with the literature, there has been a comparatively higher capacity of the CH-AC-C adsorbent. The capacities have been evaluated to be the best for case (d) 8.17– 74.06 mg/g followed by case (c) 8.08 – 70.14 mg/g, case (b) 6.56 – 42.54 mg/g and case (a) 5.73 – 29.01 mg/g). Thus, based on both capacity and removal profiles for various adsorbents, it can be inferred that the crosslinked chitosan composites perform better than chitosan impregnated adsorbents. Also, it can be said that while literature data does not confirm upon the efficacy of the chitosan impregnated adsorbents, this work confirmed that the impregnation method is ineffective to maximize the Pd recovery and capacity of the composite adsorbents. Thus, crosslinking of chitosan needs to be more thoroughly evaluated from preparation as well as process engineering perspectives. The significant variation in Pd (II) characteristics for CH-AC-C adsorbent in comparison to BPMC (literature) is possibly due to the variation in the solution pH (which was 2 for the literature case and 10/12 for the investigated cases) and inclusion of other chemicals such as sodium EDTA, NH_3 and optional CTAB surfactant (Sharififard *et al*., 2012; Snyder's *et al*., 2012).

7.5 Isotherm equilibrium modelling

Fig. 7.6 represents the validation of batch adsorption data using isotherm models such as Langmuir and Freundlich for all cases. Fig. 7.6 (a) represents the Langmuir isotherm model validation for four cases which refer to Pd adsorption on (a) CH-AC-I using ELP solution without surfactant (b) CH-AC-IS using ELP solution without surfactant (c) CH-AC-C using solution without surfactant and (d) CH-AC-C using 2 CMC CTAB surfactant containing solution. The fitness of Langmuir isotherm model parameters refers to a regression coefficient (R^2) of 0.9509, 0.9268, 0.9153 and 0.8346 for cases a-d respectively. Corresponding separation

factor (K_R) values obtained are 0.266, 0.001, 0.298 and 0.308 for cases a-d. Thus, it is confirmed that the adsorbents are favourable for adsorption. Other relevant parameters are presented in the Table 7.2.

Table 7.2: Langmuir isotherm model fitness parameters for Pd (II) adsorption on CH – AC-I, CH-AC-IS, CH-AC-C adsorbents.

Case	R^2	q_{max}(mg/g)	B	K_R	RMS Error
Pd-CH-AC-I	0.9153	38.02	0.00723	0.2982	8.78
Pd-CH-AC-IS	0.9268	58.82	0.00878	0.0016	6.14
Pd-CH-AC-C	0.9509	90.91	0.03486	0.26603	13.95
Pd-CH-AC-C-S	0.8314	95.23	0.04024	0.308752	21.68

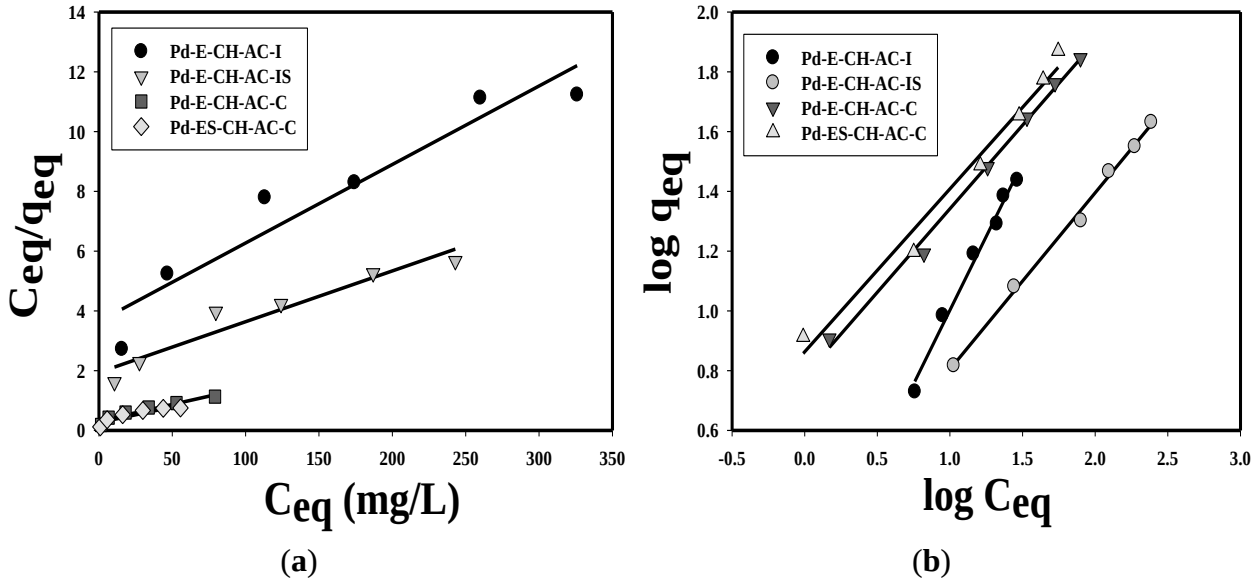

(**a**) (**b**)

Fig. 7.6: Fitness of (a) Langmuir and (b) Freundlich isotherm models for Pd-CH-AC-I, Pd-CH-AC-IS and Pd-CH-AC-C cases.

Table 7.3 Freundlich isotherm model fitness parameters for Pd (II) adsorption on chitosan–AC composite adsorbents.

Case	R^2	k_f	n	RMS Error
Pd-CH-AC-I	0.987	1.228	11.173	1.108
Pd-CH-AC-IS	0.994	1.634	4.686	0.5562
Pd-CH-AC-C	0.996	6.06	1.278	0.5219
Pd-CH-AC-C-S	0.997	7.29	1.1587	3.8752

Among all cases, Pd adsorption on CH-AC-C (case (d)) provided best fitness for the Langmuir isotherm with an estimated monolayer adsorption capacity of 95.23 mg/g. The obtained monolayer capacity and separation factor for CH-AC-C are significantly higher (70.14 mg/g and 74.06 mg/g respectively for without/with CTAB an initial Pd (II) concentration of 500 mg/L) than those reported by Sharififard *et al*. (2012) (43.48 mg/g and 0.188 respectively for a solution concentration of 300 mg/L). Based on the evaluated RMS error values, it can be concluded that significant error exists for the fitness of the Langmuir isotherm and the fitness of the model is satisfactory but not excellent.

For all cases, Fig. 7.6 (b) represents the fitness plot for batch adsorption data with Freundlich isotherm model. Regression coefficient (R^2) values for various cases correspond to 0.997, 0.996, 0.994 and 0.987 for cases a-d respectively. Thus, it can be concluded that Freundlich isotherm had good fitness with the measured data.

Table 7.3 summarizes Freundlich isotherm parameters obtained for various cases. It can be observed that for various cases, k_f and n varied from 1.228 – 7.29 and 11.173 – 1.1587

Table 7.4: A summary of Pd (II) batch adsorption capacities for various adsorbents.

Adsorbent	Type of Solution	Pd solution concentration (Feed) mg/L	Adsorbent Capacity (mg/g)	Reference
CH-AC-I	Synthetic ELP solution	50-500	5.73-29.01	Present work
CH-AC-IS	Synthetic ELP solution	50-500	6.5-42.84	Present work
CH-AC-C	Synthetic ELP solution	50-500	8.08-70.145	Present work
CH-AC-C	ELP solution + CTAB	50-500	8.17-74.061	Present work
Activated carbon	Pd (A)	50-300	5.3-35.7	(Sharififard *et al*., 2012)
BPMC	Pd (A)	50-300	6-43.4	(Sharififard *et al*., 2012)
Activated carbon	Synthetic ELP solution	50-500	5.76–43.33 (Physisorption)	Chapter 4
Activated carbon	Synthetic ELP solution	50-500	6.34 – 45.5 (Sonication)	Chapter 4
Activated carbon	Synthetic ELP solution + CTAB	50-500	6.69 – 50.13 (Physisorption)	Chapter 4
Activated carbon	Synthetic ELP solution + CTAB	50-500	7.52 – 60.03 (Sonication)	Chapter 4
Activated carbon	Aqueous chloride solution	20-225	1.5-27	(Kasani *et al.*, 2000)
Thiourea-modified chitosan microspheres	Aqueous	10-400	8.28-112.4	(Zhou *et al.*, 2009)
L-lysine Cross linked chitosan resin	Aqueous	50-400	9.5-109.7	(Fujuwara *et al.*,2007)
Racomitrium lanuginosum	Aqueous	25-300	5-30.2	(Saria *et al.*, 2009)
BTICF	Aqueous	43.8-48.8	22.4-27.5	(Ma *et al.*,2006)

respectively. Thus, it is apparent that heterogeneous phenomena occur for the Pd adsorption from synthetic electroless plating with and without surfactant on various adsorbents. For comparison purposes, it can be noted that for BPMC adsorbent, (Sharififard *et al*., 2012) reported Freundlich isotherm parameters of regression coefficient (R^2), k_f and n as 0.99, 8.11and 2.08 respectively for an initial Pd (II) aqueous solution concentration of 50-300 mg/L.

A comparative assessment of Pd adsorption characteristics obtained for CH-AC-I, CH-AC-IS and CH-AC-C adsorbents and literature data is presented in Table 7.4. The Pd adsorption characteristics of commercial activated carbon and laboratory prepared BSAC were comparable for various cases like physisorption, sonication assisted adsorption etc. Among all adsorbents, it can be inferred that only CH-AC-C provided excellent adsorption characteristics. The deviations in the solution formulations need to be noted for comparative purposes, as literature data corresponds to Pd adsorption on aqueous solutions which is not the case in this work. In summary, it can be concluded that the CH-AC- C adsorbent is effective for Pd recovery and reuse from spent electroless plating rinse waters. Further experimentation in this regard could affirm the same. However, desorption studies shall also be targeted and the results obtained for few studies carried out in this regard are being presented in the next section.

7.6 Kinetic Modeling

Amongst the two kinetic models tested for their fitness towards representing experimentally measured kinetic data of Pd (II) adsorption on Activated charcoal in the presence of CTAB surfactant, it has been observed that the first order model did not fit well as the plots did not pass through the origin. However, good fitness was observed for the second order kinetic model. Fig. 7.7 presents the fitness of the second order kinetic model for the measured kinetic data for the case of 2 CMC surfactant solution concentration and Pd solution concentrations

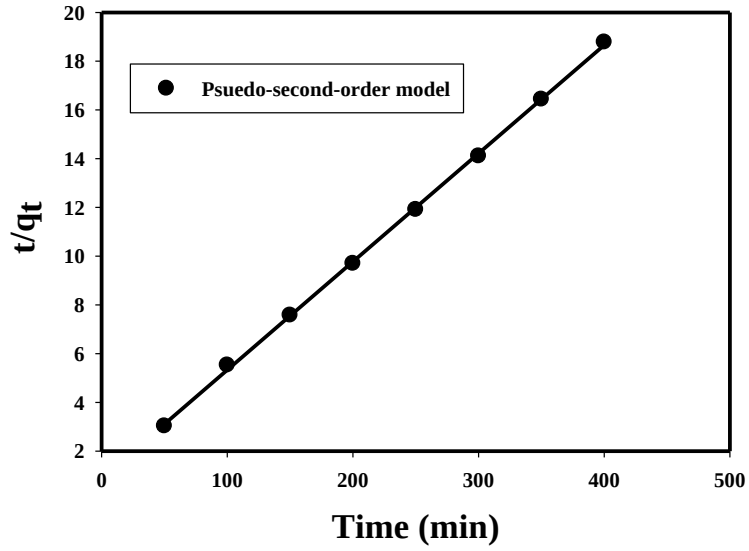

Fig. 7.7: Fitness of Psuedo second order kinetic model for CH-AC-C adsorbent with 2 CMC CTAB containing synthetic ELP solutions.

Table 7.5: Pseudo-second order kinetic model parameters for Pd (II) adsorption on CH-AC-C adsorbent with 2 CMC CTAB containing synthetic ELP solutions.

Ce	q_e (mg/g)			$k_2 x10^{-3}$	Error			
(mg/L)	Exp	Cal	R^2	(g.mol/min)	RMS	Avg	max	Min
50	21.3	22.5	0.9996	2.21	1.47	1.17	3.62	0.06

varying from 50 – 500 mg/L. Corresponding model parameters and errors are summarized in Table 7.5. As presented in Table 7.5, there is a good agreement with the q_e values determined experimentally and from pseudo second order model. Similar modelling trends were observed for other sets of palladium concentrations.

7.7 Desorption Characteristics

Table 7.6 summarizes the elution efficiency of CH-AC-C adsorbent. The CH-AC-C adsorbent that reached saturated adsorption with 300 mg/L initial Pd concentration was evaluated for its elution efficiency in batch desorption study. For the case, the experimentally determined capacity corresponds to 44.345 mg/g. Based on the Pd solution concentrations obtained after desorption study, it has been evaluated that Pd elution efficiency is significantly lower while using 0.1 M HCl. For this case, the equilibrium Pd concentration on the adsorbent after adsorption has been estimated to be 43.106 mg/L, which is very high and not promising. This corresponds to a desorption efficiency of 2.792% for 0.1 M HCl. For the NaOH based desorption study, the equilibrium concentration has been estimated to be about 33.835 mg/L which is significantly high and promising to provide a desorption efficiency of 23.698%. On comparing the desorption efficiency for the two cases, it can be observed that NaOH gave a higher desorption performance. This is due to the optimality of adsorption characteristics at a higher pH, as discussed in section 4.3.3 of the chapter. Hence, the use of a strong base like NaOH is favourable for desorption studies.

Table 7.6: Summary of batch desorption characteristics for Pd-CH-AC-C prepared with 300 mg/L initial Pd (II) solution concentration.

Reagent used	Chemical used	Adsorbent Capacity mg/g	Initial solution concentration mg/L	Final adsorbent concentration (mg/g)	% Recovery
HCl	0.1M	44.345	2.96	43.106	2.792
NaOH	0.1M	44.345	25.6	33.835	23.698

The overall desorption efficiency is not significantly high and promising for chitosan AC adsorbents. Therefore, the applicability of Pd adsorbed AC for desorption is limiting and product development, such as in catalysis, would be the appropriate application for the Pd adsorbed AC adsorbent. Further, lower desorption efficiencies confirm irreversible chemisorption.

7.8 Summary

Commercial activated charcoal was modified with several combinations of chemical reagents and approaches such as impregnated chitosan, impregnated chitosan-surfactant and cross linked chitosan (using oxalic acid) to develop CH-AC composite adsorbents for the removal and recovery of palladium from synthetic electroless plating solutions. Among various classes of adsorbents developed, CH-AC-C provided the highest enhancement in BET surface area (from 1057 to 1317.2 m^2/g). During impregnation process which was not effective, about 50–60 % chitosan was evaluated to have been adsorbed on the surface but without enhancing its adsorption properties. For CH-AC-C adsorbent, the optimal adsorption parameters were identified as pH of 12, equilibrium contact time of 300 min and dosage of 6 g/L. Using these conditions, for a variation in Pd solution concentration from 50–500 mg/L, the adsorbent was evaluated to have 8.08-70.14 mg/g capacity and 84.17–97.04% removal, which is comparatively higher than those obtained for AC adsorbent that was investigated earlier in this work (5.76–43.33 mg/g capacity and 69.12–52%). Compared to the most appropriate data available in the literature (for BPMC adsorbent), the CH-AC-C adsorbent provided comparatively higher capacities and removal % for Pd adsorption from synthetic electroless plating solutions. With a poor fitness, the monolayer adsorbent capacities were 38.02, 58.82 90.91 and 95.6 mg/g for Pd-E-CH-AC-I, Pd-E-CH-AC-IS, Pd-E-CH-AC-C and Pd-E(S)-CH-AC-C, respectively. The batch

adsorption was further evaluated and was found to fit well with the Freundlich isotherm model. Desorption studies inferred that the maximum recovery from CH-AC-C during desorption was about 23.6% which is not very promising for recovery applications.

Chapter 8

Conclusions and Recommendations for Future Work

This chapter summarizes various relevant conclusions and Recommendations for future work.

8.1 Conclusions

Based on experimental investigations and modeling related studies, the various relevant conclusions have been presented in the following sub-sections.

8.1.1 Biosorbents for heavy and precious metal removal

- Among various waste biomass plant resources in the North-eastern region, biosorbents prepared from bamboo stem and pineapple stem waste biomass provided stable performance for Ni (II) removal from aqueous solutions.
- The BET surface area of bamboo stem based biosorbent is significantly higher (116 m^2/g) in comparison to that evaluated for pineapple stem based biosorbent (11.47 m^2/g).
- Amongst NaOH and phosphoric acid based activation, phosphoric acid based activation is the most effective.

8.1.2 Ni (II) adsorption characteristics

- For Ni (II) removal using both bamboo stem and pineapple stem based biosorbents, the optimal adsorption parameters are pH = 5, equilibrium time = 300 min. and dosage = 2 g/L.
- At a solution concentration of 300 mg/L, the bamboo stem based biosorbent (BSAC) provided highest adsorption capacity (121.72 mg/g), which is 45 % higher than that reported in the literature for BSAC adsorbent prepared with similar preparation method (Lalhruaitluanga *et al.*, 2011).

- Ni (II) adsorption studies for both BSAC and PS adsorbents indicated the fitness of Freundlich equilibrium isotherm and pseudo-kinetic second order kinetic models. Further, Ni (II) adsorption with these biosorbents has been evaluated to be endothermic and irreversible in nature.

8.1.3 Laboratory fabricated AC adsorbent

- The high temperature inert environment based H_3PO_4 activation at a bamboo to acid ratio of 1:4 provided BSAC 14 adsorbent that possessed high BET surface area of 1014.4 m^2/g.
- The BSAC 14 adsorbent surface area is comparable with the BET surface area of the commercial AC adsorbent (1057.7 m^2/g).

8.1.4 Pd (II) adsorption characteristics of commercial AC adsorbent

- For the commercial AC adsorbent, using synthetic Pd ELP solutions without CTAB surfactant, the optimal adsorption parameters refer to a contact time of 300 min, pH of 10 and dosage of 6 g/L.
- For synthetic ELP solutions without surfactant, for a variation in Pd (II) solution concentration of 50-500 mg/L, the metal uptake and % removal varied from 5.76-43.33 mg/g and 69.12-52 % respectively for physisorption case. It has been evaluated that sonication assisted adsorption performed slightly better than the physisorption case.
- Compared to the synthetic ELP solutions without surfactant, the metal uptake and removal efficiency values were higher for the cases corresponding to synthetic ELP solutions containing CTAB surfactant (1-4 CMC). However, there has not been any variation in the trends i.e., with increasing Pd solution concentration, an enhancement in metal uptake is accompanied with reduction in removal efficiency.

- For all cases, Freundlich equilibrium isotherm and psuedo second order kinetic model have been evaluated to be the best fit models. Thermodynamic evaluations indicated that the Pd (II) adsorption is spontaneous and endothermic.

8.1.5 Pd (II) adsorption characteristics of laboratory fabricated AC adsorbent

- For the laboratory fabricated AC adsorbent, using synthetic Pd ELP solutions without CTAB surfactant, the optimal adsorption parameters refer to a contact time of 300 min, pH of 8 and dosage of 6 g/L.
- For synthetic ELP solutions without surfactant, for a variation in Pd (II) solution concentration from 50-500 mg/L, the metal uptake and % removal varied from 6.01-43.23 mg/g and 72.12-53.2 % respectively for sonication case. It has been evaluated that sonication assisted adsorption performed slightly better than the physisorption case.
- For synthetic ELP solutions with 2 CMC surfactant solution concentrations and agitated assisted adsorption case and for a variation in Pd (II) solution from 50-500 mg/L, the metal uptake enhanced from 6.35-45.08 mg/g and % removal decreased from 76.24–54.1%.
- From modelling perspective, batch adsorption followed Freundlich equilibrium isotherm and psuedo-second order kinetic models. Other trends are similar to those obtained for Pd (II) adsorption on commercial AC.
- With respect to the Pd (II) adsorption characteristics, the commercial AC performed a little better than the laboratory fabricated AC. This is due to insignificant enhancement in the BET surface area of the commercial AC in comparison with that of the laboratory fabricated AC.

8.1.6 Continuous Pd (II) adsorption using AC packed beds

- 15 % PVA provided optimal binding strength for the preparation of AC based packed beds.
- The operating conditions of flow rate = 15 mL/min, initial metal ion concentration of 50 mg/L and 5 cm bed height provided better combinations of % removal and capacity.
- For Pd aqueous solutions, the metal uptake, % removal and elution efficiency were evaluated to be about 18.09-152.39 mg/g, 9.60-52.39% and 51.81-68.28% respectively. These values are significantly higher than those obtained for the Pd ELP solutions without CTAB surfactant (10.78-68.66 mg/g, 5.21-34.27% and 40.84-71.54% respectively). Thus, bath chemistry is inferred to be an important variable in influencing Pd (II) sorption characteristics.
- Desorption breakthrough curves indicated that a combination of increasing and C_e/C_o decreasing profiles exist for all cases.
- Among various standard models, BDST model fit well to represent the measured Pd (II) adsorption data for both aqueous and synthetic ELP solutions.

Compared with the literature, the obtained data is inferred to serve as a reference for further research in the recovery and reuse of Pd (II) from electroplating industries.

8.1.7 Pd (II) adsorption characteristics of chitosan-AC composite adsorbents

- Crosslinked chitosan AC adsorbent (CH-AC-C) possessed higher BET surface area (1317.2 m^2/g) than AC (1014.4 m^2/g) and impregnated chitosan AC adsorbents (789.6-962.8 m^2/g).

- The impregnation confirmed 50-60% chitosan adsorption to the commercial AC but did not enhance the BET surface area (789.6-962.8 m^2/g).
- For the CH-AC-C adsorbent, the optimal batch adsorption parameters correspond to pH = 12, equilibrium time = 300 min and dosage = 6 g/L, where 97.04% Pd removal has been achieved.
- Freundlich equilibrium model fit well to represent the measured batch adsorption data for all composite biosorbents.
- For the CH-AC-C adsorbent, using 0.1 M NaOH solution, the batch desorption efficiency has been evaluated to be significantly low (23.69 %). However, it is expected to increase for continuous desorption process.

Table 8.1 summarizes the most appropriate research findings of this work along with the few most competent literature data. With a careful observation of the table, the following can be outlined as the promising output of the Ph.D. thesis:

a) Commercial AC offers significantly lower Ni (II) batch adsorption characteristics for synthetic ELP solutions in comparison with those obtained for aqueous solutions. This is a notable issue in the thesis which has clearly indicated upon the role of complex solution chemistry in altering the Ni (II) adsorption characteristics.

b) Commercial AC provides lower Pd (II) continuous adsorption characteristics than for synthetic ELP solutions. This has also confirmed the greater role of solution chemistry in influencing the evaluated characteristics.

c) CH-AC-C provided higher metal uptake but not removal for batch Pd (II) adsorption from synthetic ELP solutions.

d) The batch desorption efficiencies of commercial AC and CH-AC-C adsorbent are not promising. However, continuous Pd (II) adsorption efficiencies are promising but lower than those reported in the literature for aqueous solutions.

In summary, it can be inferred that AC are potential resources for the recovery of Pd (II) from spent ELP solutions. AC has been analyzed to provide moderate metal capacities of 50-70 mg and satisfactory elution efficiency of 50-70%. Further, AC is inexpensive (Commercial AC costs ₹ 390/- per 500g). On the other hand, ion-exchange resins such as Lewatit 14 provide excellent metal capacities (100-200 mg/g) and elution efficiencies (60-80%) but are highly expensive (retail cost of Lewatit 14 is about ₹ 3900 per 100 g). Thus, the cheating resins have 2-3 times higher capacity and about 10 times lower adsorbent dosage (30 mg/L of Lewatit14 and 300 mg/L for the AC) with a cost of about 50 times higher than those values corresponding to the AC. Considering these aspects, AC can be regarded to be cost effective by a factor of 1-2. Thus, it can be inferred that AC can be regarded to possess significant potential for the recovery and reuse of Pd (II) from electroplating wastewaters, provided AC offers good reusability performance.

8.2 Recommendations for Future Work

The following areas of work have been identified to consider in the near future consolidating further research in the vast field of noble metal recovery and reusing from industrial streams:

- Further extending the role of solution chemistry in altering adsorption characteristics is required. These refer to variant concentrations of stabilizer (Na_2EDTA/Trisodium citrate)

Table 8.1: A summary of research findings in the thesis and most relevant literature data for comparative assessment purposes.

S.No	Adsorbent	Metal	Solution	Mode of Adsorption	Optimal adsorption parameters	Concentration range (mg/L)	Max. Metal capacity (mg/g)	Removal % (at max. capacity)	Desorption (%)
1	PS	Ni (II)	Aqueous	Batch	t =300 min, pH=5, Dosage=2g/L	50-300	29.9	58.2	-
2	BSAC	Ni (II)	Aqueous	Batch	t =90 min, pH=5, Dosage=2g/L	50-300	98.7	61.23	-
3	BSAC (Lalthuranga *et al*., 2011)	Ni (II)	Aqueous	Batch	t =360 min, pH=5, Dosage=4g/L	30-70	52.9	62.35	37.42
4	Commercial AC	Ni (II)	Synthetic ELP	Batch	t =120 min, pH=10.5, Dosage=4g/L	50-500	17.75	5.56	-
5	Low *et al*., 1995	Ni (II)	Electroplating	Batch	t =60 min, pH=5, Dosage=2.5g/L	0.28-28	11.42	2.59	-
6	Commercial AC	Pd (II)	Synthetic ELP	Batch	t =300 min, pH=10, Dosage=6g/L	50-500	43.33	52	4.5
7	BSAC14	Pd (II)	Synthetic ELP	Batch	t =300 min, pH=8, Dosage=6g/L	50-500	42.5	51	-
8	Commercial AC (Sharififard *et al*., 2012)	Pd (II)	Aqueous	Batch	t =360 min, pH=2, Dosage=10g/L	50-300	35.7	85.6	-
9	Commercial AC	Pd (II)	Aqueous	Continuous	t =140 min, pH=3.5, Dosage=13g/L	50-150	152.39	9.60	68.28
10	Commercial AC	Pd (II)	Synthetic ELP	Continuous	t =140 min, pH=10.5, Dosage=13g/L	50-150	68.66	5.21	71.54
11	Coconut AC (Synders *et al*., 2013)	Pd (II)	Cyanide leach	Continuous	t=72h,pH=10 and 10g/L	0.63-2.3	-	64	95.4
12	CH-AC-C	Pd (II)	Synthetic ELP	Batch	t =300 min, pH=12, Dosage=6g/L	50-500	70.14	84.17	23.69
13	BPMC (Sharififard *et al*., 2012)	Pd (II)	Synthetic ELP	Batch	t =360 min, pH=2, Dosage=10g/L	50-300	6-43.4	86.9	-

and ammonia/NaOH and their potential to critically influence and alter Ni (II) and Pd (II) adsorption characteristics. Thereby, alternate pre-treatment process strategies can be researched for the better understanding of the recovery and reuse of Pd (II) from waste streams.

- For the commercial AC adsorbent, continuous Pd (II) adsorption and desorption studies can be carried out for synthetic ELP solutions containing CTAB surfactant. For these systems, the specific role of CTAB surfactant to influence the Pd (II) adsorption characteristics will be an interesting feature to investigate upon.
- For the BSAC 14 adsorbent or commercial adsorbent, continuous Ni (II) adsorption study from synthetic ELP solutions can be carried out.
- Pd (II) continuous adsorption study for CH-AC-C adsorbent.
- Reusability studies for commercial AC to recover Pd (II) from synthetic ELP solutions.
- Batch and continuous Adsorption characteristics of AC for the recovery of other noble metals such as Pt, Au and Ag.
- Batch and continuous Pd (II) adsorption using commercial chelating ion-exchange resins (such as Lewatit 14) for the recovery of Pd (II) from synthetic ELP solutions.
- Adsorption of multiple metals on AC from synthetic ELP and electroplating solutions.
- Batch and continuous Pd (II) adsorption studies from real electroplating industry wastewaters.
- Catalysis using Pd (II) adsorbed on CH-AC-C adsorbent. Possible investigations include phenol hydrogenation in wastewater streams (Diaz *et al.*, 2007),

hydrodechlroination of phenols (Calvo *et al*., 2004) and insitu H_2O_2 generation for phenol dehydration (Mohammad *et al*., 2011).

References

Aharoni, C. and Ungarish, M., "Kinetics of activated chemisorption, Part 2, Theoretical model," *J Chem Soc.*, 73, 456 - 464 (1977).

Ajmal, M., Khan Rao, R. A., Ahmad, R. and Ahmad, J., "Adsorption studies on citrus reticulate fruit peel of orange: removal and recovery of Ni (II) from electroplating wastewater," *J. Hazard. Mater., B* 79, 117 - 131 (2000).

Akar, T. and Kiran, S., "Botrytis cinerea as a new fungal biosorbent for removal of Pb (II) from aqueous solutions," *Biochem. Eng.J*, I25(3) 227 - 235(2005)

Akhthar, N., Iqbal, J. and Iqbal, M., "Removal and recovery of Ni (II) from aqueous solution by loofa sponge immobilized biomass of Chlorella sorokiniana: characterization studies," *J. Hazard. Mater.,* B 108, 85 - 94 (2004)

Aksu, Z., "Biosorption of heavy metals by microalgae in batch and continuous systems. In: Y.S. Wong, N.F.Y. Tam, (ed.), Algae for waste water treatment, Germany: *Springer-verlog and Landes Bioscience*., 37 - 53 (1998).

Aksu, Z., Acikel, U., Kabasakal, E. and Tezer, S., "Equilibrium modelling of individual and simultaneous biosorption of chromium (VI) and nickel (II) onto dried activated sludge," *Water Res.*, 36**,** 3063 - 3073 (2002).

Alhawas, M., Alwabel, M., Ghoneim, A., Alfarraj, A. and Sallam, A., "Removal of nickel from aqueous solution by low-cost clay adsorbents," *Intern. Acad. Ecol. Envi. Sci.*, 3 (2) 160 - 169 (2013).

Alimohamadi, M., Abolhamd, G. and Keshtkar, A., "Pb (II) and Cu (II) biosorption of *hizopus arrhizus* Modeling Mono- and Multi-Component Systems," *Miner. Eng*., 18, 1325 - 1330 (2005).

Altunoglu and Abdulkadir, "Hydrogen Permeation Through Nickel and Nickel Alloys: Surface Reactions and Trapping", Ph.D. Thesis, The Open University, (1994)

Anand kumar, J. and Mandal, B., "Removal of Cr (VI) from aqueous solution using Beal fruit (*Aeglemarmeloscorrea*) shell as an adsorbent," *J. Hazard. Mater*, 168, 633 - 640 (2009).

Applications of guidelines for drinking water quality, Document EHE/EHC/81.27 WHO (World Health Organization), *Beszedits. Eng. Dig., 18* - 25 (1982)

Awoyale, H., Eloka, A. A., Eboka, A. C. and Odubiyi, O. A.," Production and experimental efficiency of activated carbon from local waste bamboo for waste water treatment," *Int. J. Eng. Appl. Sci.*, 3 (2), 8 - 17 (2013)

Bayat, B., "Comparative study of adsorption properties of Turkish fly ashes I. The case of Nickel (II), Copper (II) and Zinc (II)." *J. Hazard. Mater.*, B 95, 251 - 273 (2002)

Benguerel, E., Demopoulos, G. P. and Harris, G. B., "Speciation and separation of rhodium (III) from chloride solutions: a critical review," *Hydrometallurgy*, 40, 135 - 152 (1996).

Birinci, E., Mustafa, G. and Ali O.A., "Separation and recovery of palladium (II) from base metal ions by melamine–formaldehyde–thiourea (MFT) chelating resin." *Hydrometallurgy*., 95 (1) 15-21 (2009).

Bohart, G. S. and Adams, E. O., "Some aspects of the behaviour of charcoal with respect to chlorine." *J. Am. Chem. Soc.*, 43, 545 - 523 (1920).

Brown, P. A., Gill, S. A. and Allen, S. T., "Metal removal from wastewater using peats," *Water Res.,* 34 (16), 3907 - 3916 (2000).

Brunauer, B., Emmett, P. H. and Teller, E., "Adsorption of gases in multi molecular layer." *J. Am. Chem. Soc.,* 60,309 - 319 (1938).

Calvo, L., Mohedano, A. F., Casas, J. A., Gilarranz, M. A. and Rodriguez, J. J., "Treatment of chlorophenols-bearing wastewaters through hydrodechlorination using Pd-activated carbon catalysts," *Carbon,* 7 (42), 1377 - 1381 (2004).

Cashton, J. C. and Sercombe, E.J., "Palladium on charcoal catalysts, some effects of variables on hydrogenation activity," *Platinum Met. Rev.,* 5 (4), 122 – 125 (1961).

Cavalcante, C. L., "Industrial adsorption separation processes: Fundamentals, modeling and applications," *Latin American Applied Research JR.,* 30, 357-364.

Chand-Bansal, R. and Goyal, M., "Activated carbon adsorption," *Taylor & Francis Group*," (2005).

Chaohui, L. Z., Jianming, W. H., Cheng, H., Bilan, L., Zimian, N., Jianzhang, Z. and Jink, F., "Adsorption and reduction of palladium (Pd^{2+}) by *Bacillus*," *licheniformis Chin. Sci. Bull,* 47, 15 (2002).

Chassary, P., Vincent, T., Jose, S. M., Macaskie, L. E. and Guibal, E., "Palladium and Platinum recovery from bicomponent mixtures using chitosan derivatives," *Hydrometallurgy,* 76, 131 – 147 (2005).

Chenxi, L. and Pascale. C., "Fixed-bed column study for the removal of cadmium (II) and nickel

(II) ions from aqueous solutions using peat and *mollusc shells*," *J. Hazard. Mater.***,** 171, (1–3) 872 - 878 (2009).

Chi K. A., Donghee, P., Seung, H. W. and Jong, M. P., "Removal of cationic heavy metal from aqueous solution by activated carbon impregnated with anionic surfactants," *J. Hazard. Mater.*, 164, 1130-1136 (2009).

Covelo, E. F., Vega, F. A. and Andrade, M. L., "Sorption and desorption of Cd, Cr, Cu, Ni, Pb and Zn by a Fibric Histosol and its organo-mineral fraction*," J. Hazard. Mater.,* 159,342-347 (2008).

Das, N., Karhika, P., Vimala, R. and Vinodhini., "Use of natural products as biosorbent of heavy metals o an overview." *Natural Product radiance*, 7 (2), 133 - 138 (2008).

Dastgheib, S. A. and Rockstraw, D. A., "A model for the adsorption of single metal ion solutes in aqueous solution onto activated carbon produced from pecan shells," *Carbon 40*" 843–1851(2002).

Dave, R. S., Dave, G. B., Mishra, V. P., "Removal of nickel from electroplating wastewater by weakly Basic chelating anion exchange resins: dowex 50x4, dowex 50x2 And dowex m-4195", *J Appl. Sci. Environ. Sanit.,* 6(1) 39-44 (2011).

Dhiraj, S., Garima, M. and Kaur, M.P., "Agricultural waste material as potential adsorbent for sequestering heavy metal ions from aqueous solutions-review," *Bioresour. Technol*., 99 (4), 6017 - 6027 (2008).

Diaz, E., Mohendano, A. F., Calvo, L., Gilarranz, M. A., Casas, J. A. and Rodriguez, J. J., "Hydrogenation of phenol in aqueous phase with palladium on activated carbon catalysts,"

Chem. Eng. J., 131 (1 - 3), 66 - 71 (2007).

Doan, H. D., Lohi, A., Dang, V. B. H. and Dang, T.," Removal of Zn (II) and Ni (II) by adsorption in a fixed bed of wheat straw," *Process Saf. Environ. Prot.*, 86, 259 - 267 (2008).

Emine, M., Yasar, N. and Yuksel, A., "Cr (VI) adsorption by waste acorn of Quercus ithaburensis in fixed beds: Prediction of breakthrough curves," *Chem. Eng. J.*, 119, 61- 68 (2006).

Fan, Y., Wang, B., Songhu, Y., Xiaohui, W., Jing, C. and Wang, L., "Adsorptive removal of chloramphenicol from wastewater by NaOH modified bamboo charcoal." *Bioresour. Technol.*, 101, 7661 - 7664 (2010).

Fatemeh, S., Mahboubeh, S., and Vajihe, S., "removal of nickel (ii) and palladium (ii) from surface waters," *Chem. Soc. Ethiopia.*, 27, (1) 1 - 9 (2013).

Fazeli, M. S., Khosravan, F., Hossini, M., Sathyanarayan, S. and Satish, P.N., " Enrichment of heavy metals in paddy crops irrigated by paper mill effluents near Narijangud, Mysore District, Karnatka, India*," Environ. Geolog*., 34, 297 - 302 (1998).

Ferda, G. and Selen, D., "Adsorption study on orange peel: Removal of Ni (II) ions from aqueous solution," *Afr. J. Biotechnol.*, 11 (5) 1250 – 1258 (2012).

Foersterling, H. U., Beer, M. and Hallmeier K. H., "Investigations of the Adsorption of Palladium on Carbonaceous Adsorbents Modified With Dimethylglyoxime II the Adsorption of Palladium on A Lignite in Its Unmodified Form and Modified With Dimethylglyoxime," *Carbon.*, 28 (4) 503 – 508 (1990).

Freundlich, M. F., "Over the adsorption in solution," *J Phys Chem B.*, 57, 385 - 470.

Fujiwara, K., Ramesh A., Maki T., Hasegawa, H. and Ueda, K., "Adsorption of platinum (IV), palladium (II) and gold (III) from aqueous solutions onto l-lysine modified cross linked chitosan resin," *J. Hazard.* , 146, 39 - 50 (2007).

Garcia. L., Torrent, A., Antico, E., Fonta, S. C. and Roglans, A., "Selective Pd (II) and Pt(IV) sorption using novel polymers containing azamacrocycle functional groups," *React Funct Polym.*, 68, 1088 – 96 (2008).

Gavrilescu, M., "Removal of heavy metals from the environment by biosorption," *Engineering in life sciences*, 4 219 - 232 (2004).

Gelb L. D. and Gubbins, K. E., "Pore size distributions in porous glasses: A computer simulation study," *Langmuir.*, 15, 305 – 308 (1999).

Goel, J., Kadirvelu, K., Rajagopal, C., and Garg, V. K., "Removal of lead (II) by adsorption using treated granular activated carbon. Batch and column studies," *J. Hazard. Mater.*, 125, 211 – 220 (2005).

Greenwood, N.N. and Earnshaw, A., "Chemistry of the elements," *Pergamon Press, oxford, UK* (1989).

Gupta, V. K., Jain, C. K., Ali, I., Sharma, M. and Saini, V. K., "Removal of cadmium and nickel from wastewater using bagasse fly ash- a sugar industry waste," *Water Res.*, 37 (16) 4038 - 4044 (2003).

Hamdaoui, O., "Removal of cadmium from aqueous medium under ultrasound assistance using

olive leaves as sorbent, chemical Engineering and processing," *Process intensification*, 48 (6) 1157 - 1166 (2009).

Hameed, B. H., Krishni, R. R., Sata, S. A., "A novel agricultural waste adsorbent for the removal of cationic dye from aqueous solutions," *J. Hazard. Mater.*, 162, 305 - 311 (2009).

Hasar, H., "Adsorption of Nickel (II) from aqueous solution onto activated carbon prepared from almond husk," *J. Hazard. Mater.*, 97 (1 - 3) 49 – 57 (2003).

Helen, K., Karthik, B. and Lima, M., "Removal and recovery of Ni and Zn from aqueous solution using activated carbon from Hevea brasiliensis: batch and column studies," *Colloids Surf. B: Biointer.*, 78, 2 (1), 291 – 302 (2010).

Henry, K. and Richard, K. M.," Continuous adsorption of Pt ions in a batch and packed bed column," *Hydrometallurgy*, 97 (1 - 2), 111 - 118 (2009).

Hibachi, Z. and Wolowicz, A., "Adsorption of palladium (II) from chloride solutions on Amberlyst A 29 and Amberlyst A 21 resins," *Hydrometallurgy*, 96, 159 - 65 (2009).

Ho, Y. S. and McKay, G., "Pseudo- second order model for sorption process," *Process Biochem.*, 34, 451 - 465 (1999).

Ho, Y. S., Huang, C. T., Huang, H. W., "Equilibrium sorption isotherm for metal ions on tree fern," *Process Biochem.*, 37, 1421 - 1430 (2002).

Ho, Y.S., "Review of second order models for adsorption systems," *J Hazard Mater., B*, 136, 681 - 689 (2006).

Hsieh, Y. J. and Teng, Z., "Industrial Wastewater Treatment Kyoto," *Imperial College Press*.

(2000)

Hubicki, Z. and Wolowicz, A., " A comparative study of chelating and cationic ion exchange resins for the removal of palladium(II) complexes from acidic chloride media," *J Hazard Mater.*, 164, (2 - 3), 1414 - 1419 (2009).

Hubicki, Z., Wolowicz, A. and Wawrzkiewicz, M., "Application of commercially available anion exchange resins for preconcentration of palladium (II) complexes from chloride-nitrate solutions," *Chem. Eng. J.*, 150 (1), 96 - 103 (2009).

Hutchins, R. A., "New method simplifies design of activated carbon systems, *Chemical Engineering,"* 80, 133 -138 (1973).

Iqbal, M. and Edyvean, R. G. J. "Biosorption of lead, copper and zinc ions on loofa sponge immobilized biomass of Phanerochaete chrysosporium," *Miner. Eng.*, 17, 217 - 223 (2004).

Jagtoyen, M. and Derbyshire, F. "Activated carbons from yellow poplar and white oak by H_3PO_4 activation," *Carbon*, 36, 1085 -1097 (1998).

Johnson Matthey Inc., "Platinum metals review" www.matthey.com, (2001 -2013).

Jossens, L., Prausnitz, J. M., Fritz, W., Schlunder, E. U., Myers, A. L., "Thermodynamics of multi-solute adsorption from dilute aqueous solution," *Chem Eng Sci.*, 33, 1097 - 1106 (1978).

Kadirvelu, K., Thamaraiselvi, K. and Namasivayam, C., "Removal of heavy metals from industrial wastewaters by adsorption onto activated carbon prepared from an agricultural solid waste," *Bioresour Technol.*, 76 (1), 63 - 65 (2001).

Kadirvelu, K., Thamaraiselyi, K. and Namasivayam, C., "Adsorption of Ni (II) from aqueous

solution onto activated carbon prepared from coir pith," *Sep. Purif. Technol.*, 24, 497 - 505 (2001).

Kasaini, H., Goto, M. and Furusaki, S., "Selective removal of Pd (II), Rh (III) and Ru (III) ions from a mixed chloride solution using activated carbon pellets," *Sep. Sci. Tech.*, 35, 1307 – 27 (2000).

Kayanuma, Y., Okabe, T.H, Mitsuda, Y. and Maeda, M., "New recovery process for rhodium using metal vapour," *J. Alloys Compd.*, 365, 211 - 220, (2004).

Kielhorn, J., Melber, C., Keller, D. and Mangelsdorf, I., "Palladium – a review of exposure and effects to human health," *Int. J. Hyg. Environ. Health.*, 205, 417 - 32 (2002).

Kinhikar, V. R., "Removal of nickel (II) from aqueous solutions by adsorption with granular activated carbon (GAC)," *Res. J. Chem. Sci.*, 2 (6) 6-11 (2012).

Kobya, M., "Removal of Cr (VI) from aqueous solutions by adsorption onto hazelnut shell activated carbon: Kinetic and equilibrium studies," *Bioresour. Technol.*, 91 (3) 317-321 (2004).

Kononova, O., Kholmogorov, A.G., Danilenko, N. V. and Goryaeva, N. G., Shatnykh, K. A., Kachin, S. V., "Recovery of silver from thiosulfate and thiocyanate leach solutions by adsorption on anion exchange resins and activated carbon," *Hydrometallurgy*, 88,189–195 (2007).

Lalhruaitluanga, H., Prasad, M. N. V., Radha, K., " Potential of chemically activated and raw charcoals of melcoanna baccifera for removal of Ni (II) and Zn (II) from aqueous solutions," *Desalination*, 271, 301 - 308 (2011).

Langmuir, I., "The adsorption gases on plane surface of glass,"

mica and platinum. J A C S, 40, 1316 - 1368 (1916).

LeVan, M. D., "Adsorption processes and modelling present and future," *Fundamentals of Adsorption* 6, F. Meunier (ed.), 19 - 29 (1998).

Li, Z., Mei, P. and Chen, W., "Adsorption rule of bamboo charcoal for nickel (II) in aqueous solution," *ChangjiangDaxueXuebaoZiranKexuebanBianjibu*, 5 (4) 62 - 64 (2008).

Lin, S. H. and Juan, R. S., "Heavy metal removal from water by sorption using surfactant-modified montmorillonite*," J. Hazard. Mater.*, 92 (3), 315 - 326 (2002).

Loderro, P., Cordero, B., Grille, Z., Herrero, R., Sastre, V. M. E., "Physicochemical studies of Cd (II). Biosorption by the invasive algae in Europe, Sargassummuticum." *Biotechnol. Bioeng.*, 88, 237 - 247 (2004).

Low, K. S., Lee, C. K. and Leo A. C., "Removal of metals from electroplating wastes using banana pith," *Bioresour. Technol.*, 51, 227 - 330 (1995).

Low, K.S. and Lee, C. K. "Quatermized rice husk as sorbent for reactive dyes." *Bioresour. Technol.*, 61 (2) 121 – 125 (1997).

Low, K.S. and Lee, C.K. "Removal of nickel (II) from aqueous solution and nickel plating industry wastewater using an agricultural waste," *Peanut hulls, waste manage.*, 15 (1),63 - 65 (1995).

Ma, H. W., Liao, X. P., Liu, X. and Shi, B., "Recovery of platinum (IV) and palladium (II) by bayberry tannin immobilized collagen fiber membrane from water solution," *J. Membr. Sci.*, 278, 373 - 380 (2006).

Ma, X. and Ouyang, F., "Adsorption properties of biomass based activated carbon prepared with spent coffee grounds and pomelo skin by phosphoric acid activation", *Appl. Surf. Sci*. (2013).

Macaskie, L.E., Creamer, N.J., Essa, A. M. M., Brown, N. L., "A New Approach for the Recovery of Precious Metals from Solution and From Leachates Derived From Electronic Scrap," *Biotechnology and bio engineering*, 96 (4) (2007).

Mahlatse, M., Sekhula, J. O., Okonkwo, Caliphs, M., Zvinowanda, Nana, N., and Abdul, J., "Fixed bed column adsorption of Cu (II) onto Maize Tassel - PVA beads," *Chem. Engg. Process Technol.*, 3(2), 1 - 5 (2012).

McKay, G., Barford, J. P. and Ip, A.W.P., "Production and comparison of high surface area bamboo derived active carbons," *Bioresour Technol.*, 99, 8909 - 8916 (2008).

Mclean, J.E., and Bledsoe, B.E., "Behavior of metals in soils", EPA/540/S-92/018. Washington, DC: U.S.EPA.

Mehta, S. K. and Gaur, J. P., "Use of algae for removing heavy metal ions from wastewater: Progress and prospects," *Crit. Rev. Bioethanol.*, 25, 113 - 152 (2005).

Merdivan, M., Aygun, R. S., Kulcu, N., Flame AAS Determination of Platinum, Palladium, and Rhodium in Catalysts. *Atomic spectroscopy,* 18,122-126 (1997).

Minero, C., Pelizzetti, C., Piccini, P., Vinceti, M., "Photo catalyzed transformation of nitrobenzene on TiO_2 and ZnO," *Chemosphere*, 28, 1229 -1244, (1994).

Mizuta, K., Matsumoto, T., Hatate, Y., Nishihara, K. and Tomoki, N., "Removal of nitrate-nitrogen from drinking water using bamboo powder charcoal," *Bioresour. Technol*., 95, 255–257

(2004).

Mohammad, S.Y., Francesc, M. and Sandra, C., "New catalytic advanced oxidation processes for wastewater treatment," *Doctoral Thesis* (2011).

Mohanty, K., Jha, M.., Meikap, B.C. and Biswas, M.N., "Removal of chromium (VI) from dilute aqueous solutions by activated carbon developed from Terminalia arjuna nuts activated with zinc chloride," *Chem. Eng. Sci.*, 60, 3049 - 3059 (2005).

Moonis, A. K., Mohammad, N., Thomas, S.Y., Choong, H. M. and Luqman, A. C., "Biosorption and desorption of Nickel on oil cake: Batch and column studies," *Bioresour Technol.,* 103, 35 – 42 (2012).

Morisada, S., Kim Y. H., Ogata, T., Marutani,Y., Nakano, Y., "Improved Adsorption behaviors of Amine-Modified Tannin Gel for Palladium and Platinum Ions in Acidic Chloride Solutions", *Ind. Eng. Chem.,* 50,1875-1880 (2011) .

Murali, P., Amrita, A., Ramgopal, U., Anil, V., "Effect of Surfactant Concentration and Loading Ratio on the Electroless Plating Characteristics of Dense Pd Composite Membranes," *Ind. Eng. Chem. Res.,* 53:3105-3115 (2014).

Muqing, Y., Daowei, S., Wei, T., Guoping, W., Wanbin, S. and Ning, X., " Systematic studies on adsorption of trace elements Pt, Pd, Au, Se, Te, As, Hg, Sb on thiol cotton fiber**,"** *Analytica Chimica Acta.*, 456 (1) 147-155 (2002).

Namasivayam, C., Suresh, K. M. V., "Removal of chromium (VI) from water and wastewater using surfactant modified coconut coir pith as a biosorbent*," Bioresour. Technol.,* 99, 2218 - 2225 (2008).

Nasehir, K., Yahaya. E. M., Ismail, A., Muhammad, F. P., Mohamed, L., Olugabenga, S. B. and Mohd, A. A., "Fixed bed column study for Cu (II) removal from aqueous solutions using rise husk based activated carbon," *Int. J Eng. Technol.*, 11(1) 186-190 (2011).

Nassar, M. M., "The kinetics of basic dye removal using palm fruit bunch." *Adsorpt. Sci. Technol.*, 15(8), 609-617, (1997).

Nehrenheim, E. and Gustafsson, J. P., "Kinetic sorption modeling of Cu, Ni, Zn, Pb and Cr ions to pine bark and blast furnace slag by using batch experiments," *Bioresour. Technol.*, 99, 1571–1577 (2008).

Noeline, B. F., Manohar, D. M., Anirudhan, T. S., " Kinetic and equilibrium modelling of lead(II) sorption from water and wastewater by polymerized banana stem in a batch reactor," *Sep. Purif. Technol.*, 45, 131 – 140 (2005).

Nur Hamizah Shaidan, Usama Eldemerdash, Sherine Awad, "Removal of Ni (II) ions from aqueous solutions using fixed-bed ion exchange column technique", *J Taiwan Inst. Chem. Eng.*, 43, 40–45 (2012).

Occupational Safety and Health Administration (OSHA), Permissible exposure limit (PEL) for various elements and compounds, http://www.osha.gov/dsg/topics/pel/.

Ozaki, H., Sharma, K., Saktaywin, W., "Performance of an ultra-low pressure reverses osmosis membrane (ULPROM) for separating heavy metal: Effects of Interference parameters", *Desalination*, 144: 287-294 (2002).

Paola, R. E., Girlado, L., Juan, C. M. P., "Nickel (II) ion adsorption onto activated carbon. Relationship between physicochemical properties and adsorption capacity", *Adsorpt. Sci.*

Technol., 29(6):541-551 (2011).

Parajuli, D., Kawakita, H., Inoue, K., Funaoka, M., "Recovery of Gold (III), Palladium (II), and Platinum (IV) by Aminated Lignin Derivatives", *Ind Eng Chem Res,* 45:6405-6412 (2006).

Paria, S. and Khilar, K. C., "Reviews on experimental studies of surfactant adsorption at the hydrophilic solid –water interface", *Adv. Colloid Interface Sci.,* 110 75-95 (2004).

Park, C. I., Chung, J. S., Cha, K. W., "Separation and pre concentration method for palladium, platinum and gold from some heavy metals using amberlite IRC 718 chelating resin". *Kor Chem Soc*, 21 (1): 121-124 (2000).

Park, J., Sung, W. W., Mao, J., Kwak I.S., Yeoung S. Y., "Recovery of Pd from HCL solution using PAH –modified Escherichia coli biomass", *J. Hazard. Mater.* 181,794-800 (2010).

Pilli, S.R., Goud, V.V., Mohanty, K., "Biosorption of Cr (IV) on immobilized hydrilla verticillata in a continuous up-flow packed bed: prediction of kinetic parameters and breakthrough curves", *Desalination and water treatment*, 50, 115-124 (2012).

Pitakchon, C. P. J. F. T., "Impregnation of Chitosan onto Activated Carbon for High Adsorption Selectivity towards CO_2: CO_2 Capture from Biohydrogen, Biogas and Flue Gas," *J. Sustainable Energy Environ.,* 3, 153 - 157 (2012).

Radenovic, A.; Malina, J., Strkalj, A., "Removal of Ni (II) from aqueous solution by low-cost adsorbents", *The Holistic Approch. Environ.,* 1 (3) 109 - 120 (2011).

Rai L.C.,Gour J. P. and Kumar H. D., " Phycology and heavy metal pollution," *Biological reviews,* 56, 99 - 51 (1981).

Ramesh, A.; Hasegawa, H.; Sugimoto, W., Maki, T., Ueda, K., "Adsorption of gold (III), platinum (IV) and palladium (II) onto glycine modified cross-linked chitosan resin", *Bioresour. Technol.*, 99:3801–3809 (2008).

Ravindra, K., Bencs, L., van Grieken, R., "Platinum group elements in the environment and their health risk", *The science of the total environment.*, 318, 1-43 (2004).

Redlich, O., Peterson, D. L., "A useful adsorption isotherm", *J .Phys. Chem.,* 63 **(**1024) (1959).

Remoudaki E., Tsezos M., Hatzikioseyian A., Karakoussis V., "Mechanism of palladium biosorption by microbial biomass, The effect of metal ionic separation and solution co-ions", 449 - 462 (2007).

Ruey-Shin Juang, Hsiang-Chien Kao, Wei Chen, "Column removal of Ni (II) from synthetic electroplating waste water using a strong-acid resin", *Sep. Purif. Technol.***,** 49 (1) 36–42 (2006).

Saeed, A., Iqbal, M., Akhtar, M. W., "Removal and recovery of lead (II) from single and multimetal (Cd, Cu, Ni, and Zn) solution by crop milling waste (black gram husk)", *J. Hazard. Mater.*, B 117: 65–73 (2005)

Sandau, E., Sandau, P. and Pulz, O., "Heavy metal sorption by microalgae", *Acta. Biotechnol.* , 16 : 227-25 (1996a).

Sari A., Durali M., Mustafa T., Mustafa S., "Biosorption of palladium form aqueous solution buy moss Racomitriumlanuginosum biomass: Equilibrium, kinetic and thermodynamic studies". *J. Hazard. Mater.* , 162, 874 – 879 (2009).

Sarkar S., Satheshkumar A., Jayanthi R., Premkumar R., "Biosorption of Nickel by Live biomass

of *Trichodemahazianum*". *Res. J Agricult. Sci.*, 1 (2) 69 -74 (2010).

Sekar, M., Sakthi, V., Rengaraj, S., "Kinetics and equilibrium study of lead (II) onto activated carbon prepared from coconut shell". *J. Colloid Interface Sci.*, 279 (2) 307-313 (2004).

Senthil kumar, S., Kalaamani, P., Porkodi, K., Veradarajan, P.R., Subburaam, C.V., "Adsorption of dissolved reactive red dye from aqueous phase onto activated carbon prepared from agriculture waste", *Bioresour. Technol.*, 97, 1618 (2006).

Senthil kumar, P., Ramakrishnan, K., Gayathri R., "Removal of nickel(ii) from aqueous solutions by Ceralite IR 120 cationic exchange resins", *J Eng. Sci. Technol.*, 5 (2) 232 – 243 (2010).

Shafaghat, A., Salimi, F., Valiei, M., Salehzadeh, J., Shafaghat, M., "Removal of heavy metals (Pb^{2+}, Cu^{2+} and Cr^{3+}) from aqueous solutions using five plants materials", *Afr. J. Biotechnol.* 11: 852–855 (2011).

Sharififard, H., Soleimani, M. and Ashtiani, F. Z., "Evaluation of activated carbon and bio-polymer modified activated carbon performance for palladium and platinum removal," *J. Taiwan. Inst. Chem. Eng.*, 43, 696 – 703 (2012).

Shukla, S. R., Pai, R. S., "Adsorption of Cu (II), Ni (II) and Zn (II) on modified jute fibers". *Bioresour. Technol.*, 96:1430–1438 (2005).

Sincero, A. P. and Sincero, G. A., "Physical-Chemical Treatment of Water and Wastewater", *IWA Publishing* (2003).

Sing, K. S. W., Everett, D. H., Haul, R. A. W., Moscou, L., Pierotti, R.A., Rouquerol, J., Siemieniewska, T,. "Reporting physisorption data for gas and solid systems with special

reference to the determination of surface area and porosity", *Pure. Appl. Chem.*, 57:603-619 (1985).

Singh, R. and Singh, P., "Pollution in Abu drainage –a preliminary report", *Adv. Plant Sci*., 13: 43-45 (2000).

Singh, S. N., "Effect of effluents from the sindri factory in the river Damodar", *J. Ecobiol*., 6: 27-32 (1994).

Singh, U. and Kaushal, R. K., "Treatment of Waste Water with Low Cost Adsorbent – A Review", *VSRD I. J. Techn. Non-Techn. Research.*, 4 (13) 33 (2013)

Snyder's, C. A., Mpinga, C. N., Bradshaw, S. M., Akdogan., G. and Eksteen, J.J., "The application of activated carbon from the adsorption and elution of platinum group metals from dilute cyanide leach solutions, "*J. South. Inst. Mining and Metal*., 113, 381 - 388 (2013).

Srinivastava, V. C., Swamy, M. M., Mall, I. D., Prasad, B., Mishra, I. M., "Adsorptive removal of phenol by Bagasse flies ash and activated carbon: equilibrium, kinetics and thermodynamics", *Colloid surf Physicochem Eng Aspects.*, 272, 89-104 (2006).

Sudha, B. R. and Abraham, T. E., "Studies on enhancement of Cr (VI) biosorption by chemically modified biomass of Rhizopus nigricans," *Water Res*. 36, 1224 - 1236 (2002).

Sun, Z. Y., Tang, Y. Q., Iwanaga, T., Sho, T., Kida, K., "Production of fuel ethanol from bamboo by concentrated sulfuric acid hydrolysis followed by continuous ethanol fermentation", *Bioresour. Technol*., 102, 10929–10935 (2011)

Tan, I. A. W., Hameed, B. H., Ahmed, A. L., "Equilibrium and kinetic studies on basic dye

adsorption by oil palm fibre activated carbon". *Chem. Eng. J.*, 127 111–119 (2007).

Tharanitharan, V. and Srinivasan K., "Removal of water and wastewater using modified Duolite XAD-761 resin", *Indian J. Chem. Technol.*, 16, 245-253 (2009).

Thomas, H. C., "Heterogeneous ion exchange in a flowing system", *J. Amer. Chem. Soc.*, 66 1664–1666 (1944).

Tiberg, F., Jonsson, B. and Lindman, B., "Ellipsometry studies of the self-assembly of non-ionic surfactants at the silica-water interface: kinetic aspects," *Langmuir.*, 10, 3714-3722 (1994).

Tran, A. V., "Chemical analysis and pulping study of pineapple crown leaves", *Ind. Crops Prod.*, 24:66-74 (2006).

Uer, A., Uyanik, A., Aygun, S. F., "Adsorption of Cu (II), Cd (II), Zn (II), Mn (II) and Fe (III) ions by tannic acid immobilized activated carbon", *Sep. Purif. Technol.*, 47:113–118 (2006).

Vijay, P., Dhande, G. A., Dipak, T., Rajput, J. C., "Micro propagation of pomegranate (Punica granatum L.) Bhagava cultival from nodale explant" *Afr. J. Biotechnol.*, 10:79, 18130-18136 (2011).

Vijayakumaran, V. and Srivoli, S., "Equilibrium, thermodynamic and kinetic studies of nickel (II) ions on ODINA WODIER bark carbon", *Elixir online journal*, 2889-2896 (2011).

Vijayaraghavan, K., Jegan, J., Palanivelu, Velan, K. M. "Removal of nickel (II) ions from aqueous solution using crab shell particles in a packed bed up-flow column," *J. Hazard. Mater., B*, 113, 223 - 230 (2004).

Wang, G., Li, A. Li, M., "Sorption of nickel ions from aqueous solutions using activated carbon

derived from walnut shell waste", *Desalination*, 16(1-3):282-289 (2010).

Wang, H., Bao, C., Li, F., Kong, X., Xu, J., "Preparation and application of 4-amino-40- nitro azobenzene modified chitosan as a selective adsorbent for the determination of Au (III) and Pd (II)". *Microchimica Acta.*, 168:99–105 (2010).

Wang, J. and Chen, C., "Biosorption of heavy metals by *Saccharomyces cerevisiae*: A review". *Bioethanol. Advan.*, 24,427-451 (2006).

Wang, L., Xinga, R., Song, L., Huahua, Y., Yukun, Q. L., Kecheng, L., Jinhua, F., Rongfeng, L., Pengcheng, L., "Recovery of silver (I) using a thiourea-modified chitosan resin", *J. Hazard. Mater.*, 180, 577–582 (2010).

Wilde, E. W. and Benemann, J. R., "Bioremoval of heavy metals by use of microalgae". *Biotechnol. Adv.*, 11: 781-812 (1993).

Woinska, S. and Godlewska, B., "Determination of platinum and palladium in road dust after their separation on immobilized fungus by electro thermal atomic absorption spectrometry". *Spectrochimica Acta Part B*: *Atomic Spectroscopy*, 66(7):522-528 (2011).

Wollmann., "Water Resources. National Academy of Sciences, National Research Council", Washington DC Publication No. 100-B (1962).

Wolowicz, A. and Hubicki Z., "Palladium (II) complexes adsorption from the chloride solutions with macro component addition using strongly basic anion exchange resins, type 1". Hydrometallurgy, 98:206–12 (2009)

Wu. F. C., Tseng, R. L., Juang, R. S., "Preparation of activated carbons from bamboo and their

adsorption abilities for dyes and phenol". *J. Environ. Sci. Health*, Part A 34(9):1753-1775 (1999).

Xiong, Y., Raj Adhikari, C., Kawakita, H., Ohto, K., Inoue, K., Harada, H., "Selective recovery of precious metals by persimmon waste chemically modified with dimethylamine", *Bioresour. Technol*, 100:4083–9 (2009).

Yan, G. and Viraraghavan, T., "Heavy metal removal in a biosorption column by Immobilization, *M. rouxi* biomass". *Bioresour. Technol.*, 78**:** 243-249 (2001).

Yang Y., Chun Y., Sheng, G., Huang, M., "pH dependent of pesticide adsorption by wheat residue derived black carbon, *Langmuir*". 20 6736-6741 (2004).

Yang, Y., Chun, Y., Sheng, G., Huang, M., "pH dependent of pesticide adsorption by wheat residue derived black carbon. *Langmuir*", 20:6736-6741 (2004).

Yoon, Y. H. and Nelson J. H., "Application of gas adsorption kinetics. I. A theoretical model for respirator cartridge service time", *Am. Ind. Hyg. Assoc. J.*, 45 509–516 (1984).

Zhou, L., Liu, J., Liu, Z., "Adsorption of Platinum (IV) and Palladium (II) from aqueous solution by thiourea-modified chitosan microspheres", *J. Hazard. Mater.*, 172: 439-446 (2009).

Zhou, L., Liu, J., Liu, Z., "Adsorption of platinum (IV) and palladium (II) from aqueous solution by thiourea-modified chitosan microspheres". *J. Hazard. Mater.*, 172:439–446 (2009).

Appendix A: Calibration Curve for the determination of Ni (II) solution concentration

The analysis of Ni (II) adsorbate samples before and after adsorption were analyzed using atomic absorption spectrophotometer (AAS) (Make: /S Varian BV, Model: Spectra AA 220FS) using flame mode at a wavelength of 232.8 nm. A calibration curve is required to determine the Ni (II) solution concentration from measured adsorbate absorbance value. Since it would be possible to obtain different calibration curves for aqueous and synthetic Ni (II) ELP solutions, two different calibration curves have been prepared.

While Ni (II) aqueous solution was prepared using nickel sulfate, the aqueous Ni (II) solution was prepared using specified amounts of nickel sulfate and tri-sodium citrate in millipore water. The synthetic ELP solution was prepared with 500 mL of stock solution with 50 ppm concentration of nickel (119.5 mg of nickel sulfate heptahydrate) and 313.12 mg of trisodium

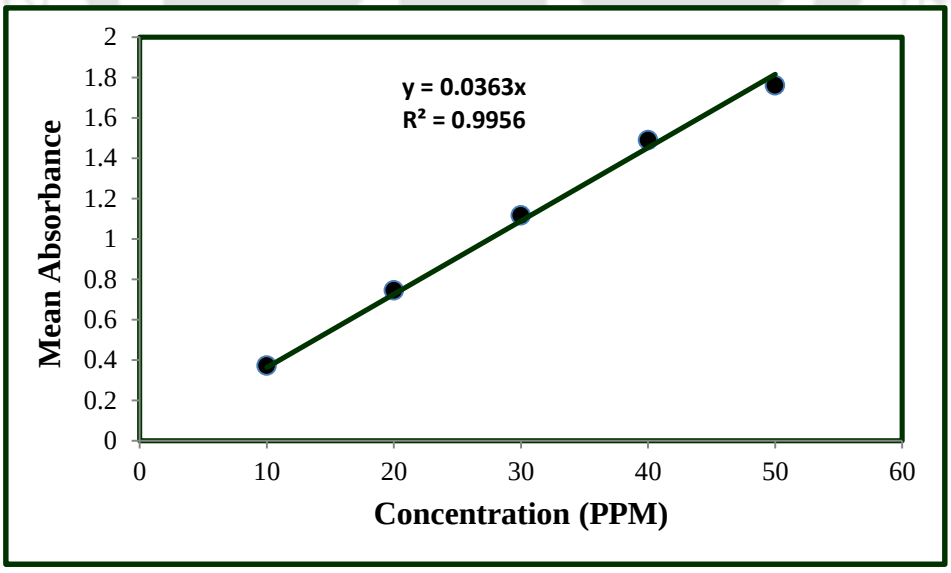

Fig. A1: Calibration curve for the determination of Ni (II) in aqueous solutions

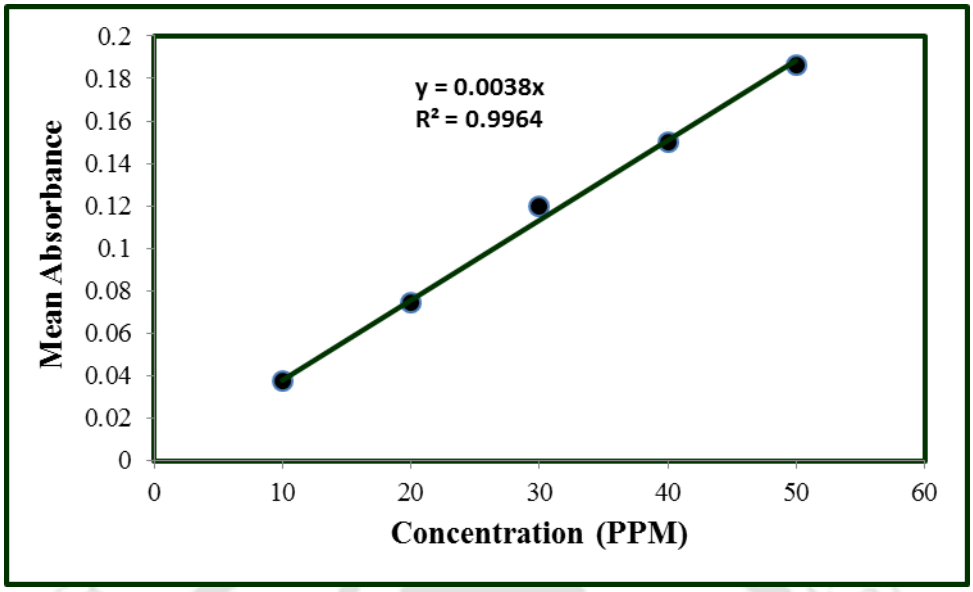

Fig. A2: Calibration curve for the determination of Ni (II) in synthetic electroless plating solutions.

citrate. Thereby, using the stock solution, 5 – 50 ppm nickel solutions were prepared using dilution approaches and these have been considered as the standards. For all standards, absorbance has been measured using the AAS. The obtained calibration curve for the variation of absorbance with Ni (II) solution concentration is presented in Figure A1 and A2 for aqueous and synthetic ELP solutions respectively. It can be observed from the figures that the absorbance varies linearly with Ni (II) solution concentration for both aqueous and synthetic ELP cases. Thereby, using these calibration curves and measured absorbance of adsorbate sample, the unknown metal solution concentration (after adsorption) is determined.

Appendix B: Calibration Curves for the determination of Pd (II) and Chitosan solution concentrations

In this section, the obtained calibration curves for the evaluation of unknown Pd (II) and chitosan solution concentrations in adsorbate samples is presented. The B1 sub-section refers to the Pd (II) calibration curves for various cases. Finally sub-section B2 refers to the prepared calibration curve for chitosan solution concentration estimation.

B1: Pd (II) Calibration Curves

The atomic absorption spectrophotometer (Make: M/S Varian BV, Model: Spectra AA 220FS) was used to analyse the concentration of the samples that were obtained after performing the various adsorption experiments on the palladium electroless plating solution. The spectrophotometer was used in the flame mode with a Pd lamp of wavelength 247.8 nm (Merdivan *et al*., 1997). Three different sets of calibration curves were prepared. These correspond to various cases such as (a) aqueous solutions (b) synthetic ELP solutions not containing CTAB surfactant and (c) synthetic ELP solutions containing CTAB surfactant. The solution concentration of synthetic ELP solutions with and without CTAB surfactant has been presented in Table 2.1 of the thesis. Thus, solutions with these specified concentrations of various chemicals and reagents were prepared as standards.

Based on the prepared standards, the calibration curves were prepared for three different cases.

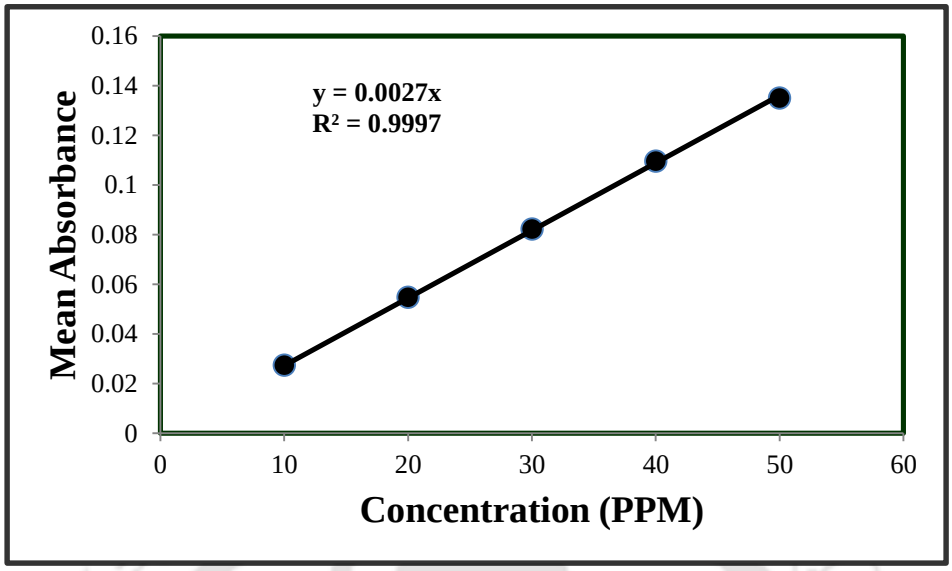

Fig. B1: Calibration curve for the evaluation of Pd (II) concentrations in aqueous solutions.

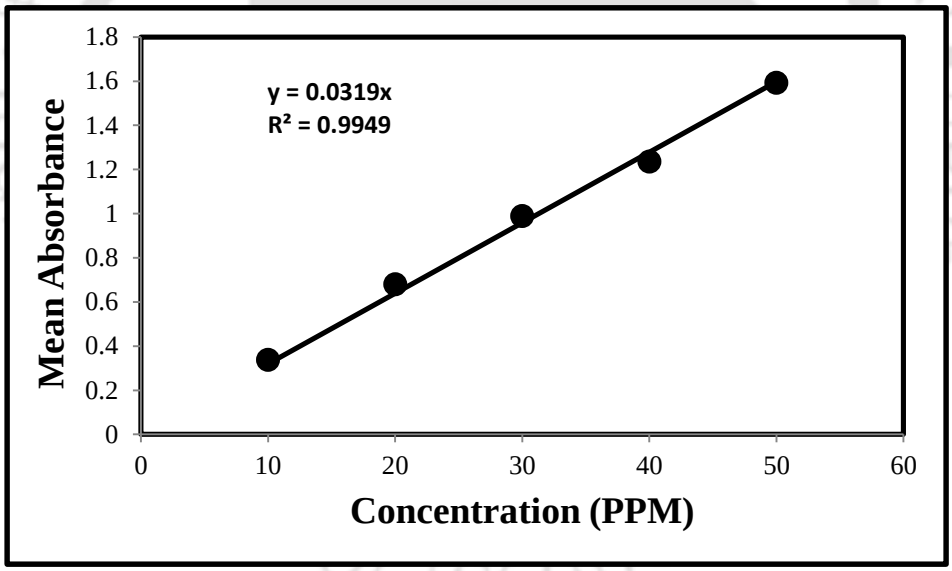

Fig. B2: Calibration curve for the evaluation of Pd (II) solution concentration in synthetic electroless plating solutions not containing CTAB surfactant.

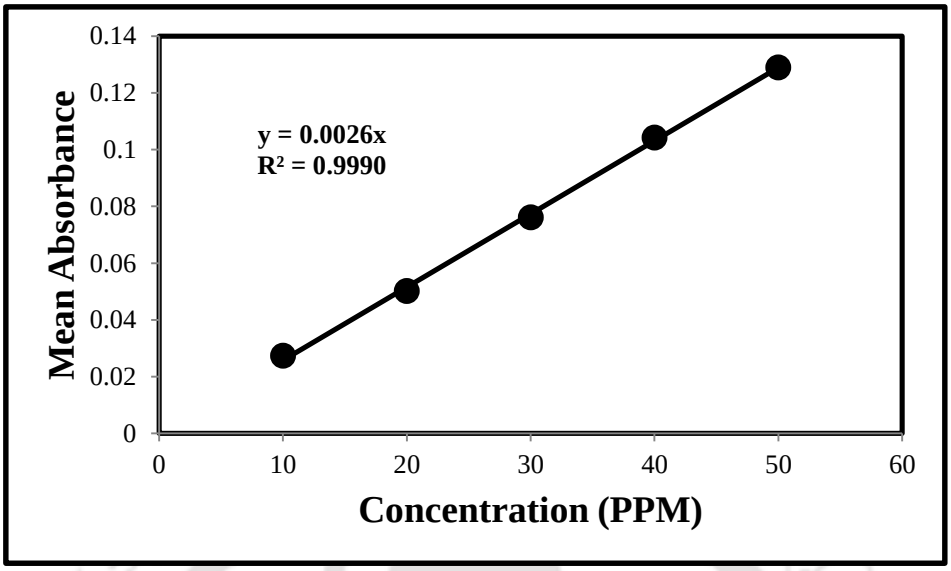

Fig. B3: Calibration curve for the evaluation of Pd (II) solution concentration in synthetic electroless plating solutions containing 2 CMC CTAB surfactant.

Figure B1, B2 and B3 illustrate the calibration curves obtained for aqueous solutions, synthetic ELP solutions (without CTAB) and (c) 2 CMC CTAB concentration containing Pd (II) synthetic ELP solutions. It can be observed that the calibration curve is linear for all three cases and different absorbance profiles exist for different cases. Using these calibration curves, the unknown Pd (II) solution concentration in the adsorbate has been determined by measuring their absorbance value using the AAS instrument.

B2: Chitosan calibration curve

The chitosan calibration curve was prepared to obtain chitosan solution concentration in the absorbate left after preparing the chitosan – AC composite adsorbent. To prepare the

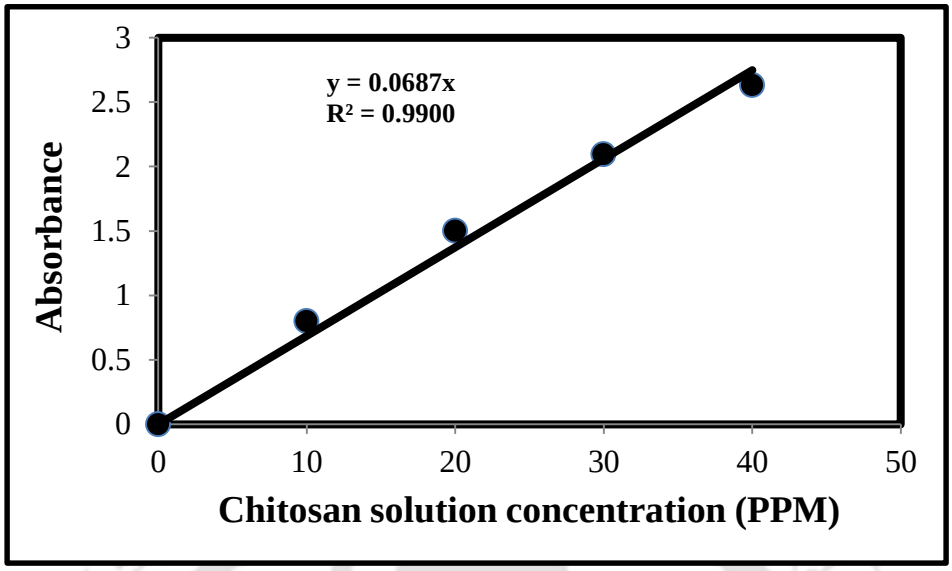

Fig. B4: Calibration curve for the evaluation of chitosan solution concentration after carrying out the fabrication of impregnated chitosan-activated carbon adsorbent.

calibration curve, standard aqueous chitosan solutions were prepared with specified amount of chitosan (in the range of 0.1-2 g/L) in Millipore water. Thereby, the prepared standards were evaluated for their absorbance using UV-Visible spectrophotometer (Make: Perkin Elmer, Model: Lamda 35), to obtain the calibration curve. Figure B4 depicts the obtained calibration curve for chitosan solution concentrations of 10 – 40 mg/L. The calibration curve is linear with respect to variation in chitosan solution concentration. Using the calibration curve, the unknown chitosan solution concentration after composite adsorbent preparation is evaluated by determining the absorbance of the spent adsorbate sample with the instrument.

Appendix C: Sample Calculations

The following steps summarize the evaluation of Pd (II) adsorption characteristics

a) Adsorption parameters: Adsorbent Dosage: 0.3g; Volume of aqueous solution: 50ml; Contact Time: 300 min; Initial Concentration: 50 mg/L.

b) Final equilibrium Pd (II) solution concentration (C_{eq}): From AAS and calibration curve, C_{eq} = 9.83 mg/L.

c) Using eq. (**2.1**), % Adsorption $= \frac{(50-9.83)}{50} \times 100 = 80.32\%$

d) Using eq. (**2.2**), Metal Uptake= $\frac{50 \times (50-9.83)}{0.3 \times 1000} = 6.69$ mg/g

e) Langmuir isotherm Parameters:

The above calculation carried palladium solution concentration from 50 to 500 mg/L. using those adsorption equilibrium data.

For the plot of C_{eq}/q_{eq} and C_{eq}, the slope, intercept and regression coefficient were obtained as 0.0145, 0.0112, R^2=0.9688 respectively.

Using slope, q_{max} (monolayer capacity) = 1/slope = 68.96 mg/g

Using intercept and q_{max}, b = 1/(q_{max} , x intercept) = 0.0112.

f) Freundlich isotherm parameters:

For a plot between log C_{eq} and log q_{eq}, the slope, intercept and regression coefficient were obtained 0.6503, 0.2358 and R^2=0.989 respectively.

Using slope, m = 0.6503.

Using intercept, K_f = exp (0.2358) = 1.721

g) Psuedo-second order model parameters

For a plot between t and t/q_t, the slope, intercept and regression coefficient were obtained as, 0.0288, 0.1759 and R^2=0.9999 respectively.

Using slope, m = 0.0288 and using intercept c=0.1759, k_2=0.004715.

h) Thermodynamic model parameters:

For a plot between 1/T and ln K_L, the slope, intercept and regression coefficient were obtained as -5926.7, 23.375 and 0.9413.

Using slope m= -5926.7 and intercept c= 23.375.

Using slope and intercept, the thermodynamic parameters are evaluated as

Slope =($-\Delta H/R$)

ΔH^o= (-slope ×R) = 5926.7×8.314 = 49.275 kJ/mol

ΔS^o = (intercept×R) = 0.194 kJ/mol. K

$\Delta G^o = \Delta H^o - T\Delta S^o$ = -528.84

Appendix D: Error Analysis

For several cases investigated in this work, two samples were simultaneously evaluated for the Ni (II) and Pd (II) adsorption characteristics. Based on the carried out measurements, the average values for various cases have been presented throughout the thesis. Based on at least two sets of experiments conducted for any case, based on the least count of the weighing balance, the maximum error in the measurement of adsorbent mass is about 0.33%. For the volume measurements using 50 mL measuring jar with least count of 0.1 mL, the error in the measurement of solution volume is 0.2%. The maximum error in the evaluation of metal solution concentration using AAS absorbance and calibration curve is about 4%. Based on atleast two sets of data, the maximum and minimum error in the estimation of metal uptake is about 2.36% and 0.932%. Similarly, for removal efficiency, the maximum and minimum error in its evaluation is about 0.58% and 0.35% respectively.

Appendix E: Images of Laboratory Research

Pineapple stem adsorbent

	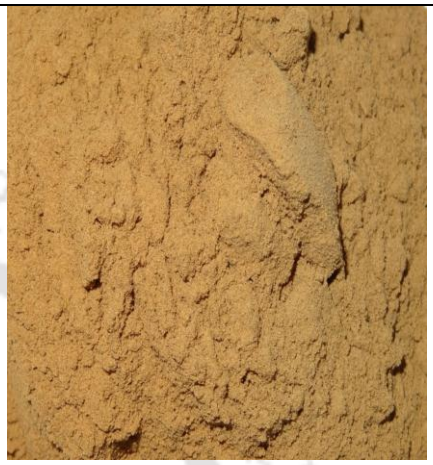
Raw Pineapple stem	**PS Powder**

BSAC14 Adsorbent

	
Raw bamboo stems	**Raw bamboostem powder**

H_3PO_4 treated bamboo powder (BSAC)

BSAC14 Adsorbent

Activated carbon-PVA beads

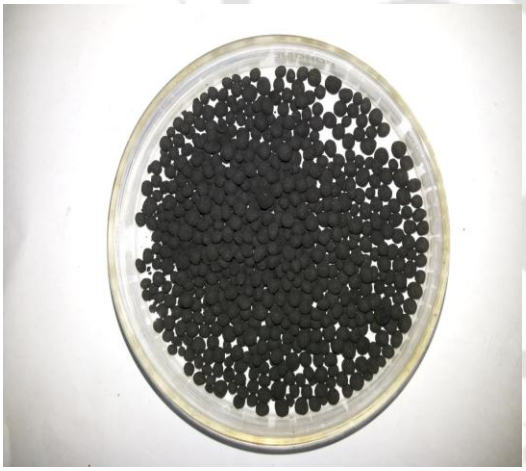

AC-PVA beads

AC-PVA beads-Pd

AC-PVA beads-Pd-NaOH

CH-AC-C Adsorbent

Commercial Activated carbon

Cross-linked with chitosan-AC

Packed bed adsorption setup for the evaluation of continuous Pd (II) adsorption characteristics

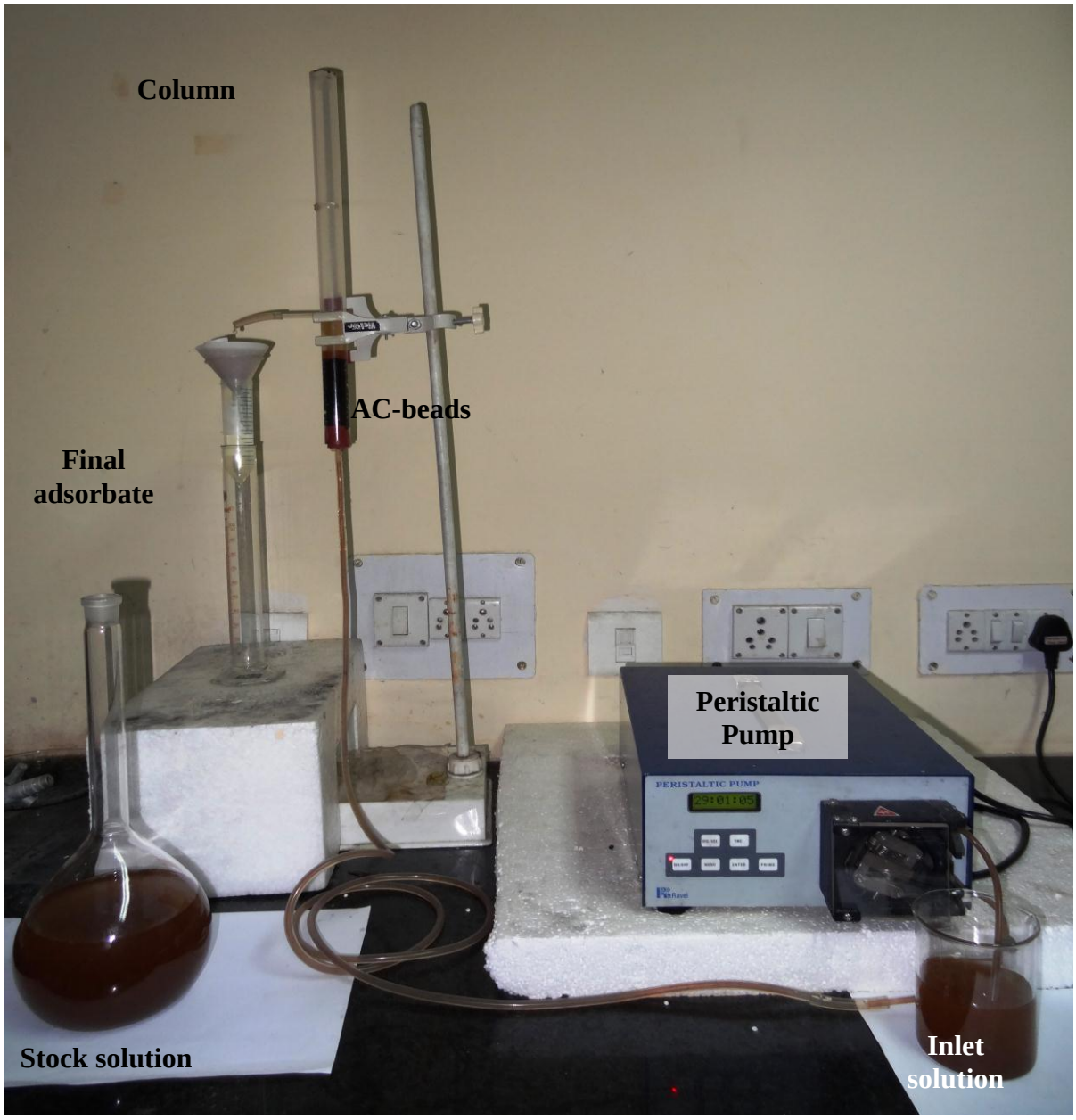

List of Publications

Published/Accepted Articles in International Refereed Journals

[1] **Yennam Rajesh**, Pujari Murali and Uppaluri Ramgopal. **"**Equilibrium and Kinetic studies of Ni (II) adsorption using Pineapple and Bamboo Stem based adsorbents" Separation Science and Technology, 49:4,533-544.

Communicated/Under preparation

[1] **Yennam Rajesh** and Uppaluri Ramgopal. "Pd (II) Adsorption on commercial activated charcoal from synthetic electroless plating solutions" [under preparation].

[2] **Yennam Rajesh** and Uppaluri Ramgopal. "Development of activated charcoal adsorbent from bamboo (Bambuseae) waste for the removal of Pd (II) from synthetic electroless plating solutions" [under preparation].

[3] **Yennam Rajesh** and Uppaluri Ramgopal. "Pd (II) Adsorption on commercial activated charcoal from industrial waste streams: Prediction of breakthrough curves" [under preparation].

[4] **Yennam Rajesh,** Nagireddi Srinu and Uppaluri Ramgopal. "Development of cross-linked chitosan based activated charcoal for the adsorption of Pd (II) from synthetic electroless plating solutions" [under preparation].

[5] **Yennam Rajesh,** Gummalla Namrata and Uppaluri Ramgopal. "Efficacy of activated carbon for the adsorption of Ni (II) from synthetic electroless plating solutions" [under preparation].

Conference Presentations (National and International)

[1] Yennam Rajesh and Uppaluri Ramgopal. **"**Preparation and Characterization of Natural Wood based Biosorbents from North-Eastern India". Third International Conference on Natural polymers, Bio-Polymers, Bio-Materials, their Composites, Blends, IPNs, Polyelectrolytes and gels: Macro to Nano Scales organized by center for Nano science and Nanotechnology held in Mahatma Gandhi University, Kottayam, Kerala, 26th to 28th, October, 2012.

[2] Yennam Rajesh and Uppaluri Ramgopal. **"**Removal of Ni (II) from aqueous solution using Banana pith as biosorbent". Reflux-I held at Department of Chemical Engineering, Indian Institute of Technology Guwahati, Guwahati, 6th to 7th, April, 2013.

[3] Yennam Rajesh and Uppaluri Ramgopal. **"**Removal of Ni (II) from aqueous solution using Pine apple stem as biosorbent". Reflux-I held at Department of Chemical Engineering, Indian Institute of Technology Guwahati, Guwahati, 6th to 7th, April, 2013.

[4] Yennam Rajesh and Uppaluri Ramgopal. **"**Fixed bed adsorption characteristics of Pd (II) on activated charcoal beads using synthetic electroless plating solutions". Reflux-II held at Department of Chemical Engineering, Indian Institute of Technology Guwahati, Guwahati, 28th to 29th, March, 2014.

[5] Yennam Rajesh and Uppaluri Ramgopal. **"**Development of novel adsorbent from bamboo stem plant wastes for the application of wastewater treatment using adsorption process". Recycle-I held at Department of Civil Engineering, Indian Institute of Technology Guwahati, Guwahati, 6th, April, 2014.